Signalling Pathways Linking Interleukin 13 Receptor Activation to Lung Epithelial Cell Function

Proctor, Victoria

Award date:
2013

Awarding institution:
University of Bath

Signalling pathways linking interleukin 13 receptor activation to lung epithelial cell function

Victoria Kate Proctor

A thesis submitted for the degree of Doctor of Philosophy

University of Bath

Department of Pharmacy and Pharmacology

March 2013

Acknowledgements

Firstly, I would like to thank my supervisor Dr Malcolm Watson for all his help and encouragement with this project. It was a steep learning curve coming from a chemistry background and I am very grateful for the opportunity to change my field and work on an area that has always interested me.

I would also like say a massive thank you to my husband Saul and my mother Diane, for without their constant help and emotional support this thesis would not have been possible.

A special thank you goes to Malika El Oualitti and Charlotte McDonnell, the best colleagues and friends a girl could wish for! I would like to thank all members of the Ward and Welham lab past and present, for their help and friendship. Gratitude also goes to Joseph Dukes, Adrian Rogers and Ursula Potter for all their imaging help.

Finally I would like to give my thanks to my funding bodies, BBSRC and Novartis without whom I wouldn't have been able to buy nearly as many pairs of shoes so in that respect they deserve the biggest thank you of all!

Abstract

The passage of fluid, ions and macromolecules across the epithelium is controlled primarily by epithelial tight junctions. Altered epithelial permeability is associated with lung disease, and barrier function is impaired by the Th2 cytokine IL-13. This thesis investigates the signalling pathways involved in the modulation of the epithelial barrier by IL-13 stimulation.

Initial experiments demonstrated that the human sub-bronchial epithelial cell line Calu-3 could be easily manipulated when grown using an air-liquid culture system. Expression of various key tight junction proteins was demonstrated, as well as a high trans-epithelial resistance (TER) for up to 7 days. Stimulation with IL-13 resulted in a decrease in TER compared with controls and this decrease was shown to be prevented with the PI3K inhibitor ZSTK474. IL-13 did not increase paracellular permeability of the epithelial monolayer to FITC-dextran from the apical to the basolateral chamber and ZSTK474 did not influence FITC-dextran flux. Immunocytochemistry showed that the expression of the tight junction protein claudin 2 was increased by IL-13 stimulation and this change in expression was shown to be PI3K dependent with the PI3K inhibitor ZSKT474 preventing the increase.

Further studies were carried out in an attempt to uncover the PI3K isoform responsible for the effects seen on both the TER and the TJ expression. It was shown that inhibition of the p110α isoform with PIK75 mimicked the result observed with the pan-PI3K inhibitor ZSTK474 and prevented the IL-13-induced claudin 2 upregulation. However none of the PI3K isoform inhibitiors showed the prevention of TER, as shown by the pan PI3K inhibitor ZSTK474. The role of STAT6 in TJ modulation was shown to be similar to that of PI3K, in that inhibition of STAT6 had a positive effect on the epithelial barrier by preventing the IL-13-induced TER decrease and the increase in the expression of claudin 2. In addition, both PI3K inhibition and STAT6 inhibition demonstrated effects on basal TER and claudin 2 expression, indicating that both pathways are involved in maintenance of epithelial barrier integrity.

Table of Contents

Table of figures

Chapter 1

Chapter 2

Chapter 3

Chapter 4

Chapter 5

Chapter 6

Chapter 7

List of Tables

Chapter 1

Chapter 2

Abbreviations

AH	Airway hyperresponsiveness
AJC	Apical junctional complex
ALI	Air liquid interface
AMPK	5' adenosine monophosphate-activated protein kinase
AMPS	Ammonium persulphate
ATP	Adenosine triphosphate
BSA	Bovine serum albumin
CD	Crohn’s Disease
cDNA	Complementary DNA
CF	Cystic fibrosis
CFTR	cystic fibrosis transmembrane conductance regulator gene
COPD	Chronic Obstructive Pulmonary Disease
DAPI	4',6-diamidino-2-phenylindole
DMEM	Dulbecco's Modified Eagle Medium
DMSO	Dimethyl Sulfoxide
DNA	Deoxyribonucleic acid
ECL	Enhanced chemiluminescence
EDTA	Ethylenediaminetetraacetic acid
EGFR	Epidermal growth factor receptor
EGTA	Ethylene glycol tetraacetic acid
EL	Extracellular loop
EMT	Epithelial to mesenchymal transition
FBS	Fetal bovine serum
FITC	Fluorescein isothiocyanate
GC	Glucocorticoid
GCM	Goblet cell metaplasia
GDP	Guanosine diphosphate
GMP	Guanosine monophosphate
GSK	Glycogen synthase kinase
GTP	Guanosine-5'-triphosphate
HAT	Histone acetyltransferase

HBE	Human bronchial epithelial
HBSS	Hank's Balanced Salt Solution
HDAC	Histone deacetylase
HL	Hodgkin Lymphoma
IBD	Inflammatory bowel disease
IC_{50}	Half maximal inhibitory concentration
IFN	Interferon
IL	Interleukin
IPF	Idiopathic pulmonary fibrosis
JAM	Junction adhesion molecule
JEAP	Junction-enriched and –associated protein
K_d	Dissociation constant
K_m	Michaelis constant (binding affinity)
LCC	Liquid covered culture
LDH	Lactate dehydrogenase
MAGUK	Membrane associated guanylate kinase
MAPK	Mitogen activated protein kinase
MDCK	Madin-Darby Canine Kidney
MEM	Minimal essential media
MH	Mucus hypersecretion
MHC	Major histocompatibility complex
MLCK	Myosin light chain kinase
mRNA	Messenger RNA
mTOR	Mammalian target of rapamycin
MUPP1	Multi PDZ-domain protein 1
NADP	Nicotinamide adenine dinucleotide phosphate
NO	Nitric Oxide
NOS	Nitric oxide synthase
OVA	Ovalbumin
PBS	Phosphate Buffered Saline
PCR	Polymerase chain reaction
PDK1	3-phosphoinositide dependent protein kinase-1
PGE	Prostaglandin

PH	Plekstrin homology
$PI(3,4)P_2$	Phosphatidylinositol 4,5-bisphosphate
$PI(3,4,5)P_3$	Phosphatidylinositol (3,4,5)-trisphosphate
PI3K	Phosphatidylinositol 3-phosphate
PKC	Protein kinase C
PTEN	Phosphatase and tensin homolog
RNA	Ribonucleic acid
RTK	Receptor tyrosine kinase
SAHA	Suberoylanilide hydroxamic acid
SDS	Sodium dodecyl sulfate
SEM	Scanning electron microscopy
siRNA	Small interfering RNA
STAT	Signal transducer and activator of transcription
TEMED	Tetramethylethylenediamine
TER	Transepithelial resistance
TGFβ	Transforming growth factor
Th2	T helper type 2 cells
TJ	Tight junction
TNF	Tumour necrosis factor
UC	Ulcerative colitis
VEGF	Vascular endothelial growth factor
ZO	Zonula occluden

Chapter 1 : Introduction

1.1 Inflammatory lung diseases

Lung diseases are the cause of around 14.5% of all deaths worldwide every year according to the world health organisation [1]. The term lung disease refers to disorders that prevent optimal function of the lungs, such as asthma, Chronic Obstructive Pulmonary Disease (COPD), cystic fibrosis, pneumonia, influenza and lung cancer. Chronic respiratory diseases are chronic diseases of the airways and other structures in the lung, some of the most common are asthma, COPD and pulmonary hypertension. COPD is an umbrella term for the disorders chronic bronchitis and emphysema and is thought to be the third leading cause of death by 2020.

A defining characteristic of all respiratory diseases is an increase in inflammatory leukocytes. These white blood cells are recruited to the site of inflammation and their presence results in the activation of multiple cell signalling pathways to prolong and increase the inflammatory response.

1.2 Innate and Adaptive immune system

In order for multicellular organisms to survive they must have a line of defence in place against pathogens and be able to efficiently repair and regenerate after damage caused by injury and infection. In humans our defence is known as the immune system, which can be separated into two branches, innate and adaptive immunity. Innate immunity is the first line of defence for the body, it involves a number of leukocytes including eosinophils, basophils, natural killer (NK) cells, mast cells along with the phagocytic cells macrophages, neutrophils and dentritic cells. Innate immune cells recognise the pathogen-associated molecular patterns which are broadly shared by pathogens with their own pattern recognition receptors. Innate immune cells either engulf pathogens (phagocytes) or

release inflammatory mediators such as histamine and leukotrienes (mast cells).

The adaptive immune response involves dentritic cells which are known as professional antigen presenting cells. Dentritic cells present selected peptides on MHC class II molecules to naive T-cells [2]. Naive T cells then differentiate into a range of cell types including T helper type 2 cells (T_H2) which produce many cytokines such as IL-13, IL-4, IL-5 and IL-9. These cytokines have been shown to be responsible for IgE production leading to mast cell activation and eosinophil recruitment both of which play an important role in sustaining inflammation [3].

1.3 Asthma

Asthma is a common respiratory disease with some 5.4 million people currently receiving treatment for this condition in the UK alone and 3 asthma related deaths per day [4]. The number of patients suffering with asthma increased dramatically between 2001 and 2010 in the USA and it is now thought to affect between 7-10% of the world's population [5, 6]. Over half of asthma is allergic, also known as atopic, which is triggered by inhaled allergens such as house dust mite allergen, pet dander and pollen. Non-allergic asthma was originally thought not to involve the immune system, a claim which has been widely challenged of late [7], nonetheless the symptoms are the same. Asthma is characterised by chronic inflammation of the airways, smooth muscle hypersensitivity and mucus overproduction causing narrowing of the airways resulting in the common symptoms of coughing and shortness of breath. In chronic cases of asthma these features cause increased smooth muscle mass and subepithelial fibrosis through a process known as airway remodelling. Unlike features apparent in mild asthma, airway remodelling is an irreversible process. Mild asthma can be adequately treated in most patients by existing medication which consists of beta-adrenergic agonists and glucocorticoid steroids. β_2 agonists are fast acting and exert their effects by relaxing the underlying airway

smooth muscle which leads to airway widening, making breathing much easier. Inhaled glucocorticoids are given as an ongoing daily treatment to reduce overall inflammation but they need to be taken for prolonged periods of time to ensure efficacy. As the results are not immediate, patient compliance plays a role as sufferers are less likely to religiously administer this treatment when the effects are not obvious. GCs are considered the most effective treatment for asthma as they improve overall lung function and quality of life by reducing airway hyperresponsiveness, disease exacerbations and hospitalisations. Withdrawal from GCs however will result in airways reverting back to their 'natural' inflamed state [8]. Over recent years asthma has been shown to have a number of sub-phenotypes, which include displaying a high or low Th2 response [9, 10]. Results from the severe asthma research program in 2010 identified five separate sub-phenotypes of asthma using cluster analysis; asthma subjects were placed in groups according to parameters such as pulmonary lung function, age, sex and response to current treatment [11]. This heterogeneity can explain why a varied response to current treatments has been observed. The subset of patients who do not display any bronchodilator reversibility are somewhat ignored when it comes to research with many studies and clinical trials only using patients who respond to beta-agonists [12]. These patients often undergo an accelerated loss of pulmonary function, hence there is clearly an urgent need for greater understanding and new potential drug targets in this field.

1.4 Chronic Inflammation in the lung

Upon allergic activation T-lymphocytes and mast cells become activated and release cytokines which can signal to endothelial and epithelial cells to express cellular adhesion molecules (CAMs). Infiltrating cells such as lymphocytes, basophils and eosinophils adhere to these CAMs and can travel through the junctional complexes of both the endothelium and epithelium. This is an important feature of allergic inflammation as the

intrusion by leukocytes sustains inflammation and causes disruption to the epithelial layer. Asthmatic patients have been shown to have a disrupted epithelium [13] and in chronic asthma the main histological changes are infiltration of macrophages and lymphocytes along with an increase in fibroblast proliferation, angiogenesis, fibrosis and tissue damage [14, 15].

As well as producing cytokines and chemokines activated mast cells also release histamine and lipid compounds such as leukotrienes and prostaglandins, which cause smooth muscle contraction leading to bronchoconstriction. Airway hyperresponsiveness (AH) has been shown to be a result of airway remodelling rather than sustained inflammation [16]. AH is characterized by exaggerated narrowing of the airways in response to non-specific stimuli such as histamine, methacholine, cold and exercise.

As mentioned previously in cases of chronic asthma airway remodelling occurs, a process describing the irreversible changes that take place in the lung after a period of sustained inflammation. It is characterised by an increase in fibrotic cells, smooth muscle hypertrophy and basement membrane thickening [17]. Two key features that contribute to airway remodelling in asthma are epithelial to mesenchymal transitions and goblet cell metaplasia [18].

1.4.1 Epithelial to mesenchymal transitions

An epithelial-mesenchymal-transition (EMT) is one where an adherent epithelial cell is converted to an individual migratory cell which then travels into the extracellular matrix to promote the activation of the process again (Figure 1.1). The term ‘transition’ is now widely used for this event as it is known to be a reversible process [19]. Cells can also undergo mesenchymal-epithelial transitions (MET) and this transition is seen in embryonic development as the mesoderm and ectoderm are generated and begin to contribute to many adult tissues by undergoing EMT and MET transitions [20]. In a healthy adult the EMT-MET transition is seen in wound repair and tissue regeneration, but it is also observed in cancer progression and metastasis [21, 22].

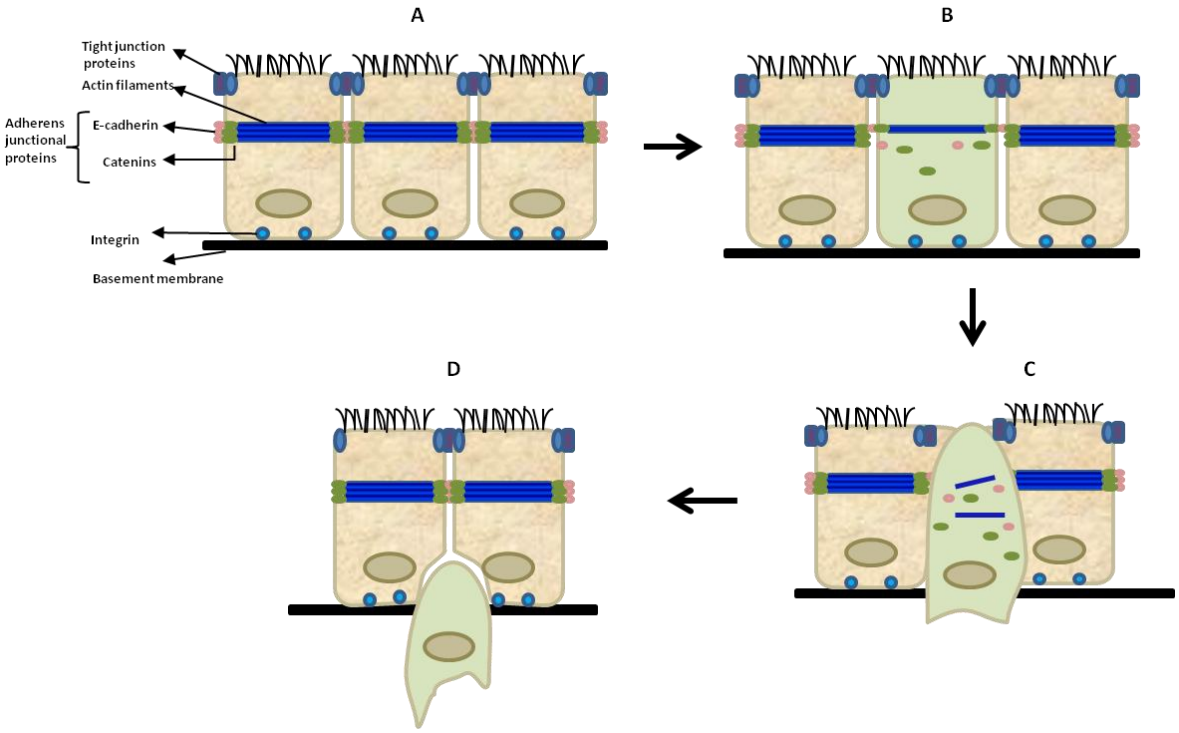

Figure 1.1 An epithelial-to-mesenchymal (EMT) transition.

The epithelial-to-mesenchymal transition consists of a normal intact epithelial cell (A) that begins to lose its connection to adjacent cells through adherens junctional proteins and actin filament breakdown, followed by internalisation (B+C). The cell then loses its tight junctions and its structure begins to change to that of a mobile myofibroblast which then passes through the basement membrane and into the submucosal epithelium (D).

1.4.2 Goblet cell metaplasia

Goblet cell metaplasia is a process where epithelial cells differentiate into goblet cells. Goblet cells have the primary role of producing mucus and can act as a protective cell or a pathogenic cell depending on the amount present. In a normal intact epithelium there are few goblet cells and little mucus produced which has the protective role of moving debris from the surface of the cell by movement of the cilia. However in patients with severe asthma the number of goblet cells is greatly increased, which leads to mucus hypersecretion, a feature which plays a significant role in airway obstruction and contributes greatly to morbidity and mortality [18, 23].

A mucin is a very large glycosylated protein which is usually >1000 kDa. There are around 20 different mucins present in the human body but the main mucin genes present in the lung are MUC5AC and MUC5B [24]. The term 'mucus' is often used and it refers to a mixture of mucins along with cell debris, ions, water, antimicrobial proteins and proteoglycans. In a healthy airway, the mucus layer is usually between 5-50μm thick [25, 26] which increases substantially in thickness in severe asthmatics during inflammation and it is reported that this obstruction by mucus plugs is the cause of 98% of all deaths in severe asthma [27-30].

The regulation of goblet cell metaplasia (GCM), mucus production and secretion in respiratory and inflammatory bowel diseases have been popular research areas over the last 15 years where findings have shown that the cytokine IL-13 plays a crucial role in its pathogenesis [31, 32]. Other known mediators are ligands that activate the epidermal growth factor receptor (EGFR) and upregulate the calcium activated chloride channel CLCA-1 [33, 34].

1.5 IL-13 structure and its role in asthma

Interleukin-13 (IL-13) was discovered in 1989 in mice when it was named P600, it was later cloned and discovered that the human cDNA

sequence was 66% homologous to that of the murine sequence [35-37]. IL-13 is part of a group of messenger proteins called cytokines and is produced principally by T-helper type 2 cells but also by mast cells, natural killer (NK) cells, eosinophils and basophils. It has similar roles to IL-4 which is understandable given their binding regions have high sequence homology and that both are found on the cytokine gene cluster on chromosome 5q31 along with GMSF, IL-3, IL-5 and IL-9 [38].

IL-13 is a key cytokine released during allergic inflammation and has been linked to asthma in many murine models; recently the link between IL-13 and asthma has been proven in human asthma [39]. Treatment with the monoclonal IL-13-antibody, lebrikizumab was shown to reduce the late asthmatic response to an inhaled allergen by 50% along with improving the prebronchodilator forced expiratory volume (FEV_1) by 5.5%. This improvement in lung function was seen in patients with high pretreatment levels of the matricellular protein periostin. Recent studies have linked periostin to the induction of chemokines in pulmonary fibrosis and it has been shown to be a biomarker of airway eosinophilia in asthma [40, 41].

IL-13 has been shown to have many roles in asthma (Figure 1.2), it is involved in B cell maturation and differentiation as well as inducing B-cell IgE switching [42]. IL-13 activates epithelial cells to produce the chemokine eotaxin which attracts eosinophils to the lung [43], it has recently been shown that eotaxin 2 and 3 (but not 1) is produced as a result of cooperation of IL-13 with leukotriene D_4 [44]. IL-13 is also known to play an important role in the pathogenesis of severe asthma features, such as fibrosis and mucus hypersecretion [45].

IL-13 has been shown to both upregulate and downregulate nitric oxide (NO) production, where upregulation of NO can have a protective role on the epithelium as it acts as a bronchodilator [46]. This increase of NO is shown to be a result of upregulation of the enzyme nitric oxide synthase (NOS) which catalyses the oxidation of L-arginine to L-citrulline where NO is produced as a by-product [47]. IL-13 however has also been demonstrated to increase the expression of the enzyme arginase, which converts the L-

arginine to L-ornithine. Upregulation of arginase has been shown to undergo competition with NOS for the substrate L-arginine and increased levels of arginase have been reported to diminish the L-arginine pool resulting in a decrease in the production of NO. Upregulated arginase has also been shown to increase the downstream products of polyamines and L-proline which are known to produce extra-cellular matrix components and lead to increased collagen deposition and eventually fibrosis. Upregulation of arginase has also been shown to increase the formation of the procontractile peroxynitrite species which has been linked to airway hyperresponsiveness [48]. This signalling loop has therefore been labelled as a key mechanism behind the increased bronchoconstriction in asthma caused by upregulation of IL-13 and arginase inhibition has been extensively researched in the treatment of asthma [49-53].

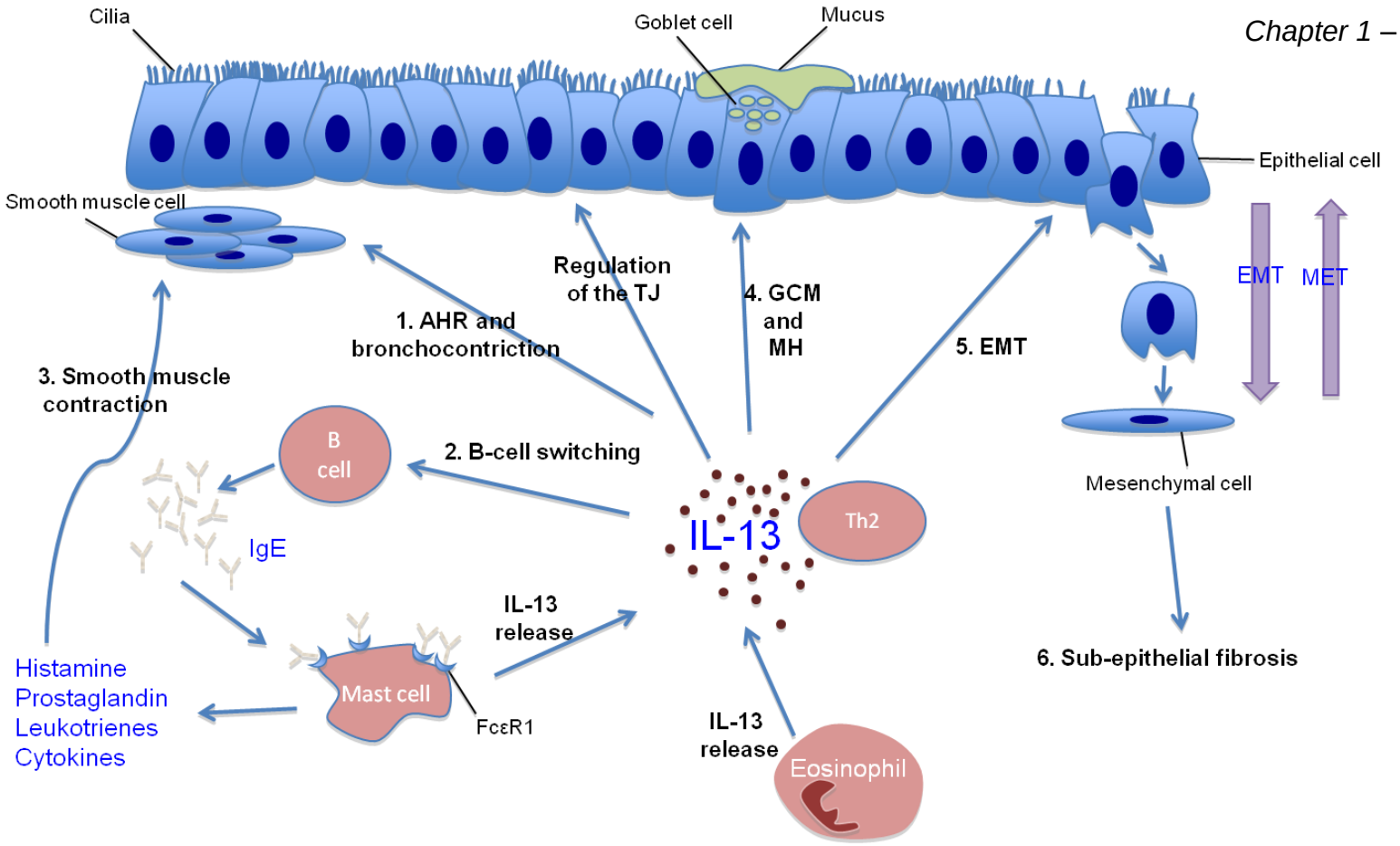

Figure 1.2 The role of IL-13 in asthma.

Upon allergic stimulation Th2 cells produce the cytokine IL-13 which has been shown to play a role in many pathological features of asthma. IL-13 stimulates B cells to produce IgE which binds to FcεRI receptors of mast cells leading to degranulation and the release of the pro-contractile compounds histamine, prostaglandins and leukotrienes which initiate smooth muscle contraction. Mast cells along with eosinophils also produce IL-13 during inflammation and upregulation of IL-13 in the airway submucosa has been shown to play a role in driving epithelial differentiation into mesenchymal cells (EMT). EMT leads to an increase of pro-fibrotic components such as collagen and fibronectin being irreversibly deposited in the sub-epithelium, if not adequately treated. Long term IL-13 stimulation causes epithelial cells to differentiate into goblet cells leading to an increase in mucus secretion and airway obstruction in severe asthma. More recently IL-13 upregulation has been linked with the regulation of the apical junction complex consisting of tight junction and adherens junction proteins; which are responsible for maintaining a strong paracellular seal between epithelial cells.

1.6.1 IL-13 receptors and signalling

IL-13 has two known receptors, IL-13Rα1 and IL-13Rα2. Human IL-13Rα1 was first cloned in 1996 shortly after the murine analogue and the cloned cDNA encodes a 270 amino acid protein. It has 76% homology to the murine IL-13Rα1 protein and has typical haematopoietic receptor patterns including a short cytoplasmic tail which contains a proline rich motif (PXXPXP) close to the transmembrane region [54, 55]. IL-13 has very little affinity for the IL-13Rα1 alone (K_d = 4.5 ± 0.5nM), however when it forms a heterodimer with the IL-4Rα receptor its affinity dramatically increases (K_d = 32 ± 8pM). The order in which the association occurs is IL-13 binds to IL-13Rα1 then it recruits the IL-4Rα complex to form the high binding affinity receptor [56].

The second IL-13 receptor IL-13Rα2 was initially thought of as a decoy receptor, however in recent years it has been found to have signalling properties [57]. IL-13Rα1 is 27% identical to the IL-13Rα2 protein which comprises of 380 amino acids and binds IL-13 but not IL-4 [54, 58]. Studies have been carried out to assess the binding properties of IL-13 with IL-13Rα2 however, the values reported in the literature are inconsistent varying from 20pM to 2.5nM [59]. IL-13Rα2 has been shown to bind with a higher affinity than IL-13 with the IL-13Rα1 complex and does not need a second receptor chain to do so [58]. However binding to IL-13Rα2 has been reported to dampen the IL-13 response as overexpression of the IL-13Rα2 complex in histiocytic lymphoma cells resulted in inhibition of IL-13 signalling [60].

IL-13 carries out its signalling principally via phosphoinositide 3-kinase (PI3K) and the signal transducer and activator of transcription 6 (STAT6) activation. IL-13 binds to the receptor IL-13Rα1 which then causes the IL-4Rα to bind to form a high affinity binding complex for IL-13. This recruitment of the receptors along with the binding of IL-13 causes activation of PI3K along with Janus kinases (JAK) and tyrosine kinase 2 (Tyk2) recruitment to the cell membrane leading to STAT6 activation.

1.7 The PI3K pathway

Phosphatidylinositols are lipids that are present in mammalian cell membranes, where the hydroxyl groups present on the inositol ring can be phosphorylated by PI3K to give many products with different functions within the cell. PI3K is activated by the dimerisation of cell surface receptors such as receptor tyrosine kinases (RTKs) caused by ligand binding, e.g. IL-13 binding to the IL-13Rα1 receptor which initiates dimerisation with IL-4Rα. PI3K becomes activated and phosphorylates the hydroxyl group on the D-3 position on the inositol ring of phosphatidylinositol 4,5-bisphosphate [$PI(4,5)P_2$] which is present in the cell membrane to produce phosphatidylinositol (3,4,5)-trisphosphate [$PI(3,4,5)P_3$] [61]. [$PI(4,5)P_3$] acts as a docking domain to plekstrin homology (PH) domain proteins such as Akt (protein kinase B) and 3-phosphoinositide dependent protein kinase-1 (PDK1) [62]. Akt is phosphorylated by PDK1 on Threonine 308 and by mTORC2 on Serine 473 which leads to a number of downstream signalling effects such as inhibiting the pro-apoptotic protein BAD, leading to increased cell survival. Akt is an important target in many cancers as it promotes tumor growth and survival [63]. This cell survival pathway is negatively regulated by phosphatase and tensin homologue deleted on chromosome ten (PTEN) [64]. PTEN de-phosphorylates [$PI(3,4,5)P_3$] at the hydroxyl group on position 3 of the inositol ring which reforms the starter [$PI(4,5)P_2$] complex. Mutations in PTEN are commonly seen in human cancers [65].

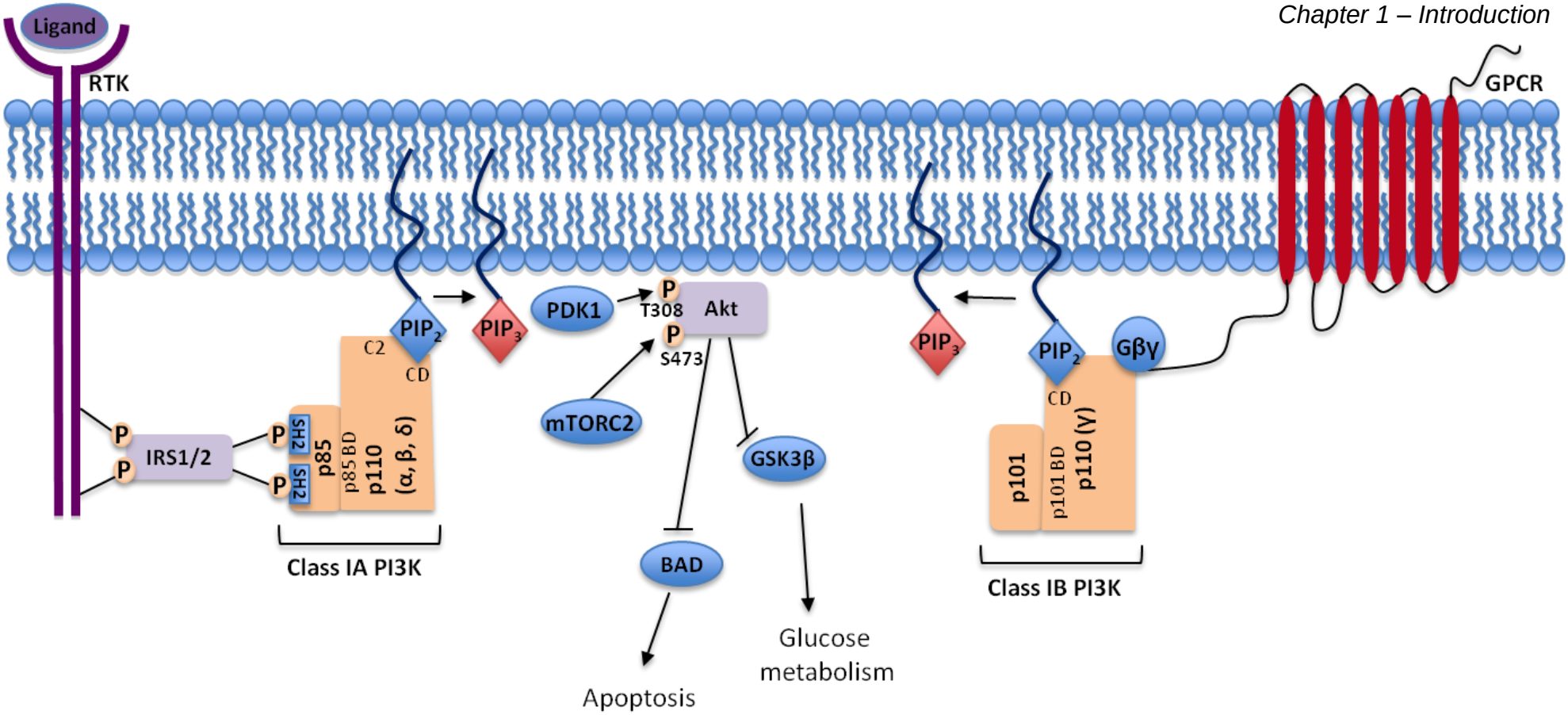

Figure 1.3 The Class I PI3K signalling pathway

The class IA PI3Ks consist of PI3Kα, β and δ; they all contain the p110 catalytic subunit and the p85 regulatory subunit. Upon ligand stimulation (IL-13 binding to IL-13Rα1) the receptor tyrosine kinase phosphorylates class IA PI3K indirectly through an interaction with the adaptor proteins insulin receptor substrate 1 or 2 (IRS1/2) via phosphorylation at the SRC-homology domains (SH2) in p85. This interaction between IRS1/2 and p85 positions PI3K at the plasma membrane in close proximity to its substrate PIP_2 and also stops p85 from having an inhibitory effect on p110, which allows PIP_2 to be converted to PIP_3. PIP_3 then recruits the serine/threonine kinases PDK1 and Akt to the cell membrane via their plekstrin homology domains (PH). PDK1 activates Akt at threonine 308 and the serine/threonine kinase mammalian target of rapamycin 2 (mTORC2) phosphorylates Akt at serine 473. Akt activation leads to a plethora of downstream events such as cell proliferation, differentiation and glucose metabolism. The class IB PI3K pathway can signal independently of Akt, p110γ consists of the p110 catalytic subunit and the p101 regulatory subunit and can be activated through the binding of chemokines to the G-protein coupled receptor (GPCR). Activation of the GPCR recruits the G-protein subunit Gβγ which directly activates p110γ resulting in PIP_2 conversion into PIP_3. BD; binding domain, C2; C2 domain, CD; catalytic domain.

1.7.1 The PI3K family

In the last decade research into the PI3K family has been very prominent and it is now widely known that four classes of PI3Ks exist. The standard 'PI3K core' consists of a catalytic subunit, a helical and a C2 binding domain [66]. Class I PI3Ks are between 110-130kDa and there are two subtypes, Class IA and Class IB, which along with the PI3K core contain a Ras binding site and a lipid binding domain. In Class IA PI3Ks there are three catalytic subunits p110α, p110β and p110δ which binds to one of five regulatory subunits: p85α, p85β, p55γ, p55α and p50α [64]. Class IB PI3Ks consist solely of the catalytic subunit p110γ which can bind to one of the three regulatory subunits p101, p87 or p84. In Class I PI3Ks the catalytic subunit binds directly to the GTPase –Ras which switches on PI3K activity via a conformation change from GTP bound-Ras converting to GDP resulting in Ras inactivation and PI3K activation. Class IA isoforms of PI3K are expressed ubiquitously whereas the Class IB isoform is mainly expressed in leukocytes.

Class II PI3Ks are larger proteins with a molecular weight of ~170kDa and lack the regulatory binding domain that Class I PI3Ks express. They have a C-terminus extension consisting of an extra C2 binding and a PX domain [67]. There are three class II PI3Ks, PI3K-C2α, PI3K-C2β and PI3K-C2γ and they phosphorylate phosphatidylinositol [PI] and phosphatidylinositol 4-phosphate [PI(4)P] to phosphatidylinositol 3-phosphate [PI(3)P] and phosphatidylinositol 3,4-bisphosphate [$PI(3,4)P_2$] respectively. PI3K-C2α and PI3K-C2β are widely expressed whereas PI3K-C2γ is more localised to liver, prostate, breast and salivary glands. PI3K-C2α is predominately localized in clathrin-coated vesicles and in the trans-Golgi network, it is suggested that PI3K-C2α binds to clathrin via its N-terminus for activation and is important in clathrin-mediated membrane trafficking.

The class III PI3K Vps34 was originally identified in yeast and phosphorylates phosphatidylinositol [PI] to phosphatidylinositol 3-phosphate [PI(3)P] [68]. Vps34 binds to the protein kinase Vps15 for activation and it is known to play an essential role in autophagy and is crucial in normal heart and liver function [69].

1.7.2 PI3K signalling and biological functions

Class I PI3Ks phosphorylate the hydroxyl group on the D-3 position on the inositol ring of phosphatidylinositol 4,5-bisphosphate [$PI(3,4)P_2$] to produce phosphatidylinositol (3,4,5)-trisphosphate [$PI(3,4,5)P_3$]. PI3K isoforms, p110α and p110β have been shown to be essential in cell survival and de-novo DNA synthesis [70, 71].

Class II PI3Ks phosphorylate PI and PI(4)P to form PIP and $PI(3,4)P_2$. The PI3K-C2α isoform has been researched more extensively than PI3K-C2β and PI3K-C2γ and clathrin is found to play a role in its signalling by binding to the N-terminal domain which alters the substrate preference resulting in an increase in its binding affinity for PI and PI(4)P [72]. Previous work in the group has showed that silencing PI3KC2β in A549 cells results in a decrease in the rate of wound healing [73]. The role of class II PI3K in biological functions is still largely unknown, which is also the case for the Class III PI3K Vps34. The involvement of Vps34 has been indicated in innate immune responses, superoxide formation and the gene PIK3C3 that encodes the protein has been associated with schizophrenia [74].

The PI3K pathway is negatively regulated by both the phosphoinositide 3-phosphate PTEN and also by the phosphoinositide 4-phosphate SHIP. PTEN de-phosphorylates the product of the class I PI3K $PI(3,4,5)P_3$ back to $PI(4,5)P_2$. It has been shown to have important roles in apoptosis, cell migration, adhesion and angiogenesis [64, 75, 76] and is frequently mutated, deleted or silenced in human cancers, especially in prostate and endometrial cancer. PTEN inactivation results in an increase in

Class	*Protein*	*Regulatory subunits*	*Activated by*	*Gene*	*Chromosome locus*	*Expression*
Class 1A PI3K	p110α	p85α, p85β, p55γ, p55α, p50α	RTKs	PIK3CA	3q26	ubiquitously
	p110β	p85α, p85β, p55γ, p55α, p50α	RTKs/GPCRs	PIK3CB	3q22	ubiquitously
	p110δ	p85α, p85β, p55γ, p55α, p50α	RTKs	PIK3CD	1q36	ubiquitously
Class 1B PI3K	p110γ	p101,p87,p84	GPCRs	PIK3CG	7q22	mainly leukocytes
Class II PI3K	PI3K-C2α	Clathrin	??	PIK3C2A	11p15	ubiquitously
	PI3K-C2β	Clathrin	??	PIK3C2B	1q32	ubiquitously
	PI3K-C2γ	Clathrin	??	PIK3C2G	12p12	liver, prostate, breast and salivary glands
Class III PI3K	Vps34	p150, VPS15	??	PIK3C3	18q12	ubiquitous but highest in heart and skeletal muscle

Table 1.1 Mammalian phosphatidylinositide kinases

Akt activity followed by uncontrolled cell proliferation [77]. SHIP de-phosphorylates the D-5 position of $PI(3,4,5)P_3$ to produce $PI(3,4)P_2$. SHIP mutations are often observed in cancers such as acute myeloid leukaemia (AML) where a dominant negative mutation of SHIP is reported to be involved [78].

1.6.3. Pharmacological inhibitors of PI3K

In 1988 the first PI3K inhibitor wortmanin was discovered which is a metabolite of the fungi Penicillium funiculosum and was found to inhibit PI3K potently with an IC_{50} of 5 nM [79]. The structure of wortmannin is shown in Figure 1.4. The primary amine on Lysine-833 in the catalytic site covalently bonds to wortmannin by its furan ring which results in irreversible inhibition of PI3K [80]. The discovery of wortmannin was shortly followed by the production of LY294002, a compound synthesised by Lilly research laboratories in 1994, which also acts as a PI3K inhibitor but, unlike wortmannin, binds reversibly to the ATP binding pocket [81]. LY294002 is a morpholine derivative from the flavanoid quertcetin and has a lower IC_{50} (1.4 μM) than wortmannin but researchers often use LY294002 due to greater stability in solution. It has been shown that both wortmanin and LY294002 inhibit mammalian target of rapamycin (mTOR), mitogen activated protein kinase (MAPK), myosin light chain kinase (MLCK) and phosphatidylinositol 4-kinases (PI4P) at high concentrations which is why these inhibitors are referred to as the ‘dirty’ inhibitors due to their numerous off target effects [82-86]. The ATP binding pocket of PI3Kγ and its interaction with wortmannin and LY294002 was obtained by X-ray crystallography in 2000 [87] and this provided a greater understanding of how inhibitors bind to PI3K and helped in the production of isoform specific inhibitors.

The first isoform selective inhibitor synthesised by the ICOS corporation (now Eli Lilly) was IC87114 which inhibits p110δ with an IC_{50} of 60 nM but does not target the other PI3K isoforms until >1000 nM (Table 1.2). p110δ has been shown to have a key role in the immune system and

IC87114 has been used in a vast array of in-vitro and in-vivo studies such as investigating airway inflammation in asthma, neutrophil accumulation in inflamed tissue and its role in chronic lymphocytic leukaemia [88-90]. The selective p110β inhibitor TGX-221 is also an ATP competitive inhibitor which is highly selective for p110β with an IC_{50} of 9 nM and does not target other isoforms until its concentration is raised to 211 nM at which point it begins to inhibit p110δ [91]. TGX-221 has been used to successfully inhibit p110β and has been shown to play a role in insulin signalling, thrombosis and cancer [92-95]. The p110β isoform was activated by the gut hormone gastric inhibitory peptide (GIP) which led to a potentiation in insulin sensitivity in adipocytes [95]. The alpha isoform of PI3K, p110α is important in many diseases, deletion of the binding domain present in p110α results in embryonic death between E9.5 and 10.5 [96]. The roles for p110α and p110β are quite similar since p110α has also been shown to play a key role in insulin activity and tumorgenesis [97]. Of the selective p110α inhibitors commercially available, PIK75 is the most selective with an IC_{50} of 8 nM (43x less than other isoforms) [98].

In recent years 'cleaner' pan-PI3K inhibitors have been generated to replace the first generation PI3K inhibitors such as wortmannin and LY294002. One such inhibitor, the triazine derivative known as ZSTK474, was produced by Zenyaku Kogyo Co (Tokyo, Japan) in 2000. Its structure differed from previous inhibitors and it proved not only to be more potent than LY294002 with an IC_{50} of 35 nM, but also more selective as it was shown not to target mTOR at low concentration [99]. ZSTK474 has been studied in human cancer xenographs and has shown strong antitumor activity without critical toxic effects [100]. The selection of highly selective PI3K isoform inhibitors available makes investigating possible roles for PI3K and its individual isoforms much easier. Other methods such as knockouts and siRNA interference can be used but as the essential roles of both p110α and p110β have been shown it is not surprising that many researchers favour the use of small molecule inhibitors through experimental ease and cost effectiveness.

Inhibitor	*p110α*	*p110β*	*p110δ*
PIK75	8	343	907
TGX-221	>1000	9	21
IC87114	>1000	>1000	60
Wortmannin	0.6	2.3	0.4
LY294002	500	970	570
ZSTK474	0.016	0.044	0.0046

Table 1.2 IC_{50} values for PI3K inhibitors (nM)

IC50 values were obtained from a cell-free lipid kinase assay, which involved recombinant expression and purification of p85α and either p110α, β or δ. Enzymatic analysis was performed with 100 μM ATP (with exception of ZSTK474 which used 10 μM ATP), the substrate PIP_2 and various concentrations of each PI3K inhibitor [91].

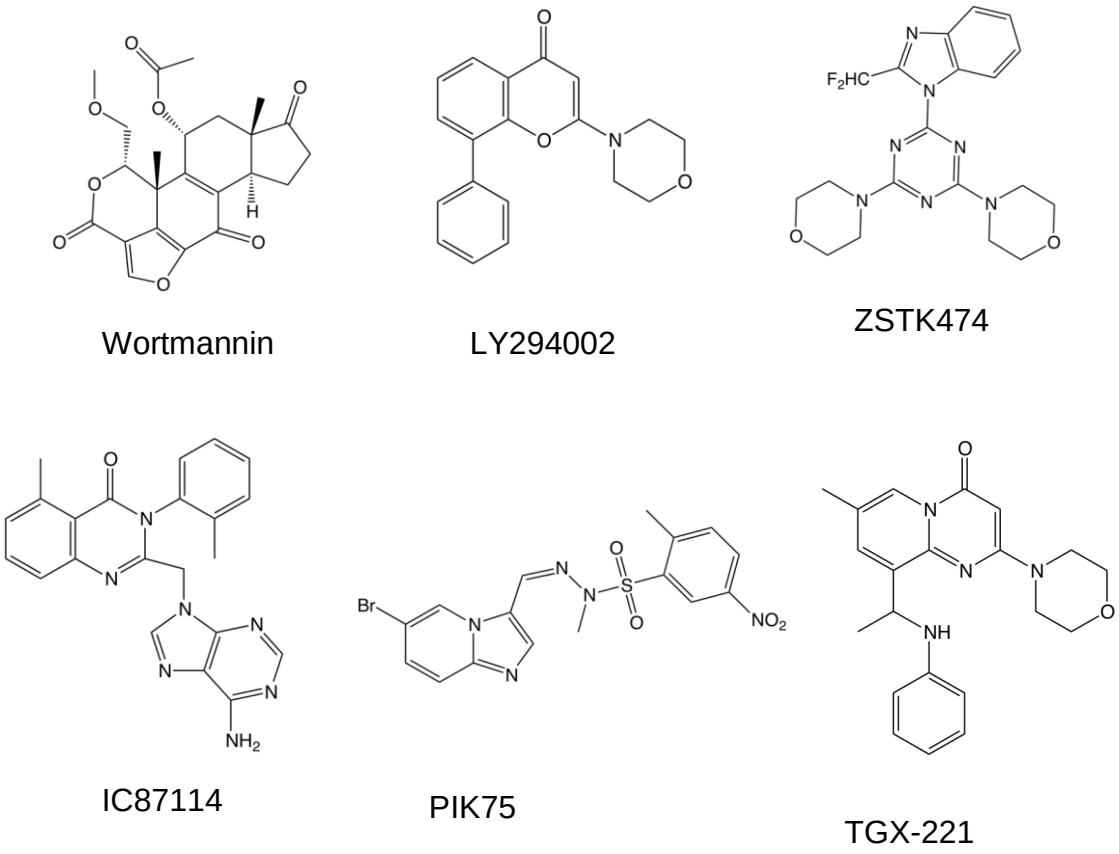

Figure 1.4 Chemical structures and IC50s of PI3K inhibitors.

The pan PI3K inhibitors consist of Wortmannin, LY294002 and ZSTK474. The isoform selective inhibitors are IC87114 (p110δ), TGX-221 (p110β) and PIK75 (p110α).

1.6.4 Role of PI3K in airway disease

The PI3K pathway has been reported to be involved in many respiratory diseases such as COPD, idiopathic pulmonary fibrosis (IPF) and chronic asthma. In one of the first PI3K related reports, in-vitro human eosinophils sensitised with ovalbumin resulted in an increase in superoxide (O_2^-) anion release and degranulation of eosinophils which was shown to be PI3K dependent as treatment with the PI3K inhibitor wortmannin reduced both superoxide formation and de-granulation [101]. The same group also investigated the role of PI3K in-vivo using a guinea pig model of asthma, in which wortmannin was administered intra-nasally in an attempt to localise the effect of the inhibitor to the lungs. It was shown that AH to histamine was prevented through treatment with wortmannin which was shown to be through the prevention of eosinophil degranulation rather than accumulation in the lung [101]. Similarly, pan class I inhibition using LY294002 attenuated the allergic response in mice by reducing cytokine production, eosinophil filtration and AH in an OVA sensitised model of asthma [102]. The isoforms responsible for causing this prevention of AH were studied by Lee et al who investigated the role of p110δ in the same murine OVA sensitization model which showed that the p110δ was responsible for the prevention in AH as inhibition with IC87114 reduced influx of neutrophils, eosinophils and leukocytes [103]. Class IA PI3K isoforms were also shown to be involved in the degranulation of mast cells in which p110β and p110δ inhibition was shown to block the upregulation of FcεR1 expression [104]. PI3K γ-deficient mice do not develop AH or bronchoconstriction in response to ovalbumin allergen challenges [105, 106] and PI3K δ-kinase dead mice resulted in impaired signalling in B-cells [107, 108] , which indicates the role of p110δ and p110γ in allergic inflammation.

1.7 STAT6 pathway

Aside from PI3K, IL-13 signalling has been linked to the signal transducer and activator of transcription 6 (STAT6). IL-13 binds to IL-13Rα1 which phosphorylates Janus kinase 2 (JAK2) which in turn activates STAT6 resulting in its dimerisation and translocation into the nucleus [109]. STAT6 plays a role in asthma and it has been shown to induce the expression of 15-lipoxgenase 1, RhoA, eotaxin, VCAM and MUC5AC, all of which are linked to airway dysregulation [109-113]. This makes it an interesting transcription factor to study, however no inhibitors exist that target STAT6 selectively.

A novel class of antineoplastic agents which mimick histone deacetylases (HDAC) have been shown to inhibit STAT proteins [114, 115]. In the nucleus of eukaryotic cells, DNA is packed into a tightly conserved structure called chromatin which consists of nucleosomes that at pH 7, carry a negative charge along with histones that carry a positive charge. Gene expression is controlled by the modification of chromatin, including histone acetylation which regulates the template accessibility to RNA polymerase II and DNA binding factors. Transcription can also be initiated through histone phosphorylation, methylation and in non-histone proteins through DNA acetylation itself [116]. This balance between acetylation and deacetylation states of histones are controlled by two groups of enzymes; histone deacetylases (HDAC) and histone acetyltransferases (HAT). HAT enzymes preferentially acetylate specific lysine residues whereas HDACs deacetylate these residues, restoring the positive charge of histones which enables them to strongly bind to the negatively charged phosphate backbone preventing transcription (Figure 1.5). Histone hyperacetylation results in an open chromatin structure which modifies gene expression and promotes a variety of features such as cell proliferation, survival, apoptosis and differentiation [117-120].

A hallmark feature of cancer is silencing of the cell cycle inhibitor p21 through hypoacetylation; gene expression can be restored through HDAC inhibition which enables acetylation. HDAC is therefore a popular drug target

tin cancer and other diseases in which there is an epigenetic imbalance [121]. The HDAC inhibitor trichostatin A (TSA) has been studied in human carcinomic cells where it was shown to be a potent inhibitor of tumour growth indicating its potential as a skin anti-cancer drug [122, 123]. In accordance with this, TSA has also been shown to possess antitumor activity against breast cancer in-vitro and in-vivo [123].

There are 11 known HDAC isoforms, which can be split into different classes through their sequence homology, location within the cell and enzymatic properties. Class I HDACs consist of 1, 2, 3 and 8, which are mostly expressed in the nuclei of all healthy cell types (excluding HDAC8), however overexpression has been reported in aggressive malignancies [124]. There are two subclasses of Class II HDACs, Class IIb (6, 10) are expressed primarily in the cytoplasm whereas class IIa (4, 5, 7 and 9) are found in both the nucleus and cytoplasm [121, 125]. Class III are the only class of HDACs that are NAD^+ dependent with other classes being zinc dependent. Suberoylanilide hydroxamic acid (SAHA) also known as Vorinostat [126], was produced by Richon *et al* in 1996 and was reported to inhibit HDAC1-3 by binding to the enzymes active site in the presence of zinc [115]. SAHA was later shown to inhibit all HDACs [127]. Similar to other HDAC inhibitors such as TSA, SAHA showed promising potential as an anticancer drug and was tested in clinical trials in 2004 [116, 128]. More recently SAHA has been shown to have anti-inflammatory effects, by reducing the expression of pro-inflammatory cytokines produced in murine macrophages after LPS stimulation [129]. SAHA was also found to have a dual effect in a model of Hodgkin Lymphoma (HL) where it had direct anti-proliferative effects and an indirect immunoregulatory effect by reducing the cytokine and chemokine release from T_H2 cells through inhibition of STAT6 [130]. This association between SAHA and STAT6 activity was first shown in 2003 by Rascle et al [84] and as knowledge of HDAC inhibitors increased it become evident that SAHA decreased the phosphorylation of STAT6 without inhibiting other STAT proteins [114].

HDAC inhibitors have also been shown to target non-histone proteins such as α-tubulin, one of the main proteins in microtubules. Microtubules

make up part of the cytoskeleton and are essential in aiding the migration of fibroblasts. Inhibition of HDAC6 deacetylation of α-tubulin resulted in inhibition of fibroblast invasive motility and decreased focal adhesion dynamics and turnover [131]. Recently, STAT5 transcription has been shown to be inhibited by the HDAC inhibitor trichostatin A (TSA) by blocking basal transcription machinery following STAT5 DNA binding [132]. Both STAT1 and STAT3 can be direct acetylated resulting in the recruitment of tyrosine phosphatases [133, 134], which render the protein resistant to further phosphorylation. It is yet to be shown if this is true for STAT6. In asthma an abnormal HDAC/HAT ratio is observed [135] along with prevalence for increased STAT6 expression; little is known about how STAT6 is regulated by HDAC.

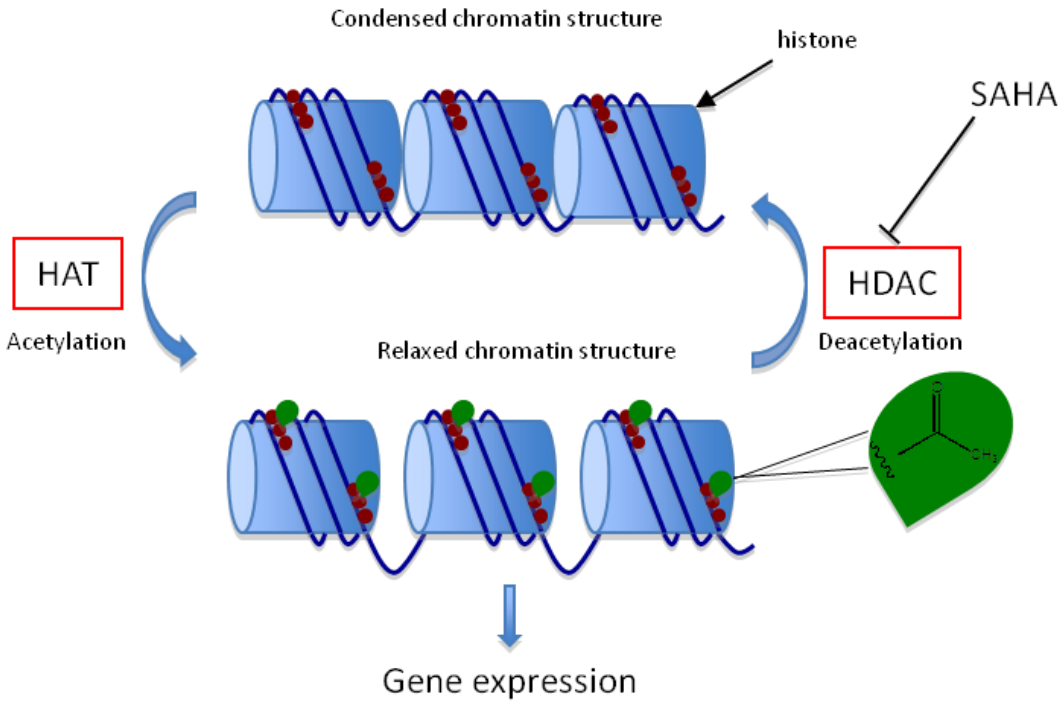

Figure 1.5 Regulation of gene expression via histone acetylation and deacetylation.

Histone actyltransferase (HAT) enzymes preferentially acetylate specific lysine residues whereas histone deacetylases (HDAC) restore the positive charge of histones through deacetylation. HDAC inhibitors such as Trichostatin A and SAHA result in hyperacetylation of histones, in which the chromatin structure is relaxed inducing gene expression. HDAC inhibitors increase the expression of 1-2% of genes such as the inhibitor of cell cycle kinase p21 resulting in cell growth arrest along with other tumour suppressing genes which account for the anti-tumour effects displayed. HDAC inhibitors also upregulate the expression of anti-inflammatory genes and can regulate the expression of transcription factors such as STATs through direct acetylation.

1.8 Glycogen synthase kinase-3- beta (GSK3β)

GSK3β is a multifunctional serine/threonine kinase that is present in all eukaryotes and plays a much more complicated role than merely catalysing the conversion of glucose to glycogen. It acts as a crucial downstream regulatory switch and responds to signals from Wnt, PI3K, RTKs as well as G-protein coupled receptors giving a variety of different signalling outcomes [136]. GSK3β has been linked to numerous diseases including Alzheimer's [137, 138], bipolar disease [139-141] and cancer [142]. It is an unusual kinase in the respect that phosphorylation renders it inactive therefore it is regulated through this inactivation.

Crystal structures of GSK3β were released in 2001 and they provided new insights into this peculiar signalling molecule [143, 144]. Phosphorylation of GSK3β at serine 9 by Akt results in formation of a pseudosubstrate which occupies the active site causing inactivation. This inhibition is described as competitive however at high concentrations of primed substrates can overcome this inhibition. Another strange feature of GSK3 is its affinity for pre-phosphorylated (primed) substrates, phosphorylation of the substrate beta-catenin reduced the K_m 30 fold resulting in a much higher affinity for the enzyme [145].

The role of GSK3 in insulin regulation has been extensively studied, insulin has been shown to inhibit GSK activity which leads to the activation of glycogen synthase and increased deposition of glycogen. GSKβ activity is upregulated in diabetes and inhibition of GSK has been shown to increase insulin sensitivity and improve glucose tolerance [146, 147]. Early studies which overexpressed GSK3 in human skeletal muscle cells showed a reduction of IRS1 phosphorylation and a decrease in the binding affinity of GS for glucose-6-phosphate, both of which impaired insulin signalling [148].

Many small molecule inhibitors have been synthesised to target GSK3, where the ATP competitive 6-bromoindirubin-3′-oxime (BIO) was the first GSK3α/β inhibitor to show the importance of GSK in self renewal of

human and mouse stem cells [149]. Since then more selective inhibitors have been synthesised, such as 1m, which was shown to be more potent than BIO and more selective for GSK3β alone [149].

1.9 MAPK signalling

The MAPK pathway is one of the most studied signalling pathways in the body. It is involved in a plethora of cellular processes such as proliferation, differentiation, apoptosis and cell cycle to name but a few and can be activated by a range of ligands such as cytokines, growth factors and viruses. MAPK signalling initiates through activation of RTKs, such as the epidermal growth factor receptor (EGFR), which are present at the cell surface. EGFR is activated by the ligand EGF and this 'switches' on the signalling cascade. The pathway begins with the activation of the small GTPase protein Ras; after GDP is removed Ras can bind to GTP and become active. Ras then proceeds to activate the protein kinase Raf which in turn phosphorylates and activates MEK. Once activated, MEK phosphorylates extracellular signal-related kinases 1/2 (ERK 1/2) (aka MAPK) at Thr 202 and Tyr 204 of Erk 1 and Thr 185 and Tyr 187 of Erk 2. The phosphorylated form of ERK activates many transcription factors such as E twenty-six (ETS)-like transcription factor 1 (ELK1) and early growth response protein 1 (EGR1) which regulate transcription, differentiation and mitogenesis.

ERK has been a popular drug target in cancer since its roles are mainly focused on cell survival and proliferation. Increased expression of ELK1 through ERK activation induces the expression of the anti-apoptotic protein myeloid cell leukaemia (Mcl-1) along with the plasminogen activator inhibitor-1 (PAI-1) whose levels are elevated in many tumours including breast cancer [150, 151].

In recent years, many compounds have been produced that inhibit the MAPK pathway. The most successful target to inhibit in the MAPK signalling

cascade was MEK 1/2. MEK is activated by Raf on residues Ser 218 and Ser 222 and requires both sites to be phosphorylated to become fully active [152]. The first inhibitor generated was PD98059 [153] shortly followed by U0126 [154], these first generation MEK inhibitors were unique as they were not competitive ATP binding inhibitors. Both were potent in preventing MEK phosphorylation and stopping ERK activation in vitro but both were unsuccessful at doing so in vivo. There was substantial controversy over the potency and mechanism of action of these inhibitors which led to a second generation of MEK inhibitors being produced. The first MEK inhibitor to reach clinical studies for treatment of cancer was CI-1040, phase I results proved promising with it being well tolerated and showing antitumor activity, however investigations were stopped at phase 2 due to insufficient antitumor activity in patients with solid tumours [155, 156]. The MEK 1/2 inhibitor PD0325901 produced by Pfizer was shown to inhibit MEK 1 and 2 more potently than CI-1040 with an IC50 of 0.33nM (compared to 17nM for CI-1040) [156-158].

TGFβ is a known ligand of EGFR and along with IL-13 has been shown to play roles in the epithelial-to-mesenchymal transition in many studies [159-161]. A synergistic role for IL-13 and TGF-β was hypothesised when IL-13+TGFβ but not IL-13 alone increased the production of the eosinophil chemokine eotaxin 1(CCL11) by airway fibroblasts [161]. It was later found that inhibition with the MEK/ERK inhibitor PD98059 after stimulation with IL-13+TGFβ resulted in an increase in IL-13Rα2 expression [162]. As eotaxin expression causes the accumulation of eosinophils in the lung, the finding linking these pathways was an interesting and a relevant one for asthma research. Zhou *et al* hypothesised that TGFβ increases eotaxin expression by dampening the IL-13 autoregulatory mechanism by reducing the amount of binding to IL-13Rα2.

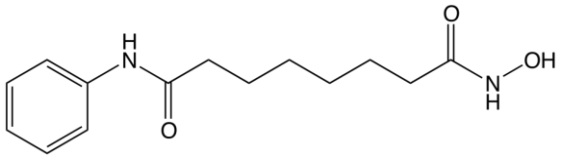

SAHA

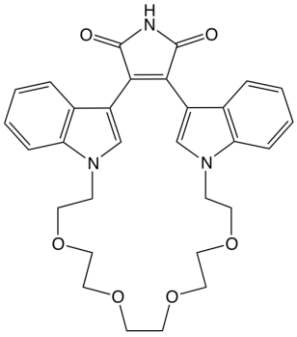

1m

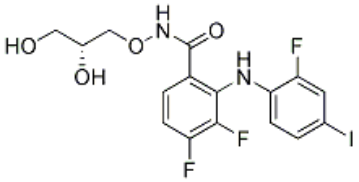

PD0325901

Figure 1.6 Chemical structures of the STAT6, GSK3β and MEK inhibitors SAHA, 1m and PD0325901

1.10 The lung epithelium

The lung epithelium has many roles, the most obvious being gas exchange in the alveoli, however another major role is in the protection of the underlying cells from inhaled pathogens from the external environment. It is made up of a heterogeneous layer of cells and is defined as a ciliated pseudostratified columnar epithelium. This description is due to the heterogeneous nature of the cells that line the trachea, bronchi and larger bronchioles (upper airways) which consist of ciliated stratified cells tightly packed together with goblet and basal cells attached to the basal lamina. The smaller bronchioles and the connecting alveoli are lined with simple squamous epithelial cells to enable quick exchange of oxygen and carbon dioxide across the membrane.

The epithelial cells in the upper airway have a much more complicated role than those at the gas exchange level, they are involved in the transport of a plethora of substances a such as cells, pathogens and tissue fluids across the membrane via paracellular permeability. Paracellular permeability is controlled by the proteins that hold adjacent epithelial cells together, which are collectively known as junctional proteins.

1.10.1 Junctional proteins

Junctional proteins that bind adjacent epithelial cells were discovered in the early 1960s but have been more extensively researched over the last 20 years [163-165]. There are 4 main groups of junctional proteins that can have roles in anchoring, communication and regulation, these groups are: adherens junctions, desmosomes, gap junctions and tight junctions. Adherens junctions and desmosomes have anchoring roles, whereas gap junctions are responsible for communication and tight junctions have roles in regulation. The tight junction complex is located at the most apical part of the adjoining membrane, it is made up of proteins such as occludin and the

complex family of claudins. These tight junction proteins are essential in regulating paracellular permeability and bind to important scaffold proteins known as zonula occludens. The adherens junction (AJ) is situated below the TJ complex and consists of catenins and cadherins proteins. The most studied adherens junction protein is E-cadherin which requires calcium ions for localisation at the junction [166]. Desmosomes and hemidesmosomes are intracellular adhesive junction proteins which anchor the intermediate filaments to the plasma membrane [167]. Desmosomes lie beneath cadherins, wheras hemidesmosomes link the epithelial cell to the basement membrane. Gap junctions are clusters of intracellular channels between adjacent epithelial cells; they link the cytoplasm of two cells and act as a form of communication [168, 169]. The main family of gap junction proteins are connexins, in which there are around 21 members.

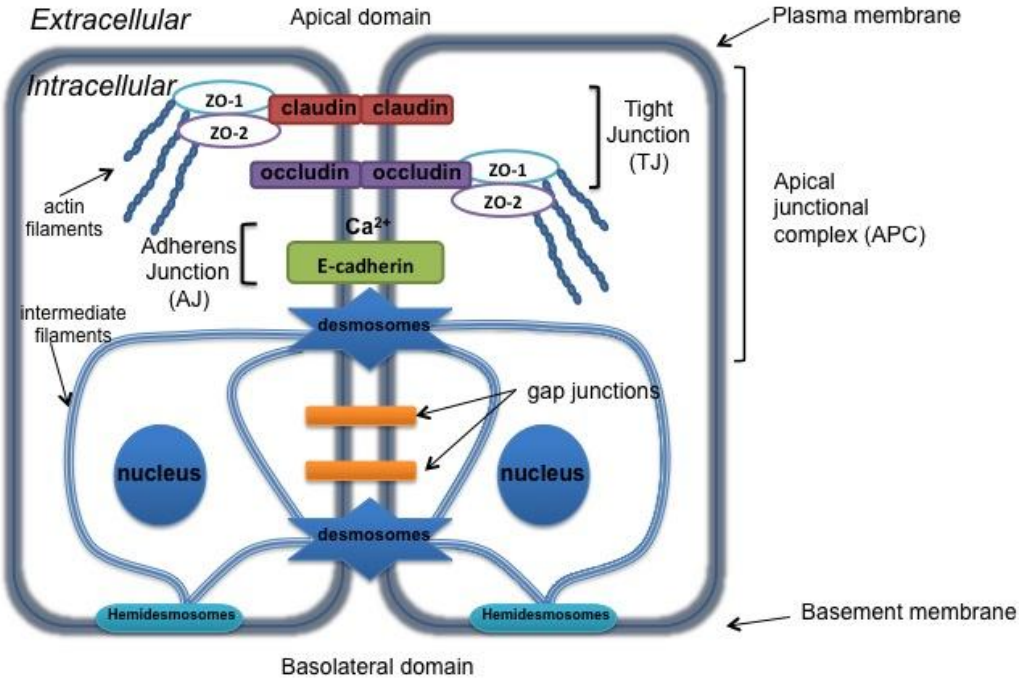

Figure 1.7 An overview of the junctional protein arrangement between adjacent epithelial cells.

Adjacent epithelial cells are connected via junctional proteins that are responsible for controlling paracellular permeability and maintaining cell polarity. The transmembrane tight junction proteins occludin and claudin bind to the scaffold proteins ZO-1 and ZO-2 anchoring them to the actin cytoskeleton. The adherens junction protein E-cadherin is positioned below the tight junction and requires Ca^{2+} ions for junctional assembly. Desmosomes and gap junctions associate below the apical junctional complex and hemidesmosomes link the epithelial cell to the basement membrane. Hemidesmosomes are connected to desmosomes via intermediate filaments; they associate with integrins and play a role in wound healing. (NB. Diagram not drawn to scale)

1.10.2 The discovery of tight junction proteins

The first transmembrane tight junction protein occludin was discovered in 1993 by Furuse *et al*, who examined chick liver and found a 65kDa protein which was observed directly over the points of contact between epithelial and endothelial cells (the tight junction) under both light and electron microscopy [170]. The structure of occludin is now well known, it is a transmembrane protein with four transmembrane domains, two extracellular loops, a short N-terminus and a long C-terminus. The importance of occludin was shown in many studies; overexpression in MDCK cells resulted in an 30-40% increase in the trans-epithelial resistance (TER) (i.e. a measure of TJ strength) as well as a 15% increase in tight junction strand density [171] and truncation of the C-terminus resulted in a decrease in TER [172]. The essential role of occludin at the TJ was questioned by two contrasting studies which altered the C-terminus of the protein and still observed an intact TJ, which posed a question as to the degree of involvement other integral transmembrane proteins have [172, 173]. During further investigation of chick liver an un-identified 22kDa protein was discovered and after sequencing was found to encode two proteins, 211 and 230 amino acids long. The structure of these proteins had four transmembrane domains similar to occludin but had no sequence homology. These proteins were named Claudin 1 and Claudin 2 and were the start of the 'claudin family'[174]. It soon became evident that Claudin 1 and 2 showed a stronger ability to form TJ strands than occludin [175] and over the years more members of the claudin family have been discovered with 24 individual claudin proteins presently known [176].

The first tight junction protein discovered was not occludin but the important tight junction associative protein zonula occluden which was discovered around 1966 [177] and was found to be present in three forms, zonula occluden 1, 2 and 3 (ZO-1, 2, 3) [178, 179]. These proteins were classed as belonging to the membrane associated guanylate kinase protein family termed MAGUK. ZO-1 was reported to associate with the transmembrane protein occludin [116] and later studies showed to also binds

members of the claudin family [180-182] this complex made up of occludin, claudin and ZO-1 and ZO-2 become known as the core tight junction complex. Today ZO-1, 2 and 3 are often referred to as scaffold proteins as their role is to anchor occludin and claudin in place by binding to the actin cytoskeleton [182].

1.10.3 Zonula occludens

Zonula occludens possess the common MAGUK modules PDZ, SH3 and GUK (the term PDZ is derived from the first letter of the proteins in which the binding domain were first witnessed, PSD-95, Drosophila lethal (1) discs large-1 and ZO-1). The PDZ domains are protein binding domains which are important in the anchoring of transmembrane proteins by recognition of certain sequences in other protein e.g. S /TXV [183]. SH3 domains contain the binding domain PXXP and are known to regulate enzymatic activity by coupling substrates. The guanylate kinase domain is thought to be enzymatically inactive as it doesn't catalyse the reaction of GMP to GDP [183].

ZO-1 is a 220-225kDa protein, which is mainly expressed in epithelial and endothelial cells although it has been reported in fibroblasts, astrocytes and Schwann cells [184]. The C-terminal domain in ZO-1 is 3 and 10 times longer than that of ZO-2 and ZO-3 respectively. The C-terminus is important in anchoring transmembrane proteins such as occludin to the actin cytoskeleton.

ZO-1 has many binding partners, the most well known being the TJ proteins occludin along with many members of the claudin family (Figure 1.7). ZO-1 has been shown to interact with the peripheral membrane protein, junction-enriched and –associated protein, JEAP [185], along with the second member of the connexin family, connexin 45 which also associates with ZO-3 via its PDZ domain but not with ZO-2 [186]. The junctional adhesion molecule (JAM) interacts with the PDZ domain in the N-

terminal region of ZO-1 along with cingulin, both interactions are thought to stabilise the association between ZO-1 and occludin [187]. Cingulin is a component of the multiprotein TJ complex and has been shown to interact with ZO-1 via activation of Rho A; unlike ZO-1 its expression is restricted to epithelial tissues [188]. ZO-2 is similar to ZO-1 with 51% amino acid identity, however its C-terminal tail is quite different only displaying 25% sequence homology which indicates that ZO-2 will function differently to ZO-1 as the C-terminus is responsible for the regulation of the protein [189].

ZO-3 was identified in 1998 by Haskins *et al* and was shown to be homologous to ZO-1 and ZO-2 with 3 PDZ domains, an SH3 domain and an acidic C-terminal tail. It differed from ZO-1 and ZO-2 by containing a proline rich region between the second and third PDZ domains [178]. The exact roles of these three MAGUK proteins are still not fully characterised. ZO-2 was shown to be essential for embryonic development as ZO-2 deficient embryos died shortly after implantation, whereas ZO-3 was shown to be dispensable and cells even remained polarized [190].

1.10.4 Occludin

Occludin is a four transmembrane protein, with 2 extracellular loops, a long C-terminus and a shorter N-terminus shown in Figure 1.8. The C-terminus has been shown to be vital in TJ assembly, it spans 254 amino acids and the COOH-terminal domain contains a 27-amino acid stretch which binds ZO-1, this region contains hydrophobic clusters and is termed the coiled-coil domain [191]. This coiled-coil region was found to be redox sensitive and occludin was shown to undergo dimerisation by forming a disulphide bridge at cysteine 408 [192, 193].

The N-terminus domain consists of 149 amino acids and has also shown to be essential in the function of occludin at the TJ, as an occludin construct which lacked the N-terminus was found to inhibit the production of a high TER and increased paracellular mannitol flux [194].

A crucial role for the second extracellular loop of occludin was reported by Medina *et al* who found that deletion of the second but not the first extracellular loop proved detrimental to its function and location at the TJ. These data were consistent with other studies which showed that the extracellular loops can impair adhesion, tight junction re-sealing and localization [173, 195-197].

Occludin has many binding partners, the first shown to interact with the TJ protein were ZO-1 and ZO-2 [198]. In recent years occludin has been shown to bind VAP33, caveolin and PKCη to name but a few [199-201]. Occludin phosphorylation at the coiled-coil domain of the C-terminus is reportedly involved in the regulation of the TJ protein. Highly phosphorylated occludin was found localised at the tight junction whereas non-phosphorylated occludin was distributed on the basement membrane [202]. The effect that phosphorylation has on occludin was shown when phosphorylation on serine and threonine residues led to the assembly of occludin at the tight junction [203], whereas tyrosine phosphorylation was shown to disrupt occludin function. Phosphorylation of tyrosine on residues 398 and 402 prevents it interaction with ZO-1 and prevents TJ assembly [204]. Protein kinase C η (PKCη), a novel isoform found only in epithelial cells, was shown to phosphorylate threonine 403 and 404 at the coiled-coiled domain which was shown to be essential for assembly and maintenance of occludin at the TJ [199]. Although tyrosine phosphorylation has been shown to be damaging to the integrity of the TJ, it plays a role in the re-formation of occludin, ZO-2 and ZO-3 and hence the recovery of the paracellular barrier after injury [205].

1.10.5 The Claudin family

Since the discovery of claudin 1 and 2 in 1998, a further 22 members of the claudin family have been discovered. Claudins are named after the latin word ‘claudere’ which means to close, as they were understood to have an important role in the tight junction. They are comprised of four

transmembrane domains, two extracellular loops, a longer cytosolic C-terminus and a shorter cytosolic N-terminus (Figure 1.8). Compared to other TJ proteins claudins are quite small ranging from 22-27kDa, the first extracellular loop (EL) is larger than the second at around 50 amino acids long and is thought to regulate paracellular tightness and control selective ion paracellular permeability [206]. It contains charged amino acids and reactive cysteine residues that are thought to form di-sulphide bridges to stabilize the protein as many claudins are insensitive to thio-reactive agents [207]. The second extracellular loop (EL2) comprises of around 16-33 residues and contains the receptor for Clostridium perfringens enterotoxin (CPE), an interesting finding from a drug delivery perspective [208]. The EL2 is also thought to contribute to various interactions between claudin members. Interactions between the same claudin members are termed homotypic or homomeric depending on whether the proteins interact head to head or side to side respectively. If these interactions occur with differing claudin members they are termed hetrotypic and heterometric [180]. Claudins are thought to restrict the paracellular space through these interactions and different claudins have varying selectivity to size and charge. Claudin 1 and 5 have been reported to be involved in homotypic and hetrotypic interactions and their dimerisation is thought to be aided by the aromatic amino acids present in the EL2 [209]. It is likely that this variety of possible claudin associations can shed some light on why paracellular permeability is such a dynamic process.

The C-terminal region of claudins ranges greatly between different isoforms suggesting that it is responsible for the differing roles observed. It contains a PDZ domain which binds the MAGUK proteins ZO-1, 2 and 3, [182] as in occludin. It has also been shown to bind junctional adhesion molecule (JAM-1) through binding of ZO-1 which triggers the binding of protease activated receptor 3 (PAR-3) to the tight junction [210]. ZO-1 and ZO-2 are responsible for the organization of the spatial arrangement of claudin strands in epithelial cells but are not required for claudin strand formation shown by claudin transfection into non-polar fibroblasts [175, 211].

The N-terminus of claudin is very short only spanning around 7 amino acids and has no known functionality. There are two classes of claudins, each of which have opposing functions, class I are made up of proteins that seal the tight junction and class II are made up of pore forming tight junctions. The pore forming tight junctions are claudin 2, 10, 15 and 20. Claudin 2 and 10 are expressed in the lung whereas 15 and 20 have not been shown to be present [212]. The most studied pore forming tight junction is claudin 2, which forms pores that have been shown to be oligomeric and dependent on cysteine 66, as manipulation of this residue lead to blockage of the pore [213]. Claudin 1 and 8 are known to interact with the multi PDZ-domain protein 1 (MUPP1) which is found localised in the tight junction [214].

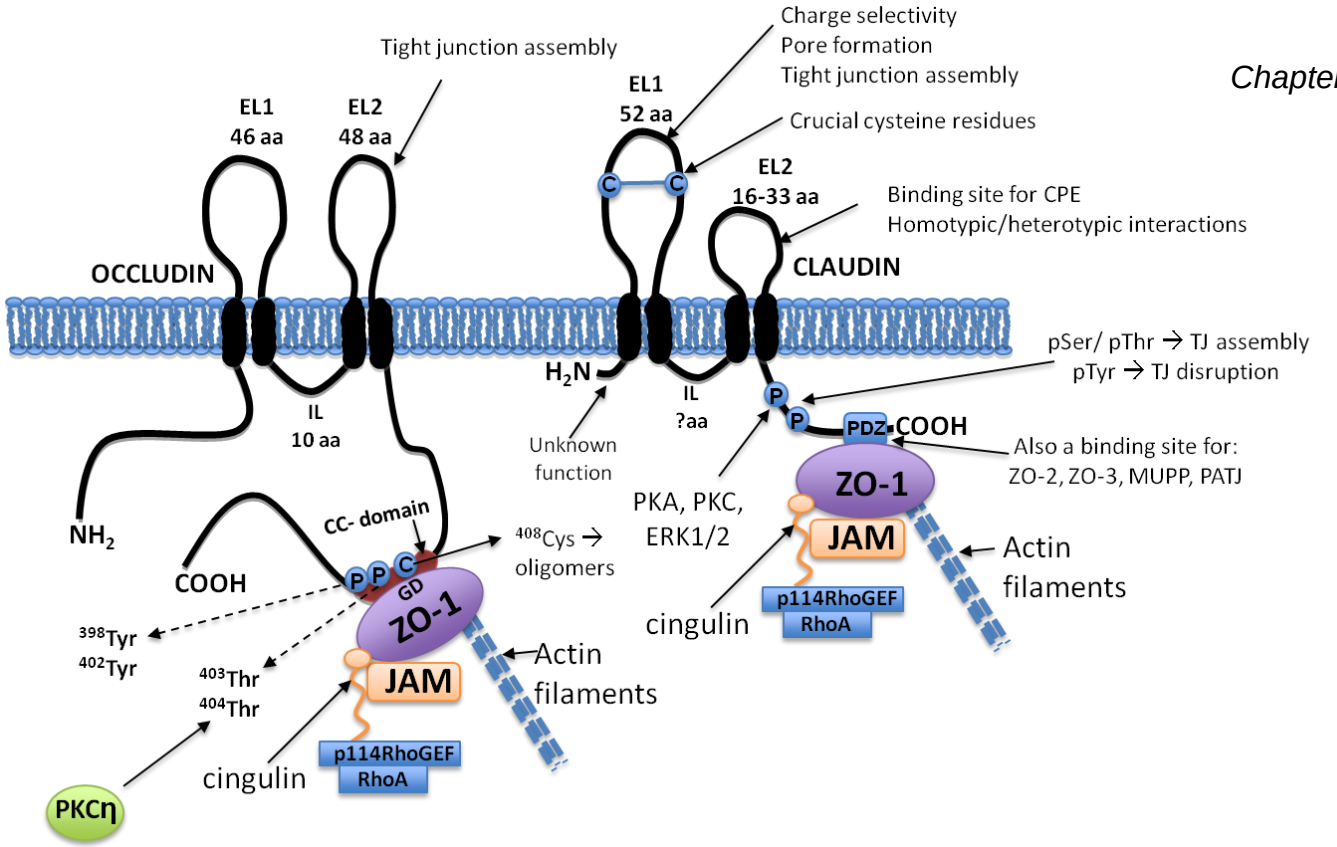

Figure 1.8 The structure of occludin and claudin at the apical junctional complex. The tight junction transmembrane proteins occludin and the family of claudins consist of 2 extracellular loops, 4 transmembrane domains, an N-terminal and a C-terminal intracellular domain. The first extracellular loop (EL1) of claudins is responsible for their assembly at the TJ and for charge selective pore formation. All claudins contain 2 reactive cysteine residues in their EL1, which form a disulphide bridge and are crucial to the structure and function of claudins. Site directed mutagenesis at either cysteine residue results in a decrease in TER and disruption of TJ assembly [207, 213, 215]. The second extracellular loop (EL2) has been linked with claudin oligomerisation across adjacent epithelial cells and is known to contain the binding domain for Clostridium perfringens enterotoxin (CPE) [208]. The C-terminal tail of occludin contains the redox sensitive coiled-coil (CC) domain. Phosphorylation at threonine 403 and 404 present in the CC domain is critical for assembly and maintenance at the TJ, whereas phosphorylation of tyrosine 398 and 402 prevents the interaction with ZO-1 and disrupts TJ formation [204]. In contrast to claudins, the EL2 of occludin is required for its localization at the TJ [216]. GD; guanylate kinase domain, CC; colied-coil domain, JAM; junctional adhesion molecule, PDZ; PSD95/dlg/ZO-1.

1.10.6 The cadherin family – E-cadherin

The 135 kDa intracellular adherens junctional protein E-cadherin was discovered in 1984 and is part of the cadherin family of junctional proteins [217]. Other original members of the cadherin family are N-cadherin and P-cadherin, where the letter denotes the location of protein expression in the body, E-cadherin is expressed in epithelial tissue. N-cadherin is mainly expressed in neural tissue and P-cadherin expression was first identified in the placenta [217-220]. This family of proteins got their name from their "calcium dependent adhesion" properties; hence they depend on calcium ions to function adequately.

E-cadherin has around 723-748 amino acids, its structure consists of a single transmembrane domain, an extracellular N-terminus and a cytoplasmic C-terminus domain [217]. The amino acid sequence is highly conserved (between 69-89%) in the cytoplasmic tail and this was the region found to regulate cell-cell binding [221].

1.10.7 Regulation of the TJ in the intestine and the kidney

The regulation of the epithelial barrier through modulation of tight junction proteins in the intestine and kidney has been researched in relation to Ulcerative colitis (UC) and Crohn's Disease (CD), which are both conditions involving the breakdown of the epithelial barrier of the intestine leading to uncontrolled flux of solutes resulting in a common symptom of severe diarrhoea. Epithelial breakdown is characterised in UC by a disruption of tight junction proteins and a decrease in the number of tight junction strands at the apical membrane [222]. Tight junction strand breaks can also be seen in CD [223, 224], along with cell apoptosis and epithelial cell lesions [225]. Although TJ strand numbers are reduced, an increase in the expression of the TJ protein claudin 2 has been reported in UC and decreases in claudin 5 and claudin 8 have also been observed [226, 227].

Extracellular calcium levels were one of the first known regulators of the apical junction complex (AJC). Depletion of calcium levels resulted in diffuse TJ staining in the cell and upon returning to normal calcium levels, TJ proteins becomes localised to the AJC (an experiment known as a 'calcium switch') [166, 228-231]. The tight junction protein ZO-1 was the first protein shown to be modulated by calcium in this way [228].

AMP-activated protein kinase (AMPK) has a prominent role in regulating cell metabolism and was also shown to be involved in the regulation of the TJ. AMPK was phosphorylated at threronine 172 and this phosphorylation decreased during calcium depletion leading to re-distribution of ZO-1 from the TJ to the cytoplasm [232, 233]. To ensure the TJ regulation was due to AMPK not just calcium changes, AMPK was activated through addition of the AMP precursor 5-aminoimidizole-4carboxamide riboside (AICAR) and the result remained the same, indicating an important role for AMPK in TJ regulation. AMPK is activated by the serine-threonine kinase LKB1 which has been shown to inhibit GSK3β, an association which lead Zhang et al to investigate the role of GSK3β in TJ modulation. Inhibition of GSK3β by LiCl or SB216763 resulted in the deposition of TJ components ZO-1 and occludin even before the restoration of normal calcium levels indiating that GSK3β modulation of the TJ is independent of calcium [234]. GSK3β inhibiton further increased the deopsition of TJ components even after maximum AMPK activation was reached. GSK3β inhibtion by SB415286 in intestine (SKCO-15) and kidney cells (MDCK) resulted in an increase in paracellular permeability coupled with a decrease in claudin 1, occludin and E-cadherin expression [235].

The MAPK pathway has been shown to be involved in the protection of epithelial integrity from hydrogen peroxide through EGF activation. EGF has been reported to achieve this through prevention of tyrosine phosphorylation on ZO-1 and occludin [236]. Protein kinase C (PKC) has been pinpointed as a player in the regulation of the TJ with a specific role in the assembly of the tight junction proteins ZO-1, claudin1, claudin 4 and occludin [199, 237-239]. Claudin 1 and claudin 4 are specifically regulated by phosphorylation through the novel isoform PKCθ, which doesn't require

calcium for activation. On the other hand occludin assembly has been reported to involve PKCη [238] and PKCβ has been shown in an opposite role in endothelial cells, by controlling the paracellular permeability of VEGF by phosphorylating occludin which leads to its ubiquitination [240-242]. There has also been a correlation to the amount of PKCα at the membrane and the level of paracellular permeability [199]. The spatial organization of the TJ was shown to be associated with the small GTPase proteins RhoA and Rac1, the epithelial barrier was disrupted resulting in a leaky system when RhoA and Rac1 were constitutively active or dominant negative, although ZO-1 and occludin expression remained constant [243]. This notion of controlling the spatial arrangement of the TJ was followed up by Terry et al who discovered that RhoA is driven by a junction-associated Rho signalling molecule called p114RhoGEF that spatially restricts the activation of Rho which results in TJ formation [244].

The pore forming tight junction protein claudin 2 was reported to be upregulated by IL-13 [245] a discovery which pin-pointed the Th2 cytokine as a key effector in UC. IL-13 was shown to induce apoptosis, increase claudin 2 expression and mucus secretion. The signalling mechanisms by which IL-13 elicits its responses has come under some scrutiny with Rosen et al proposing an involvement for STAT6 in epithelial barrier dysfunction in UC which is consistent with results from Maddon et al [246, 247]. However, these data have been opposed by Ceponis et al who believe IL-13 signals via PI3K and is independent of STAT6 activation [248]. Although the argument has not been settled there seems to be a role played by both PI3K and STAT6 which raises the question of whether a complementary effect or cross-over in their signalling pathways exists. Claudin 2 up-regulation has also been shown to be attributable to the pro-inflammatory cytokine tumour necrosis factor-α (TNFα). TNFα up-regulates claudin 2 in colonic HT29/B6 cells after 24 hours stimulation and is shown to be mediated by the PI3K pathway as the up-regulation was prevented by inhibition with the pan-PI3K inhibitor LY294002 [249].

Combination of the pro-inflammatory cytokines TNFα and IFN-γ altered expression of claudin 1, claudin 2, claudin 3 and occludin in MDCK

cells and inhibition of ERK 1/2 enhanced the expression of occludin and claudin 1 at the TJ interface [250]. This indicated a role for the MAPK pathway in TJ regulation which has been examined in a number of studies which found that activation of ERK1/2 has been shown to both up-regulate claudin 2 in intestine cells [249] and down-regulate claudin 2 in kidney cells, [250] this discrepancy may be a result of TJ proteins having different regulation patterns in respect to their location in the body.

1.10.8 Regulation of the TJ in the airway

There is significantly less research on the regulation of the AJC in the lung epithelial layer although it has been found that cytokines, bacteria and oxidative stress can play a significant role in both assembly and dysfunction of the highly dynamic TJ complex. Combined treatment with T_H1 cytokines TNFα and IFNγ in primary human airway epithelial cells has been reported to alter the localisation of ZO-1 and junctional adhesion molecule (JAM) and decrease their expression after 24 hours treatment [251]. IL-13 and IL-4 were shown to disrupt the epithelial TJ complex as is seen in the intestine, treatment with both cytokines for 72 hours increased mannitol permeability 2.5 fold compared with controls [252]. In human epithelial Calu-3 cells IFNγ has been shown to reduce the levels of occludin and ZO-1 but it also plays an unusual role as it enhances the barrier by increasing the transepithelial resistance and prevents disruption of the TJ by IL-4 and IL-13. This observation is interesting as it is not observed in the intestine, T84 cells show a decrease in TER and paracellular permeability after IFNγ stimulation [253].

The role of inhaled allergens in the regulation of the TJ has been researched. The alkaline serine protease from P.*chrysogenum* (Pen ch 13) was reported to upregulate the expression of prostaglandin 2 (PGE_2), IL-8 and TGFβ in A549, and 16-HBE lung epithelial cell lines. PGE_2 has been shown to dampen the T_H1 response and enhance the T_H2 inflammation leading to TJ disruption [254, 255]. The non-proteolytic group 2 allergen Der p 2 is derived from house dust mite and has been linked to triggering asthma

attacks, the mechanism by which Der p 2 exerts its effects was recently researched where it was shown that Der p 2 increases the cell surface expression of claudin 2 in A549 cells via ERK 1/2 and GSK3β phosphorylation [256]. A Der p2 DNA mutant vaccine was shown to prevent AH and allergenic airway inflammation in mice by upregulating Toll-like receptor 9 (TLR9) and inhibiting STAT6 [257, 258]. Der p 2 and Der p 1 have also been shown to disrupt the TJ by cleavage of occludin [256, 259].

Oxidative stress has been linked to epithelial barrier disruption with an inflamed epithelium producing increased amounts of nitric oxide via upregulation of the enzyme nitric oxide synthase NOS in the airways [260]. Nitric oxide synthase has many isoforms, inducible nitric oxide synthase (iNOS) has been shown to promote epithelial wound healing in the lung epithelial cell line 16-HBE [46]. Research carried out on NO in the lung has mainly focused on Cystic Fibrosis (CF) as a key characteristic in patients is their deficiency of nitric oxide production due to an alteration in the signalling pathways that produce NO and the expression of NOS [261, 262]. CF has a mutated cystic fibrosis transmembrane conductance regulator gene (CFTR) which affects the chloride ion transport. Cells with a CFTR mutation (CFBE41o and AF508) were reported not to increase their expression of iNOS after IFNγ, IL-1β and TNFα stimulation whereas normal HBE cells showed a dramatic increase [263]. This finding may explain why patients with CF are much more susceptible to infection. In 16-HBE airway epithelial cells nitric oxide was shown not to impair the TJ integrity but has a role in the assembly of the TJ [46].

Rho A and Rac are involved in TJ maintenance through regulation of the actin cytoskeleton (see review [264]). Rho and Rac mutants cause a decrease in TER but do not alter the TJ protein expression, however cause apical clumping and actin strand loss at the basolateral side [243]. Cytoskeletal modulation via activation of Rho kinase (ROCK) and myosin light chain kinase (MLCK) has been linked to cigarette smoke. Treatment with cigarette smoke resulted in a decreased association between ZO-1 and occludin via destabilisation of occludin through tyrosine phosphorylation [265]. ROCK has been shown to increase F-actin expression at the

periphery of the cell [266] through phosphorylation of the myosin binding subunit (MBS) [267], which results in increased permeability [268] and TJ redistribution resulting in disruption of the epithelial barrier. TGFβ is also shown to play a role in upregulating RhoA in the mobilization of the actin cytoskeleton at the TJ [269].

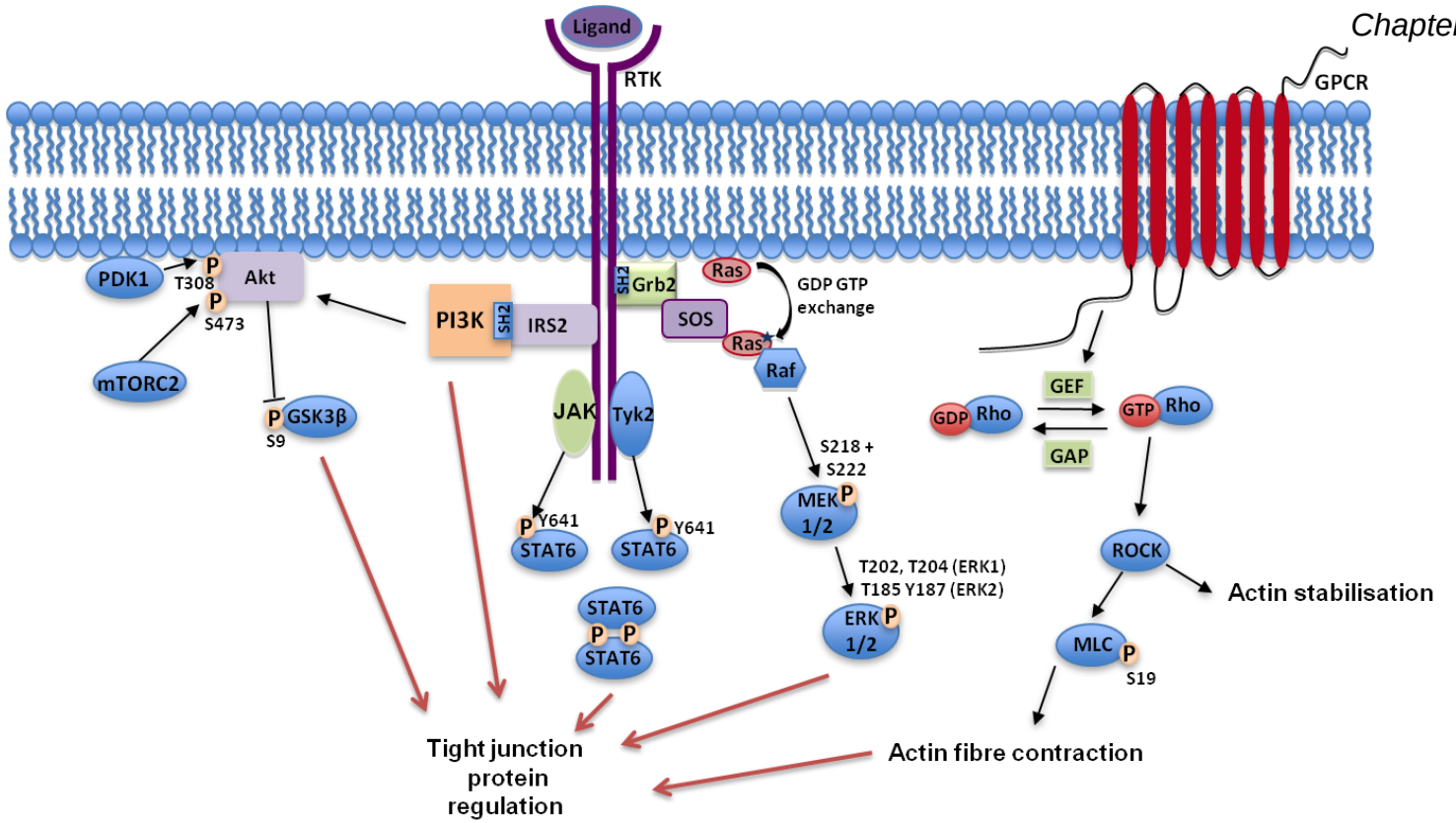

Figure 1.9 Overview of important signalling pathways in TJ regulation.

The complexity of the multiple interconnecting signalling pathways behind the highly dynamic regulation of the tight junction complex has given rise to many conflicting results. The MAPK pathway is activated through receptor tyrosine kinase (RTK) activation and has been shown to both disrupt the TJ complex in corneal epithelial cells [270] as well as stabilise it in intestinal cells [271]. RhoA kinase is activated through G-protein coupled receptors (GPCR) via the guanine nucleotide exchange factor (GEF) which activates GTPases leading to ROCK activation. ROCK phosphorylates myosin light chain (MLC) at serine 19 and also inhibits MLC phosphatase activity, which dephosphorylates MLC. The ROCK/Rho signalling pathway has been linked with regulation of the actin cytoskeleton [266]. PI3K is activated via RTKs such as the cytokine receptor IL-13Rα1 through IL-13 binding and can inhibit GSK3β through phosphorylation at Serine 9. GSK3β inhibition has been shown to be beneficial to barrier integrity by increasing occludin and ZO-1 expression and deposition at the TJ [234]. STAT6 is activated by RTK activation leading to the recruitment of janus kinases (JAK) and tyrosine kinase 2 (Tyk2) which phosphorylate STAT6. There is limited research on the role of PI3K and STAT6 in TJ regulation in the lung, however both have been shown to play a role in altering the barrier integrity in IBD [247, 248].

1.11 Aims of the project

The junctional complex is responsible for the maintenance of epithelial polarity along with the control of paracellular permeability. As shown in this introductory chapter, asthmatic patients have a disrupted epithelial layer during allergic inflammation, resulting in loss of barrier integrity which becomes a vicious circle sustaining inflammation. The regulation of the tight junction is highly dynamic and not well established in lung epithelial cells. IL-13 has been shown to play a key role in the modulation of the TJ in IBD, however research into regulation of the TJ in the lung is lacking. The overall aim of this thesis was to characterise the role of IL-13 in the regulation of the TJ. This can be subdivided into the following aims:

1. To establish a physiologically relevant airway epithelial model which could be easily manipulated
2. To investigate the role of IL-13 in the regulation of the TJ, in particular the main objectives were:
    - To investigate the effect of IL-13 on the integrity of the epithelial barrier, by monitoring resistance and paracellular permeability
    - To assess the effects of IL-13 on junctional protein expression and distribution within Calu-3 cells
    - To interpret the signalling pathways that are involved in the effects of IL-13 in the modulation of the epithelial barrier.

Chapter 2 : Materials and methods

2.1 Cell culture

2.1.1 Calu-3 cells

Human sub-mucosal Calu-3 cells from a pleural effusion [272] (HTB-55) were obtained from the American Type Culture Collection (ATCC). Calu-3 cells were cultured in Minimal essential media (MEM) supplemented with 10% fetal bovine serum (FBS), 2 mM glutamine, 5% non essential amino acids (NEAA) 100 U/ml pencillin, 100 µg/ml streptomycin, 1% fungizone and 5 µg/ml plasmocin (referred to as complete MEM media) at 37°C in a 5% CO_2 humidified atmosphere. Calu-3 cells were cultured in flasks or multi-well plates which were pre-treated with a coating solution (1 mg/ml bovine serum albumin, 3 mg/ml collagen I and 1 mg/ml human fibronectin in LHC basal media) overnight to ensure cell adherence.

Calu-3 cells were grown using an air-liquid-interface (ALI) culture system with 12-well transwell plates which comprised of 12 mm polyester filters with a 0.4 µm pore size (Figure 2.1). 300 µl of cells were plated onto the apical side of the filter and 1 ml of complete media was placed in the basolateral chamber, cells were placed in incubation at 37°C for 48 hours. After this time the cells have attached to the filter, the media was removed from the apical chamber and the cell monolayer was exposed to air at the apical side and media at the basolateral side so ALI was established. In either ALI or normal immersion culture, media was changed every other day until confluency. Calu-3 cells were used between passages 20-40 which is similar to other research groups who study them between passages 24-40 [273].

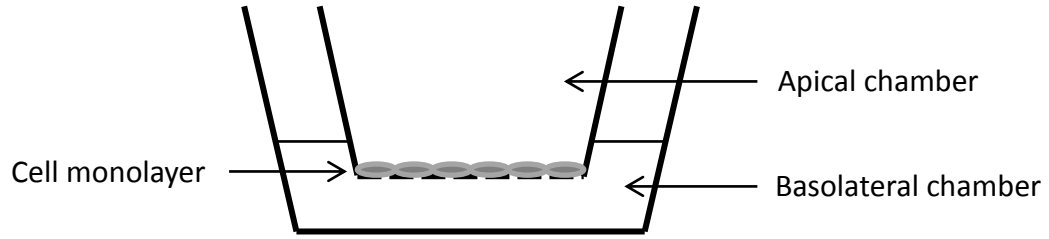

Figure 2.1 Schematic diagram of an air-liquid interface culture system. Cells are seeded onto the apical chamber, a polycarbonate filter with 0.4 µm pores. Cells were left with complete media in the apical chamber (immersion culture) for 2 days after which time the media was removed to establish the air-liquid-interface. Basolateral media was changed every other day

.

2.1.2 A549 cells

Human alveolar epithelial cells A549s were obtained from the European Collection of Animal Cell Culture and cultured in a 1:1 mix of Dulbecco's Modified Eagle Media (DMEM) and Ham's F-12 nutrient mixture (DMEM/F-12) supplemented with 10% FBS, 2 mM glutamine, 100 U/ml pencillin, 100 µg/ml streptomycin and 1% fungizone at 37°C in a 5% CO_2 humidified atmosphere. Culture media was changed every other day until confluency.

2.1.3 Subculture

When cells reached 80-90% confluency, the medium in the 75 cm^2 flask was removed and cells were washed with pre-warmed PBS to wash away any traces of serum. They were then placed in 7ml of 0.25% Trypsin/EDTA for 15-20 minutes at 37°C. Once cells had detached from the flask, 15 ml of complete media was added to stop the reaction. Cells were centrifuged at 25000 g for 5 minutes at 25°C, the media was removed and the cell pellet was dissolved in 2ml of complete media for cell counting using a dye exclusion method with trypan blue. Cells were mixed with trypan blue

in a 1:1 ratio and 10 µl of the mixture was placed in a haemocytometer and a cell count was performed. Dye exclusion works as intact cells will not allow trypan blue in whereas cells which are dying will have a compromised cell membrane and will let the dye enter, therefore, all cells that are stained blue are excluded from the count. Cells were then plated either into flasks or into multiwall plates at a seeding density of $2x10^5$ cells/ml for subsequent experiments. A549 subculture is as detailed for Calu-3 cells except cells were placed in 3ml of 0.05% Tryspin/EDTA for 3 minutes and plated in larger 175 cm^2 flasks due to an increased rate of growth.

2.1.4. Thawing and freezing cell lines

Vials were removed from liquid nitrogen and quickly thawed in a 37°C water bath, cells were added to 9ml of complete media and centrifuged for 10mins at 250 g at 25°C. The media was aspirated off and the pellet was re-dissolved in 1 ml of complete media followed by the addition of another 9ml and centrifuged as before, cells were then placed into a small 25 cm^2 flask (coated for Calu-3 cells) and incubated for 24 hours. After 24 h the media was changed and then cells were cultured normally with a media change every 2 days.

Cells were frozen down at 60-80% confluency, they were detached using trypsin/EDTA, checked for viability and counted using trypan blue. Freezing media consisted of 50% FBS, 40% complete media and 10% DMSO. Cells were resuspended at $1x10^6$ cells/ml into cryotubes and placed at -80°C for 24 hours after which time they were transferred to liquid nitrogen.

2.1.5 Routine testing for mycoplasma

Every three months cell lines were screened for the presence of a mycoplasma infection. Mycoplasma are a group of bacteria which lack a cell wall, this feature makes them resistant to many antibiotics such as penicillin. Cells were cultured in 75 cm^2 flasks and when they reached 50% confluence, 2 ml of media was removed after it had been in contact with the cells for at least 24 hours. The sample was tested using a mycoplasma kit (Lonza), 600

µl of assay buffer was added to both substrate and reagent vials. The media was centrifuged at 11000 g for 5 minutes at room temperature and reading A was obtained by adding 100 µl of media to 100 µl of reagent in a 96 well white plate. The luminescence was read on a Fluostar optima plate reader, after which 100 µl of the substrate was added to the well and left for 5 minutes before reading B was taken. The result of the test was dependant on the ratio of reading B/reading A, if the answer was less than one then cells were mycoplasma free however if it was greater than one then cells were infected. If cells were infected they could be treated with Plasmocin to eliminate the infection in 2 weeks and to prevent further infection Plasmocin was routinely added to the media.

2.2 Transepithelial resistance

Calu-3 cells grown via ALI were monitored using transepithelial resistance measurements to check on their confluency this was necessary as the standard method using light microscopy proved inefficient due to poor lighting on the surface of the filter. Resistance was measured using STX-2 chopstick electrodes which have one long and one short arm, the short arm rests in the apical chamber media and the longer arm in the basolateral chamber media, the resistance between the electrodes is measured using an EVOM voltohmmeter to give the raw value in ohms. The higher the resistance between the electrodes the more confluent the cells are as less ions can flow between them. The TER was measured everyday once ALI culture had begun and the value obtained was converted into ohms.cm^2. Pre-warmed serum-free media (300 µl) was placed in the apical chamber and incubated at 37°C for 30 minutes to equilibrate. During this time, the STX-2 electrodes were sterilized using 100% ethanol for 30 minutes, they were then placed in serum free media to wash off all traces of ethanol. As a background reading a well without cells (just media) was used before every experimental plate. The chopsticks were placed in undiluted bleach for 3 minutes followed by rinsing with water for 20 minutes to ensure a deep clean, this was done every 3-4 months and their performance was also routinely

checked using a CALICELL12 (WPI instruments) to check for any variations in TER measurements. TER is a useful technique as it is seen as an indirect measure of epithelial integrity and presence of tight junction proteins [274].

2.2.1 Cytokine stimulation

Once the raw resistance value had reached over 400 Ωcm^2 the cells were considered confluent and if none of the basolateral media was seeping into the apical chamber i.e non 'leaky' then they were ready for cytokine stimulation. For long term experiments cytokines were added to the basolateral chamber in serum media and the TER was monitored every 24 hours, cytokines were refreshed every 72 hours. For shorter stimulations, cells were starved overnight prior to experimental use.

2.3. FITC Dextran permeability

To investigate the integrity of the epithelial barrier a FITC dextran permeability study was used. Dextran is a high molecular weight polymer of glucose and when tagged with fluorescein isothiocyanate (FITC) it can be used to look at paracellular barrier properties. FITC dextran (4 kDa) was dissolved in HBSS buffer to a concentration of 500 µg/ml.

Cells were grown via ALI culture and after 7 days confluent cells were stimulated with IL-13 or treated with various inhibitors. Cells were washed with pre-warmed HBSS to remove all the phenol red in the media and 600 µl of HBSS was added to the basolateral chamber. FITC-dextran (200 µl) at 500 µg/ml was added to the apical chamber and incubated for 30 minutes, triplicate samples (100µl each) were taken from the basolateral chamber of each well and placed into a black 96 well plate to measure fluorescence intensity on a Fluostar optima plate reader at excitation and emission wavelength of 485 nm and 530 nm respectively.

2.4 Immunocytochemistry

Immunocytochemistry is an extremely useful technique and in this thesis it is used to assess the distribution of junctional proteins within the cell after stimulation with cytokines or inhibitors.

2.4.1 Sample preparation and antibody staining

It was necessary to use two methods in order to achieve the optimal staining outcome, some antibodies can be very sensitive to the fixing method. Method 1 was used for all junctional antibodies except for E-cadherin which used method 2.

Fixing method one

Cells were grown via ALI (see section 2.1.1) and once confluent, various cytokines and/or inhibitors were administered to the basolateral chamber for 24-72 hours. Cells were washed twice with PBS and fixed in 4% paraformaldehyde for 20 minutes at room temperature. Cells were permeabilized using 0.1% Triton-X-100 in PBS for 30 minutes and blocked for 30 minutes in a 10% blocking buffer (Roche). Cells were covered with the primary antibody (1 in 100 dilution) in 2% blocking buffer in PBS and left on the rocker at 4°C overnight. After which they were washed three times with PBS for 15 minutes per wash and then covered with either an anti-mouse or anti-rabbit Alexa Fluor secondary antibody which was conjugated with a 488 (green) or 546 dye (red) in 2% blocking buffer in PBS for 1 hour in the dark. Cells were washed three times with PBS for 15 minutes and on the final wash the fluorescent stain 4',6-diamidino-2-phenylindole (DAPI) was added to the wash to stain the nuclei by strongly binding A-T rich regions in DNA. Cells were placed in water to rinse off any remaining PBS and the filters were cut out using a scalpel and fixed onto glass slides using a mounting media solution containing Mowiol 4-88, which has the same refractive index as immersion oil. The slides were kept in the dark at 4°C overnight and then viewed on a LSM510META confocal laser scanning microscope. Images were digitally recorded and manipulated using LSM image examiner software (Carl Zeiss Microscopy).

Fixing method two

Cells were grown via ALI and once confluent, various cytokines and/or inhibitors were administered to the basolateral chamber for 24-72 hours. Cells were quickly washed twice with PBS and fixed in ethanol at 4°C for 30 minutes. Cells were permeabilized using acetone cooled to -20°C for 3 minutes at room temperature and then washed twice with PBS and blocked in 10% FBS in PBS for 30 minutes (or overnight at 4°C is desired). Cells were washed twice with 2% FBS in PBS and once with PBS and then covered with the primary antibody (1 in 100 dilution) in 2% FBS in PBS and left on the rocker at 4°C overnight. The cells were washed three-to-five times with 2% FBS in PBS and three times with PBS for a mixture of very quick or 5 minute washes. Cells were then covered with either an anti-mouse or anti-rabbit Alexa Fluor secondary antibody which was conjugated with a 488 (green) or 546 dye (red) in 2% FBS in PBS for 1 hour in the dark. Cells were washed as before and then placed in DAPI in PBS (1 in 20,000 dilution) for 10 minutes. Cells were placed in water to rinse off any remaining PBS and the filters were cut out using a scalpel and mounted onto glass slides using Mowiol.

2.5 Flow cytometry

The surface expression of the IL-13 receptor IL-13Rα2 was analysed to determine its possible role in IL-13 treated cells with and without PI3K inhibition. Calu-3 cells were cultured by ALI and stimulated with a variety of PI3K inhibitors along with varying concentrations of IL-13. Cells were washed with pre-warmed PBS and placed in 300 µl of 0.25% trypsin/EDTA in the incubator for 15 minutes. Once cells had detached the reaction was stopped with the addition of 700 µl of complete media, and each well was pipetted several times and placed in a 1.5 ml plastic tubes (Eppendorf), which were incubated for 30 minutes to allow cells to recover. Cells were

washed once with ice-cold PBS and then re-suspended in the anti-IL-13Rα2 antibody and incubated at 4°C for 1 hour, cells were washed with ice-cold 2% FBS in PBS three times. Cells were placed in an anti-mouse secondary antibody labelled with Alexa Fluor 488 dye for 1 hour at 4°C in the dark. They were washed twice with ice-cold 1% FBS in PBS and re-suspended in 500 µl PBS and analysed on a FACSCanto flow cytometer (Becton Dickinson).

2.6 Quantitative real-time PCR

To evaluate the mRNA expression of the junctional proteins after IL-13 and PI3K inhibition quantitative PCR was carried out. In this process a single RNA strand is first reversed transcribed to its DNA complement, this double strand of DNA is then denatured which allows specifically made primers to anneal to the single stranded DNA template. This DNA strand is then elongated using polymerase enzymes and the whole process is repeated causing amplification of the DNA.

RNA was extracted from Calu-3 cells using an RNeasy mini kit (Qiagen) according to the manufacturer's instructions. Cells were washed twice with PBS then 250 µl of lysis buffer (with added 2-mercaptoethanol 10 µl/ml) was added to the well and the sample was pipetted up and down a few times to ensure homogeneity. The lysate was pipetted into QIAshredder spin column and centrifuged at 5000 g for 2 minutes, 70% ethanol was added to the lysate and mixed well. The sample was then transferred to an RNeasy spin column in a 2ml collection tube and centrifuged at 5000 g for 15 seconds. The sample was subjected to DNase digestion, was cleaned using RPE washes and then eluted using RNase free water.

The RNA was quantified using a Qubit 2.0 fluorimeter and was then reverse transcribed using a high capacity cDNA reverse transcription kit (see section 8.3 for more details). Reactions were performed on a StepOnePlus Real-time PCR system (Applied Biosystems) using a SYBR Green system,

for each well 10 µl of SYBR green was added to 0.4 µl of forward and 0.4 µl of reverse primers, 9.2 µl of cDNA was added to this mixture. The PCR reaction consisted of 2 steps, firstly heating to 95°C for 10 minutes for the initial hold, then 40 cycles of 95°C for 15 seconds followed by 1 minute at 60°C.

2.7 Immunoblotting

Immunoblotting (also known as western blotting) is a technique whereby visualisation of specific proteins in a cell is achieved using gel electrophoresis. Gel electrophoresis is a method by which proteins are separated by charge and size. Protein samples are run through a polyacrylamide gel and then transferred onto a nitrocellulose membrane by using an electric current. The membrane is then blocked and probed using primary antibodies that are specific to the protein of interest followed by further washing and secondary antibodies which recognise the primary antibodies that are used via the species in which they were raised in (e.g mouse or rabbit). The secondary antibodies are tagged with a horseradish peroxidise (HRP) enzyme and detection is achieved in the presence of chemiluminescence agents which catalyse the HRP which causes emission of light (luminescence) which is picked up on a photosensitive film.

2.7.1 Cell lysis

After incubation with cytokines and various inhibitors, cells were washed three times in ice cold PBS and were then placed in lysis buffer (see section 8.1) for 5 minutes on ice. Cells were detached from the plate/well using a cell scraper and the sample was pipetted multiple times before being place in a pre-cooled 1.5ml plastic tube (Eppendorf). The samples were then centrifuged at 4°C at 7000 g for 3 minutes to pellet the cell debris and the supernatant was carefully removed and placed in another pre-cooled 1.5ml plastic tube.

2.7.2 Quantification of protein

To ensure each sample contained the same amount of protein a Bradford assay was carried out. This assay works by colorimetric analysis, when the coomassie dye present binds to the hydrophobic amino acids residues found in protein it undergoes an absorbance shift. Samples were prepared with varying concentrations of bovine serum albumin (BSA) 0, 2, 4, 6, 8 and 10 µg/ml from which a standard curve was constructed. The Bradford dye reagent was diluted in water (1:5) and 198 µl was placed in each 1.5 ml plastic tube, 2 µl of sample was added to the dye and the tube was mixed well. 100 µl was pipetted out of each sample in triplicate into a clear 96 well plate and the concentration of protein was measured at 595nm using a VersaMax plate reader (Molecular Devices). The protein concentration in each sample was calculated using the standard curve.

2.7.3 Sample preparation

After the amount of protein was calculated, each sample was made up to 25 µg (or as close to it as possible) of protein in 20 µl with the addition of water to dilute if necessary. 5 µl of 5X sample buffer (see section 8.1) was added to each sample and the tubes were heated to 90°C for 7 minutes, after which they were quickly centrifuged at 200 g and placed back on ice.

2.7.4 Gel electrophoresis

One dimensional gel electrophoresis was used, in which proteins are separated by size using an electrical current by moving through pores in a gel matrix, the size of the pore depends on the percentage of acrylamide used, the higher the percentage the smaller the pores so the slower the proteins will migrate. As the size of the protein determines how quickly it migrates through the gel it is necessary to pick the correct acrylamide percentage gel to use, for larger proteins lower percentage gels are required and vice versa.

Different percentage gels 7.5, 10 or 12% were prepared to make up the resolving gel, this was pipetted between the assembled glass plates to around 75% total volume, the remaining 25% was filled with water to ensure the resolving gel set flat. After around 20-30 minutes the gel would polymerise and the water could be tipped out. A gel comb containing either 10 or 15 wells was placed on top of the resolving gel and a stacking gel consisting of 5% acrylamide was pipetted around the comb carefully ensuring no bubbles were present. After 15 minutes the stacking gel set and the comb was carefully removed leaving intact wells in its place. The wells were washed well with MQ water and the gel was placed in a Bio-Rad Mini Protean II system with running buffer (see section 8.1). The first well was reserved for a standard protein ladder (5-10 µl) which is a molecular weight marker. All subsequent wells were filled with the specific protein samples. Gels were run for 15 minutes at 80V to ensure the proteins moved though the stacking gel and lined up at the edge of the resolving gel, then the voltage was turned up to 150-180V for 1 hour.

2.7.5 Semi-dry transfer of proteins

The proteins were transferred onto nitrocellulose membrane in order to be accessible to antibody detection. The graphite plates of the Flowgen E702 (Consort) transfer machine were dampened with semi-dry transfer buffer (section 8.1) The gel was placed in a 'sandwich' containing 4 pieces of Whatman filter paper, followed by a piece of nitrocellulose paper, the gel itself and then another 4 pieces of Whatman filter paper, all cut to the size of the gel and soaked in buffer before placing onto the plate. The sandwich was gently rolled after the first set of Whatman paper and at the end to gently expel any bubbles. The apparatus was assembled and run for 1 hour at 40 mA per gel. The proteins move according to an electric current as in the last stage. After the transfer was complete, the membranes were quickly washed in phosphate buffered saline (PBS) and a ponceau stain was added which enabled visualisation of all bound protein on the membrane and helped in verifying the success of the transfer.

2.7.6 Antibody probing and Immunoblot developing

After the transfer was complete, the ponceau stain was washed off with phosphate buffered saline with 0.1% Tween 20 (PBST) for 10 minutes and then the membrane was blocked for 1 hour at room temperature on a rocking platform in either 5% (w/v) powdered milk or 5% BSA (w/v), 1% ovalbumin (w/v) both in PBS with the addition of 0.05% azide. The block was rinsed off with a phosphate-buffered-saline solution with 0.1% Tween-20 (PBST) and the primary antibody was diluted (see section 8.2 for specific antibody dilutions) 1:5 with blocking buffer in PBST and incubated overnight at 4°C on a rocking platform. The next day the primary antibody was removed and the membrane was washed 3 times with PBST for 10 minutes per wash and then once with PBS for 10 minutes. After washing the secondary antibody was diluted (1:10000) in PBST and placed onto the membrane for 2-3 hours at room temperature on the rocker. The membrane was then washed again with PBST and PBS as after the primary antibody step and the membrane was prepared for the detection step. An enhanced chemiluminescent lumigen (ECL, Pierce) reagent was added to membrane for 1 minute after which time the membrane was placed on absorbent paper to remove the excess reagent. The membrane was then placed between two layers of cling film in a photosensitive cassette and in a dark room photosensitive film was placed upon the membrane for varying length exposures depending on the antibody used. The film was developed and computer scanned to be analysed using ImageJ software (Wayne Rasband, National Institutes of Health, USA)

2.7.7 Membrane stripping

With many immunoblotting experiments protein phosphorylation is examined, both the phosphorylated and non-phosphorylated proteins will appear at the same size therefore it is necessary to probe for one and then strip the membrane and re-probe for the other. The membrane was placed in 20 ml of 1X stripping buffer supplemented with 2-mercaptoethanol (see section 8.1) in a sealed container for 30 minutes at 60°C on a rocking platform in a water bath. After which the stripping buffer was disposed of into

a solvent bottle in the hood and membrane was transferred to a clean container. The membrane was washed three times with PBS for 15 minutes per wash and then once with PBS, after the final wash, the membrane was blocked again as described in section 2.7.

2.7.8 Poly-acrylamide gel recipes

	Sufficient for 2x 1mm thick gels Final % gel			
	6	**7.5**	**10**	**12**
30% Acrylamide-Bis solution (ml)	3	2.5	5	4
MQ water (ml)	6.35	5	4.35	3.5
1M Tris pH 8.8 (ml)	5.6	2.5	5.6	2.5
10% SDS (ml)	0.25	0.16	0.25	0.16

- *Before pouring add 50µl of 10% AMPS and 20µl of TEMED*

	Sufficient for 2 x 1mm thick gels Final % gel
	5
30% Acrylamide-Bis solution (ml)	0.84
MQ water (ml)	3
1M Tris pH 6.8 (ml)	0.63
10% SDS (ml)	0.075

- *Before pouring add 20µl of 10% AMPS and 13µl of TEMED*

Table 2.1 Resolving and stacking gel recipes.

The size of the protein of interest depends on the percentage of resolving gel used, with larger proteins a lower percentage gel is used (6 or 7.5%) as the pores are much larger to allow the protein to pass through. The reverse is true when blotting for smaller proteins.

2.8 Scanning electron microscopy (SEM)

To assess the surface of the cells, electron microscopy was used. Calu-3 cells were grown via air-liquid interface culture for 7 days, then washed with serum free media and placed in the fixative solution, 2.5% GDA and 0.5 g potassium ferrocyanide were dissolved in 50 ml normal strength culture media. Cells were washed again with serum free media and then the fixative solution was added for 2 hours at 37°C. Cells were then washed with serum-free media and postfixed with 1% osmium tetroxide + 1% potassium ferrocyanide for 1 hour at room temperature. Cells are washed twice with water over 10 minutes,the filters are cut out and placed in small glass vials and stained with 2% uranyl acetate for 1 hour in the dark. The filters are further washed with acetone 50, 70 and 90% each one over 10 minutes and then twice with 100% acetone, followed by one 15 minute wash with an equal mix of acetone and HMDS and then two final 15 minute washes with HMDS. The cells are then coated with an ultrathin layer of gold and viewed on a JEOL SEM6480LV scanning electron microscope.

2.9 Wound healing

A common method of examining the ability of cells to repair wounds is the scratch assay. Cells were grown on 12-well plates and when confluent were scratched with a small plastic pipette tip (10-200 µl) to make a horizontal scratch and a needle tip to make a vertical scratch (as shown in Figure 2.2). The method of crossing over the scratches allowed for the area photographed each time to remain constant. Cells were washed twice with serum-free media to remove any cell debris and were viewed on an Olympus CKX41 microscope with an attached C-3030 camera and photographs were taken in the area directly left of the vertical needle scratch. Cells were placed in media containing IL-13 and/or inhibitors and incubated for 24 hours, after which time the media was removed and cells were washed with serum free

media twice to remove any cell debris and photographed again. The photos were then analysed using Tscratch software (CSElab) and the amount of wound that had closed was given as a percentage of the initial wound area.

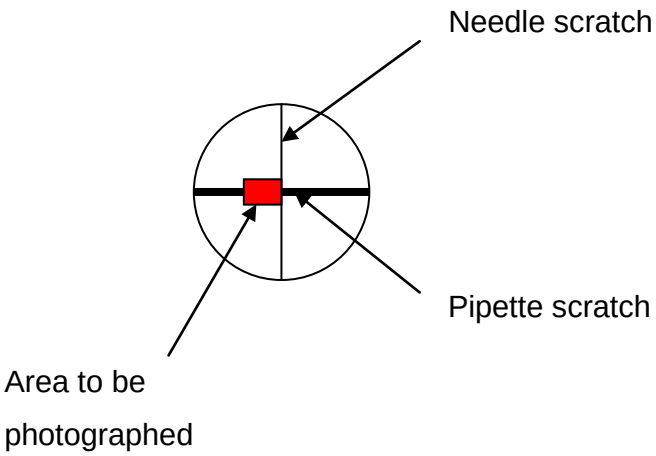

Figure 2.2 Wound healing assay

2.10 Calcium switch Assay

Another method useful in investigating the mechanisms behind cell repair and regrowth is a calcium switch assay [230] in which cells are subjected to low calcium followed by normal levels of calcium and monitored by TER measurements. Confluent cells grown via ALI were measured by TER to get an initial value, they were then placed in 4 mM EGTA for 30 minutes to destroy tight junctions and adherens junctions and their TER was measured again to check that this was the case (depicted by a large decrease in TER). Cells were then placed back in normal calcium containing media with the addition of IL-13 and/or inhibitors for 24 hours in the incubator. After which time the TER was measured and compared with the initial value to see the effect the various cytokines/inhibitors had on tight junction re-formation.

2.11 Lactate dehydrogenase (LDH) assay

To assess the membrane integrity of the cells as a measure of cell necrosis after treatment of the various inhibitors the TOX7 Lactate dehydrogenase (LDH) kit was used. The assay measures the amount of NADP reduced to NADPH by LDH through the stoichiometric conversion of a tetrazolium dye by the reduced NADPH. The red coloured result can then be measured spectroscopically by monitoring the absorbance at 490 nm. Cells were grown to confluency in 12-well plates and treated with inhibitors for 24 hours after which the media from each sample was sampled to assess the amount of LDH released. In each experiment media was placed in a cell containing no cells (negative control) and triplicate wells were lysed and averaged to give the total LDH present in each sample.

2.12 Statistical analysis

To test the statistical significance the following tests were used: either a 1-way or 2-way ANOVA followed by Dunnett's or Tukeys post-hoc test. A paired t-test was also used when only comparing 2 groups. A P value of less than 0.05 was considered to be statistically significant.

2.13 Materials

Material	Catalogue No	Source
10ml plastic pipettes	CC114	Appleton Woods, Birmingham UK.
12-well plates	665180	Greiner Bio-One, Gloucestershire UK
13mm cover slips	MNJ-500-010G	Fisher Scientific, Loughborough UK.
25ml plastic pipettes	CC116	Appleton Woods, Birmingham UK.
2-mercaptoethanol	M3148	Sigma-Aldrich, Dorset UK
30% Acrylamide/Bis	161-0154	Bio-rad, Hertfordshire UK
35mm tissue culture dishes	BC150	Appleton Woods, Birmingham UK.
4-well plates	TKT190130	Fisher Scientific, Loughborough UK.
6-well plates	657160	Greiner Bio-One, Gloucestershire UK
Ammonium persulphate (AMPS)	A/P470/46	Fisher Scientific, Loughborough UK.
Anti beta-actin antibody	4967S	New England Biolabs, Hertfordshire UK
Anti- phospho STAT6 antibody	9361S	New England Biolabs, Hertfordshire UK
Anti- STAT6 antibody	9362S	New England Biolabs, Hertfordshire UK
Anti-Akt (1/2/3) antibody	sc-8312	Santa Cruz, Heidelberg, Germany
Anti-claudin 2 antibody	32-5600	Invitrogen,Paisley UK
Anti-Ecadherin antibody	3195S	New England Biolabs, Hertfordshire UK
Anti-GSK3β antibody	9315S	New England Biolabs, Hertfordshire UK
Anti-IL-13Rα2	ab55275	Abcam, Cambridge UK
Anti-mouse alexa fluor 488 antibody	A11001	Fisher Scientific, Loughborough UK.
Anti-mouse PE conjugated IL-13Rα1	12-2130-80	ebioscience, Hatfield UK
Anti-MUC5AC antibody	ab24070	Abcam, Cambridge UK
anti-occludin antibody	55065	New England Biolabs, Hertfordshire UK
Anti-phospho Akt (ser473)	9271S	New England Biolabs, Hertfordshire UK
Anti-phospho GSK3β antibody	9331S	New England Biolabs, Hertfordshire UK
Anti-phospho-p44/42 MAPK antibody	4377	New England Biolabs, Hertfordshire UK
Anti-rabbit alexa fluor 546 antibody	A11010	Fisher Scientific, Loughborough UK.
Anti-rabbit Claudin 1 antibody	4933S	New England Biolabs, Hertfordshire UK
Anti-rabbit Claudin 8	40-2600	Invitrogen,Paisley UK
Anti-rabbit phosphoβ-catenin antibody	9561P	New England Biolabs, Hertfordshire UK
Anti-rabbit ZO-1 antibody	VX339100	Fisher Scientific, Loughborough UK.
Anti-rabbit β-catenin antibody	95625	New England Biolabs, Hertfordshire UK
Aprotinin	A1152	Sigma-Aldrich, Dorset UK
Aspirating needles	FB50253	Fisher Scientific, Loughborough UK.
Autoclave tape	AUY-170-030P	Fisher Scientific, Loughborough UK.
Black 96-well plates	655086	Greiner Bio-One, Gloucestershire UK
Blocking buffer	11096176001	Roche, West Sussex UK
Bovine Collagen	354231	BD Biosciences, Oxford UK
Bovine serum albumin	A6003	Sigma-Aldrich, Dorset UK
Bradford protein assay dye	500-0006	Bio-rad, Hertfordshire UK
Bromophenol blue	B/P620/44	Fisher Scientific, Loughborough UK.
Calibration kit for TER experiments	CALICELL12	World Precision Instruments

Cell scrapers	541070	Greiner Bio-One, Gloucestershire UK
Clear 96-well plates	655180	Greiner Bio-One, Gloucestershire UK
Dimethyl sulphoxide	D8418	Sigma-Aldrich, Dorset UK
DMEM/F12 media	21331-046	Invitrogen, Paisley UK
ECL kit	32109	Pierce, Northumberland UK
ECL prime blocking agent	RPN2232	GE Healthcare, Amersham UK
ECL prime kit	RPN418	GE Healthcare, Amersham UK
EDTA pH8 0.5M	BPE2482-500	Fisher Scientific, Loughborough UK.
EGTA	E0396	Sigma-Aldrich, Dorset UK
Fetal bovine serum (FBS)	10082147	Invitrogen, Paisley UK
FITC-dextran (Mwt 3000-5000)	FDR	Sigma-Aldrich, Dorset UK
FUJI X-ray film	2731261	Fisher Scientific, Loughborough UK.
Fungizone	15290-026	Invitrogen, Paisley UK
Gel loading pipette tips	PMP-130-100A	Fisher Scientific, Loughborough UK.
Glass plates for western blotting	1653308	Bio-rad, Hertfordshire UK
Glucose	G7021	Sigma-Aldrich, Dorset UK
Glutamine	25030024	Invitrogen, Paisley UK
Glycerol	G5516	Sigma-Aldrich, Dorset UK
Glycine	G/P460/53	Fisher Scientific, Loughborough UK.
HBSS (1X)	14025-050	Invitrogen, Paisley UK
Hepes	H3784	Sigma-Aldrich, Dorset UK
High capacity cDNA RT kit	VY4368814	Fisher Scientific, Loughborough UK.
Hi-res Agarose	A4-0700-S	Geneflow, Staffordshire UK
HotstarTaq DNA polymerase	203203	Qiagen, Crawley UK
Human EGF	AF-100-15	Peprotech, London UK
Human fibronectin	354008	BD Biosciences, Oxford UK
Human IL-13	200-13	Peprotech, London UK
Human TGFα	100-16B	Peprotech, London UK
Human TGFβ	100-21	Peprotech, London UK
IC87114 inhibitor	S1268	Selleck chemicals, Suffolk UK
LDH assay kit	TOX7	Sigma-Aldrich, Dorset UK
Leupeptin	BPE2662-5	Fisher Scientific, Loughborough UK.
LHC basal medium	12677-027	Invitrogen, Paisley UK
LY294002 inhibitor	L9908	Sigma-Aldrich, Dorset UK
MicroAmp 96-well plates	VY4346906	Fisher Scientific, Loughborough UK.
MicroAmp optical adhesive film	VY4360954	Fisher Scientific, Loughborough UK.
Microscope slides	MNJ-700-010N	Fisher Scientific, Loughborough UK.
Millipore filters	FDR-050-071N	Fisher Scientific, Loughborough UK.
Minimum essential media (MEM)	21430-079	Invitrogen, Paisley UK
Mowiol	10852	Sigma-Aldrich, Dorset UK
MUC5AC antibody	ab3649	Abcam, Cambridge UK
Mycoalert mycoplasma detection kit	LT07-218	Lonza, Blackley UK
NEAA 100X	11140035	Invitrogen, Paisley UK
Nitrocellulose membrane	162-0115	Bio-rad, Hertfordshire UK
Nonidet P-40	56009	Sigma-Aldrich, Dorset UK

Oligo $(dT)_{15}$ primer	C1101	Promega, Southampton UK
Omniscript RT kit	205111	Qiagen, Crawley UK
p10 pipette tips	FB34511	Fisher Scientific, Loughborough UK.
p1000 pipette tips	FB34611	Fisher Scientific, Loughborough UK.
p200 pipette tips	FB34541	Fisher Scientific, Loughborough UK.
PBS (without Ca^{2+} and Mg^{2+})	14190-169	Invitrogen, Paisley UK
PBS tablets	P4417	Sigma-Aldrich, Dorset UK
PCR mixed colour tubes	FB68729	Fisher Scientific, Loughborough UK.
PD0325901 inhibitor	4192	Tocris Bioscience, Bristol UK
Pencillin/Streptomycin	15140122	Invitrogen, Paisley UK
Pepstatin A	BPE2671-250	Fisher Scientific, Loughborough UK.
pH electrode	PHL-650-520T	Fisher Scientific, Loughborough UK.
Phenol Red	P0290	Sigma-Aldrich, Dorset UK
PIK75 inhibitor	S1205	Selleck chemicals, Suffolk UK
Plasmocin	ant-mpt	Source Bioscience, Nottingham UK
Presept tablets	HYG-210-010P	Fisher Scientific, Loughborough UK.
Primers	N/A	Sigma-Aldrich, Dorset UK
Protein standard marker	161-0375	Bio-rad, Hertfordshire UK
QIA shredders	79654	Qiagen, Crawley UK
Qubit RNA BR Buffer	Q10210	Invitrogen, Paisley UK
Recombinant Dnase I	AM2235	Ambion, Paisley UK
Rnase free water	BPE561-1	Fisher Scientific, Loughborough UK.
Rnase-free Dnase set	79254	Qiagen, Crawley UK
Rnasin Plus Rnase inhibitor	N2611	Promega, Southampton UK
Rneasy mini kit	74104	Qiagen, Crawley UK
SAHA inhibitor	1604-1	Cambridge Bioscience, UK
Set of dNTPs	U1330	Promega, Southampton UK
Sodium	S/P530/53	Fisher Scientific, Loughborough UK.
Sodium azide	S2360	Sigma-Aldrich, Dorset UK
Sodium fluoride	S1504	Sigma-Aldrich, Dorset UK
Sodium molybdate	S6646	Sigma-Aldrich, Dorset UK
Sodium orthovanadate	S6508	Sigma-Aldrich, Dorset UK
STX2 Tweezer electrode for TER	STX2	World Precision Instruments, Florida
SYBR Green PCR master mix	VY4364344	Fisher Scientific, Loughborough UK.
TEMED	T/P190104	Fisher Scientific, Loughborough UK.
Tissue culture flasks 175 cm^2	660175	Greiner Bio-One, Gloucestershire UK
Tissue culture flasks 25 cm^2	690175	Greiner Bio-One, Gloucestershire UK
Tissue culture flasks 75 cm^2	658175	Greiner Bio-One, Gloucestershire UK
Transwell plates 12mm	CLS3460	Sigma-Aldrich, Dorset UK
Trizol	15596-018	Invitrogen, Paisley UK
Trypan blue dye	T8154	Sigma-Aldrich, Dorset UK
Trypsin/EDTA 0.05%	25300062	Invitrogen, Paisley UK
Trypsin/EDTA 0.25%	25200072	Invitrogen, Paisley UK
Tween-20	P1379	Sigma-Aldrich, Dorset UK

Water bath clean treatment	S5525-40Z	Sigma-Aldrich, Dorset UK
Whatman chromatography paper	FB59515	Fisher Scientific, Loughborough UK.
Wortmanin inhibitor	W1628	Sigma-Aldrich, Dorset UK
ZSTK474 inhibitor	1597-100	Cambridge Bioscience, UK

Chapter 3 : Characterisation of Calu-3 cells

3.1 Assessing the transepithelial resistance of Calu-3 cells

This thesis investigates the role of IL-13 and PI3K in lung epithelial barrier modulation. To establish a model that was physiologically relevant to that of the lung, the cell line had to be characterised and optimised to achieve an air-liquid interface (ALI) culture system that could be easily manipulated. Calu-3 cells were grown on transwell filters that comprised of a 12 mm membrane with 0.4 µm pores. 300 µl of cells were placed in the apical chamber and 1 ml of complete media was placed in the basolateral chamber, cells were grown under immersion culture for 2 days then the media was removed from the apical chamber to establish ALI (see Figure 2.1).

It was important to optimise both the seeding density as well as the culture time period. Calu-3 cells were first plated onto the transwell filters at $2.5x10^5$ cells/ml and their transepithelial resistance (TER) was monitored daily up to 23 days. TER increased dramatically after day 12 and peaked at day 16 (Figure 3.1). This seeding concentration was unsuitable for further studies due to the length of incubation time before cells reach confluency and then the immediate decrease after the maximal TER, giving no time period where cells maintained a stable TER in order to carry out various stimulations. Subsequently cells were seeded at the higher concentration of $5x10^5$ cells/ml and this proved far more effective with a maximal TER being reached at day 7 which remained constant up to day 14 as shown in Figure 3.1. All later experiments were seeded at $5x10^5$ cells/ml and stimulated with various cytokines and inhibitors at confluency.

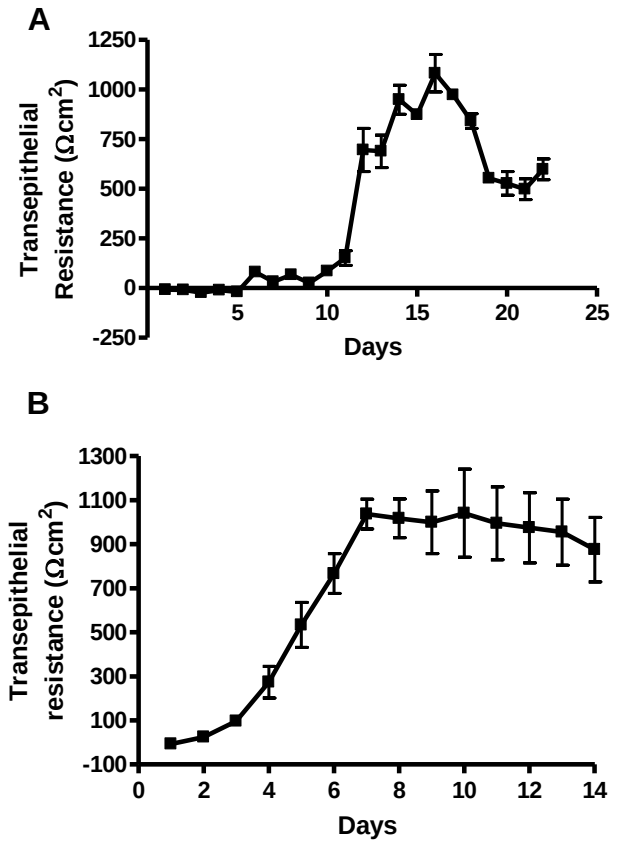

Figure 3.1 Optmising the seeding density of Calu-3 cells grown at ALI. Cells were seeded at $2.5x10^5$ cells/ml (A) and $5x10^5$ cells/ml (B) and the transepithelial resistance was measured with STX2 electrodes every day. The background was measured using a transwell without cells and was subtracted from the raw resistance which was then multiplied by the area of the transwell to get the units Ωcm^2. Data are expressed as mean values ± SEM from n=5 independent experiments.

3.2 Surface morphology of Calu-3 cells grown via ALI culture

After monitoring the TER of Calu-3 cells, it was necessary to study the surface properties of the cells grown via air-liquid interface. Under immersion culture, which is often termed liquid covered culture (LCC), cells have a different phenotype to those exposed to the air. Cells grown via LCC have been shown to produce less mucus and are less differentiated than those grown via ALI [275]. Scanning electron microscopy was used to study the surface of the cells after 7 days in ALI culture, the point at which the TER reached its peak and the cell layer was presumed to be 'intact' with fully formed tight junction proteins (Figure 3.1).

Calu-3 cells were clearly shown to express cilia after 7 days in culture (Figure 3.2); a feature only present in a differentiated pseudostratified epithelium. Around 90% of all cells in each sample displayed cilia, with each cell showing a different degree of differentiation with the shape and length of cilia also varying between cells. The cell boundary between cells can also be observed, clearly shown in figure 3.2B as indicated by red arrows. Figure 3.2D is a highly magnified image of a cell in which the cilia present appear to be clumping together in a star-like appearance, with the tips of four or five cilia touching, this is thought to be an effect of the fixing method and was only observed on some cells. SEM imaging gives a good indication that the culture method used is providing a physiologically relevant airway model to study further.

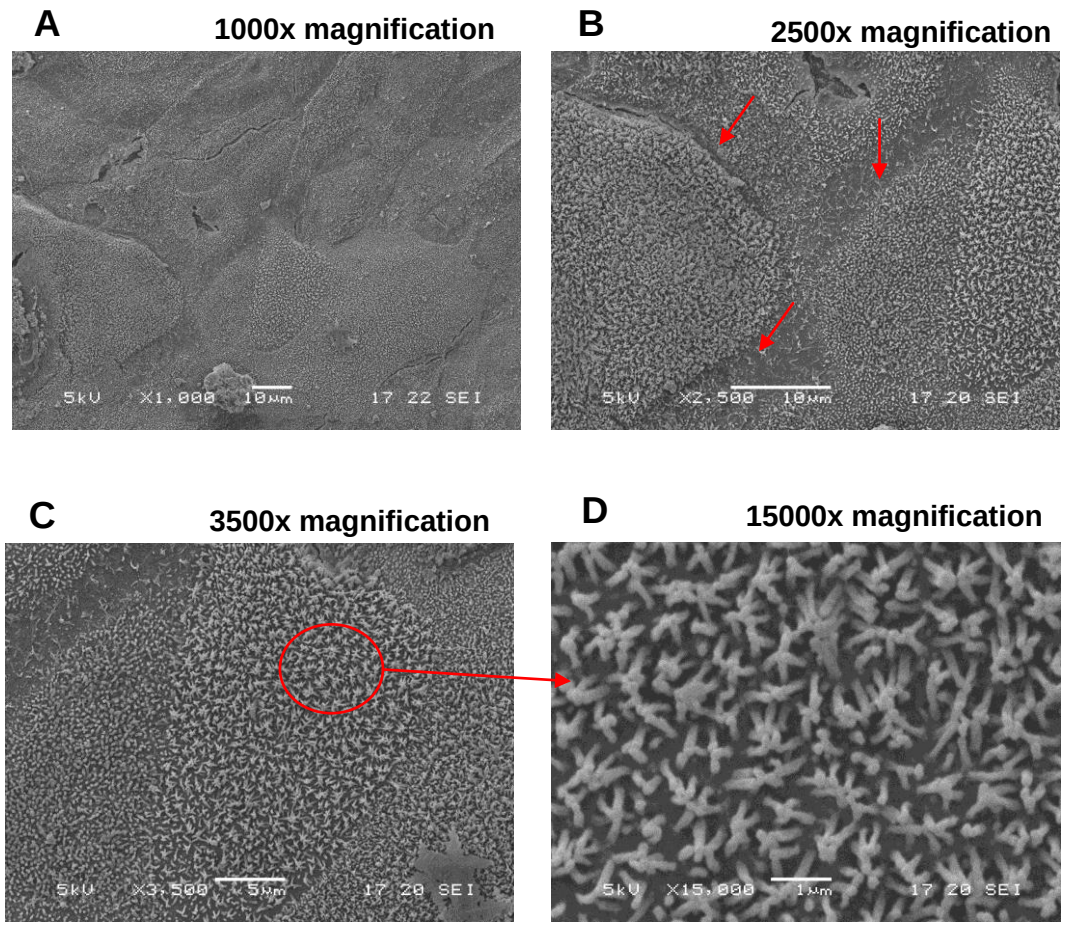

Figure 3.2 The surface profile of Calu-3 cells using scanning electron microscopy (SEM).

Calu-3 cells grown via air-liquid interface culture for 7 days were washed with serum free media and placed in the fixative solution, 2.5% glutaraldehyde, 0.5g potassium ferrocyanide in media for 2h at 37°C. Cells were then washed and postfixed with 1% osmium tetroxide and 1% potassium ferrocyanide for 1 hour at room temperature. After washing with water, cells were stained with 2% uranyl acetate for 1 hour in the dark, followed by slow dehydration with acetone and HDMS washes. Cells were coated with an ultra thin layer of gold and viewed on a JEOL SEM6480LV scanning electron microscope. Image A was the lowest magnification (1000x) taken of the surface area showing > 10 individual cells. Image B was taken at a higher magnification and the junctions can be clearly seen between ciliated cells, depicted by red arrows. Image C (3500x) shows the cilia forming a star like appearance and the area encircled in red is shown at the higher magnification of 15000x in image D. Images are representative of three independent experiments.

3.3 Expression of tight junction proteins via immunocytochemistry

Tight junction proteins which are present at the most apical part of the junctional complex between cells are essential in maintaining epithelial barrier function and controlling what can pass through via paracellular permeation. The intestinal epithelial cell lines Caco-2 and T84 have been extensively researched in relation to tight junction modulation, and they have been shown to express many tight junction proteins from the claudin family along with occludin and the tight junction associated proteins zonula occludens 1-3 [199, 236, 276, 277]. In order to begin studying the signalling pathways involved in lung epithelial modulation, it was necessary to check the basal expression of key junctional proteins present in Calu-3 cells. Of the various methods available to monitor protein expression immunoblotting would not be the obvious first choice, however due to the vast size of some TJ proteins, it is the most suitable method. Such proteins include ZO-1, which has a molecular weight of 225 kDa and often appears as numerous sized unclear bands on an SDS-PAGE gel, a feature explained by its many phosphorylated forms [278]. Immunofluorescence was used and proved useful as although the expression could not be quantified as it would with immunoblotting the distribution of the proteins were also observed.

As shown in Figure 3.3 Calu-3 cells were found to express the junctional proteins occludin, ZO-1, claudin 1, claudin 2, claudin 8, E-cadherin and beta-catenin. Occludin was found at the edges of cells forming a continuous ring around each individual cell, a similar situation was seen for ZO-1, E-cadherin and beta-catenin. Claudin 2 basal expression was found to be very low compared to the other proteins and appears scattered throughout the cell. Claudin 1 was expressed but the distribution was shown to be a mixture between localisation at the cell junctional complex and random scattering throughout the cytoplasm. Claudin 8 was expressed at a very low level in basal cells and appeared to be cytoplasmic.

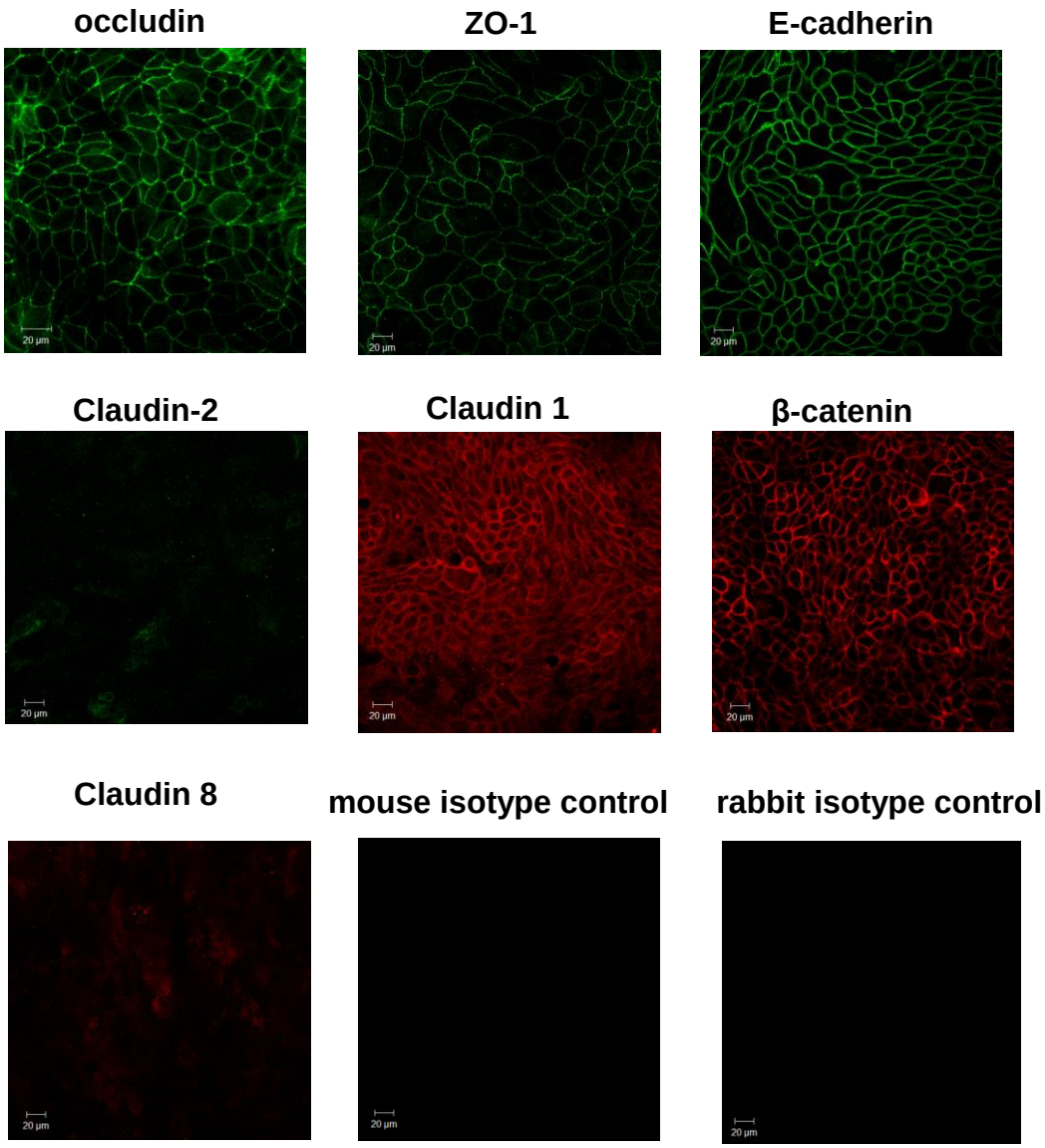

Figure 3.3 Basal expression of junctional proteins via immunofluorescence.

Calu-3 cells were grown via ALI culture for 7 days, then washed with PBS and fixed using 4% PFA (except for E-cadherin which was fixed with ethanol). Cells were permeabilised and stained for various junctional proteins overnight at 4°C. They were then washed and labelled with a secondary antibody conjugated to either a 488 or 546 dye. After a series of washing steps, filters were cut out, mounted onto to glass slides and left to dry overnight at 4°C. Cells were visualised using an LSM510META confocal microscope. Occludin, ZO-1, E-cadherin, Claudin 1 and beta-catenin were shown to be expressed as a continuous band surrounding each cell at the tight junction. The expression of claudins 2 and 8 were lower than the other junctional proteins and were shown to be localised sporadically throughout the cytoplasm rather than concentrated at the cell junction. Images are representative of three independent experiments.

3.4 Discussion

3.4.1 Characterisation of Calu-3 cells

Calu-3 cells are a carcinomic cell line derived from a pleural effusion. They are a well characterized bronchial cell line which has serous cell properties [279] and can be referred to as a submucosal cell line. When confluent, Calu-3s become polarised and express the same membrane associated protein and mRNA profiles as that of a normal human lung epithelium, with the expression of many key drug transporter proteins such as the multidrug resistance-associated transporter protein 1 [280]. There are many advantages of using this cell line over primary cells, the most important with respect to research ease being their immortality and cost effectiveness. Primary cells often give irreproducible results due to donor variability, whereas Calu-3 cells are known to be reproducible and unlike many SV-40 transformed cell lines they maintain their phenotype after many repeat passages [273].

3.4.2 Transepithelial resistance as a measure of confluency

Calu-3 cells form an 'intact' cell monolayer which reaches a TER of around 1000 Ωcm^2 after 7 days in culture. TER values are often used as an indirect measure of presence of tight junctions [274] and so it was assumed that tight junction proteins were expressed in the Calu-3 cell line. The alveolar epithelial cell line A549 and the bronchial epithelial cell line, 16-HBE were also grown on transwell filters and both failed to reach a TER of >300 Ωcm^2 (data not shown). A leaky transwell filter was also observed which occurs when media from the basolateral chamber travels through the membrane and is a tell-tale sign of cells that have yet to, or are unable to form tight junctions between adjacent cells resulting in little resistance to liquid passing through. This finding was consistent with other research in

which A549 cells are labelled as a leaky cell line in terms of TER, however they are still studied in relation to tight junction modulation [256, 281-284] but are known to be unreliable for drug transport studies [285].

3.4.3 Calu-3 cell surface morphology by SEM

After determining the presence of a high TER and thus concluding that tight junction proteins were present, the surface properties of Calu-3 cells were studied by SEM. Calu-3 cells are clearly shown to be differentiated after ALI culture for 7 days, with cilia present on 90% of the overall cell surface and a clear definition between cell boundaries. The difference between Calu-3 cells grown under ALI compared to that of liquid covered cells was examined by Zhu *et al* and it was shown that ALI cells form a thicker pseudostratified cell layer in which cells display long cilia whereas those grown in immersion culture did not, with the cell layer being so thin that the pores of the transwell could be seen on the image [286]. The permeability of peptides through the epithelial layer was also shown to be different depending on the culture method used, the apical uptake of the peptide glycyl-sarcosine was much higher in ALI cultured cells than those in LCC [287]. The transwell filter can be composed of polyethylene terephthalate (PET) or polycarbonate, however studies have shown that there is no difference between using either [286], the factor which influences the inconsistencies in the data is the method of culture. This may explain why there are such contrasting conclusions in research undergone using this cell line with some researchers using LCC and others ALI culture.

3.4.3 Expression of tight junction proteins in Calu-3 cells shown by immunofluorescence

Calu-3 cells are known to have a wide range of junctional protein expression which is one of the reasons why they are a good cell model to use when studying the integrity of the airway epithelium. Of the many junctional proteins commonly expressed by epithelial cells, some were examined by immunofluorecence studies. Occludin, ZO-1, claudins 1, 2, 8 and beta-catenin were all found to be expressed at some level in basal Calu-3 cells. The expression of these proteins in Calu-3 cells is already known however it was useful to get an idea of their localisation within the cell before beginning various stimulations to study their modulation.

3.4.4 Limitations and future experiments

Although Calu-3 cells have been shown to be a good model to study the tight junction, they are still a carcinomic cell line and undoubtedly have many altered signalling pathways. In terms of tight junction expression and degree of ciliogenesis, it would be interesting to compare Calu-3 cells to that of a primary bronchial epithelial cell culture.

3.5 Conclusions

In this initial part of the study it was determined that Calu-3 cells are a suitable model to further study the modulation of tight junction proteins as they basally express all the key junctional proteins studied and reach high TER values when cultured on filters at ALI. They were proven to be polarised after 7 days of culture by SEM where cilia were observed throughout the cell monolayer.

In summary, this chapter shows that:

- Calu-3 cells form a high TER of up to 1000 Ω cm^2 after 7 days in ALI culture.
- SEM images prove that the cells are differentiated and display cilia on their surface.
- ZO-1, occludin, claudin 1, 2, 8 and beta-catenin are all present in Calu-3 cells shown by immunofluorescence.

Chapter 4 : Role of IL-13 in epithelial barrier modulation

4.1 Effect of cytokines IL-13, IL-4, IL-1β and IFN-γ on transepithelial resistance in Calu-3 cells

IL-13 is known to be up-regulated in the lung of asthmatic patients. It has been shown to play a role in many features of allergic asthma such as epithelial-to-mesenchymal transitions [288] and goblet cell metaplasia [34]. The role of IL-13 in lung barrier modulation has been extensively researched in the intestine where it is known to play a key role in the inflammatory bowel disease ulcerative colitis [227, 245]. However much less in known about TJ regulation in the lung, here the effect of IL-13 on transepithelial resistance was researched. IL-13 was added to the basolateral chamber of the culture system on day 7 when the cells had reached a maximum TER and were non 'leaky'. IL-13 was administered at 10 ng/ml and the TER was monitored every 24 hours over 3 days. IL-13 caused a ~40% decrease in transepithelial resistance after 24 hours which was sustained for 72 hours. (Figure 4.1). In addition to IL-13, the effect of IL-4, IL-1β and IFNγ were investigated after 24 hour stimulation. The T_H2 cytokine IL-4 also demonstrated a decrease in TER of 35% compared to control. The proinflammatory cytokine IL-1β which is part of the IL-1 cytokine family did not have any significant effect on TER compared with the control. Interestingly the T_H1 cytokine interferon-γ (IFN-γ) resulted in a 40% increase in TER over control cells. Unfortunately, only the role of IL-13 was investigated due to time constraints.

4.2 Role of IL-13 in tight junction distribution by immunocytochemistry

In order to investigate the underlying mechanism responsible for the decrease in TER caused by IL-13 the distribution of key junctional proteins were examined by immunocytochemistry. Cells were grown via ALI and when confluent were stimulated with IL-13 at 10 ng/ml for 24 hours, they were then fixed and stained as described in section 2.4.

The junctional proteins claudin 1, claudin 2, ZO-1, E-cadherin, occludin and β-catenin were investigated. IL-13 caused an obvious change in claudin 2 expression and distribution and a slight change in claudin 1 expression. Claudin 2 was found to be expressed more highly after IL-13 stimulation and its distribution became more membrane associated.

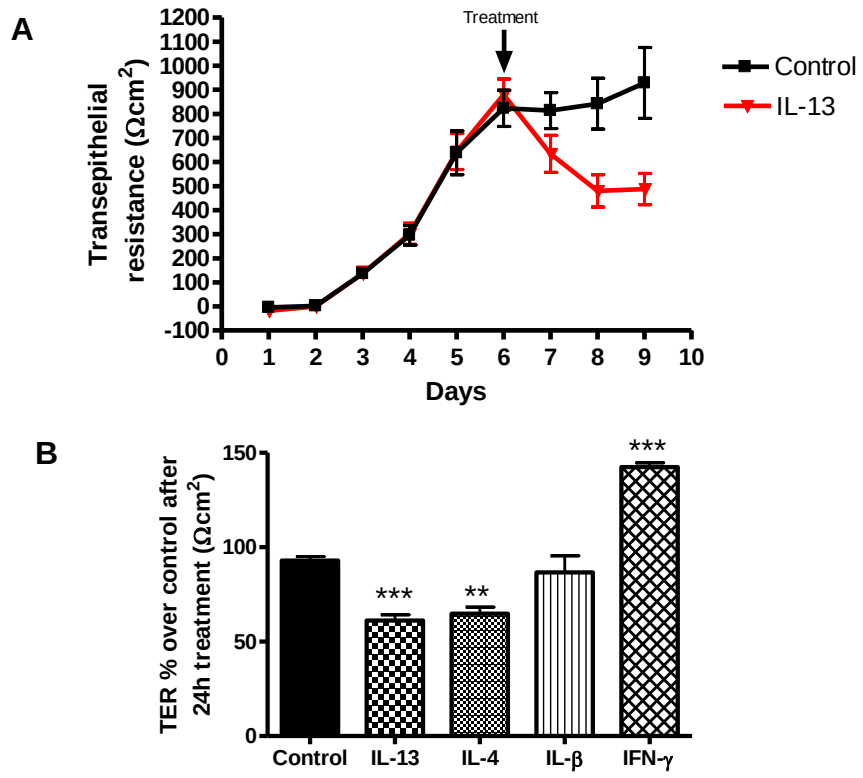

Figure 4.1 Effect of cytokine stimulation on transepithelial resistance in Calu-3 cells.

For each experiment $5x10^5$ cells/ml were seeded onto transwell filters and their transepithelial resistance was monitored every 24 hours. On Day#7 when the maximum TER was reached, IL-13 (10 ng/ml) was added to the basolateral chamber and TER was measured after 24, 48 and 72 hours (A). Confluent Calu-3 cells grown via ALI were starved in serum free media overnight and stimulated with IL-13 (10 ng/ml), IL-4 (5 ng/ml), IL-1β (10 ng/ml) and IFN-γ (10 ng/ml) for 24 hours. The TER was then compared to that of the same well 24 h prior to obtain the TER % of control after 24 h treatment (B). Data expressed as mean values ± SEM from n=9 (IL-13) and n=3 (IL-4, IL-1β and IFN-γ) independent experiments and statistical significance is represented as (***) for $p<0.001$ and (**) for $p<0.01$.

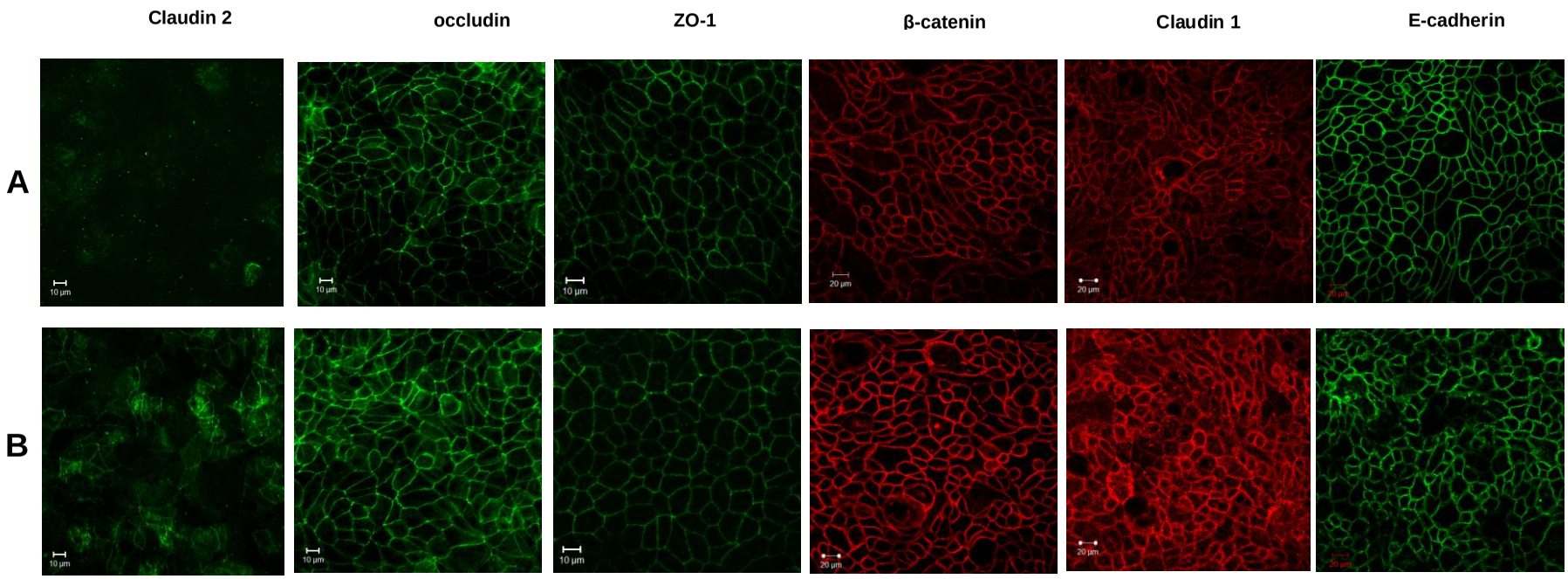

Figure 4.2 Effect of IL-13 on junctional protein distribution in Calu-3 cells.

Calu-3 cells were stimulated with 10ng/ml IL-13 for 24 hours, row A are untreated controls and row B are IL-13 treated. They were then fixed and probed for specific junctional proteins (see section 2.4 for details), mounted onto glass slides and viewed using a LSM510META confocal laser scanning microscope. Each image is representative of three similar images taken during three independent experiments (n=3)

Claudin 1 was shown to have a slight increase in expression following IL-13 treatment whereas distribution at the cell junction remained the same as in the untreated control. The distribution or relative expression of occludin, E-cadherin and ZO-1 did not change with IL-13 treatment (Figure 4.2). The graph in Figure 4.3 is representative of the claudin 2 images semi-quantified by calculating the intensity per pixel using LSM image examiner.

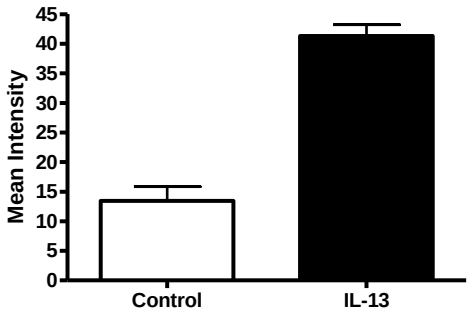

Figure 4.3 Semi-quantification of the effect of IL-13 on claudin 2 expression in Calu-3 cells via immunocytochemistry.
Images taken from immunocytochemistry (as shown in Figure 4.2) were quantified by intensity per pixel using LSM image examiner software. The data plotted is expressed as mean ± SEM from n=3 independent experiments.

4.3 Effect of IL-13 on tight junction expression by immunoblotting

To further investigate the changes in protein expression seen in immunofluorescence data, immunoblotting was used. Claudin 1, claudin 2, occludin, E-cadherin and ZO-1 were blotted following the method described in 2.7. The results mimicked the immunocytochemistry data in that the only proteins that changed in expression after IL-13 stimulation were claudin 1 and claudin 2 (Figure 4.4). Claudin 1 was only increased slightly with the largest increase being 1.5 fold over basal after 48 hours stimulation, the increase being gradual up to this point and then dropping slightly after 72

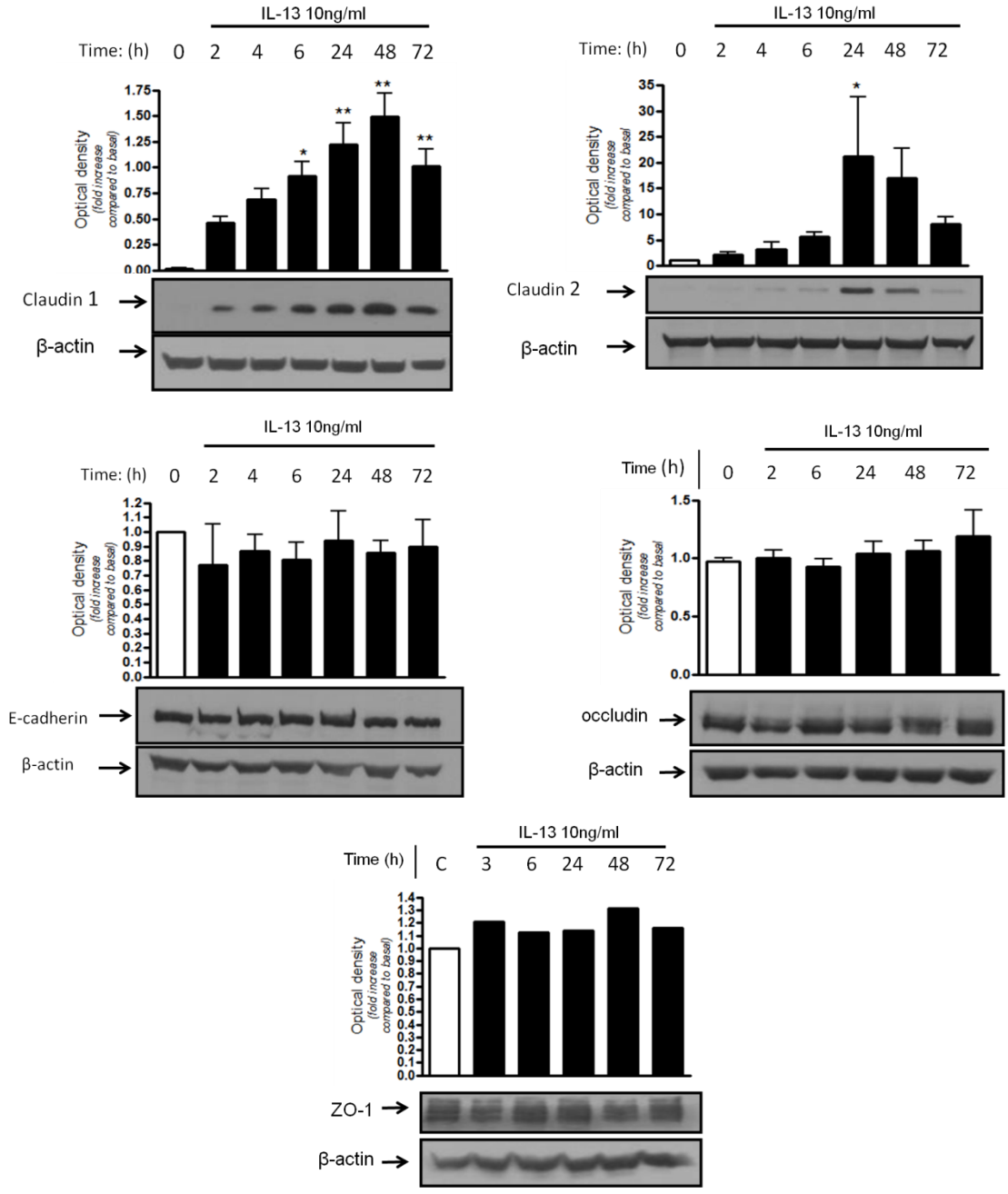

Figure 4.4 The effect of IL-13 on junctional protein expression by immunoblotting.

For each experiment, cells were plated onto 3 cm^2 dishes in complete MEM. When confluent, cells were incubated with IL-13 (10 ng/ml) for up to 72 h. Samples were resolved on SDS-PAGE gel, transferred to nitrocellulose membranes and immunoblotted, using antibodies against claudin 1 at 20 kDa, claudin 2 at 23 kDa, E-cadherin at 120 kDa, occludin at 65 kDa and ZO-1 at 225 kDa. Each immunoblot is representative of 3 independent experiments (except for ZO-1 which is only one experiment). All groups were compared to vehicle control (0 h) for statistical significance, which is expressed as (**) for $p<0.01$ and (*) for $p<0.05$.

hours. IL-13 treatment induced the upregulation of claudin 2 after 24 hours with a 25-fold increase over basal which decreased to 15 fold after 48 hours and after 72h was almost returned to basal levels. E-cadherin, occludin and ZO-1 protein levels did not alter with IL-13 stimulation up to 72 hours.

4.4 Effect of IL-13 on paracellular permeability

To further investigate the role of IL-13 in lung barrier modulation, the effect of IL-13 on macromolecule paracellular permeability was explored. To standardise the experiment fluorescein isothiocyanate (FITC) dextran (4kDa) was diluted to between 0.1-1000 µg/ml to construct a standard curve of known FITC concentrations in the absence of cells. It was important to ensure the amount of FITC detected in the basolateral chamber of untreated Calu-3 cells was not at the top end of the intensity limit; giving no window to monitor changes. FITC-dextran at 500 µg/ml in HBSS buffer is a standard concentration to use in this assay; 200 µl was added to the apical chamber of fully confluent untreated cells for 15, 30 and 45 minutes. The optimal incubation time was found to be 30 minutes (Figure 4.5), which has also been used by other studies investigating paracellular permeability [289]. Calu-3 cells were grown for 7 days until confluent, they were treated with IL-13 at 10 ng/ml for 24 hours. The apical chamber was washed with HBSS and 500 µg/ml FITC-dextran in HBSS was added to the chamber for 30 minutes. The amount of FITC-dextran in the basolateral chamber was measured using a fluorescent plate reader at excitation and emission wavelengths of 485 and 530 nm respectively. There was no change observed in the paracellular permeability of FITC dextran between the IL-13 treated cells to that of control untreated cells (Figure 4.6).

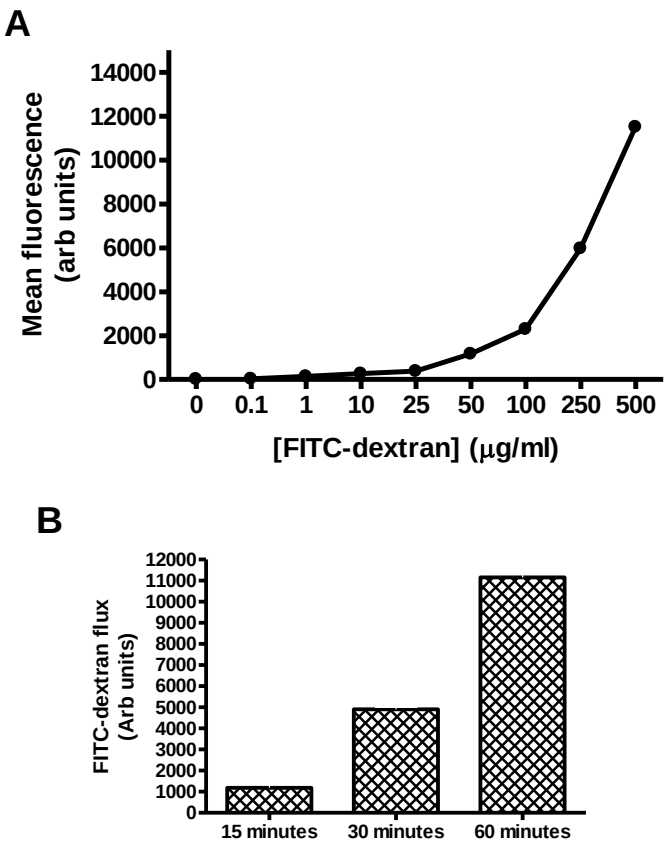

Figure 4.5 Optimisation of the FITC-dextran paracellular permeability assay.

To ensure that changes in FITC-dextran flux were detected a standard curve was constructed using samples of known FITC-dextran concentration in the absence of cells (A). Untreated Calu-3 cells were monitored by TER and when confluent the apical chamber was washed with HBSS and 200 µl of FITC-dextran at 500 µg/ml was added for 15, 30 and 60 minutes. Triplicate samples (100 µl) were extracted from the basolateral chamber and placed into a black 96-well plate. The fluorescence intensity was measured at excitation 485 nm and emission 530 nm on a Fluorstar optima plate reader. The optimal incubation time with 500 µg/ml FITC-dextran was 30 minutes which gave a mid range intensity (~5000) on the standard curve, giving a window for change throughout subsequent experiments (B). Data shown are from two independent experiments.

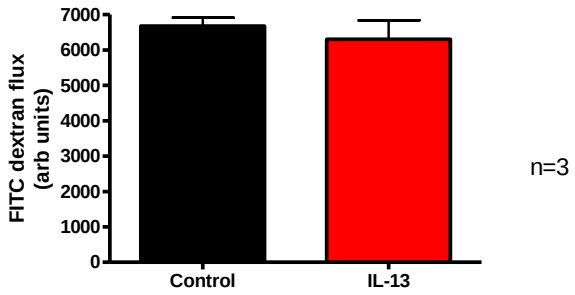

Figure 4.6 Effect of IL-13 on paracellular permeability.
Confluent Calu-3 cells were stimulated with IL-13 (10 ng/ml) for 24 hours, after which they were washed twice with HBSS to remove all traces of phenol red. HBSS (600 µl) was placed in the basolateral chamber and 200 µl of 500 µg/ml FITC-dextran was placed in the apical chamber. Cells were incubated at 37°C for 30 minutes and triplicate samples (each 100 µl) were taken from the basolateral chamber and placed into a black 96-well plate. The fluorescence intensity was measured at excitation 485 nm and emission 530 nm on a Fluorstar optima plate reader. Data are expressed as mean values ± SEM from n=3 independent experiments.

4.5 Effect of IL-13 on epithelial surface properties by scanning electron microscopy (SEM)

Calu-3 cells were stimulated with IL-13 for 24 hours and their surface properties were studied using SEM (Figure 4.7). Vehicle treated cells (Figure 4.7 A, B and C) displayed the same ciliated appearance as shown in the last chapter in Figure 3.2, the cilia were present on 90% of all cells in the monolayer and displayed the same star-like form. After 24 hour IL-13-treatment (Figure 4.7 D, E and F), 70% of the cell surface area was covered in tangled stringy structures which are believed to be secreted mucus. These structures are seen most clearly in image F which is a highly magnified area of image E. Images B and E clearly show the cell boundaries labelled with red arrows

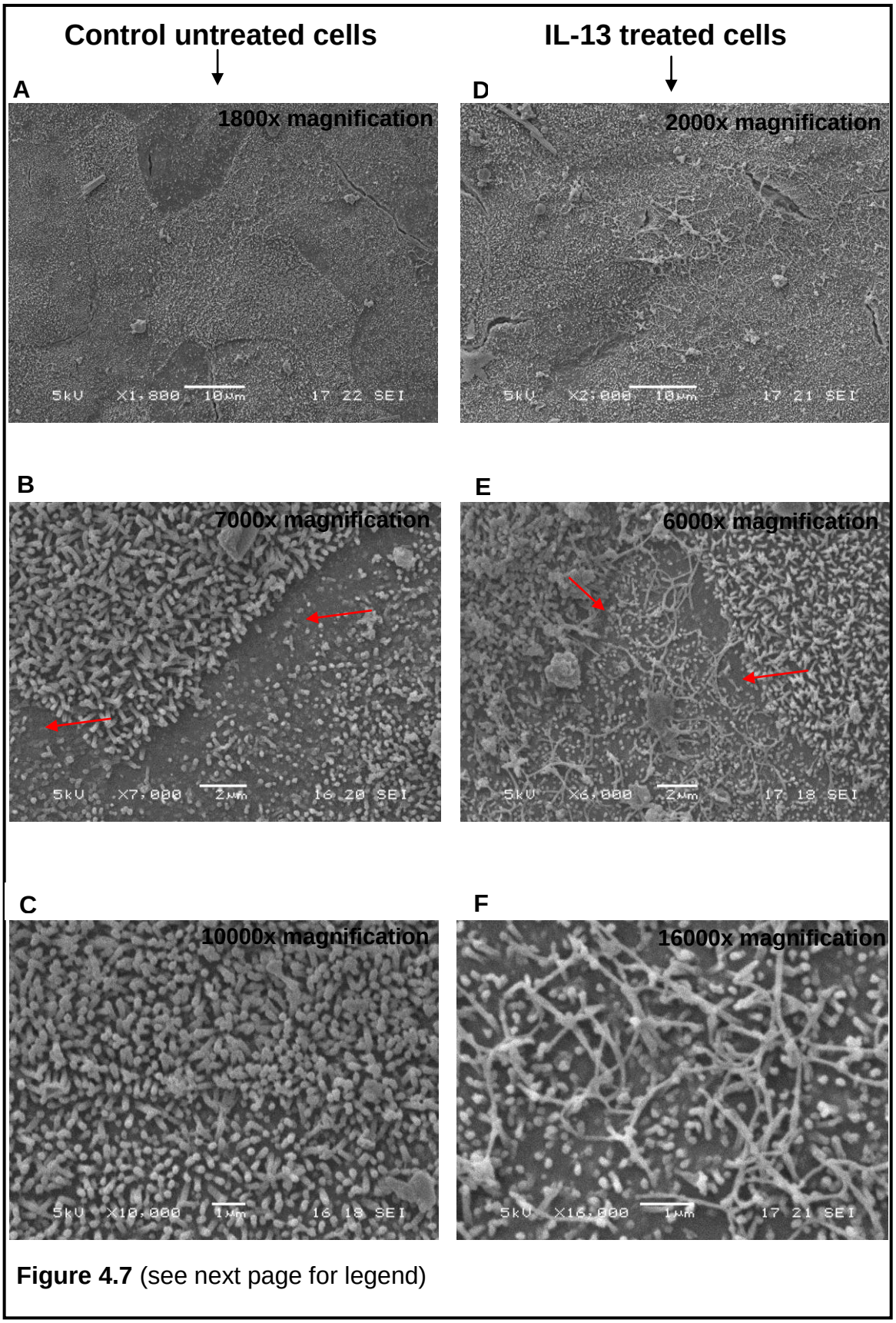

Figure 4.7 (see next page for legend)

Figure 4.7 Effect of IL-13 on the surface properties of Calu-3 cells by SEM imaging.

Calu-3 cells were grown via air-liquid interface culture for 7 days, they were then stimulated for 24 hours with IL-13 (10 ng/ml). Cells were washed with serum free MEM and placed in the fixative solution, , 2.5% glutaraldehyde, 0.5g potassium ferrocyanide in media for 2 hours at 37°C. Cells were then washed and postfixed with 1% osmium tetroxide and 1% potassium ferrocyanide for 1 hour at room temperature. Cells were washed with water and were then stained with 2% uranyl acetate for 1 hour in the dark. They were then slowly dehydrated with acetone and HDMS washes, then coated with an ultrathin layer of gold and viewed on a JEOL SEM6480LV scanning electron microscope. Vehicle control treated cells (A-C) do not display the stringy cell surface feature that is displayed on the IL-13 treated cells (D-F). Images A and D are at low magnification and give an overall idea of the cell surface with many cells visible. B and E are taken at a higher magnification and show the junctional space between cells, illustrated with red arrows. Images C and F are the highest magnification taken and clearly show the difference in cell surface features between control and IL-13 treated cells. Images are representative of n=3 independent experiments.

4.6 Effect of IL-13 on MUC5AC expression

To investigate whether the 'stringy' cell surface features observed by SEM were mucus as believed, the expression of one of the main mucins present in the lung, MUC5AC protein was investigated using immunofluorescence. Calu-3 cells were grown to confluence at ALI and treated with IL-13 for 24 hours; cells were then stained for the MUC5AC protein and examined on a confocal microscope. IL-13 treatment resulted in an increase in MUC5AC expression after 24 hours (Figure 4.8 A). The mRNA expression of MUC5AC was explored after long-term IL-13 stimulation up to 21 days which is the longest time in which cells can be studied at ALI by quantitative PCR (Figure 4.8 B). IL-13 treatment demonstrated a noticeable upregulation of MUC5AC after 48 hours which continued to increase up to 7 days when the increase was shown to be statistically significant compared to control cells. After 14 days IL-13 stimulation the level of MUC5AC dipped (due to one low data point) and then increased back up to significantly higher levels at days 14 and 21. The data indicates that IL-13 upregulates mRNA after 48 hours however upregulation of the IL-13 protein level occurs after just 24 hours.

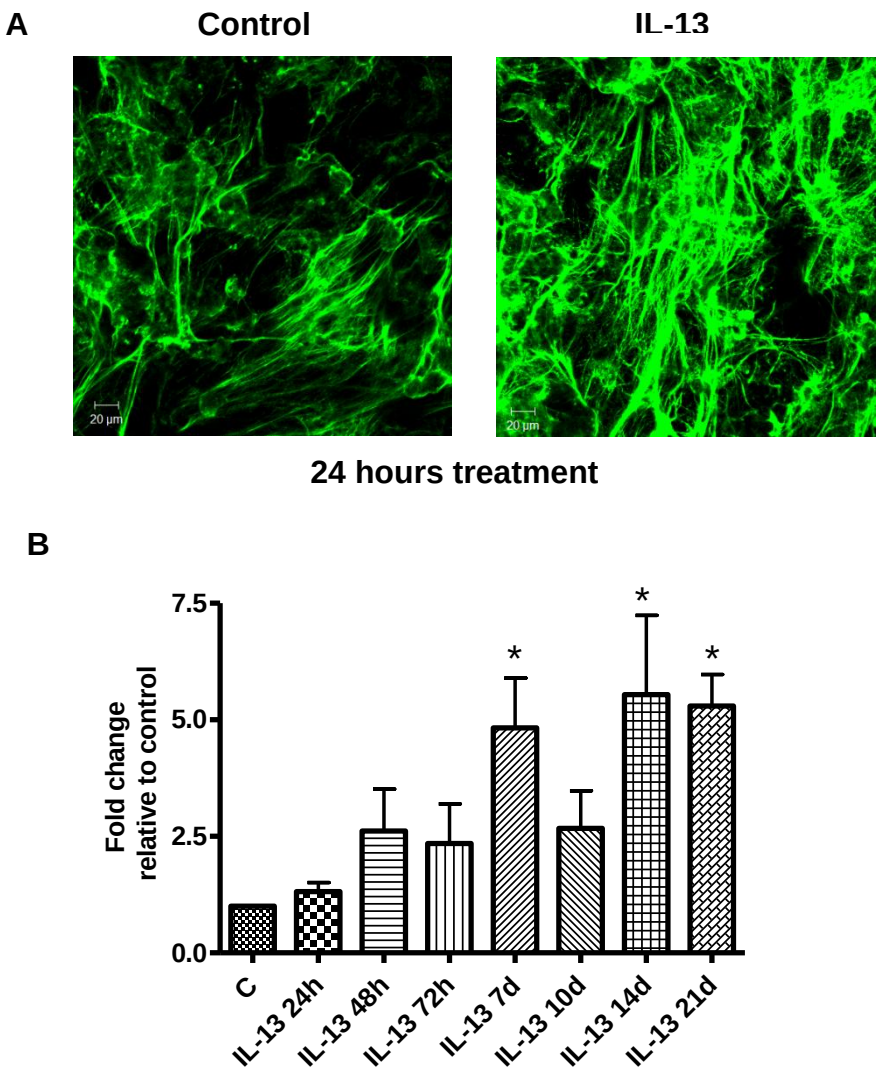

Figure 4.8 Effect of IL-13 stimulation on MUC5AC protein and mRNA expression.

Cells were treated with IL-13 at 10ng/ml for 24 hours (A) and up to 21 days (B), IL-13 and culture media were changed every other day. Cells were washed, fixed and stained with antibodies against the mucin MUC5AC. Transwell filters were cut out and mounted onto glass sides and viewed with a LSM510META confocal laser scanning microscope. In B, cells were lysed and RNA was extracted using an RNeasy mini kit. qRT-PCR reactions were run on a StepOne Plus PCR machine and MUC5AC mRNA expression was compared to β-actin as an equal loading gene and then normalised to the control group. A, images are representative of three independent experiments. B, data are shown as mean ± SEM for three independent experiments, in which all groups were compared to control for statistical significance which is expressed as (*) for $p<0.05$.

4.7 The signalling pathways that are activated by IL-13

In order to establish how IL-13 plays a role in epithelial barrier modulation, the signalling pathways activated by IL-13 were investigated. Figure 4.9 shows that IL-13 phosphorylates Akt which is a common measure of PI3K activity; this phosphorylation reaches a maximum at 15 minutes, but it not significantly different from the untreated control. Calu-3 cells are known to have very high basal level of phosphorylated Akt [290] which may explain why there is no significant stimulation. Repeating the same experiment in the alveolar epithelial cell line A549 showed a significant increase in Akt phosphorylation at 10 minutes.

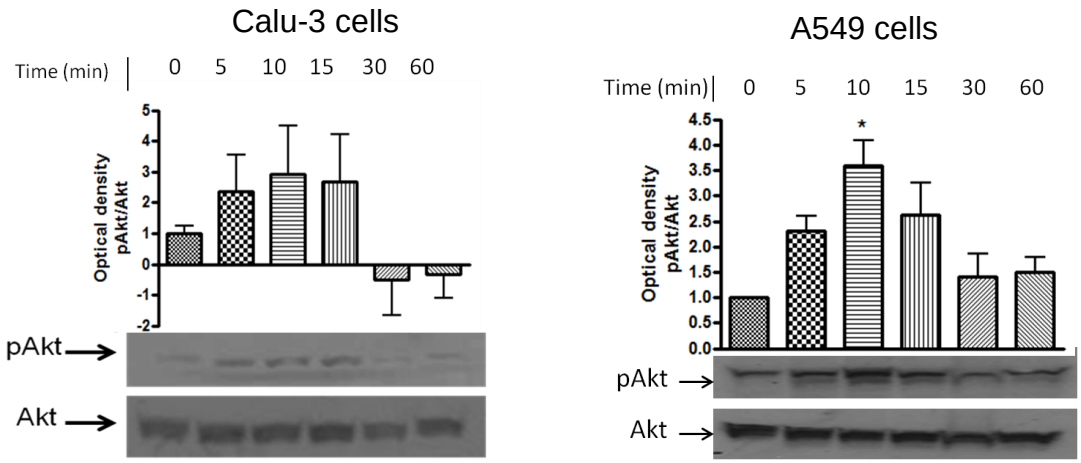

Figure 4.9 IL-13 timecourse study on Akt phosphorylation in Calu-3 cells and A549 cells.

For each experiment Calu-3 cells and A549 cells were seeded onto 12-well plates until confluency. The cells were then placed in serum free media at 37°C at 5% CO_2 overnight. Cells were treated with IL-13 at 10 ng for up to 90 minutes and then cells were washed with ice-cold PBS and lysed to extract all available protein. Protein concentration was measured using a Bradford assay and samples were boiled with 5X sample buffer and resolved on an SDS-PAGE gel with 25 µg protein in each sample. Samples were transferred onto nitrocellulose membrane and immunoblotted using antibodies against phosphoSer473 – Akt (pAkt) and Akt1 with both protein bands detected at 60 kDa. Data shown are from three independent experiments. Optical density values are expressed as mean fold increase compared with control ± SEM.

4.8 Discussion

4.8.1 The effect of cytokines IL-13, IL-4 and IFN-γ on TJ modulation of Calu-3 cells grown at ALI

IL-13 has been shown to be highly upregulated in allergic asthma; here its role in TJ regulation was examined. IL-13 stimulation resulted in a significant decrease in TER of 40% after 24 hours treatment, this decrease was mimicked using the T_H2 cytokine IL-4 which resulted in a 35% decrease. The cytokine IL-1β did not have any effect on the TER compared to control, however the T_H1 cytokine IFN-γ brought about the opposite result to IL-13 and IL-4 and increased the TER 40% over basal levels. This difference between T_H1 and T_H2 cytokines is interesting and the effect shown by IFN-γ has not been shown in studies investigating TJ regulation in IBD whereby IFN-γ has a negative effect on the epithelial barrier by disrupting the tight junction through internalisation of the TJ proteins occludin, claudin 1, claudin 4 and JAM-1 [291].

The decrease shown by IL-13 stimulation in the TER assay was not accompanied by an increase in paracellular permeability by FITC-dextran as would be expected if a paracellular space had opened up. There are three scenarios which can occur that connect TER and FITC-dextran permeability, shown in Figure 4.10 below. The data in the first part of this chapter indicate scenario 2 where the result is the formation of an ion channel.

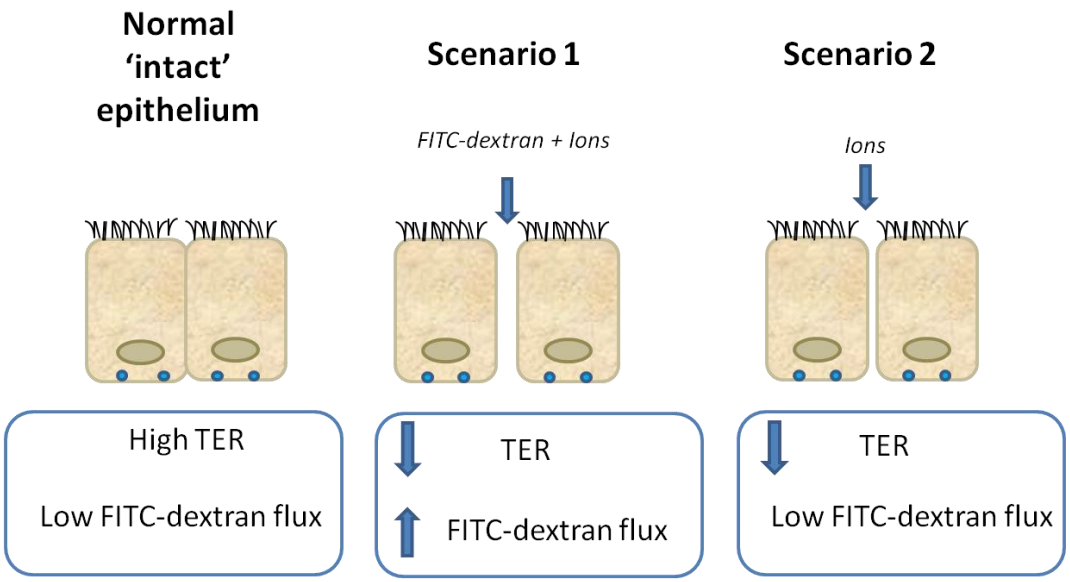

Figure 4.10 Possible outcomes in TER vs FITC dextran.

There are 3 possible scenarios that can occur when looking at TER and FITC dextran permeability. A normal intact epithelial layer will possess a high TER and a low FITC dextran flux. If there is a decrease in TER it is often accompanied by an increase in FITC dextran flux as shown in scenario 1, but it is also possible to see a decrease in TER coupled with no change in FITC-dextran flux which indicates a small gap opening between cells and could also indicate an ion channel forming which would decrease the TER but be too small to let FITC-dextran pass through.

4.8.2 The role of IL-13 in regulating TJ expression

The expression of the TJ protein claudin 2 was upregulated 25-fold compared to control by IL-13 after 24 hours, it was shown to move from a very low level of expression in the cytoplasm to more ordered junctional location in rings around each cell. Claudin 2 has been shown to be upregulated in the intestine [292] and has been reported to form a cation selective ion channel in MDCK cells with a pore diameter of 6.5 ± 0.3 Å [293]. Transfection of human claudin 2 into MDCK C7 cells resulted in a cation channel forming which was responsible for the paracellular water flux through the tight junction [294].

Claudin 2 and claudin 15 have recently been reported to control paracellular Na^+ ion flow in the intestine. Claudin 2 $^{-/-}$ and claudin 15 $^{-/-}$ double knockout mice were shown to have a reduced concentration of Na^+ in the lumen as well as a disruption in the absorption of amino acids and glucose resulting in death by day 25 from malnutrition [295]. Tamura *et al* argue that claudin 15 but not claudin 2 is responsible for this Na^+ ion flow regulation in the intestine [296].

IL-13 may regulate claudin 2 by post-translational modification, Van Itallie *et al* have recently published data which shows that phosphorylation of claudin 2 at Serine 208 is responsible for its retention at the plasma membrane [297]. However, to rule out this theory future experiments investigating the effect of IL-13 on mRNA expression could be undertaken to show whether IL-13 is acting in a transcriptional or post-transcriptional manner.

4.8.3 The effect of IL-13 on the surface morphology and mucus secretion of Calu-3 cells

Calu-3 cells treated with IL-13 for 24 hours displayed long stringy structures on their surface determined by SEM images at various magnifications. These structures were labelled as mucus. IL-13 has been shown to play a role in the feature of asthma where an overproduction of mucus blocks the airways, termed goblet cell metaplasia (GCM) and mucus hypersecretion. Treatment with IL-13 resulted in an increase in MUC5AC protein on the cell surface after 24 hours shown by immunofluorescence data which correlates with Nakano *et al* who showed that IL-13 treatment increases the number of goblet cells in mouse tracheal after only 24hours [298]. In primary epithelial cells IL-13 was shown to increase the number of goblet cells, MUC5AC mRNA and protein expression after 14 days [299, 300], which is consistent with the results shown here in the quantitative PCR experiment, which demonstrated an increase in MUC5AC mRNA at 7,14 and 21 days IL-13 treatment. The expression of the calcium activated chloride channel hCLCA1 has also been shown to be up-regulated by IL-13 after

14days and was shown to co-localise with MUC5AC in goblet cells suggesting a role for hCLCA in IL-13-incuced mucus hypersecretion [300]. Anti-IL-13Rα1 reduces the IL-13 MUC5AC and goblet cell protein and mRNA upregulation in NHBECs in accordance with previous publications stating that IL-13 is mediating its affects via the IL-13Rα1 complex. Tanabe *et al* also studied the role of IL-13Rα2 in GCM and found that recombinant IL-13Rα2 but not anti-IL-13Rα2 decreased goblet cell numbers, PAS positive cells, MUC5AC protein and mRNA expression when combined with IL-13, implying that soluble the IL-13Rα2 plays a role in the regulation of GCM.

4.8.4 Limitations and future experiments

To further explore the effect of IL-13 on the proposed ion channel formation shown in Figure 4.10, scenario 2, an ion flux assay could be carried out. Ion binding dyes such as fluor-2 and ANG-2 which bind to Ca2+ and Na+ ions respectively can be added to the apical chamber in the concentrations 10-100 μM. The ion-bound dye can then be detected by sampling the basolateral media and testing the fluorescence [301]. An unfortunate limitation of the work in this chapter was the inability to further investigate the effect of IFN-γ on barrier modulation after the result observed in the TER assay. Stimulation with the T_H1 cytokine IFNγ resulted in the opposite effect on TER to that of IL-13, with an increase in resistance above control. This result is conflicting with studies that have shown that IFNγ disrupts the epithelial barrier in intestinal bowel disease and decreases the TER [302]. This indicates that the regulation of tight junctions in the lung may not be the same as those in the intestine.

4.9 Conclusions

In this chapter the role of IL-13 in the modulation of tight junction proteins was explored. IL-13 was shown to decrease TER by ~30% after 24 hours treatment, however, this was not coupled with an increase in the paracellular permeability of the macromolecule FITC-dextran which indicates that an ion channel has formed in response to IL-13 stimulation. Claudin 2 protein upregulation by IL-13 shown by both immunoblotting and immunofluorescence after 24 hours emphasises the validity of the theory of ion channel formation as it is known to be a pore forming tight junction protein which is involved in forming a paracellular water channel [294].

In summary, in this chapter the following was determined:

- IL-13 causes a decrease in TER of up to ~30% after 24 hours treatment.
- IL-13 has no effect on the paracellular permeability of FITC-dextran.
- The TJ proteins claudin 1 and 2 were upregulated by IL-13 shown by immunoblotting.
- The distribution of claudin 2 altered from cytoplasmic to junctional after 24 hour IL-13 treatment.
- Junctional proteins occludin, ZO-1, E-cadherin and β-catenin were not altered by IL-13 treatment.
- IL-13 causes an upregulation of mucus on the cell surface of Calu-3 cells after 24 hour treatment.

With the results in this chapter indicating a role for IL-13 in the modulation of the tight junction, the next step was to look at the signalling pathways behind these IL-13-induced responses.

Chapter 5 : Role of PI3K in epithelial barrier modulation

One of the most common signalling pathways activated by IL-13 is the PI3K pathway. In the context of this thesis, it was necessary to investigate the possible role of this pathway in the regulation of the TJ complex in the lung and particularly the IL-13-induced effects on TJ proteins mentioned in chapter 4.

The PI3K pathway has been extensively researched in a variety of cancers [65, 74, 303-305] as well as in inflammatory diseases [73, 76, 88, 89, 106, 277, 306]. Class IA PI3Ks are involved in human cancers as they drive Akt activation by producing PtdIns(3,4,5)P3 which promotes tumor cell survival and proliferation [61]. PI3K has been reportedly involved in inflammatory bowel disease (IBD), where it was found to control adherens junction formation as well as activating the p38 MAPK cascade [277]. Over the last decade the dysregulation of the PI3K pathway has been shown to be involved in the pathogenesis of respiratory diseases such as severe asthma, yet its exact role and the key isoforms involved are yet to be discovered.

IL-13 has been shown to phosphorylate Akt, the key protein kinase downstream of PI3K, at Serine 473 [307] and this phosphorylation is often used as a measure of PI3K activity. PI3K can be silenced using synthetically generated siRNA specific to individual isoforms or inhibited by the addition of small molecule inhibitors which usually competitively block to the ATP binding pocket. Previous members of the group have used siRNA systems to observe PI3K due to the lack of commercially available isoform selective inhibitors [73], however recently many highly selective class I PI3K isoform inhibitors have been produced (see Figure 1.4). This chapter will assess the role of class I PI3K inhibition in the modulation of junctional proteins in the lung using small molecule inhibitors.

5.1 Effect of PI3K inhibition on the IL-13-induced decrease in transepithelial resistance

IL-13 was shown to cause a 30-40% decrease in TER, in order to discover the signalling pathways behind this response, cells were pretreated with the Class I PI3K inhibitor ZSTK474 for 30 minutes and then subsequently subjected to IL-13 stimulation for up to 72 hours. Class I PI3K inhibition with the highest concentration of ZSTK474 (10 μM) resulted in the prevention of the IL-13-induced decrease in TER (shown in Figure 5.1 A). Treatment with ZSTK474 and IL-13 resulted in a 60% increase in TER over IL-13-stimulated cells (Figure 5.1 B). Cells were treated with lower concentrations of ZSTK474 (1 and 0.1 μM) for 24 hours; neither 1 μM nor 0.1μM ZSTK474 showed a significant effect on the IL-13-induced decrease in TER. Pre-treatment with ZSTK474 at the lowest concentration 0.1 μM followed by IL-13 was statistically different from the control groups as was the case with the IL-13 stimulated cells. Cells were also treated with the pan-PI3K inhibitor LY294002 for 24 hours which prevented the IL-13 induced decrease in TER (Figure 5.1 B).

In an attempt to uncover the PI3K isoform responsible for the effect shown, selective small molecule PI3K isoform inhibitors were used. The PI3K selective isoform inhibitor IC87114 targets the p110δ isoform of PI3K and cells treated with this inhibitor alone showed a slightly higher TER than that of untreated cells, however this increase was not statistically significant (Figure 5.2). There was also no significant difference between the IL-13 treated cells and those pre-treated with the p110δ inhibitor followed by IL-13. The same was observed for the p110β inhibitor TGX-221. Addition of TGX-221 alone resulted in TER that was identical to that of control cells and the decrease in TER observed when cells were pretreated with TGX-221 before IL-13 stimulation mimicked the IL-13 alone result. Treatment with the p110α inhibitor PIK75 resulted in a large decrease in TER indicating that the p110α isoform is required to maintain a high basal TER. The dual p110β and p110δ inhibitor TGX-121 had no effect on TER and produced the same results with

or without inhibitor addition. These data do not correlate with the results seen using the pan-class I inhibitor ZSTK474, which indicates that either all isoforms play individual but vital roles in maintaining the TER or that the ZSTK474 inhibitor is having off target effects.

In order to investigate whether each class I PI3K isoform had an essential role in modulating the epithelial barrier, all the selective isoform inhibitors were added at the same time and the TER was monitored. Cells treated with IC87114, TGX-221 and PIK75 together resulted in a 20% decrease in TER (Figure 5.3) which did not change upon IL-13 stimulation. To eliminate the possible involvement of the class II PI3Ks along with the key serine/threonine kinase mammalian target of rapamycin (mTOR), cells were treated with PI-103 which had been shown to inhibit PI3K C2β, p110α and mTOR at high concentration [308]. Pre-treatment with PI-103 (300 nM) alone had no effect on TER and the same was shown for the combined PI-103 and IL-13 treatment (Figure 5.3 B)

The PI3K inhibitors LY294002 and wortmannin have been reported to inhibit mTOR by irreversibly inhibiting its serine specific autokinase activity; [85] ZSTK474 has been shown not inhibit mTOR in this way [99]. To investigate whether mTOR inhibition was the reason behind the IL-13-induced TER recovery seen by ZSTK474, Calu-3 cells were treated with the potent mTOR inhibitor, Rapamycin. In this experiment, Rapmycin was administered in two concentrations, the highest of which (20 nM) resulted in a decrease in TER in both inhibitor and inhibitor + IL-13 treatments. The lower concentration of Rapamycin (2 nM) was shown to have little to no effect on the TER (Figure 5.3 C), indicating that mTOR is not responsible for causing the IL-13-induced decrease in TER.

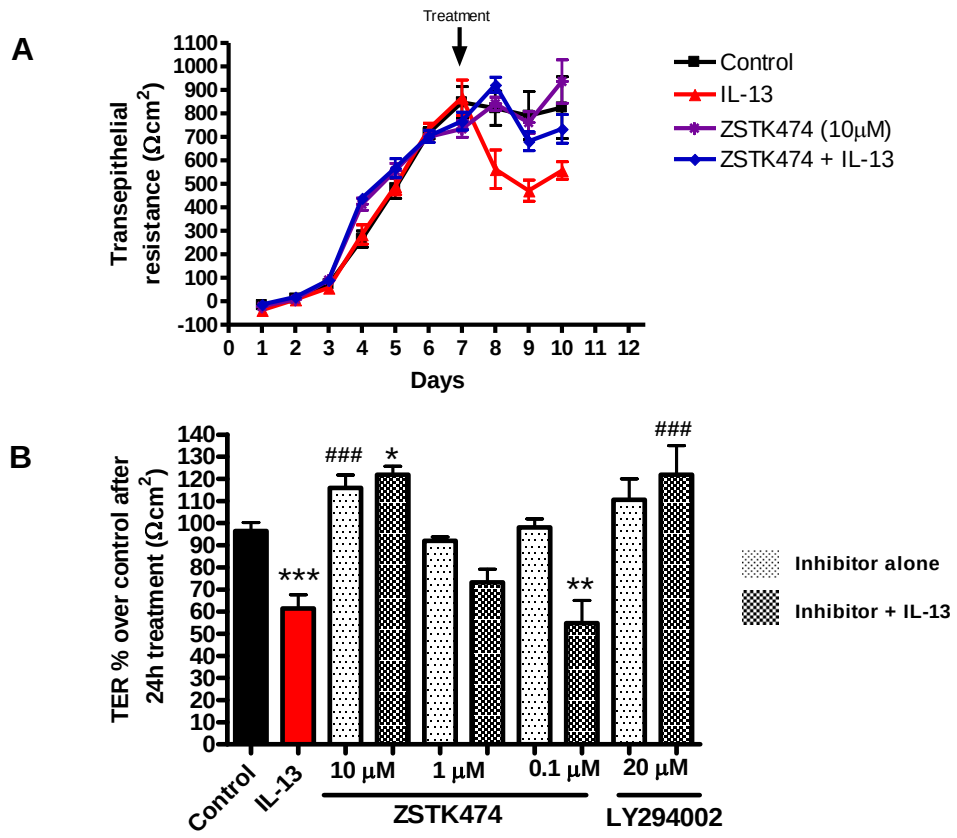

Figure 5.1 Effect of Class I PI3K inhibition on transepithelial resistance.

For each experiment $5x10^5$ cells/ml were seeded onto transwell filters and their transepithelial resistance was monitored every 24 hours. When cells reached confluency on day#7 they were treated with ZSTK474 (10 μM) followed by addition of IL-13 (10 ng/ml) for up to 72 hours. The TER was measured after 24, 48 and 72 hours, this raw value was subtracted from the background reading (obtained from a transwell insert without cells) and multiplied by the transwell area to obtain TER Ωcm^2 (A). Confluent cells at day#7 were treated with ZSTK474 (10, 1 and 0.1 μM) or LY294002 (20 μM) and IL-13 (10 ng/ml) for 24 hours. The TER was measured before treatment and after 24 hours and the raw value was converted to a percentage of the TER prior to treatment (B). Data expressed as mean values ± SEM from n=5 (C, IL-13 and ZSTK474 10μM) and n=3 (ZSTK474 1μM, ZSTK474 0.1μM and LY294002 20 μM) independent experiments. All inhibitor + IL-13 treated groups were compared to IL-13 stimulation alone and statistical significance is expressed as (###) for $p<0.001$. All groups were compared to control and statistical significance is expressed as (*) for $p<0.05$, (**) for $p<0.01$ and (***) for $p<0.001$.

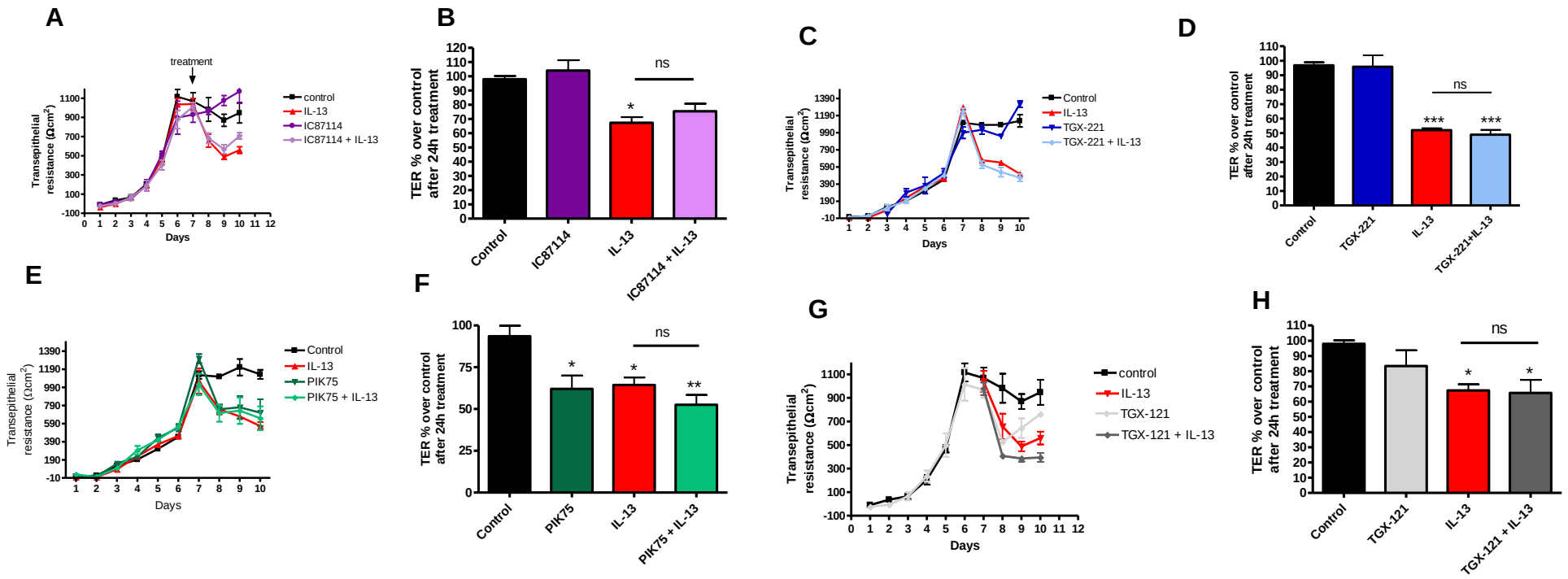

Figure 5.2 Effect of isoform selective PI3K inhibitors on transepithelial resistance.

For each experiment $5x10^5$ cells/ml were seeded onto transwell filters and their transepithelial resistance was monitored every 24 hours. On day#7 when the maximum TER was reached IC87114 (p110δ inhibitor, 10 μM) TGX-221 (p110β inhibitor, 100 nM), PIK75 (p110α inhibitor, 100 nM) and TGX-121 (p110β and p110δ dual inhibitor, 10 nM) were added to the basolateral chamber for 30mins followed by IL-13 (10 ng/ml) and the TER was measured after 24, 48 and 72 hours (A,C, E and G). The TER was then compared to that of the same well 24 h prior to obtain the TER as a percentage of the control after 24 h treatment (B, D, F and H). Data expressed as mean values ± SEM n=6 (A,B), n=3 (C,D), n=3 (E,F), n=6 (G,H) independent experiments. All groups were compared to each other and statistical significance is expressed as (*) for $p<0.05$, (**) for $p<0.01$ and (***) for $p<0.001$. ns; not significant.

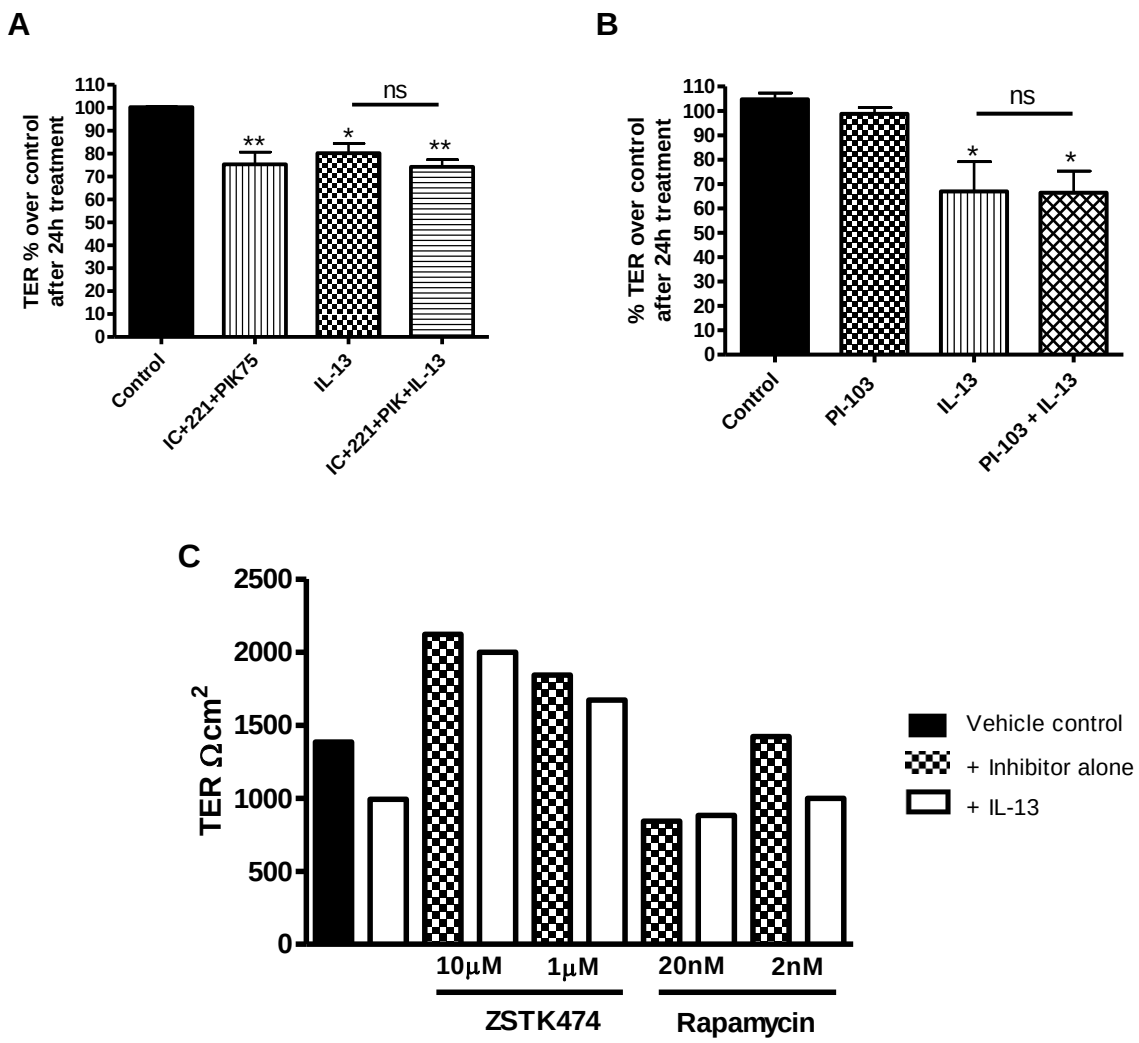

Figure 5.3 Effect of combined PI3K individual class I isoform addition, PI-103 and Rapamycin on transepithelial resistance.

For each experiment $5x10^5$ cells/ml were seeded onto transwell filters and their transepithelial resistance was monitored every 24 hours. On Day#7 when the maximum TER was reached IC87114 (p110δ inhibitor, 10 µM) TGX-221 (p110β inhibitor, 100 nM), PIK75 (p110α inhibitor, 100 nM) (A), PI-103 (300 nM) (B) and Rapamycin (20 nM and 2 nM) (C) were added to the basolateral chamber for 30 min followed by IL-13 at 10 ng/ml and the TER was measured after 24 hours. Data expressed as mean values ± SEM from three independent experiments (A and B) and two independent experiments (C). All groups were compared to the control group for statistical significance which is expressed as (*) for $p<0.05$ and (**) for $p<0.01$.

5.2 Investigating the efficacy of PI3K inhibitors

Phosphorylation at serine 473 of Akt was used as a marker of PI3K activity to investigate the efficacy of the various PI3K inhibitors. An IL-13 time course of Akt phosphorylation was carried out, where cells were pre-treated with the pan Class I PI3K inhibitor ZSTK474 or the specific class I isoform inhibitors IC87114, TGX-221 and PIK75 which target the delta, beta and alpha isoforms of PI3K respectively. The Class I PI3K inhibitor ZSTK474 completely abolished the Akt phosphorylation at all time points between 5 and 90 minutes (Figure 5.4 A) The PI3Kα inhibitor PIK75 reduced the Akt phosphorylation at both 15 and 30 minutes; both the PI3Kβ and δ inhibitors TGX-221 and IC87114 only slightly decreased the Akt phosphorylation (Figure 5.4 B).

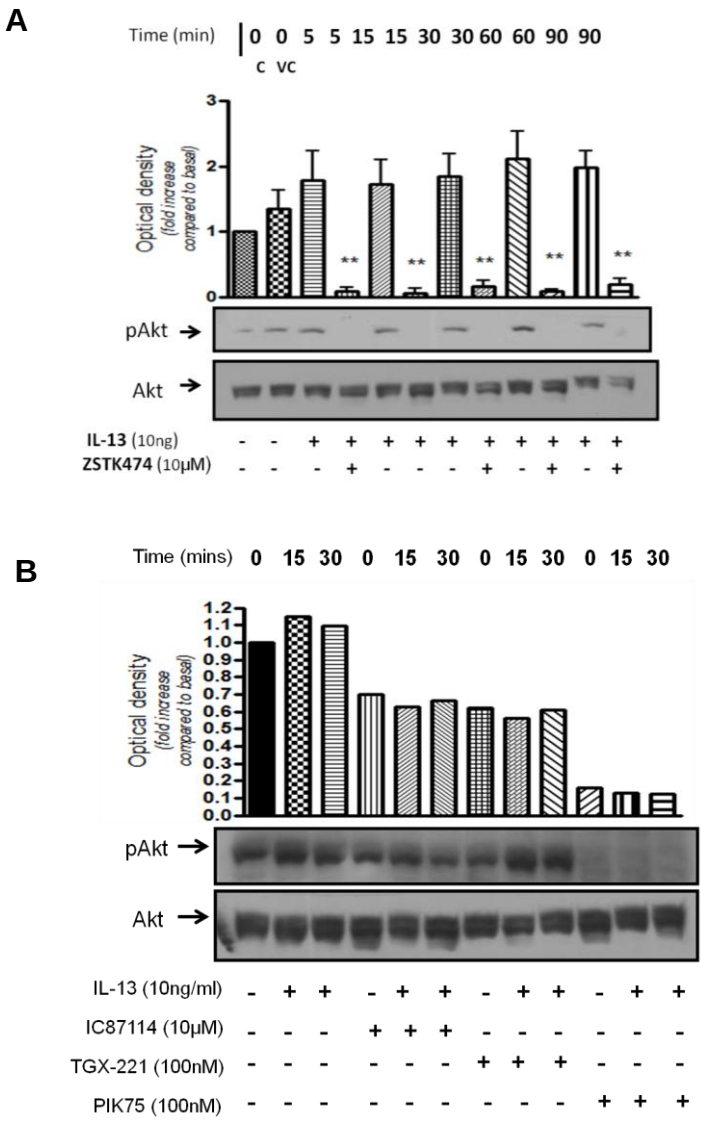

Figure 5.4 Effect of ZSTK474 pre-treatment on IL-13-induced Akt phosphorylation in Calu-3 cells.

Cells were plated onto 12-well plates in serum containing MEM. When confluent, cells were cultured in serum free MEM at 37°C at 5% CO_2 overnight. After which they were incubated for 30 minutes with ZSTK474 (10 μM) (graph A) or IC87114 (10 μM), TGX-221 (100 nM) and PIK75 (100 nM) (graph B) and then stimulated with IL-13 (10 ng/ml) for up to 90 minutes in graph A or 15 and 30 minutes in graph B. Samples were resolved by SDS-PAGE, transferred to nitrocellulose membranes and immunoblotted, using antibodies against phosphoSer473-Akt (pAkt) and Akt1 with both protein bands measured at 60 kDa. Data are presented as n=3 (A) and n=2 (B) independent experiments. All groups were compared to vehicle control for statistical significance, which is expressed as (**) for $p<0.01$ and (*) for $p<0.05$

5.3 Effect of class I PI3K inhibition on paracellular permeability

In chapter 4, IL-13 was shown to decrease TER but have no effect on the paracellular permeability of FITC-dextran, which was concluded to be through small cationic pore formation. To test the effect of PI3K inhibition on FITC-dextran flux cells were treated with PI3K inhibitors prior to IL-13 stimulation for 24 hours (see section 2.3 for more details). None of the PI3K inhibitiors tested (ZSTK474, IC87114, TGX221 and PIK75) had any significant effect on the permeability of FITC-dextran compared to that of untreated control cells. (Figure 5.5)

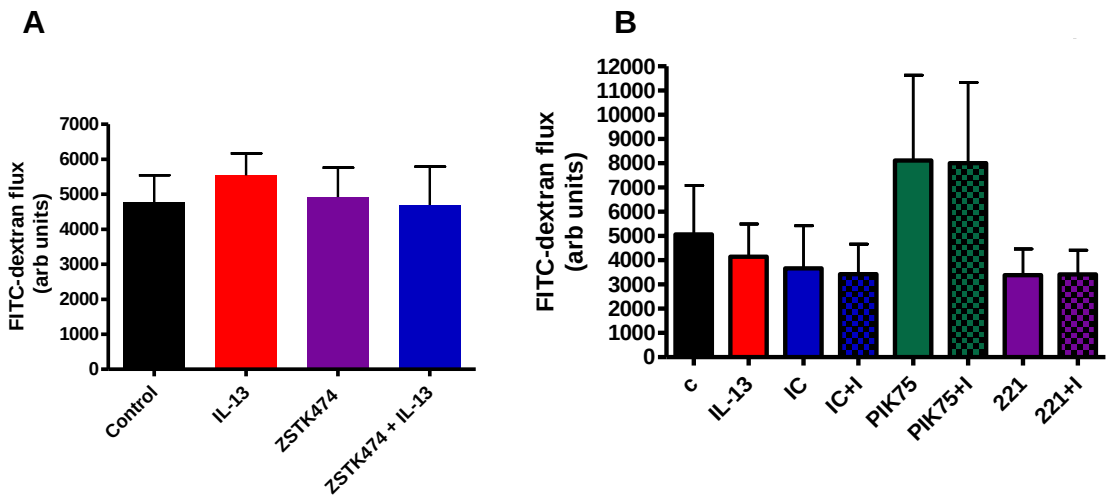

Figure 5.5 Effect of class I PI3K inhibition on paracellular permeability. Calu-3 cells were stimulated with ZSTK474 (pan-class-I-PI3K inhibitor,10 µM), IC87114 (p110δ inhibitor, 10 µM), TGX-221 (p110β inhibitor, 100 nM) and PIK75 (p110α inhibitor, 100 nM) for 30mins followed by IL-13 at 10 ng/ml. They were washed twice with HBSS to remove all traces of phenol red and 600 µl HBSS was placed in the basolateral chamber and 200 µl of 500 µg/ml FITC-dextran was placed in the apical chamber. Cells were incubated at 37°C at 5% CO_2 for 30 minutes after which 100 µl was pipetted from the basolateral chamber of each sample in triplicate onto a black 96-well plate. The fluorescence intensity was measured at excitation 485 nm and emission 530 nm on a Fluorstar optima plate reader. Data are presented as n=6 (A) and n=3 (B) independent experiments.

5.4 Effect of PI3K inhibition on junctional protein expression and distribution by immunocytochemistry

Confluent cells grown via ALI were pretreated with PI3K inhibitors for 30 minutes then stimulated with IL-13 for 24 hours and claudin 2 was probed for using immunocytochemistry (see section 2.4 for details). Treatment with ZSTK474, PIK75 and LY294002 decreased the basal expression of claudin 2 which was not restored following stimulation with IL-13; LY294002 did not completely abolish the IL-13-inducation of claudin 2 to the same extent of ZSTK474 and PIK75 (Figure 5.6). The p110β and p110δ inhibitors (IC87114 and TGX221) had no effect on basal or IL-13-stimulated claudin 2 upregulation.

5.5 Effect of PI3K inhibition on claudin 2 mRNA expression by qRT-PCR

To evaluate the mRNA expression of the TJ protein claudin 2 after IL-13 and PI3K inhibition, quantitative PCR was carried out. Confluent cells at ALI were treated with IL-13 and various PI3K inhibitors for 24 hours, they were lysed and RNA was extracted using an RNeasy mini kit (see section 2.6). Although stimulation with IL-13 seemed to show an increase in mRNA expression, there was no significant difference due to one experiment demonstrating a much higher IL-13 stimulated effect than the previous two experiments, so the result remains inconclusive and further experiments are needed to clarify this affect. Treatment with the PI3K inhibitors (ZSTK474, IC87114 and PIK75) did not show any significant difference in mRNA expression compared with that of the untreated control (Figure 5.7). Treatment with ZSTK474 appears to reduce the expression of claudin 2 compared with that of the IL-13 stimulated cells, but as previously mentioned, further experiments are needed in order to form accurate conclusions on the effect of both IL-13 and PI3K on claudin 2 mRNA expression.

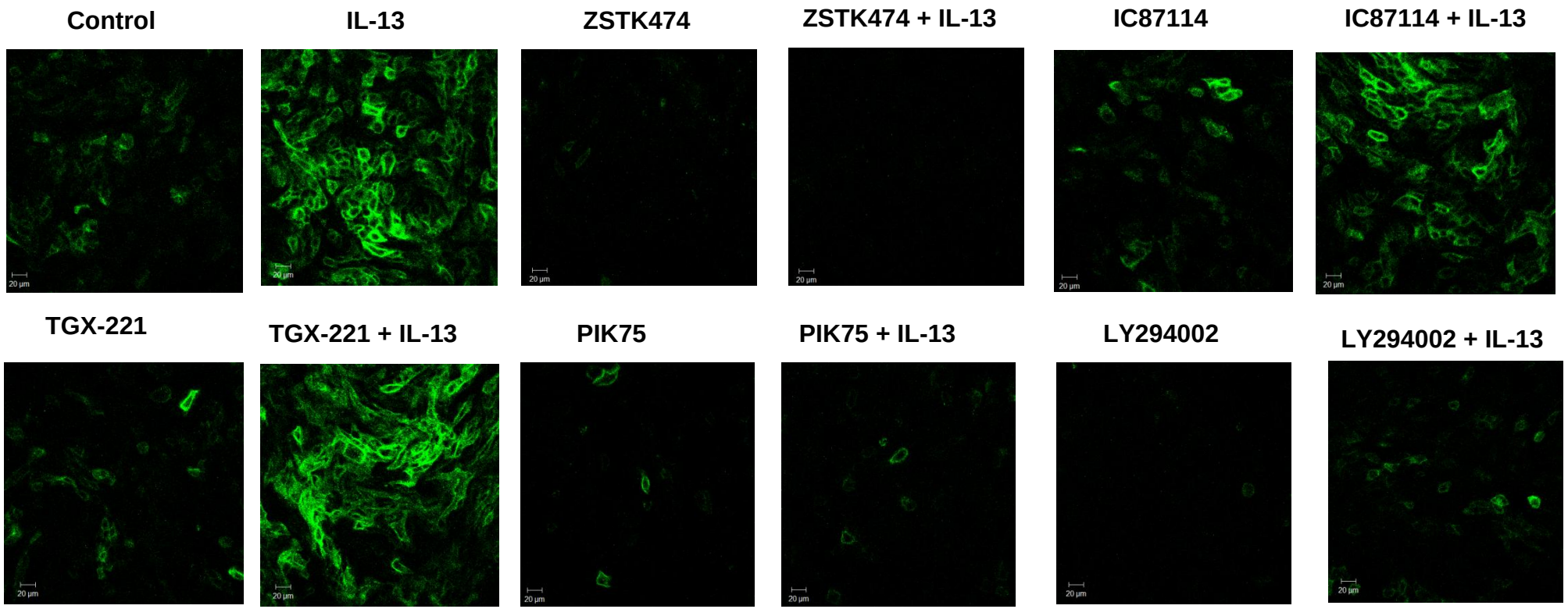

Figure 5.6 Effect of Class I PI3K inhibition on claudin 2 distribution.

Calu-3 cells were stimulated with ZSTK474 (pan-class-I-PI3K inhibitor,10 μM), IC87114 (p110δ inhibitor, 10 μM), TGX-221 (p110β inhibitor, 100 nM), PIK75 (p110α inhibitor, 100 nM) and LY294002 (20 μM) for 30mins followed by IL-13 (10 ng/ml) for 24 hours. After which they were fixed and probed for the tight junction protein claudin 2 (see section 2.4 for details). The filters were then mounted onto glass slides and viewed using a LSM510META confocal laser scanning microscope. Each image is representative of three similar images taken during three independent experiments (n=3), for magnification see scale bars displayed on each image.

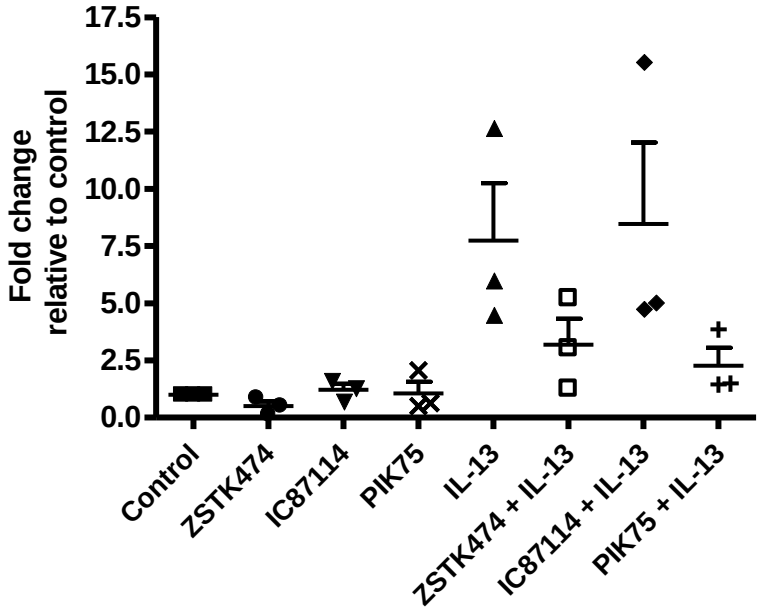

Figure 5.7 Effect of PI3K inhibition on claudin 2 mRNA expression by qRT-PCR.

Confluent Calu-3 cells grown via ALI were treated with ZSTK474 (pan-class-I-PI3K inhibitor, 10 μM), IC87114 (p110δ inhibitor, 10 μM) and PIK75 (p110α inhibitor, 100 nM) for 30mins followed by 10 ng/ml IL-13 for 24 hours. Cells were lysed and RNA was extracted, reversed transcribed to cDNA and reactin were performed on a StepOnePlus Real-time PCR system. All samples were compared to the equal loading gene β-actin and normalised to the untreated control sample. Data expressed as mean values ± SEM from n=3 independent experiments.

5.6 Apical vs basolateral chamber stimulation on the role of PI3K in IL-13-induced decrease in TER

As most asthma drugs are administered by inhalation and transported from the apical side of the epithelium to the basolateral side into the underlying smooth muscle cell layer, inhibitors were placed into the basolateral chamber. Figure 5.8 shows preliminary data showing that adding the various PI3K inhibitors to the top side of the cells (apical) brought about the same response as if they were added to the basolateral (basement membrane) side. Interestingly, treatment with PIK75 to the apical chamber resulted in a ~60% decrease in TER which is around a 20% greater decrease than when administered to the basolateral side in Figure 5.2. IL-13 was administered to the basolateral side of the chamber as physiologically in the lung IL-13 will come from T-cells present in the submucosa.

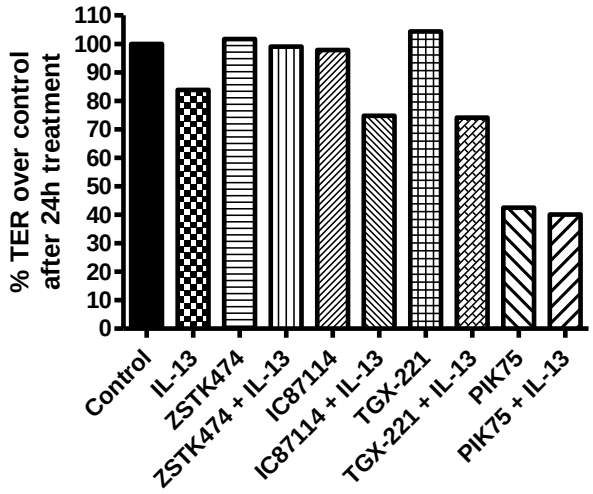

Figure 5.8 Effect of apical vs basolateral chamber administration of PI3K inhibitors on TER in Calu-3 cells.

Calu-3 cells were grown via ALI and when confluent they were placed in serum-free media overnight. PI3K inhibitors ZSTK474 (10 μM), IC87114 (10 μM), TGX-221 (100 nM) and PIK75 (100 nM) were placed in 200 μl of serum free-media and placed in the apical chamber (on top of cells) for 30 minutes prior to IL-13 addition to the basolateral chamber for 24 hours. The TER was monitored before and after as in previous TER experiments. Data shown is preliminary data expressed as the mean of triplicate values from n=1 experiment.

5.7 Effect of IL-13 and PI3K inhibition on IL-13 receptor surface expression by flow cytometry

Research has shown that increased expression of IL-13Rα2 at the cell surface can impact signalling by inhibiting IL-13 responses [60]. Higher expression of this second IL-13 receptor, IL-13Rα2 is presumed to compete against the first receptor IL-13Rα1 for IL-13 and therefore results in less IL-13 available for the IL-13Rα leading to a dampened response. It was necessary to study the expression of IL-13Rα2 on basal and stimulated Calu-3 cells, as a possible explanation of the results observed to date using the PI3K inhibitors may be due to upregulation of the IL-13Rα2 expression.

To investigate the surface expression of IL-13Rα2 fluorescence-activated cell sorting (FACS), a specific type of flow cytometry was used (Figure 5.9). Calu-3 cells proved difficult to analyse by FACS due to their heterogeneous nature being a submucosal cell line. IL-13Rα2 was expressed on 20% of control Calu-3 cells, after IL-13 stimulation with both 1 and 10 ng/ml this surface expression increased to 34% and 33% respectively. Pretreatment with the PI3K inhibitor ZSTK474 and the isoform selective inhibitors IC87114, TGX-221 and PIK75 before IL-13 stimulation returned IL-13Rα2 surface expression to control levels. These data indicate that PI3K signalling is involved in regulation of the expression of IL-13Rα2 on the cell surface of Calu-3 cells, but further experiments need to be carried out to prove this.

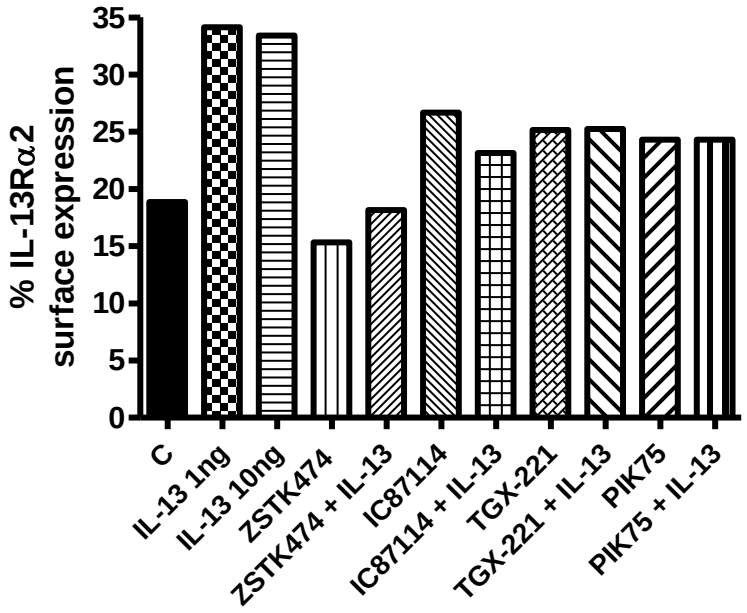

Figure 5.9 Effect of IL-13 and PI3K inhibition on IL-13Rα2 surface expression.

Cells were grown at ALI and once confluent at day#7 were stimulated with IL-13, with or without pre-treatment with ZSTK474 (10 μM), IC87114 (10 μM), TGX-221 (100 nM) and PIK75 (100 nM) for 24 hours. Cells were washed with PBS then 0.25% Trypsin/EDTA was added to detach the cells from the surface of the filter. Cells were then washed with PBS followed by addition of an antibody against IL-13Rα2 in 2% FBS in PBS for 1 hour. Cells were washed with PBS and resuspended with a secondary conjuated 488 Alexa Fluor labelled antibody for 1 hour at 4°C in the dark. Cells were washed wil PBS, resuspended in 500 μl of ice-cold PBS and samples were analysed on a FACSCanto flow cytometer. Data are presented as mean values from n=2 independent experiments.

5.8 Role of pan PI3K and selective isoforms in cell migration

The ability of cells to migrate and repair wounds is an essential part of epithelium constitution. PI3K has been shown to be involved in epithelial wound repair in skin fibroblasts and also has a role in IL-6 induced migration of BEAS2B lung epithelial cells [309].

A549 and Calu-3 cells were investigated in a wound healing assay. A549 cells had an average percentage regrowth of 33.4 ± 7% of the wound which was significantly lower than that of Calu-3 cells which was 62.6 ± 5% (Figure 5.10). In both A549 and Calu-3 cell lines IL-13 treatment resulted in little to no response after 24 hours with A549 cells staying the same at 33.6 ± 3% and Calu-3 cells decreasing to 54.9 ± 6% wound closure. PI3K was found to play an essential role in cell migration during the wound healing response, in both cell lines treatment with the pan-PI3K inhibitor ZSTK474 reduced the percentage of the wound healed to 19.9 ± 4.5% in A549 cells and -7.6 ± 4% in Calu-3 cells. The combined treatment of ZSTK474 + IL-13 did not change the percentage of wound healed in either cell line.

The PI3K response in cell migration was further investigated by addition of the PI3K isoform inhibitors PIK75, TGX-221 and IC871114 (Figure 5.11). In both cell lines the order in which the inhibitors reduced cell migration was TGX-221< IC87114 < PIK75. With p110β inhibition only resulting in a small decrease to 49.1 ± 4% in Calu-3 cells and 28.5 ± 6% in A549 cells. IC87114 showed a larger decrease in wounds with 36.9 ± 12% closure in Calu-3 cells and 16.5 ± 1.3% in A549 cells. Treatment with the p110α isoform was shown to reduce the wound healing response significantly in both cell lines with only 5.1 ± 2.1% regrowth in Calu-3 cells and 5.9 ± 2.5 % regrowth in A549 cells. These data imply the involvement of the p110α isoform in the role of PI3K in epithelial migration and wound healing.

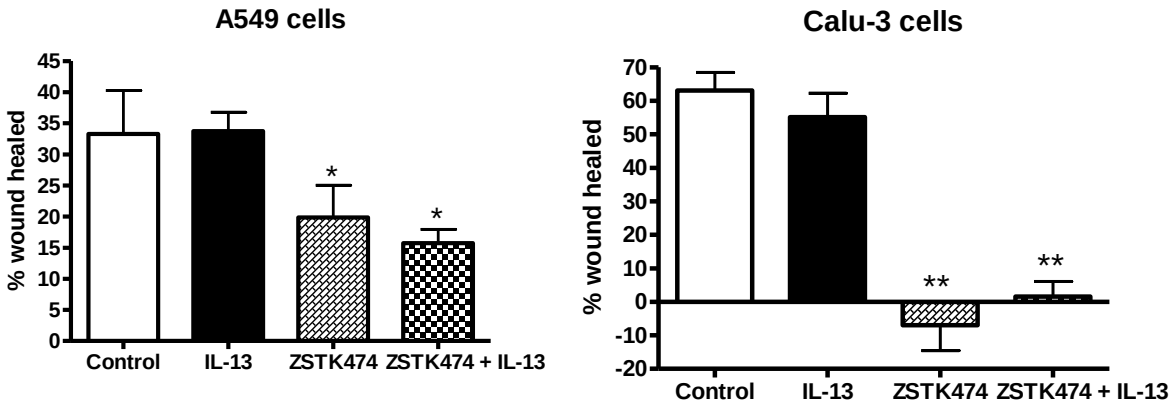

Figure 5.10 Effect of IL-13 and PI3K inhibition on cell migration in Calu-3 and A549 cells.

For each experiment, cells were plated onto 12-well plates in complete media and when confluent were placed in serum free media overnight at 37°C at 5% CO_2. Cells were then scratched with a pipette tip to make a wound, the wound was washed and photographed. PI3K was inhibited using the class-I inhibitor ZSTK474 (10 μM), which was added to serum free media for 30 minutes prior to IL-13 stimulation. IL-13 (10 ng/ml) was added to cells and they were incubated for 24 hours. Cells were washed and photographed and the % of wound healed was calculated using Tscratch software [310]. Data are presented as mean values ± SEM for three independent experiments. All groups were compared to control for statistical significance, which is expressed as (**) for $p<0.01$ and (*) for $p<0.5$

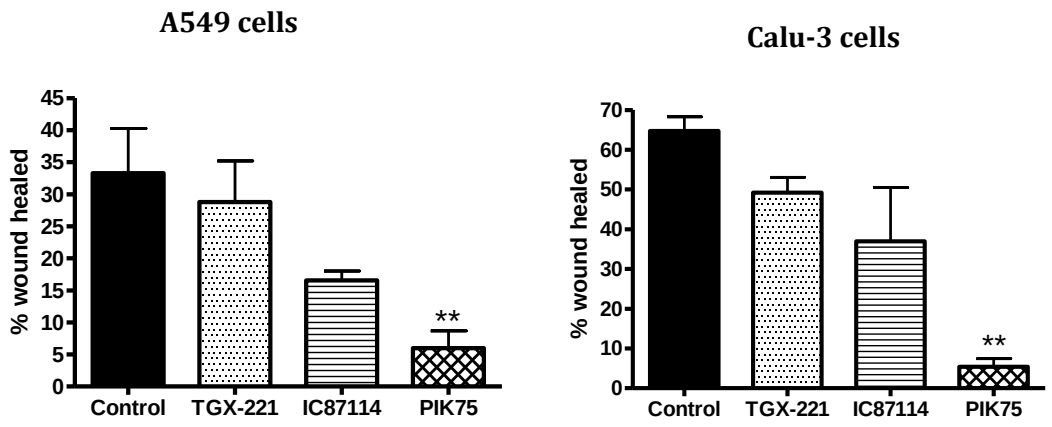

Figure 5.11 Effect of PI3K isoforms on cell migration in wound healing assay.

For each experiment, cells were plated onto 12-well plates in complete media and when confluent were placed in serum free media overnight at 37°C at 5% CO_2. Cells were then scratched with a pipette tip to make a wound which was washed and photographed. PI3K isoforms p110α, p110β and p110δ were inhibited using the selective isoforms inhibitors PIK75 (100 nM), TGX221 (100 nM) and IC87114 (10 μM) respectively, which were added to serum free media and incubated for 24 hours. Cells were washed and photographed and the % of wound healed was calculated using Tscratch software [310]. Data are presented as mean values ± SEM for three independent experiments. All groups were compared to control for statistical significance, which is expressed as (**) for $p<0.01$.

5.9 Investigating the role of PI3K in junctional protein re-formation using a calcium switch assay

The 'calcium switch' assay is useful for studying the biogenesis of epithelial polarity and junctional protein formation [230, 231]. When calcium levels are changed from <5 μM to 1.8 mM, cells change from a non-polarized state with little cell-cell contact to a polarized state with the formation of junctional protein complexes (tight junctions, adherens junctions and desmosomes) that separate the apical and basement membranes. Calcium is essential in maintaining and in the assembly of adherens junctional proteins. E-cadherin which is part of the cadherin family gets its name from being a calcium dependent adhesion molecule, as repeated cadherins are known to be the extracellular binding sites for calcium. [229, 231]

Confluent cells grown at ALI were starved overnight in serum-free media and then placed in a 4 mM solution of EGTA at pH 8 for 30mins to disrupt the adherens junctional proteins which in turn breaks open the tight junction proteins, a process which can be observed by a dramatic decrease in TER. Cells were placed back in normal calcium containing serum free media with the addition of IL-13 (10 ng/ml) or various PI3K inhibitors (ZSTK474, LY294002, IC87114, TGX-221 and PIK75). IL-13 hindered the ability of cells to re-form their junctional protein complexes after 24 hours, control cells reached a 25% higher TER than the IL-13 treated cells (Figure 5.12). Pan class I-PI3K inhibition with ZSTK474 resulted in cells reaching a higher TER than that of control cells, however this was only true for the highest concentration of ZSTK474 (10 μM), the lower concentrations (1 and 0.1 μM) displayed the same TER as control cells. From the selective isoform inhibitors tested, only PIK75 had a significant effect on the re-formation of the tight junctions with a decrease of 45% compared to control. The p110δ inhibitor IC87114 and the pan-inhibitor LY294002 slightly increased the end point TER over control but not significantly, whereas TGX-221 had no effect at all.

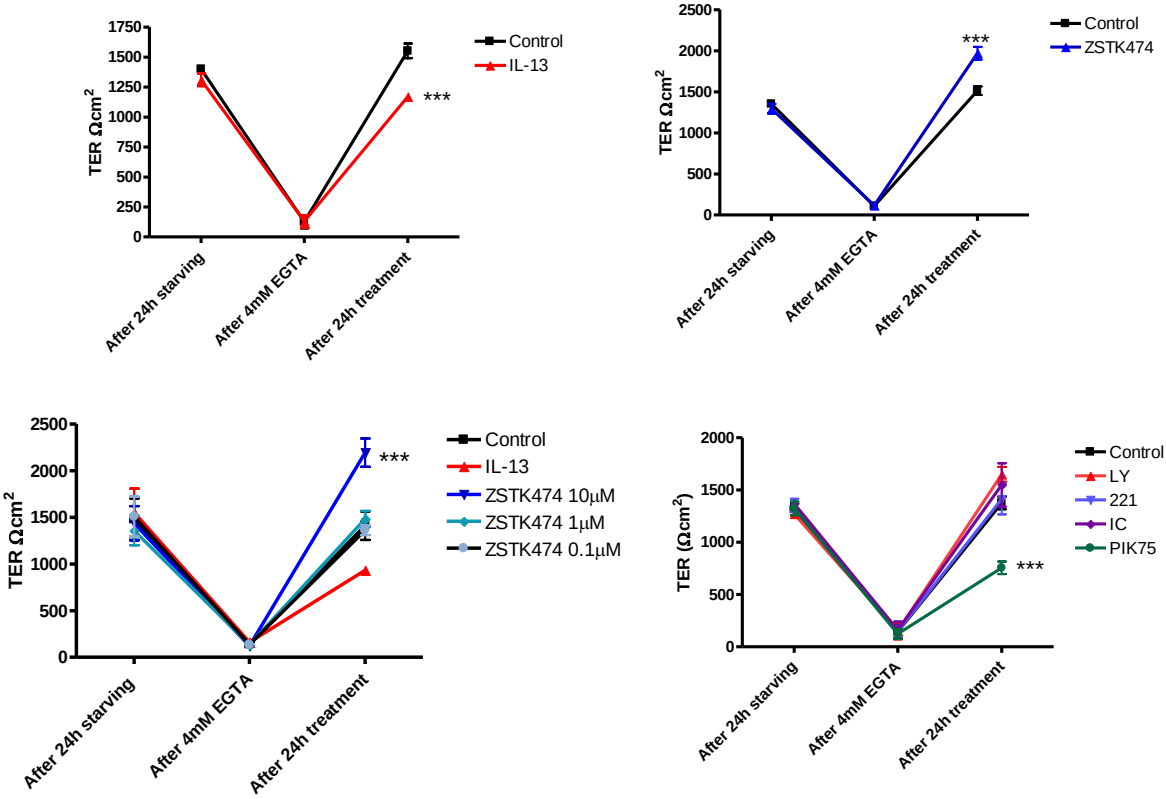

Figure 5.12 Effect of IL-13 and PI3K inhibition on tight junction re-formation.

For each experiment Calu-3 cells were grown via ALI and once confluent were placed in serum-free media for 24 hours and monitored by TER measurements. Cells were then placed in 4 mM EGTA for 30 minutes followed by serum-free media with the addition of IL-13 (10 ng/ml) or PI3K inhibitors ZSTK474 (10 µM), IC87114 (10 µM), TGX-221 (100 nM), PIK75 (100 nM) and LY294002 (20 µM) for 24 hours. Data are presented as mean values ± SEM for three independent experiments. All groups were compared to the control group using a 2-way ANOVA and statistical significance is expressed as (***) for $p<0.001$.

5.10 Investigating the effect of IL-13 and PI3K inhibition on LDH release as a marker of cell necrosis

To assess whether the various inhibitors used were having a negative effect on cell viability by inducing cell necrosis, an LDH assay was carried out. Confluent cells were exposed to IL-13 and PI3K inhibitors for 24 hours as in all previous experiments. The media from each well was sampled and examined for LDH release using a LDH assay kit which utilized a spectroscopic colour change observed with higher amounts of protein present analysed by absorbance. (see section 2.11 for more details). The LDH released from each sample was compared with that of the total LDH in the cell sample by lysing the cell to release all the protein present.

The un-stimulated control cells released 17 ± 3% LDH over the total LDH available in the sample (Figure 5.13). None of the treatments studied resulted in a statistically significant increase in LDH release after 24 hours. Treatment with IL-13 (10 ng/ml) resulted in 18.5 ± 2% LDH release whereas ZSTK474 (10 μM) and IC87114 (10 μM) treatment for 24 hours showed an LDH release of 17 ± 3% and 15 ± 5% respectively. The p110α isoform which was inhibited using PIK75 (100 nM) showed slightly higher levels of cell necrosis compared to control cells with 24 ± 4% of LDH released. p110β inhibition using TGX-221 (100nM) also displayed slightly higher levels of LDH (25 ± 8%) and results were seen to be more variable. The pan PI3K inhibitor LY294002 (20 μM) which is often referred to as a 'dirty' PI3K inhibitor released the highest amount of LDH 37 ± 8% which demonstrated that the cells were not content in the presence of this concentration for 24 hours.

These data are essential when using any type of small molecule inhibitor as it is important to know if the results obtained are a consequence of blocking certain signalling pathways (as is hoped) or merely the cell being 'poisoned' by the inhibitor itself. This negative result indicates that the inhibitors used are not having adverse effects on the cells necrotic pathways

and results obtained thus far are true of the complex signalling pathways being manipulated.

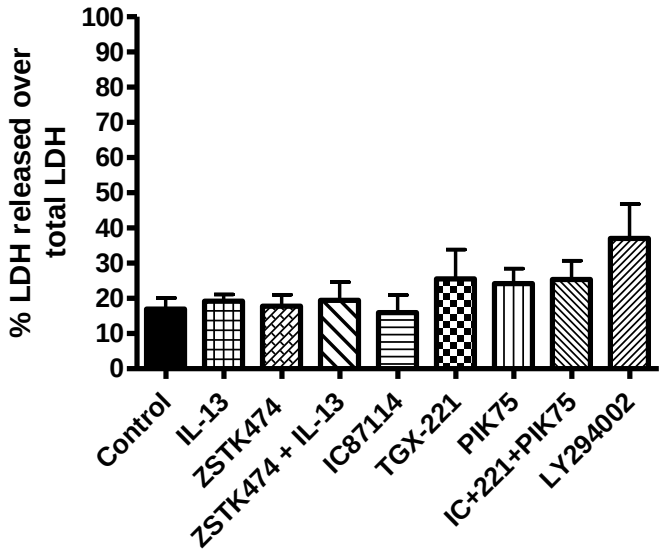

Figure 5.13 Effect of PI3K inhibition on Lactate dehydrogenase release. Cells grown to confluence at ALI were treated with IL-13 (10 ng/ml), ZSTK474 (10 μM), IC87114 (10 μM), TGX-221 (100 nM), PIK75 (100 nM) and LY294002 (20 μM) for 24 hours. Samples from the media were tested for LDH presence by measuring the reduction of NADP to NADPH which results in a shift to a deep red colour and can be monitored spectroscopically at a wavelength of 490 nm. These values were converted to a percentage of released LDH over the total LDH in each sample which was obtained through lysing the transwell to release all protein present. Data are plotted as mean values ± SEM for three independent experiments.

5.11 Effect of PI3K inhibition on the IL-13-induced increase in MUC5AC expression by immunocytochemistry

IL-13 was shown to increase the expression of the mucin protein MUC5AC (Figure 4.9) after 24 hours treatment. The role of PI3K in this upregulation was investigated; ZSTK474 was added to the basolateral chamber 30 minutes prior to IL-13 to ensure its entry into the cell. MUC5AC protein expression was shown to be reduced following PI3K inhibition (Figure 5.14 A). The reduction is seen more clearly in the images in Figure 5.14 B, where the images are represented as a z stack. A z-stack is where the whole layer of the cell monolayer is observed e.g. 10 x 4 µm slices are imaged then placed together on top of each other, so you look at the cell monolayer side on instead of from the top. In the control and the IL-13 stimulated groups MUC5AC expression is mainly located on the surface, whereas in the ZSTK474 and ZSTK474 + IL-13 treated cells show less MUC5AC surface staining and more intracellular staining in the same plane with the nuclear stain. IL-13 appears to increase the MUC5AC expression according to the images in 5.14 A and B, however there is no significant difference when the images are quantified to give fluorescence intensity per pixel (Figure 5.14, C). PI3K inhibition with ZSTK474 alone and in combination with IL-13 significantly reduces MUC5AC levels 32% and 24% respectively compared to control.

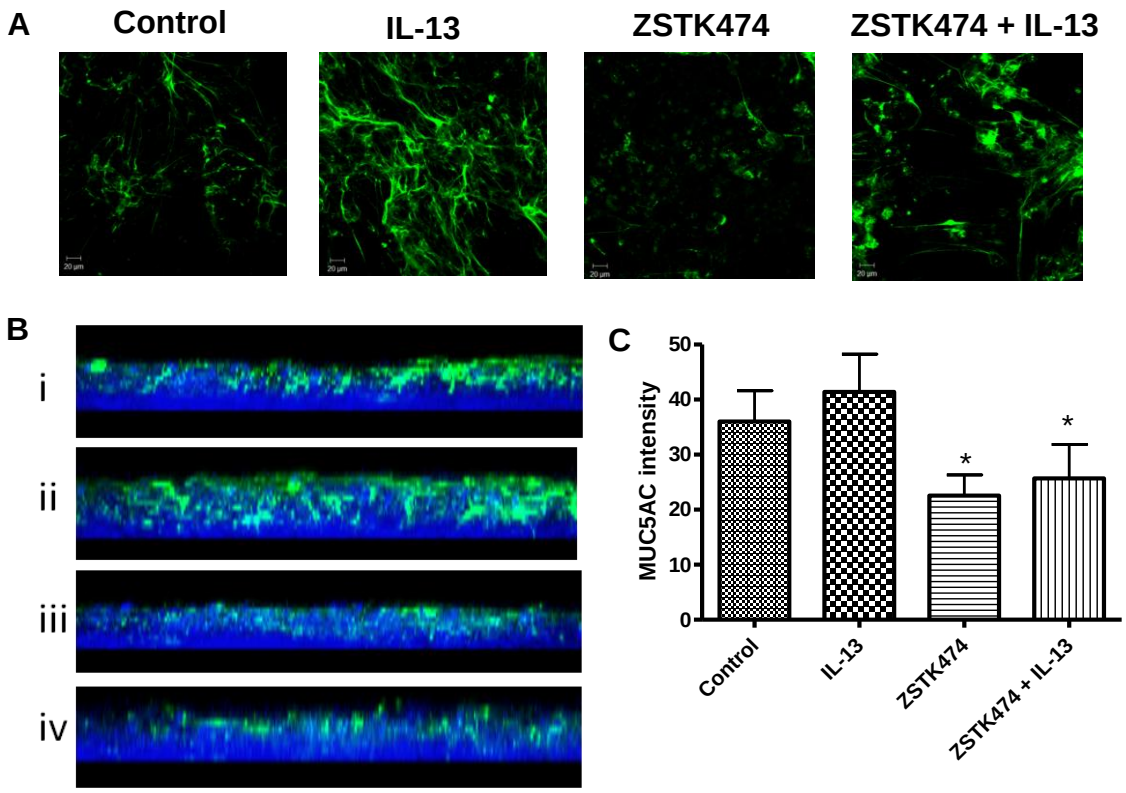

Figure 5.14 Effect of IL-13 and PI3K inhibition on MUC5AC expression in Calu-3 cells. Confluent cells grown at ALI were stimulated with IL-13 with or without pre-treatment with ZSTK474 for 24 hours, after which they were fixed in 4% PFA and probed with a mouse monoclonal antibody against MUC5AC, followed by an Alexa Fluor 488 conjugated secondary antibody Filters were cut out, mounted onto glass slides and viewed using a LSM510META confocal laser scanning microscope. The images in A show MUC5AC staining taken at the focal point immediately after the disappearance of the DAPI blue stain (i.e the top section or surface of the cells) after IL-13 stimulation(10 ng/ml) and/or ZSTK474 treatment (10 μM). The Z-stack images in B are side on profiles from the images shown in A (i = control, ii = IL-13, iii = ZSTK474 iv = ZSTK474 + IL-13). Images in A and B are representative of three similar images taken during three independent experiments. C shows the semi quantified graph of the average intensity per pixel expressed as mean ±SEM from n=3 experiments.

5.12 Discussion

5.12.1 The role of PI3K in IL-13-induced TER decrease

PI3K pan-class I inhibition reverses the IL-13-induced decrease in TER after 24 hours, a finding that is consistent with Ceponis *et al.* who reported the involvement of PI3K in the IL-4/IL-13 induced decrease in TER in intestinal epithelial cells [248]. The isoform of PI3K that was responsible for its role in the regulation of the TJ however had not been studied. This data shows that the inhibition of p110δ using IC87114 produced a slightly higher TER than vehicle treated cells, although this increase was not statistically significant in this study, p110δ has been recently been reviewed in relation to having potential as an effective drug target in allergic asthma [311]. The only selective inhibitor that caused a statistically significant difference in TER was PIK75 which resulted in a decrease in TER of 30% below control cells when administered alone. When combined with IL-13 treatment this decreased a further 10% indicating that p110α signalling to the TJ may be involved in the maintenance of basal TER.

None of the selective isoform inhibitors brought about the same response as the pan PI3K inhibitor ZSTK474, so they were studied in combination to rule out isoform redundancy. Combined treatment with TGX-221, IC87114 and PIK75 reduced basal TER and had no effect on IL-13 stimulation. These data suggest that ZSTK474 is having off target effects and isn't as selective as previously claimed [99]. The possible role of mTOR and the class II PI3Kβ, which are reported as being off target effects of the first generation PI3K inhibitors wortmannin and LY294002 [85] were studied. Treatment with PI-103 which is equipotent against both PI3K C2β, p110α and also targets mTOR [308] resulted in no change in TER compared to controls. The potent mTOR inhibitor rapamycin displayed a 35% decrease in TER when administered alone and in combination with IL-13 at the highest concentration of 20 nM, but this was not seen for the lower concentration 2 nM and neither concentration mimicked the effects observed with ZSTK474

in the prevention of the IL-13-induced decrease. These results indicate that mTOR is not involved in the prevention of TER observed by ZSTK474.

Inhibitor location between basolateral and apical chambers did not change the effect of PI3K inhibition, with apical inhibitor incubation also preventing the IL-13-induced decrease in TER which was previously shown by the basolateral incubation. This finding was useful as if a PI3K inhibitor was to become a new drug for treatment in severe asthma then it would be administered to the apical side (top side) of the epithelial cells.

5.12.2 Investigating the efficacy of pan PI3K and isoform selective inhibition in Calu-3 cells

In order to ensure that ZSTK474, IC87114, TGX-221 and PIK75 were inhibiting the PI3K pathway effectively, cells were pre-treated with the inhibitor for 30 minutes to allow penetration into the cell and then treated with IL-13 for up to 90 minutes. Phosphorylation of Akt at Serine 473 was measured as a marker of PI3K activity. ZSTK474 was shown to successfully inhibit Akt phosphorylation proving it adequately inhibited PI3K as claimed [99]. The only isoform selective inhibitor that caused a decrease in Akt phosphorylation was PIK75 which inhibits the p110α isoform, IC87114 and TGX-221 which inhibit p110δ and β respectively did not significantly reduce Akt phosphorylation in the given time scale. This finding initially proved concerning, however it was consistent with related research that has shown that IC87114 has little effect on Akt phosphorylation in HUVEC endothelial cells which was concluded to be due to the low levels of p110δ present [289]. Another explanation for this finding is the idea of isoform redundancy i.e Akt is phosphorylated by all isoforms of PI3K and if one is blocked then another will simply take over in its place. Further studies into the expression of individual isoforms and their effect on IL-13 stimulated Akt phosphorylation in Calu-3 cells is needed in order to come to an accurate conclusion.

5.12.3 The role of PI3K on the expression and distribution of TJ proteins and IL-13Rα2

The effect of PI3K inhibition on the IL-13 induced increase in claudin 2 was studied using immunofluorescence and mRNA levels of the TJ protein were investigated using qRT-PCR. Pan-PI3K inhibition with ZSTK474 prevented the IL-13-induced upregulation of the tight junction protein claudin 2 shown by immunofluorescence. Claudin 2 has been previously shown to be upregulated by the non-proteolytic house dust mite allergen in A549 cells and the PI3K pathway was found to be involved through inhibition with wortmannin [256]. In addition to the role of PI3K the EGFR pathway has also been linked to an upregulation of claudin 2 [281]. This is the first study investigating the role of the selective PI3K isoform inhibitors in TJ modulation.

Pre-treatment with the selective p110α inhibitor PIK75 mimicked this result observed by ZSTK474 and LY294002 in that, claudin 2 was barely visible in either the inhibitor alone or inhibitor + IL-13 treatments, indicating a basal effect on claudin 2 expression as well as blocking its upregulation after IL-13 stimulation.

In addition to studying the protein expression of the TJ protein claudin 2, its mRNA expression was also monitored by qRT-PCR. IL-13 was shown to increase claudin 2 mRNA compared to control cells, however this was not significant due to one anomaly experiment. Pretreatment with ZSTK474 and PIK75 reduced the expression of claudin compared with IL-13 stimulation, however as results were not significant, the experiment needs to be repeated in order to come to an accurate conclusion.

The expression of the IL-13 receptor alpha 2 after PI3K inhibition was studied due to research which reported that it can play an inhibitory role on IL-13 effects in the cell if expressed highly enough [60]. It was necessary to check that the effects being observed from PI3K inhibition on the expression and TER studies were not due to the upregulation of the IL-13Rα2 at the cell surface thus inhibiting the IL-13 response. FACS studies showed that IL-

13Rα2 was basally expressed on the cell surface of Calu-3 cells and that IL-13 treatment resulted in an increase in IL-13Rα2 surface expression from 20% to 35% which is consistent with results published by Daines et al [60]. Pretreatment with ZSTK474 reduced this IL-13-induced expression to 15%, which hints that the concern that PI3K was only having an effect through increasing the IL-13Rα2 expression and dampening the IL-13 response is not true. However this experiment needs to be repeated in order to demonstrate the role of PI3K signalling on the expression of IL-13Rα2 on the cell surface of Calu-3 cells.

5.12.4 The role of PI3K on cell migration and reformation of the TJ

A typical scratch assay was used in order to study the role of PI3K in the process of epithelial wound healing, also termed re-epithelisation. Other methods such as the chemical wounding using NaOH [312] are also used but the mechanical scratch method is the least harmful to the cell monolayer. PI3K inhibition was shown to inhibit the wound healing response in both A549 and Calu-3 cell lines, a finding which is not entirely surprising as PI3K signalling is known affect cell migration and proliferation. Involvement of PI3K in wound repair is supported by Lai *et al* who have shown that inhibition of the negative regulator of PI3K pathway, PTEN increases the wound healing response in BEAS2B cells [313, 314]. An interesting result in this experiment was the difference observed in the basal cell healing response between Calu-3 and A549 cells, with Calu-3 cells closing the wound almost double the distance of that of A549s in the same amount of time. It has been reported that the tight junction protein claudin 2 is expressed 160-fold higher in basal A549 cells than in normal tissue and that this decreases cell motility and the expression of the matrix metallopeptidase 9 (MMP-9), which is also referred to as Gelatinase B [282]. Claudin 2 levels between normal lung tissue and Calu-3 cells have been shown to be comparable [286] which may explain the vast difference seen between the cell lines basal motility in this study. The PI3K pathway has been shown to reduce the expression of many

MMPs which are responsible for the degradation of the extracellular matrix (ECM). Andrographolide, a potential chemotherapeutic agent was shown to reduce cell migration and motility by suppressing the PI3K pathway through Akt and AP1 by reducing MMP-7 expression [315]. Regulation of the epidermis has also been reported to involve the PI3K pathway where it strongly enhances keratinocyte migration and proliferation [316].

The level of extracellular calcium has been reported to play a role in TJ maintenance, permeability and regulation [317]. Calcium was shown to be important in assembly of the junctional complex in keratinocytes in 1987 following the discovery of the cadherin family in 1984 which were named after their "calcium dependent adhesion" properties [217]. Depletion of extracellular calcium leads to disruption of the adherens junctional proteins including E-cadherin and subsequently breaks open the tight junction complex. Here, we used a common technique called a calcium switch assay which utilizes this dependence on calcium by lowering levels to deplete all junctional proteins and then restores levels to monitor the de-novo synthesis of the junctional complex [318].

The calcium switch experiment showed that IL-13 treatment decreases the ability of cells to reform an intact junctional complex and hence display a high TER. It is not known whether IL-13 affects the rate of junctional formation or the expression of a particular junctional protein which hinders the re-formation. Previous results show that IL-13 upregulates the pore forming junctional protein claudin 2 so this may explain the observed result, however it cannot be assumed that the regulation of basal tight junctions is the same as that of de-novo synthesis of tight junctions required for epithelial reconstitution. PI3K inhibition alone at high concentration resulted in an increase in TER above basal levels as witnessed in the regular TER experiment. This increase was not observed in the lower concentrations of ZSTK474 which displayed the same TER after 24 hours treatment as the vehicle controls; a finding which strongly indicates off-target effects of the inhibitor. The role of the PI3K-class I isoforms were also studied in the reformation of the TJ and it was shown that p110β and p110δ inhibition had no effect on TJ reformation after 24 hours compared with controls.

Interestingly, inhibition of p110α significantly reduced the TER compared to control cells after 24 hours, which suggests a role for p110α signalling in the formation of tight junction proteins in Calu-3 cells.

5.12.5 The role of PI3K in IL-13-induced goblet cell metaplasia

IL-13 was shown to increase MUC5AC after 24 hours treatment in accordance with Nakano *et al* who reported IL-13 increased MUC5AC expression in mice trachea at this time [298]. The role of PI3K in IL-13-induced mucus hypersecretion was investigated and it was shown to reduce the expression of MUC5AC present on the surface of the cells, shown clearly in z-stack images. This increased expression was not replicated to the same extent in the semi-quantification graph, which only portrays a small difference between control, IL-13 and ZSTK474 treatments. An explanation for this finding could be that IL-13 and PI3K have a more substantial effect on the distribution/secretion of the mucin rather than its expression alone. In the IL-13 stimulated cells, MUC5AC is highly localised on top of the cells; PI3K inhibition may block the IL-13-induced release of MUC5AC from intracellular stores. Although this result itself is interesting this section of work was not followed up due to time constraints. Recently, IL-13 –induced MUC5AC expression has been shown to be mediated by 15-lipooxygenase 1 in bronchial epithelial cells [319], which has been shown to rely on the two IL-13 receptors, soluble IL-13Rα2 and surface IL-13Rα1 [299].

5.12.6 Limitations and future work

The main limitation in this chapter is: the use of small compound inhibitors to study the role of PI3K. Firstly, the starting point for using this approach should have been to assess the isoform expression within the Calu-3 cell line. Subsequent concentration and dose response experiments should have been carried out to ensure that the both the optimal concentration and experimental time was being used. PI3K silencing with

synthetically generated siRNAs that target each isoform of PI3K could have also been used, however when using siRNA technology, experiments assessing the basal cell activity would be required to ensure the was no change in cell proliferation and survival which would alter the signalling pathways and lead to misinterpretation of results. It would be interesting to verify the role of PI3Kα by either silencing or overexpressing the p110α gene and investigating its role in maintaining the junctional complex by TER, Ca^{2+} switch and tight junction expression studies. However as p110α is essential in many cell cycle processes, there would only be a small window in which experiments could be carried out following knockdown.

Another limitation with many results in this chapter is the lack of repeated independent experiments carried which was due to time constraints, repeating these data will enable statistical analysis of results and more accurate interpretation.

5.13 Conclusions

The role of PI3K in TJ regulation was researched in this chapter and it was shown to play an important role in maintaining the basal TER of the epithelial layer by keeping levels of the TJ protein claudin 2 low.

In summary, in this chapter the following was determined:

- Pan-PI3K inhibition prevents the decrease in TER shown by IL-13 in chapter 3
- The result seen with the ZSTK474 pan-PI3K inhibitor was not observed in any of the selective isoform inhibitor studies or when studying them in combination, indicating off –target effects of the ZSTK474 inhibitor.
- PI3KC2β and mTOR were shown not to be responsible for the prevention in IL-13-induced TER by ZSTK474
- ZSTK474 was shown to bring about the same response regardless of apical or basolateral addition.
- Increased claudin 2 protein and mRNA expression by IL-13 was reduced by pre-treatment with ZSTK474 and PIK75
- p110α was shown to be essential for the wound healing response in both Calu-3 and A549 cells
- The re-formation of the TJ was shown to be hindered by IL-13 treatment and p110α inhibition.

Chapter 6 : Role of STAT6, MEK and GSK3β in epithelial barrier modulation

6.1 Role of STAT6, MAPK and GSK3β in IL-13-dependent or independent junctional protein regulation

To further investigate the molecular signalling pathways involved in the highly dynamic role of tight junction regulation, STAT6, GSK3β and MAPK pathways were examined. IL-13 has been shown to exert its affects via PI3K/Akt signalling and Akt has many roles within the cell including, cell proliferation, migration and regulation of GSK3 activation through Akt phosphorylation which results in inactivation [320] [321]. IL-13 has also been shown to act via STAT6 by recruiting Jak proteins to the RTK that activates STAT proteins, which are subsequently released into the cell and have many roles including transcription [109]. The MAPK pathway is another important cellular pathway which is involved in many vital cell processes and many studies have linked IL-13 activation to MAPK signalling [23, 162, 322]

With the results so far indicating a role for PI3K in TJ regulation it was necessary to look at the other pathways that are linked to IL-13 activation and investigate their possible roles.

6.1.1 IL-13 signalling via STAT6, GSK3 and MAPK

In order to study the possible role of STAT6, MEK and GSK3 in TJ regulation it was necessary to first look at if they are activated through short term treatment with IL-13. Calu-3 cells were stimulated with IL-13 (10 ng/ml) for up to 90 minutes. Figure 6.1 shows that STAT6 is phosphorylated 40-fold over basal after 90 minutes treatment with IL-13. Phosphorylation of GSK3β and ERK were also investigated and the results were much less obvious than the STAT6 activation. Phospho-GSK levels remain exactly the same as GSK levels over the 90 minute period, indicating that IL-13 is having no effect on GSK3 activation which may be explained by GSK activity being constituently active in Calu-3 cells so the activation is masked. A similar result was seen when MAPK activity was monitored by assessing the presence of phosphorylated threonine 202 and tyrosine 204 residues on

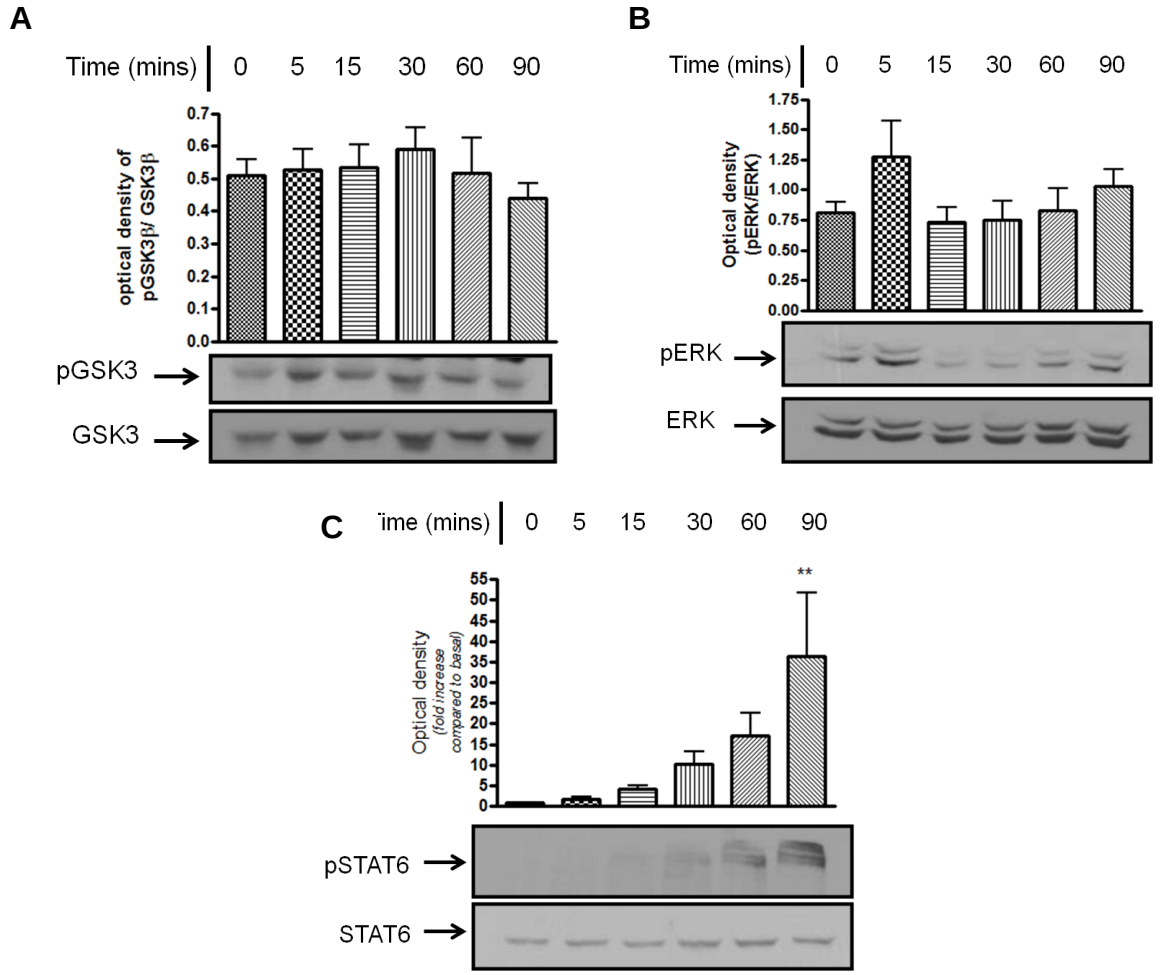

Figure 6.1 Effect of IL-13 stimulation on MAPK, GSK3β and STAT6 activation in Calu-3 cells.

For each experiment, cells were plated onto 12-well plates in serum containing MEM. When confluent, cells were placed in serum-free media overnight and then stimulated with IL-13 (10 ng/ml) for up to 90 minutes. Samples were resolved on SDS-page gel, transferred to nitrocellulose membranes and immunoblotted, using antibodies against A) phosphoThr^{202}/Tyr^{204}-ERK (pERK) at 44 and 42 kDa, B) phosphoSer^{9}-GSKβ (pGSK3β) at 46 kDa and C) phopshoTyr^{641}-STAT6 (pSTAT6) at 110 kDa. Membranes were then re-probed using antibodies against ERK1, GSK3β and STAT6. Data are presented as n=3 independent experiments. All groups were compared to vehicle control (0 h) for statistical significance, which is expressed as (**) for $p<0.01$.

ERK. IL-13 was shown to slightly increase the phosphorylation of ERK after 5 minutes stimulation; this increase was quite variable hence why the immunoblot does not match the quantified graph and is not statistically significant.

6.2 Effect on STAT6 phosphorylation using the histone deacetylase inhibitor SAHA

Suberoylanilide hydroxamic acid (SAHA) has been shown to be a potent inhibitor of all isoforms of histone deacetylases (HDAC) with highest selectivity for class I and II with an IC_{50} of <86 nM [115, 121]. It was discovered to possess antitumor properties and inhibited growth in prostate, breast and endometrial cancer cell lines [323-325]. HDAC 1 has been shown to directly acetylate STAT3, a requirement for activation by IL-6. Overexpression of HDAC-1 in hepatoblastoma cells resulted in reduced IL-6-induced STAT3 expression [134]. Treatment with SAHA has been demonstrated to inhibit STAT6 activation, which led to dampening of the IL-13 response in ulcerative colitis [247]. LPS-induced cytokines were shown to be reduced in vivo following SAHA treatment signifying its anti-inflammatory properties [129]. The role of STAT6 in the regulation of the TJ in bronchial epithelial cells has not been investigated.

To assess the effect of SAHA (5 μM) on IL-13-induced activation of STAT6, cells were cultured with SAHA 30 minutes prior to IL-13 treatment and pSTAT6 was immunoblotted after 24 and 48 hours treatment (Figure 6.2). Membranes were stripped and re-probed for STAT6 and then again for the common loading control β-actin to check if SAHA had any effect on overall protein expression. STAT6 phosphorylation increased 1.8-fold over control after 24 hours and this dropped to 1.4-fold after 48 hours both of which proved statistically significant over vehicle control. Inhibition with SAHA completely abolished the IL-13-induced STAT6 phosphorylation at

both 24 and 48 hours treatment. Additionally, SAHA didn't alter the overall STAT6 protein expression, indicating that the mechanism of inhibition is through blocking the phosphorylation site without affecting the protein itself. STAT6 phosphorylation was shown to be much higher after short term IL-13 stimulation (90 minutes) shown in figure 6.1 but as the subsequent experiments were studied for longer time periods of 24-48 hours it was necessary to see the effect of SAHA on the cells after this duration.

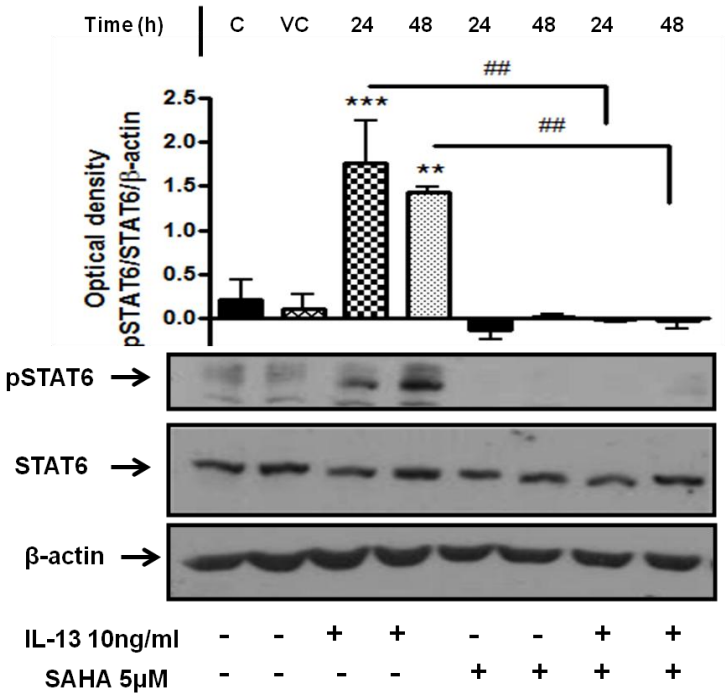

Figure 6.2 Effect of SAHA on IL-13-induced STAT6 activation.

For each experiment, cells were plated onto 12-well plates in serum containing MEM. When confluent, cells were placed in serum-free media overnight and then stimulated with IL-13 (10 ng/ml) and SAHA (5 μM) for up to 48 hours. Samples were resolved by SDS-PAGE, transferred to nitrocellulose membranes and immunoblotted, using antibodies against phopshoTyr641-STAT6 (pSTAT6) and STAT6 both at 110 kDa and β-actin at 45 kDa as an equal loading control. Data are presented as n=3 independent experiments and all groups were compared to each other for statistical significance, which is expressed as (***) for $p<0.001$ and (**) for $p<0.01$ compared to vehicle control (VC). The IL-13 treated groups were compared to the IL-13 + SAHA treated groups and statistical significance is expressed as (##) for $p<0.01$.

6.2.1 Effect of STAT6 of junctional protein regulation and formation

The role of SAHA on junctional protein regulation and formation was studied by TER and calcium switch experiments respectively. The effect of SAHA on basal TER was investigated and it was shown that both concentrations of SAHA (5 μM and 1 μM) alone increased the TER of cells over that of the vehicle control (Figure 6.3 A). The higher concentration of SAHA alone (5 μM) increased the TER over double compared to the standard baseline control. Pre-treatment and incubation of SAHA with IL-13 prevented the IL-13-induced decrease in TER in both concentrations of SAHA, however only the higher concentration was statistically significant. This data mimicked the results with the pan-PI3K inhibitor ZSTK474 (Figure 5.1) indicating that both PI3K and STAT6 pathways have an involvement in junctional protein regulation which is essential to maintaining an intact epithelial layer.

In the calcium switch assay the intact epithelial layer was disrupted by addition of an EGTA solution (4 mM) for 30 minutes which decreased the extracellular calcium concentration leading to breakdown of both adherens and tight junction proteins. The junctional protein disruption was observed by monitoring the TER and a dramatic decrease in TER is witnessed where values fall to between 200-300 Ωcm^2. When cells reached a TER between the range 200-300 Ωcm^2, they were washed to remove all traces of EGTA and were placed back in serum-free media (normal Ca^{2+} concentration) with the addition of IL-13 and SAHA for 24 hours (Figure 6.3 B). IL-13 alone caused a decrease in TER indicating that it not only has an effect on an intact epithelial layer but may also be involved in the re-formation of junctional proteins and their recruitment back to the cell membrane. STAT6 inhibition alone using SAHA lead to an increase over control cells as seen in Figure 6.3 A. In the combined treatment of SAHA and IL-13 the results mimicked the SAHA alone treated cells where SAHA prevented the IL-13-induced prevention of TER to normal basal levels. The STAT6 pathway is therefore important in both the regulation of the intact epithelial layer as well

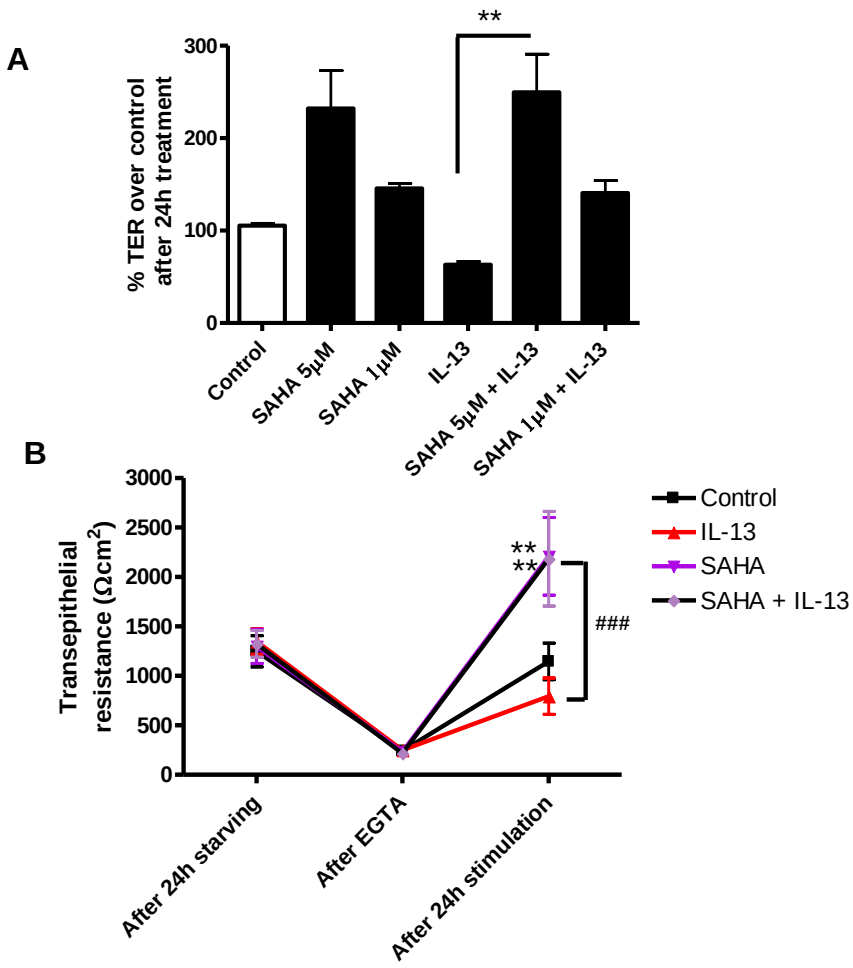

Figure 6.3 Effect of SAHA on the IL-13-induced decrease in transepithelial resistance and tight junction reformation.

For each experiment $5x10^5$ cells/ml were seeded onto transwell filters and their transepithelial resistance was monitored. For A, on Day#7 when the maximum TER was reached IL-13 (10 ng/ml) and SAHA (5 µM) were added to the basolateral chamber and the TER was measured after 24 hours. This TER was then compared to that of the same well 24 h prior to obtain the TER % over control after 24 h treatment. For B, on day#7 cells were placed in serum-free media for 24 hours after which they were placed in 4 mM EGTA for 30 minutes followed by serum-free media with the addition of IL-13 (10 ng/ml) with or without SAHA (5 µM) for 24 hours. Data are presented as mean values ±SEM from three independent experiments. All groups were compared to the control group and statistical significance which is expressed as (**) for $p<0.01$. All groups were also compared to each other and statistical significance which is expressed as (###) for $p<0.001$.

as exhibiting its importance in junctional protein re-formation. The involvement of STAT6 in this highly dynamic area is similar to that of PI3K suggesting that they may work together downstream of IL-13 or as independent pathways.

6.2.2 Effect of SAHA on tight junction protein expression and distribution by immunocytochemical studies

To investigate the role of STAT6 further in an attempt to uncover the molecular mechanisms involved in the regulation of junctional proteins, immunocytochemical studies were carried out. Cells were stimulated with SAHA for 24 hours, fixed and stained with antibodies against claudin 2 and claudin 8 (see section 2.4 for more experimental detail).

As Claudin 2 had previously shown to be affected by IL-13 treatment (chapter 4) it was observed first. IL-13 treatment alone resulted in a dramatic increase in claudin 2 expression as illustrated before and it was shown that SAHA treatment alone also resulted in a decrease of claudin 2 protein expression compared with control (Figure 6.4 A). When SAHA was combined with IL-13 treatment the expression of claudin 2 was shown to be slightly increased compared with the SAHA alone treated sample but the observed level of expression was much lower than that of the IL-13 alone treated sample. This is shown more clearly in Figure 6.4 B where the average intensity of fluorescence per pixel is shown for each of the treatments. Treatment with SAHA decreases the IL-13-induced claudin 2 upregulation from 34 ± 5 arbitrary units to 14.5 ± 1.(Figure 5.6).

The expression of claudin 8 was also examined by immunocytochemistry due to the limited research into its regulation in the lung. In control cells it was found to be expressed at a low level quite sparsely and appeared to be cytoplasmic rather than gathered at the junctional membrane in ring like structures. IL-13 was shown to increase the

expression of claudin 8 compared to control, with around 50% of cells expressing the tight junction protein (Figure 6.5). SAHA treatment alone (5 μM) resulted in a prominent increase in claudin 8 within almost every cell in the image field expressing claudin 8, this expression was shown to be mainly localised to the nucleus along with low level cytoplasmic staining. This increase in nuclear expression slightly decreased after pre-treatment of SAHA followed by IL-13 stimulation. Figure 6.5 B shows more clearly the relative expression of claudin 8 as the intensity per pixel is plotted for each treatment group, although these data are only semi-quantified they give a much clearer overall picture. IL-13 treatment alone results in a 25% increase of claudin 8 intensity and SAHA treatment alone causes an increase in claudin 8 expression levels to 90 arbitrary units which is reduced to 53 ± 4 with the combined SAHA and IL-13 treatment. This finding illustrates that STAT6 inhibition leads to a vast increase of >10 fold in the expression of claudin 8 protein after 24 hours treatment. The role of claudin 8 in the TJ is still unknown, however these results suggest that there is an important role for STAT6 signalling in normal epithelial barrier maintenance.

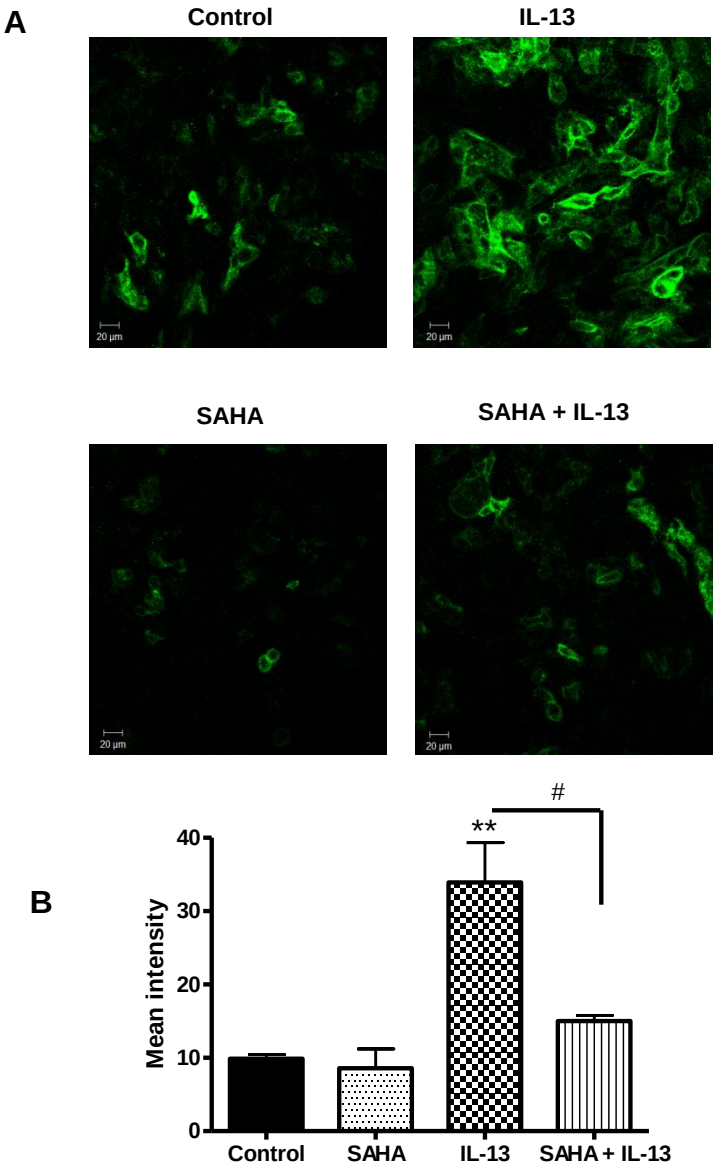

Figure 6.4 Effect of SAHA on claudin 2 protein expression and mRNA expression.

Calu-3 cells grown via ALI were stimulated with 10 ng/ml IL-13 with or without SAHA (5 µM) for 24 hours. They were fixed in 4% PFA and probed with an antibody against claudin 2 (see section 2.4 for details), They were mounted onto glass slides and viewed using a LSM510META confocal laser scanning microscope. Each image is representative of three similar images taken during three independent experiments (n=3). B is a semi-quantified representation of the mean intensity per pixel from n=3 independent experiments. All groups were compared to each other for statistical significance which is expressed as (**) for $p<0.01$ compared to control and (#) for $p<0.05$ for IL-13 vs SAHA + IL-13 groups.

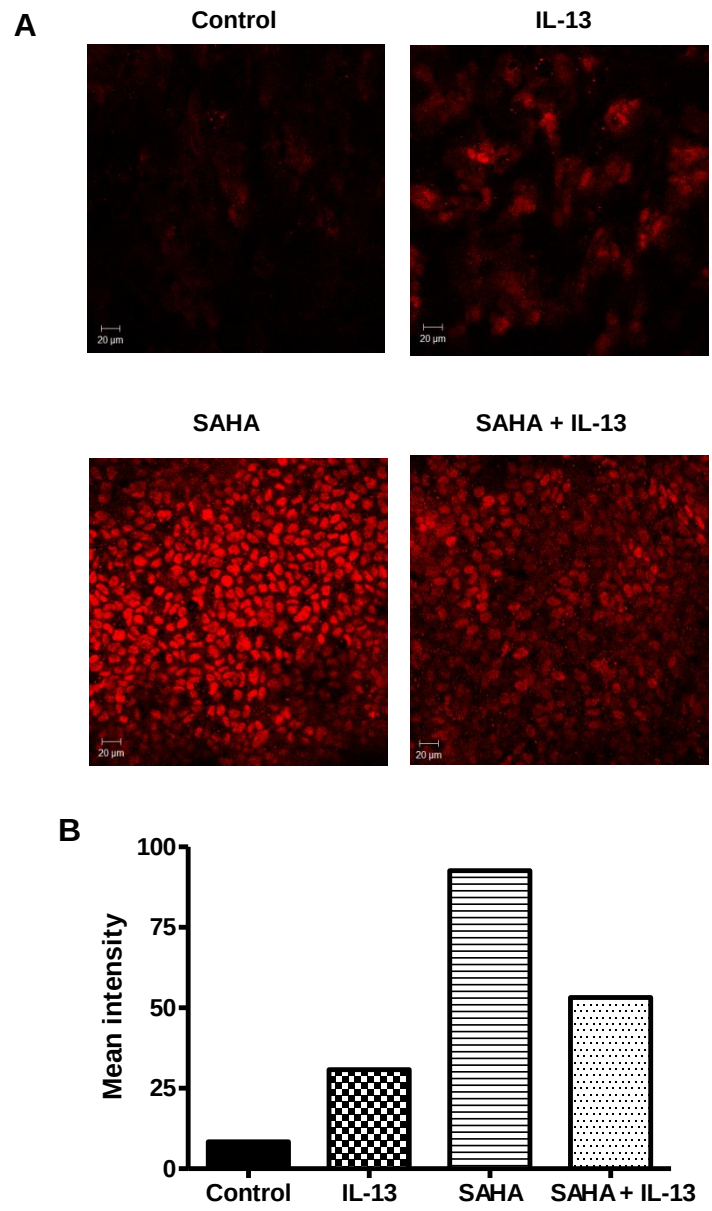

Figure 6.5 Effect of SAHA on claudin 8 protein expression and distribution.

Calu-3 cells grown via ALI were stimulated with 10 ng/ml IL-13 with or without SAHA (5 µM) for 24 hours. They were fixed in 4% PFA and probed with an antibody against claudin 8 (see section 2.4 for details), Cells were mounted onto glass slides and viewed using a LSM510META confocal laser scanning microscope. Each image is representative of three similar images taken during two independent experiments (n=2). B is a semi-quantified graph of the mean intensity per pixel from n=2 independent experiments. Data expressed as mean values ± SEM.

6.2.3 Effect of SAHA on mRNA expression of claudin 2 and claudin 8

The mRNA expression of the TJ proteins claudin 2 and 8 were studied in order to investigate a correlation between protein and mRNA expression. Quantitative PCR (qRT-PCR) was used to study the mRNA expression of claudins 2 and 8 after 24 hour treatment with SAHA. Figure 6.6 shows that the IL-13-induced increase in claudin 2 mRNA is reduced by STAT6 inhibition using SAHA from 5-fold to 2-fold higher than controls, which mimicked the results observed with the protein expression. Claudin 8 mRNA was briefly looked at after the interesting finding demonstrating the upregulation in protein expression following STAT6 inhibition. SAHA was shown to increase claudin 8 mRNA expression 12-fold over basal after 24 hours treatment. This increase was slightly abrogated with the combined SAHA and IL-13 treatment to 10-fold. IL-13 stimulation was shown to have

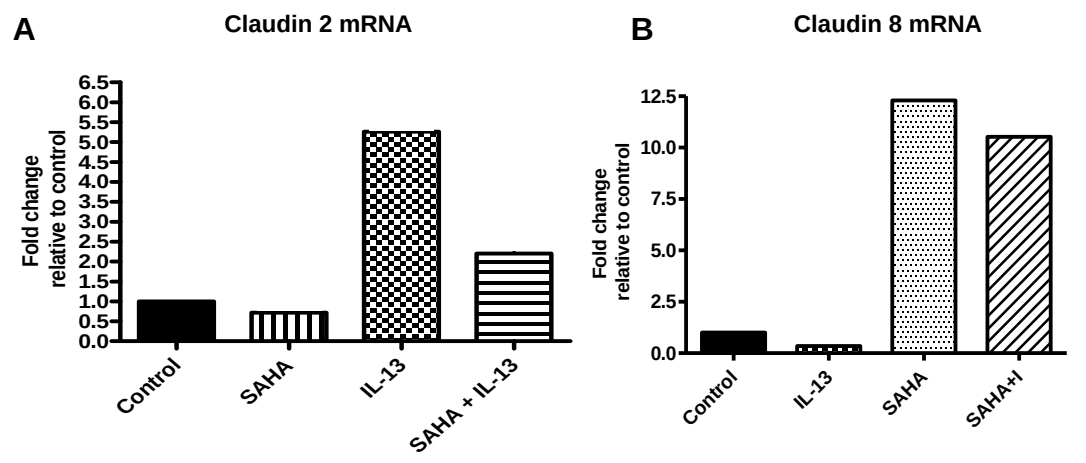

Figure 6.6 Effect of SAHA on claudin 2 and claudin 8 mRNA expression. Confluent Calu-3 cells grown via ALI were stimulated with SAHA (5 μM) for 30 min followed by 10 ng/ml IL-13 for 24 hours. Cells were lysed and RNA was extracted, reversed transcribed to cDNA and reactions were performed on a StepOnePlus Real-time PCR system. All samples were compared to the equal loading gene β-actin and normalised to the untreated control sample. Data expressed as mean values ± SEM from n=2 and n=1 independent experiments (A and B)

no effect on claudin 8 mRNA expression which contrasts what was observed in the protein expression data with IL-13 stimulation resulting in a ~25% increase in claudin-8 levels. This suggests that IL-13 may regulate claudin 8 by post-transcriptonal or post-translational modification; further experimental repeats are required before this idea can be followed up.

6.2.4 Investigating the effect of the PI3K inhibitor ZSTK474 on STAT6 signalling

As the results from the PI3K inhibitor ZSTK474 and the STAT6 inhibitor SAHA were so similar, it was necessary to look at whether the PI3K inhibitor was also having an effect on STAT6 activation. Calu-3 cells were treated with SAHA (5 μM) and ZSTK474 (10 μM) for 24 hours with or without IL-13 stimulation (10 ng/ml) and membranes were blotted against pSTAT6 and STAT6. As shown at the beginning of this chapter IL-13 phosphorylates STAT6 at both 24 and 48 hours, which is completely prevented by SAHA inhibition. The combined treatment of ZSTK474 and IL-13 showed a reduction in STAT6 phosphorylation compared to the IL-13 alone treatment after 24 hours but not 48 hours. This finding indicates that at 24 hours ZSTK474 is having off target effects and inhibiting STAT6 phosphorylation.

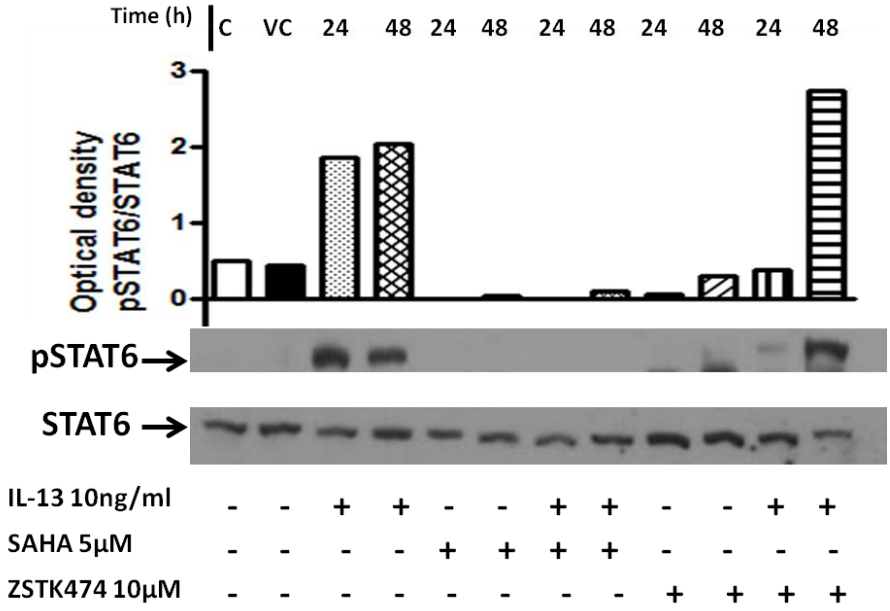

Figure 6.7 Effect of ZSTK474 and SAHA on IL-13-induced STAT6 activation.

For each experiment, cells were plated onto 12-well plates in serum containing MEM. When confluent, cells were placed in serum-free media overnight and then stimulated with IL-13 (10 ng/ml), ZSTK474 (10 µM) and SAHA (5 µM) for up to 48 hours. Samples were resolved by SDS-PAGE, transferred to nitrocellulose membranes and immunoblotted, using antibodies against phosphoTyr^{641}-STAT6 (pSTAT6) and STAT6 both at 110kDa and β-actin at 45kDa as an equal loading control. Data are presented as mean values from n=2 independent experiments.

6.3 Investigating a possible role for GSK3β in epithelial barrier regulation

GSK is a complex signalling molecule that has been shown to promote inflammation and play a role in cell migration and has been reported to be involved in alzheimers, diabetes and cancer [326, 327]. Here the role of GSK3β in epithelial barrier regulation was explored.

6.3.1 Effect of GSK3β inhibition on transepithelial resistance and calcium switch studies

GSK3β was inhibited using 1m, an extremely selective inhibitor which consists of a macrocyclic bisindolylmaleimide structure (Figure 1.6). Bone et al showed that 1m had an IC_{50} of 1-3μM in human stem cells and reduced levels of phospho-beta-catenin in a concentration dependent manner [149, 328].

The effect of 1m on the resistance between the apical and the basolateral chamber was explored in the standard TER experiment (Figure 6.8 A). 1m treatment alone (2 μM) decreased the TER 40% compared to the control. When 1m was combined with IL-13 treatment the TER dropped a further 9% compared to the 1m alone group. Tukey's post hoc test was used to check the statistical significance between all treatment groups and it was shown that the IL-13 treated group was statistically different to the IL-13 + 1m group, indicating that inhibiting GSK3β acts in aiding the actions of IL-13 further. In the calcium switch assay 1m prevented the re-formation of the junctional proteins and resulted in a 37% decrease in TER compared with that of control cells (Figure 6.8 B). The IL-13 + 1m group mimicked the 1m alone result, proving further that GSK3β has a role in not only the basal maintenance of epithelial barrier modulation but also in the reconstitution of the junctional proteins after disruption or injury.

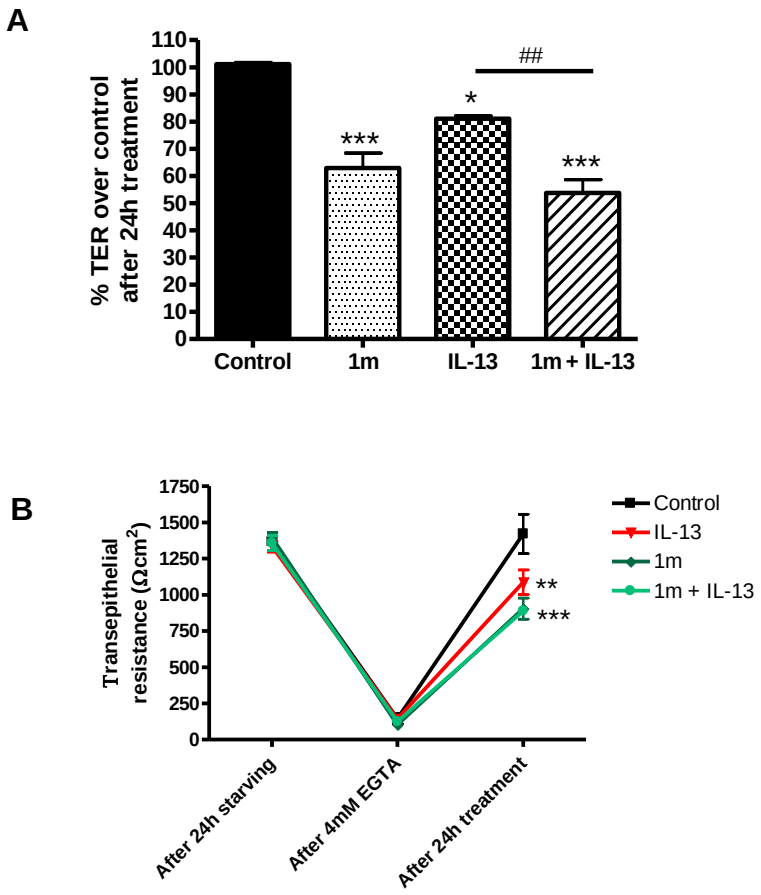

Figure 6.8 Effect of GSK3β inhibition on transepithelial resistance and junctional protein re-formation.

For each experiment 5x10^5 cells/ml were seeded onto transwell filters and their transepithelial resistance was monitored. On Day#7 when the maximum TER was reached IL-13 (10 ng/ml) and 1m (2 μM) were added to the basolateral chamber and TER was measured after 24 hours. The TER was then compared to that of the same well 24 h prior to obtain the TER % over control after 24 h treatment (A). For B, on day#7 cells were placed in serum-free media for 24 hours after which they were placed in 4 mM EGTA for 30 minutes followed by normal calcium containing serum-free media with the addition of IL-13 (10 ng/ml) with or without 1m (2 μM) for 24 hours. Data are presented as mean values ±SEM from three independent experiments. All groups were compared to the control group and statistical significance which is expressed as (*) for $p<0.05$, (**) for $p<0.01$ and (***) for $p<0.001$. All groups were also compared to each other and statistical significance which is expressed as (##) for $p<0.01$.

6.4 MAPK signalling in epithelial barrier modulation

Whilst carrying out the previous TER experiments, an interesting finding was observed while monitoring the TER of cells in serum free media overnight; a 50% increase over control was seen (Figure 6.9 A). In an attempt to discover the explanation for this result the content of the serum was explored and in particular the growth factors present. Amongst many growth factors present in serum EGF is one and it is known to activate the MAPK pathway as well as the PI3K pathway through activation of EGFR [329, 330].

To test out the hypothesis that MAPK was being activated by the presence of growth factors such as EGF in the serum containing medium, the selective inhibitor PD0325901 was used to inhibit the activation of the MAPK protein MEK and the role of MEK in the maintenance of junctional proteins and their reformation were investigated. The TER study showed that inhibition of MEK using PD0325901 (1 μM) alone increased the transepithelial resistance of the cell monolayer 50% over untreated control cells after 24 hours. This increase in TER exactly matched that of the increase in TER after incubation in serum-free media overnight, which indicated that the hypothesis predicted may be credible with an increase in TER being a result of a reduction in MEK signalling through serum starvation of the cells. The combined treatment of IL-13 with PD0325901 had no effect on the result with PD0325901 alone suggesting that MEK is not involved in the IL-13-induced effects in TER.

A similar result was observed in the calcium switch assay which investigates the re-formation of the junctional proteins after disruption through the reduction of extracellular calcium concentration. MEK inhibition by PD0325901 (1 μM) was shown to increase TER 34% over control after 24 hours. The combined treatment of PD0325901 with IL-13 gave the same result as the PD0325901 alone as is the case in the classic TER experiment. These results also indicate that IL-13 does not exert its effects on TJ re-

formation through MAPK signalling, however MAPK is shown to be involved independently.

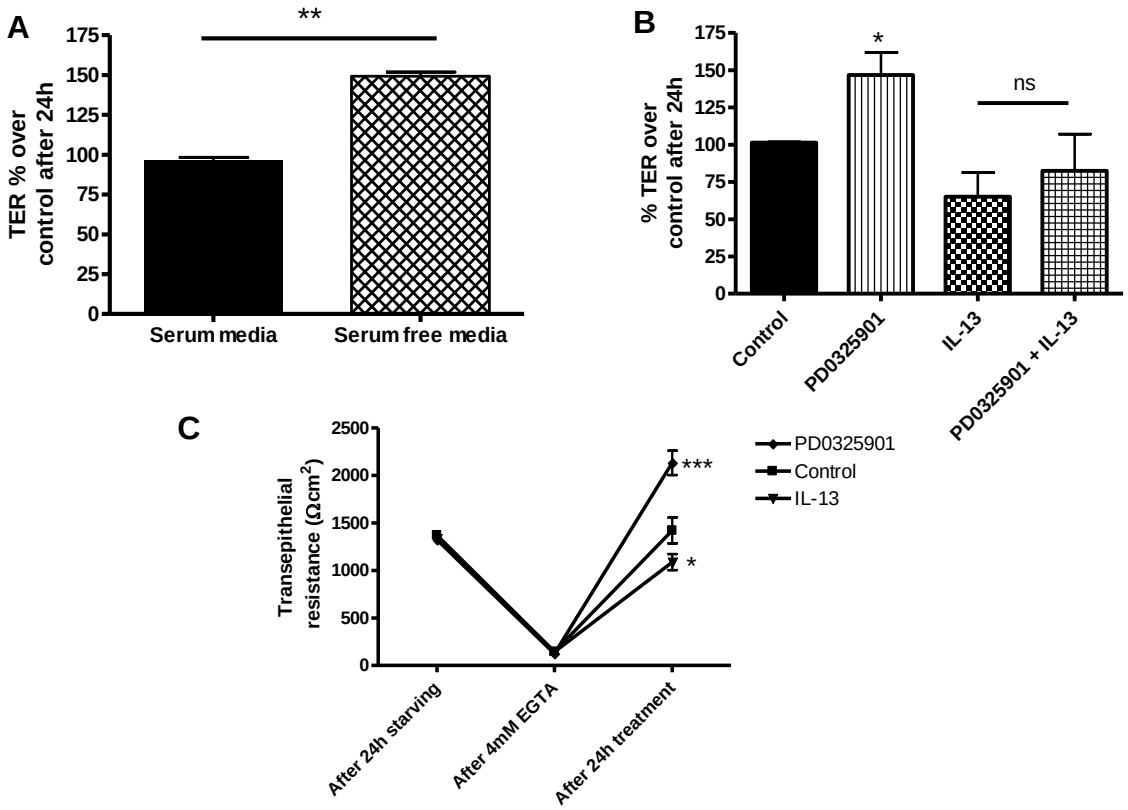

Figure 6.9 Effect of serum and MEK inhibition on TER and junctional protein re-formation.

Cells were grown via ALI and monitored by TER measurements; they were placed in serum or serum-free media for 24 hours (A). Cells were stimulated with IL-13 (10 ng/ml) with or without PD325901 (1 μM) for 24 hours and the TER was then compared to that of the same well 24 h prior to obtain the TER % over control after 24 h treatment (B). For calcium switch studies (C), cells were grown via ALI to confluency, they were starved overnight with serum-free media and their TER was measured. Serum-free media containing 4mM EGTA at pH8 was added to both the apical and basolateral chambers for 30 minutes in which time junctional proteins were diminished shown by a reduction in TER of <300 Ωcm^2. The EGTA solution was removed, cells were washed once with serum-free media and fresh serum-free media containing IL-13 (10 ng/ml) or PD0325901 (1 μM) was placed into the basolateral chamber for 24 hours. Data are presented as mean values ±SEM from n=3 independent experiments, a paired T-test (A) and a 1-way ANOVA (B and C) were used to determine statistical significance which is expressed as (*) for $p<0.05$, (**) for $p<0.01$ and (***) for $p<0.001$.

6.5 Effect of SAHA, 1m and PD0325901 on paracellular permeability using FITC-dextran.

To further investigate the role of STAT6, GSK3β and MEK in epithelial barrier modulation, the paracellular permeability was studied after 24 hour treatment with the inhibitors SAHA, 1m and PD0325901 respectively (Figure 6.10). Inhibiting STAT6 alone with SAHA (5 μM) or in combination with IL-13 did not have any effect on the paracellular permeability compared to the basal response. Inhibiting GSK3β with 1m (2 μM) resulted in a dramatic increase in the amount of FITC detected in the basolateral chamber. This increase in paracellular permeability proved to be statistically significant when compared to the untreated control with a Dunnett's post hoc test. Cells treated with 1m and IL-13 showed a reduction in FITC-dextran permeability compared to that of the 1m alone stimulated cells, but they still showed a significant increase over basal cells. MEK inhibition using PD0325901 (1 μM) alone did not have a great effect on FITC-dextran flux with the result the same as that for the IL-13 group and only slightly higher than the control group. Treating cells with the combination of IL-13 and PD0325901 resulted in a significant increase in FITC-dextran flux, which was a surprising result due to the fact that PD0325901 alone increased TER.

6.6 Effect of SAHA, 1m and PD0325901 on LDH release

To check that the cells were not undergoing cell necrosis caused by treatment of SAHA, 1m and PD0325901 the cells were treated for 24 hours with these inhibitors, after which samples of the media were collected and tested for LDH release compared to the total lysed LDH in the cell. The amount of LDH released was represented as a percentage of the total LDH. None of the inhibitors tested had high levels of LDH release which indicates that cells are happy in the inhibitors for the allocated time shown (Figure 6.11).

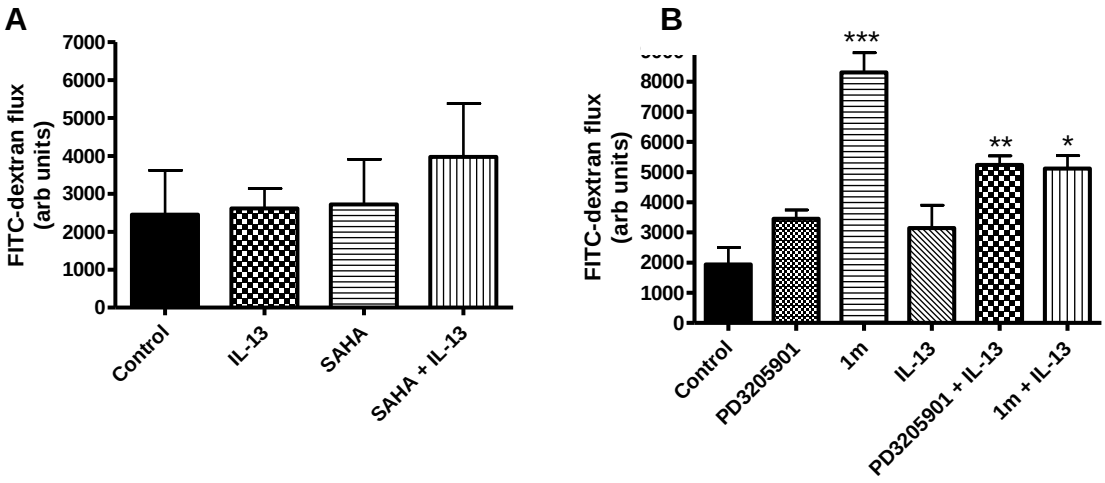

Figure 6.10 Effect of STAT6, MEK and GSK3β inhibition on FITC-dextran flux.

Calu-3 cells were stimulated with SAHA (5 μM), PD3205901 (1 μM) and 1m (2 μM) with or without IL-13 (10 ng/ml) for 24 hours (inhibitors were added 30 minutes prior to IL-13). They were washed twice with HBSS to remove all traces of phenol red and 600 μl HBSS was placed in the basolateral chamber and 200 μl of 500 μg/ml FITC-dextran was placed in the apical chamber. Cells were incubated at 37°C at 5% CO2 for 30 minutes and 100 μl was pipetted from the basolateral chamber of each sample in triplicate onto a black 96-well plate. The fluorescence intensity was measured at excitation 485 nm and emission 530 nm on a Fluorstar optima plate reader. Data are presented from n=3 independent experiments and values are expressed as mean ± SEM. All groups were compared to control and statistical significance is expressed as (*) for $p<0.05$, (**) for $p<0.01$ and (***) for $p<0.001$.

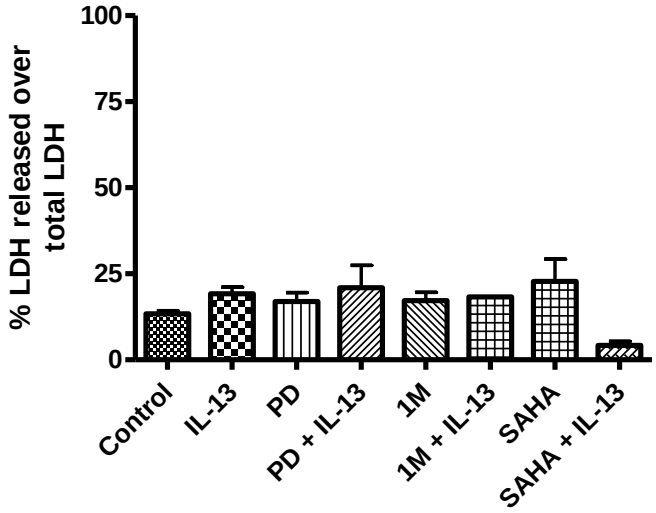

Figure 6.11 Effect of SAHA, PD3205901 and 1m on LDH release.

Cells were treated with IL-13 (10 ng/ml), PD3205901 (1 μM), 1m (2 μM) and SAHA (5 μM) for 24 hours. Samples from the media were tested for LDH presence by measuring the reduction of NADP to NADPH which results in a shift to a deep red colour and can be monitored spectroscopically at a wavelength of 490 nm. These values were converted to a percentage of released LDH over the total LDH in each sample which was obtained through lysing the transwell to release all protein present. Data are plotted as mean values ± SEM for three independent experiments.

6.7 Effect of STAT6, GSK3β, MEK and ZSTK474 inhibition on junctional protein mRNA expression via qRT-PCR

Quantitative real-time PCR was used to investigate the effect of SAHA, 1m, PD0325901 and ZSTK474 (pan class I PI3K inhibitor) on the mRNA expression of various junctional proteins (Figure 6.12). The junctional proteins examined were, claudin 2, claudin 4, claudin 5, claudin 7, claudin 8, claudin 10, occludin, E-cadherin and ZO-1. (For primer sequences see 8.4) Data shown are preliminary from triplicate values from one independent experiment; they give an idea of the expression of a wide range of TJ genes present in Calu-3 cells and with repeated data can act as a

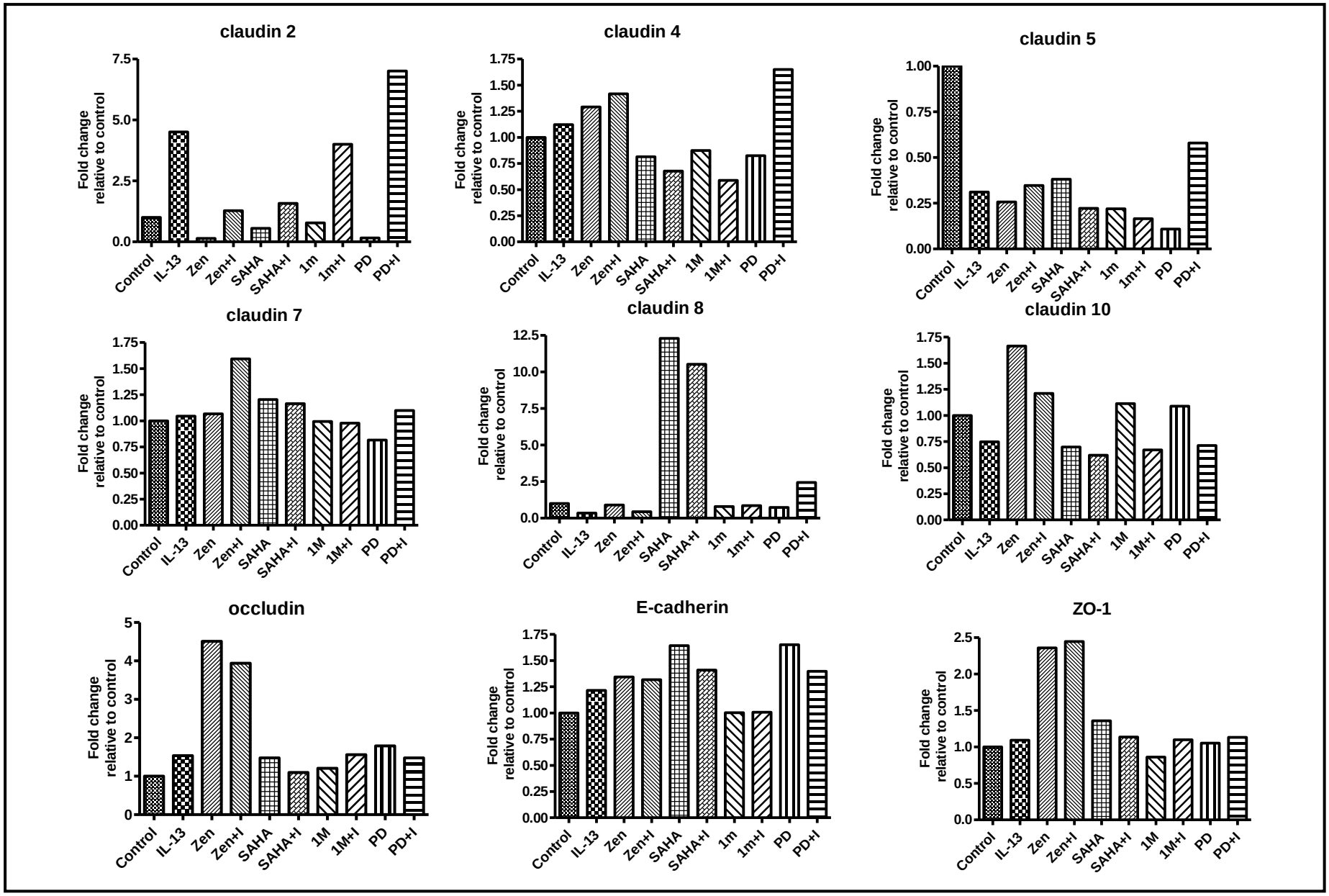
claudin 2
Fold change relative to control
7.5
5.0
2.5
0.0
Control
IL-13
Zen
Zen+I
SAHA
SAHA+I
1m
1m+I
PD
PD+I
claudin 4
Fold change relative to control
1.75
1.50
1.25
1.00
0.75
0.50
0.25
0.00
Control
IL-13
Zen
Zen+I
SAHA
SAHA+I
1M
1M+I
PD
PD+I
claudin 5
Fold change relative to control
1.00
0.75
0.50
0.25
0.00
Control
IL-13
Zen
Zen+I
SAHA
SAHA+I
1m
1m+I
PD
PD+I
claudin 7
Fold change relative to control
1.75
1.50
1.25
1.00
0.75
0.50
0.25
0.00
Control
IL-13
Zen
Zen+I
SAHA
SAHA+I
1M
1M+I
PD
PD+I
claudin 8
Fold change relative to control
12.5
10.0
7.5
5.0
2.5
0.0
Control
IL-13
Zen
Zen+I
SAHA
SAHA+I
1m
1m+I
PD
PD+I
claudin 10
Fold change relative to control
1.75
1.50
1.25
1.00
0.75
0.50
0.25
0.00
Control
IL-13
Zen
Zen+I
SAHA
SAHA+I
1M
1M+I
PD
PD+I
occludin
Fold change relative to control
5
4
3
2
1
0
Control
IL-13
Zen
Zen+I
SAHA
SAHA+I
1M
1M+I
PD
PD+I
E-cadherin
Fold change relative to control
1.75
1.50
1.25
1.00
0.75
0.50
0.25
0.00
Control
IL-13
Zen
Zen+I
SAHA
SAHA+I
1m
1m+I
PD
PD+I
ZO-1
Fold change relative to control
2.5
2.0
1.5
1.0
0.5
0.0
Control
IL-13
Zen
Zen+I
SAHA
SAHA+I
1M
1M+I
PD
PD+I

Figure 6.12 Effect of ZSTK474, SAHA, 1m and PD0325901 on junctional mRNA expression.

Confluent Calu-3 cells grown via ALI were stimulated with ZSTK474 (10 μM), SAHA (5 μM), PD0325901 (1 μM) or 1m (1 μM) for 30 min followed by 10 ng/ml IL-13 for 24 hours. Cells were lysed and RNA was extracted, reversed transcribed to cDNA and reactions were performed on a StepOnePlus Real-time PCR system (see section 2.6 for details). All samples were compared to the equal loading gene β-actin and normalised to the untreated control sample. Data expressed as mean values from preliminary n=1 experiment.

useful screen to uncover proteins which are vastly altered following inhibition of various pathways. The expression of claudin 2 mRNA was upregulated by IL-13 as previously shown and PI3K inhibition with ZSTK474 and STAT6 inhibition with SAHA reduced this upregulation. 1m treatment had no effect on claudin 2 mRNA expression and PD0325901 seemed to slightly increase the IL-13-induced upregulation when used in combination with IL-13. Treatment with SAHA, 1m (either with or without IL-13) and PD0325901 (alone) decreased the level of Claudin 4 mRNA compared to controls between 30-40% and ZSKT474 slightly increased its expression. All treatments (excluding PD+IL-13) decreased the mRNA expression of the TJ protein claudin 5 (70-85%) compared to the control after 24 hour treatment. Claudin 7 mRNA remained unchanged after all treatments, whereas claudin 8 expression was shown to drastically increase 12-fold over controls in the SAHA treated samples, but remained unchanged in all other treatments. PI3K inhibition was shown to increase the mRNA expression of claudin 10 and noticeably all IL-13 treatment groups display a decrease in expression. Occludin and ZO-1 mRNA expression were changed solely by ZSTK474, which upregulated levels 4.5 fold and 2.5 fold respectively compared to controls. All treatments excluding 1m resulted in an slight increase in E-cadherin expression with SAHA increasing levels most highly with a 1.5-1.7 fold increase.

The mRNA expression of IL-13 and IL-4 receptors was also studied after PI3K, STAT6, GSK3β and MEK inhibition (Figure 6.13). The main differences to take from these results is the 50% decrease in IL-4Rα mRNA expression by STAT6 inhibition and the 50% increase by PI3K inhibition, an interesting result as these pathways have been portrayed as having high synergy throughout this project and in research. IL-13 treatment resulted in the 4.5-fold increase of IL-13Rα2 expression which was shown to be reduced by both ZSTK474 and SAHA, data which correlates nicely with the claudin 2 expression results which could possibly suggest a role for IL-13Rα2 in regulation of claudin 2 levels. The expression of IL-13Rα1 remained fairly constant with only PI3K inhibition using ZSTK474 showing a slight increase. This experiment proved very interesting in screening junctional proteins following a variety of pathway inhibitors.

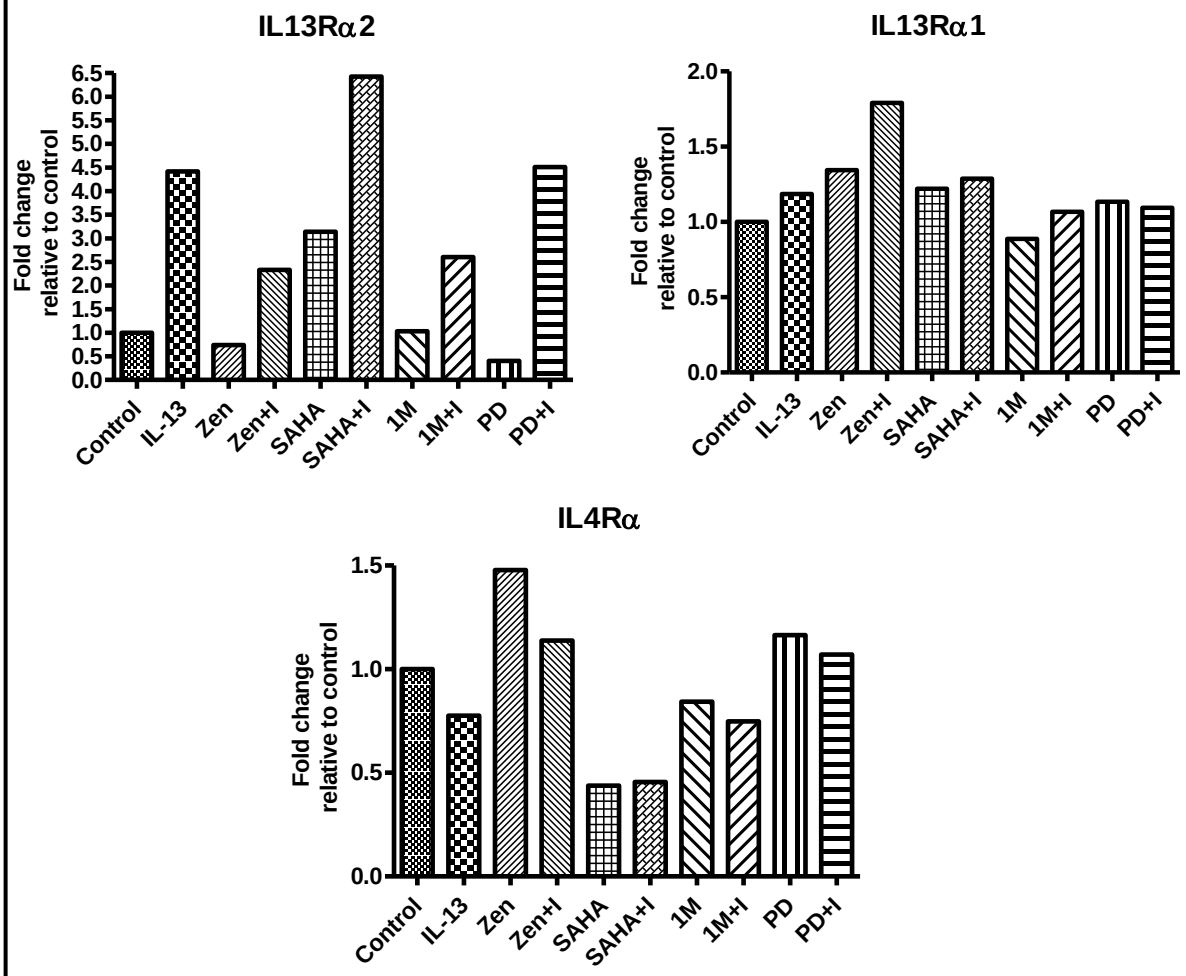

Figure 6.13 Effect of PI3K, STAT6, GSK3β and MEK inhibiton on IL-13 and IL-4 receptor mRNA expression.

Confluent Calu-3 cells grown via ALI were stimulated with ZSTK474 (10 μM), SAHA (5 μM), PD0325901 (1 μM) or 1m (2 μM) for 30 min followed by 10 ng/ml IL-13 for 24 hours. Cells were lysed and RNA was extracted, reversed transcribed to cDNA and reactions were performed on a StepOnePlus Real-time PCR system (see section 2.6 for details). All samples were compared to the equal loading gene β-actin and normalised to the untreated control sample. Data expressed as mean values from preliminary n=1 experiment.

6.8 Discussion

6.8.1 The role of STAT6 in TJ regulation and reformation

The class I and II HDAC inhibitor SAHA was used to inhibit STAT6 activation as previously reported in colonic HT29 and T84 cells [247]. To test its activity in Calu-3 cells, it was administered in combination with IL-13 treatment for up to 48 hours and was shown to completed abolish STAT6 phosphorylation after both 24 and 48 hours. SAHA was subsequently tested in the standard TER experiment carried out in this project where cells cultured at ALI are monitored by TER to confluency and then stimulated with IL-13 with or without the combination of inhibitors. STAT6 inhibition with SAHA resulted in a dramatic increase in TER over control cells when administered alone and the IL-13-induced decrease in TER was prevented when cells were pre-treated with SAHA. This data is in accordance with Madden et al who discovered that the IL-13-induced increase in mucosal permeability and chloride secretion was dependent on STAT6 signalling using knockout mice [246].

The role of STAT6 in the distribution and expression of the TJ protein claudin 2 was explored, with levels shown to be increased by IL-13 in intestinal cells [245, 292], alveolar cells [281] and now bronchial epithelial cells in this project. STAT6 inhibition through treatment with SAHA (5 μM) resulted in a 57% decrease in the IL-13 induced increase in claudin 2 shown by immunofluorescence data. This result was supported by data gained from the quantitative PCR experiment, where SAHA reduced the mRNA expression of IL-13-induced claudin by 3-fold. Together the beginning of this chapter provides strong evidence for the role of STAT6 in the IL-13-induced upregulation of claudin-2 which leads to a disruption in epithelial barrier properties.

These data obtained with the HDAC inhibitor SAHA were almost identical to that obtained using the pan class I PI3K inhibitor ZSTK474 in chapter 5. To investigate whether the pathways were acting independently to produce the same result or they were both being blocked by the same

inhibitor, ZSTK474 was administered to Calu-3 cells and STAT6 activation was studied. It was decided to investigate ZSK474 on STAT6 activation rather than SAHA on pAkt activation as a marker of PI3K due to STAT6 activation providing a far clearer signalling result than Akt. Cells treated with ZSTK474 for 24 hours completely inhibited IL-13-induced STAT6 activation providing evidence that this inhibitor is not a selective class I PI3K inhibitor as reported [99]. However this result was only witnessed after 24 hours, after 48 hours, IL-13-induced STAT6 phosphorylation returned to comparative levels to that of the IL-13 treatment alone. In retrospect, if this experiment was carried out earlier in the project a greater understanding on this PI3K and STAT6 relationship and their involvement in the IL-13 induced effects on claudin 2 expression would have been carried out. However, at this point it can only be concluded that both pathways play a role in TJ regulation and in particular both reduce the basal and IL-13-induced expression of the cationic pore forming TJ claudin 2. Whether this result of ZSTK474 and SAHA treatment is via the same target (or an off-target effect) is not known.

SAHA has recently been shown to acetylate α-tubulin in a dose dependent and concentration dependent manner; in addition the heatshock protein 90 (HSP90) was inhibited, which was demonstrated by a decrease in CDK4 expression [331]. The role of α-tubulin in tight junction regulation is yet to be explored.

6.8.2 Role of STAT6 in claudin 8 regulation

Preliminary results obtained studying claudin 8 expression proved particularly interesting with STAT6 inhibition with SAHA resulting in a 12-fold increase in claudin 8 mRNA over controls after 24 hours. This finding was supported by immunofluorescence data which also showed a significant upregulation of claudin 8 protein after 24 hours after treatment with SAHA. These data suggest that basal STAT6 signalling is required to keep levels of claudin 8 low. There is very little research presented on the role of claudin 8

at the TJ, with most papers focused on its role in the kidney. Claudin 8 has been reported to interact with claudin 4 to form an anion selective pathway in the kidney [332], a finding which was supported by Amasheh et al who reported that Na^+ absorption was coupled with claudin 8 upregulation which seals the TJ to prevent back leakage [333]. Interestingly, claudin 8 has been shown to displace claudin 2 at the TJ and increase the TER of the cell monolayer. However, it was reported to have this effect in MDCK I but not MDCK II cells [334]. This result led researchers to conclude that levels of endogenous and exogenous claudin proteins interfere with each other so the cell line used can impact the results significantly. In their study MDCK I cells were not affected by claudin 8 overexpression as they did not express endogenous claudin 2; MDCK II cells who do endogenously express claudin 2 responded, with claudin 8 transfection promoting TER by reducing claudin 2 expression at the TJ. The way in which claudin 2 and claudin 8 interact is unknown, with possible reasons being claudin 8 may destabilise claudin 2 at the junction or block its insertion into the TJ. Our data obtained from the preliminary qRT-PCR experiment revealed that claudin 4 which has been reported to associate with claudin 8 in the kidney [332] was slightly down-regulated by SAHA, however, further experimental repeats are required to properly investigate this. Claudin 1 has recently been shown to be upregulated by HDAC inhibition with sodium butyrate via an increased association between SP1 and the claudin 1 promoter [335]; this mode of action could also be true for the effects of SAHA on claudin 8.

6.8.3 Role of GSK3β and MAPK in TJ regulation

The role of GSK3β in TJ regulation has mainly focused on the synergistic activation of AMPK and inhibition of which has been reported to lead to TJ deposition in kidney and intestinal cell lines [232, 233, 336]. GSK3β inhibition was shown to induce the upregulation of ZO-1 and occludin independently of extracellular calcium [234]. Severson et al also reported an upregulation of occludin and ZO-1 protein following GSK3β inhibition

[235]. These results do not correlate with our findings in that, the preliminary data obtained from the quantitative PCR studies showed that GSK3β inhibition with 1m did not alter any of the TJ proteins studied including occludin and ZO-1. However this data is only a very basic idea and needs to be repeated in order to form any solid conclusions.

In Calu-3 cells GSK3β was not activated by IL-13 treatment, which could be explained by the cell line already expressing constituently inactive (phosphorylated) GSK3β. GSK3β inhibition alone resulted in a decrease in TER, which was unaffected when combined with IL-13, this was coupled with an increase in FITC dextran flux, indicating the GSK3β is essential for maintaining an intact TJ complex. This result is the opposite of another paper which found that inhibition of GSK3β has a beneficial effect on TER. Degradation of GSK3 by Akt following serum and glucocorticoid protein kinase (Sgk) activation resulted in E-cadherin organization and TJ sealing shown by an increase in TER through inactivation of beta-catenin [337]. Calcium switch studies showed that GSK3β also has a negative effect of the re-formation of the TJ, with decreased TER compared with control cells after 24 hours stimulation. This discrepancy between published results could be explained by the selectivity of the inhibitors used by other investigators, who used far less selective GSK3β inhibitors so their results observed may be explained through GSK3α inhibition.

IL-13 stimulation did not activate the MAPK pathway in Calu-3 cells shown by no significance in ERK phosphorylation compared with control. A recent study by Petecchia et al who investigated the effect of IL-4, IFN and TNFα on MAPK signalling also saw a small increase in ERK phosphorylation in Calu-3 cells [338]. Hence this may be a signalling defect in this cell line as other cell lines such as A549 cells, IL-13 has been shown to phosphorylate ERK 1/2 [339]. The role of the MAPK was investigated by inhibiting MEK 1/2 with the small molecule inhibitor PD0325901; a non-competitive inhibitor that has been shown to be a potent inhibitor of tumour growth in human melanoma cells [340]. Inhibition of the MAPK pathway was shown to increase the TER of Calu-3 cells 2-fold over control and this increase in TER was also observed in TJ reformation during the calcium switch assay.

Results observed after MEK inhibition were independent of IL-13 treatment in both basal and reformation TJ experiments. The combined treatment of PD0325901 and IL-13 produced a bizarre result with an increase in FITC-dextran flux observed along with increases in the mRNA of claudin 2, claudin 4 and IL-13Rα2 after 24 hours. These data indicate that inhibition of MAPK is having an additive effect on IL-13 responses, which may be through more of the IL-13 response being forced down the PI3K pathway instead of being split amongst the two. The beneficial effect seen in our TER study is supported in research in which the MAPK pathway has been shown to be involved in the protection of epithelial integrity from hydrogen peroxide through EGF activation via prevention of tyrosine phosphorylation on ZO-1 and occludin [236]

There are papers that do not agree with MAPK having a positive effect on TJ integrity and it has been shown that Der p 2 increases the cell surface expression of claudin 2 in A549 cells via ERK 1/2 and GSK3β phosphorylation which leads to a decrease in TER [256, 281]. A similar result was observed in human corneal epithelial cells where inhibition of MEK resulted in changes in ZO-1 and disruption of the TJ [270]. Cytokines IL-4, TNFα and IFNγ were shown to decrease the expression of ZO-1 and occludin via a MAPK dependent pathway [338]. These inconsistencies may be explained by different cell types having diverse expression of endogenous tight junctions, which has been shown to play a role in TJ regulation [334].

6.8.4 Limitations and future work

This chapter provides a variety of interesting findings, however many experiments need to be repeated in order to statistically analyse and form conclusions. The work conducted with the HDAC inhibitor SAHA has shown inhibition of STAT6 phosphorylation; this had a beneficial effect on TER as well as, a reduction in the expression of the pore-forming tight junction protein claudin 2. It is still unclear whether blocking phosphorylation of STAT6 is how SAHA elicits its effects on TER and TJ expression as HDAC6

inhibition has been shown to have other targets such as, α-tubulin which it directly acetylates [331]. In order to verify the exact role of STAT6 within these assays, gene silencing or overexpression studies would be required. Another limitation of the data using SAHA treatment is the use of 24 and 48 hour time points to look at IL-13-induced STAT6 phosphorylation, as after this time, there is no way of telling if IL-13 is the sole mediator, or whether there could be a secondary mediator involved. It is therefore necessary to study the effect of SAHA on IL-13-induced STAT6 phosphorylation in a much shorter time-scale of around 0-90 minutes.

To study the relationship between claudin 2 and claudin 8, protein dynamics involving fluorescent techniques such as fluorescence recovery after photobleaching (FRAP) and fluorescence loss in photobleaching (FLIP) can be utilised [341]. Claudin 2 and 8 can be green fluorescent protein (GFP) fusion tagged and their mobility within the membrane can be monitored to investigate the theory that claudin 8 may displace claudin 2 at the junction following SAHA treatment.

It would prove interesting to further study the signalling mechanism in which MEK inhibition enhances basal TER. This can be achieved through immunoblotting and immunofluorescence experiments to investigate tight junction expression and distribution. These studies could also be performed to assess the mechanisms behind the decrease in barrier resistance and increase in paracellular FITC-dextran flux after GSK3β inhibition with 1m. The effect of the PI3K inhibitor ZSTK474 on claudin 8 expression should also be examined.

6.9 Conclusions

This chapter investigated the roles of STAT6, GSK3β and MEK in TJ regulation in Calu-3 cells.

In summary, in this chapter the following was determined:

- The STAT6 pathway is upregulated by IL-13 and STAT6 phosphorylation is inhibited by treatment with the histone deacetylase inhibitor SAHA.
- Treatment with SAHA increases basal TER 2-fold over control and enhances the ability of cells to reform their TJ complex in the calcium switch assay.
- Treatment with SAHA decreases the IL-13-induced increase in claudin 2 protein and mRNA expression
- SAHA treatment dramatically increases the expression of claudin 8 protein and mRNA after 24 hours
- ZSTK474 was shown to have off target effects by inhibiting STAT6 phosphorylation after 24 hours but not 48 hours
- MEK inhibition was shown to have a positive effect on the epithelial barrier by increasing TER.
- GSK3β inhibition had a negative effect on the epithelial barrier properties of Calu-3 cells by decreasing TER and increasing paracellular flux of FITC dextran.

Chapter 7 : General discussion, conclusions and future work

7.1 PI3K in the modulation of the epithelial barrier

The aim of this project was to determine the role of PI3K in lung barrier integrity after IL-13 stimulation. IL-13 had been reported to be involved in features of asthma such as B-cell switching, mast cell degranulation and epithelial transitions such as EMT and GCM. In order to assess the role of PI3K, small molecule inhibitors were administered to the cells prior to stimulation with IL-13. The measurement of TER was used as a marker of epithelial barrier integrity as an intact epithelial layer will possess high basal resistance – whereby no ion exchange between basolateral and apical chambers can take place. Treatment with IL-13 alone resulted in a decrease in the measured resistance (inverse of ion flux), which implied a breakdown of the epithelial barrier. This breakdown has been researched in IBD and tight junctions that make up the apical junctional complex between adjacent epithelial cells, was shown to be responsible for regulating the 'tightness' of epithelial cells and therefore the barrier properties. Pre-treatment with the pan class I inhibitor ZSTK474 was shown to prevent the IL-13 induced decrease in TER. Upon further investigation of the expression and distribution of common junctional proteins known to be present in Calu-3 cells, it was shown that IL-13 treatment resulted in an increase in expression of the tight junction protein claudin 2. Levels of claudin 1 were also slightly increased following IL-13 treatment however levels of ZO-l, occludin, beta catenin and E-cadherin remained unaltered, a finding that is inconsistent with Ahdieh et al who showed that expression of ZO-1 and occludin, were downregulated by IL-13 [252]. Upregulation of claudin 2 following IL-13 treatment was shown to be PI3K dependent with ZSTK474 treatment reducing claudin 2 protein and mRNA expression significantly; ZSTK474 also reduced the basal level of claudin 2. These data indicate that, PI3K signalling is involved in the regulation of the TJ protein claudin 2, which is shown to be upregulated by IL-13.

The next part of this project focused on investigating the isoform of PI3K that was responsible for the prevention of IL-13-induced TER decrease and the reduction of claudin 2 protein. The effects of the PI3K selective inhibitors IC87114, TGX221 and PIK75, which inhibit p110δ, p110β and

p110α respectively, were studied. The IL-13-induced increase in claudin 2 protein levels was prevented by p110α inhibition with PIK75; although PIK75 treatment also reduced basal claudin 2 expression. None of the selective inhibitors alone or in a combined treatment mimicked the prevention of the IL-13 induced decrease in TER shown by the pan-inhibitor ZSK474. This finding was puzzling but may could be explained by the suggestion that whilst PI3K isoforms have their own specific role within a cell, if one is removed then another will compensate for its signalling (analogised for instance by a colleague covering another colleagues shift in work). This concept is referred to as isoform redundancy and is supported by other researchers who propose that immortalized cells can use multiple PI3K isoforms for the same function [342, 343].

7.2 STAT6 in IL-13 induced modulation of the TJ

Aside from PI3K signalling IL-13 has also been shown to activate the STAT6 pathway, which itself has been shown to be involved in the regulation of mucin expression [344] along with the attenuation of airway inflammation in mice [345]. In this project STAT6 phosphorylation was inhibited with the histone deacetylase inhibitor SAHA and pre-treatment resulted in the prevention of the IL-13-induced decrease in TER along with reduction of the tight junction protein claudin 2. These results indicated a role for STAT6 in the modulation of the airway by IL-13. Surprisingly, these data with SAHA mirrored the results seen (with regards to TER and claudin 2 regulation) with the PI3K inhibitor ZSTK474. It was considered whether both results were from inhibition of the same protein, so STAT6 phosphorylation was monitored after ZSTK474 stimulation and was shown to be reduced at 24 hours but not 48 hours, indicating an off-target effect of the apparent ‘selective’ pan-class I PI3K inhibitor. This effect of ZSTK474 on STAT6 activation may explain why none of the selective isoform inhibitors prevented the IL-13-induced TER decrease, even when administered in combination in an attempt to mimic pan-PI3K inhibition. This idea that all the results obtained with ZSTK474 were through blocking STAT6 phosphorylation rather

than through PI3K inhibition, would be a credible conclusion if it wasn't for the results obtained by the p110α selective inhibitor PIK75, which showed that p110α played a role in the claudin 2 upregulation. However, the selectivity of this inhibitor may not be quite what was reported either [98] and its effect on STAT6 phosphorylation was not tested. Another possible explanation could be that both STAT6 and PI3K pathways are equally important in the maintenance of the TJ and whether they act in synergy or independently of each other is yet to be confirmed. Research into the mechanisms behind the IL-13 effects in intestinal epithelial cells, do not shed much light on the role of PI3K vs the role of STAT6 in TJ regulation in the lung. Ceponis *et al* reported a link between IL-13-induced TER and PI3K and stated that there is no role for the STAT6 pathway [248]. This finding opposes what is predicted in this project with the main emphasis of the IL-13 effect on the epithelial barrier being put down to STAT6. An involvement for the STAT6 pathway in IL-13-induced effects has been reported in mice where inhibition reduces airway inflammation [345] as well as reducing glucose absorption and chloride secretion in the intestine [246]. In a paper published recently (January 2013), ulcerative colitis was attenuated in STAT6 knockout mice by a reduction in the tight junction protein claudin 2, proving that epithelial barrier modulation is reliant on STAT6 signalling [346]. The results on the effect of STAT6 signalling on the TJ in Calu-3s cells are, equivalent to those published in this recent paper on ulcerative colitis proving that, the mechanism behind the modulation is similar in both inflammatory diseases.

It has be taken into account that the majority of the data presented in this thesis focuses on the regulation of one tight junction protein, claudin 2, as there are 23 other claudins shown to be present in the TJ, with each one possessing its own unique role, along with an individual pattern of regulation. Whilst there are a number of other proteins to consider, every piece of knowledge on the mechanisms behind the highly dynamic process of tight junction regulation, is important in the search for new treatment for diseases, such as asthma and ulcerative colitis. An additional point to mention, which was covered in more detail in 6.8.4, is that SAHA is a HDAC inhibitor so it is

not selective for STAT6 and therefore, could be eliciting its effects through regulation of an alternative signalling mediator.

Another key finding in this project was the significant upregulation of the tight junction protein claudin 8 following treatment with SAHA. The role of claudin 8 at the TJ is relatively unknown, it has been reported to interact with claudin 4 to form an anion selective pathway in the kidney [332]; a finding which was supported by Amasheh et al who reported that, Na^+ absorption in the kidney was coupled with claudin 8 upregulation, which, seals the TJ to prevent back leakage [333]. Interestingly, claudin 8 has been shown to displace claudin 2 at the TJ and increase the TER of the cell monolayer. This finding could explain the effect seen by SAHA treatment in Calu-3 cells, whereby, IL-13 causes an upregulation of claudin 2, leading to a decrease in TER both of which are prevented by SAHA treatment. A suggestion of how this effect is brought about may be through the increase in claudin 8 displacing claudin 2 at the TJ, as in IBD. It has also been shown that along with displacing claudin 2, claudin 8 also reduces the gene expression of claudin 2 and impedes its insertion back into the TJ, however the reason for this is unknown [334]. This result led its researchers to conclude that, levels of endogenous and exogenous claudin proteins interfere with each other, so the cell line used can impact the results significantly. The complexity of claudins regulation is increased further by, their ability to interact with the same or different claudins in homomeric, homotopic, heteromeric and heterotopic interactions.

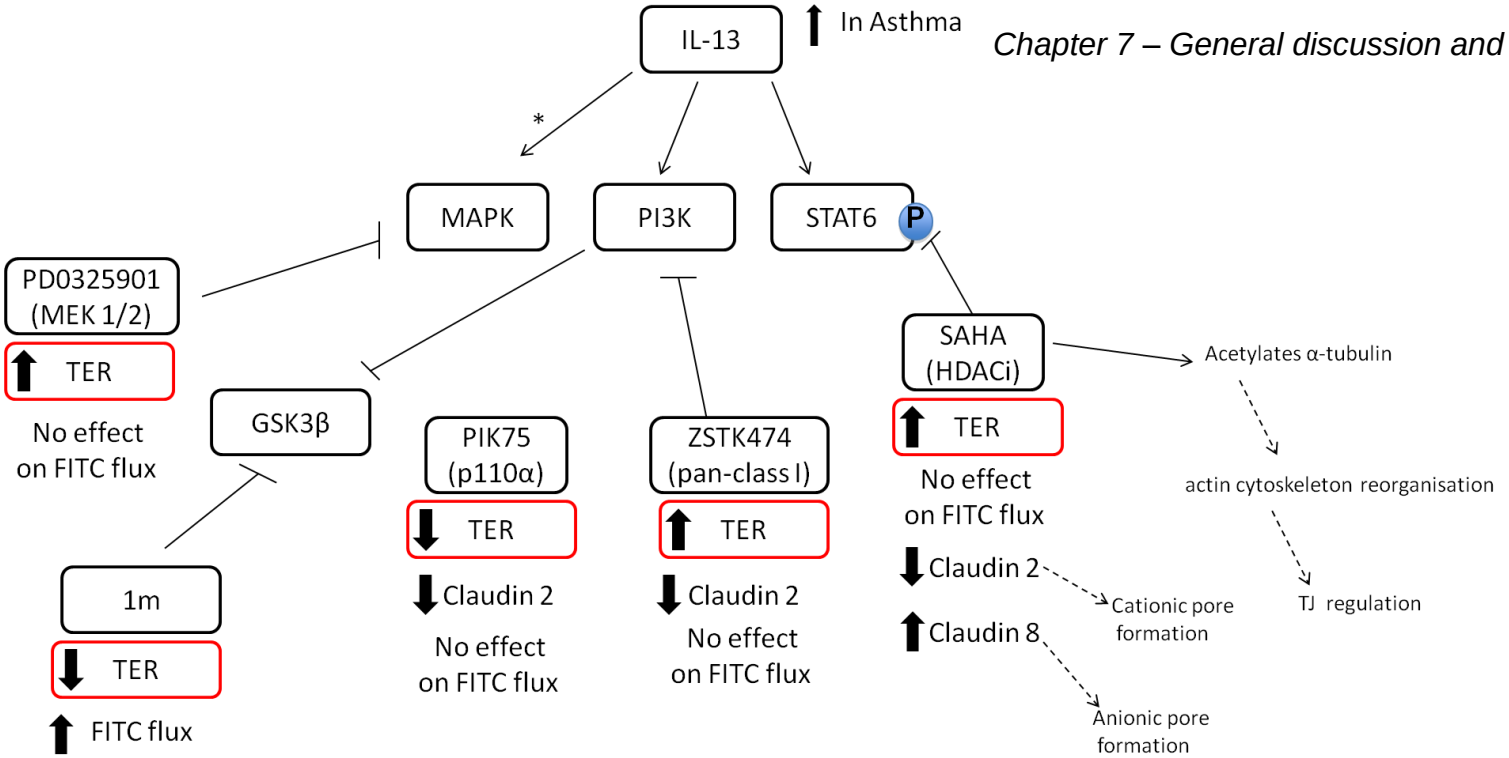

Figure 7.1 Overview of signalling pathways involved in TJ regulation in Calu-3 cells.

This thesis has studied the signalling pathways involved in tight junction regulation in Calu-3 cells. IL-13 stimulation decreases epithelial barrier resistance, has no effect on the paracellular permeability to FITC-dextran flux and dramatically increases claudin 2 protein expression. PI3K class I inhibition with ZSTK474 prevents the IL-13-induced TER decrease and reduces both basal and IL-13-induced claudin 2 expression. Only the PI3K α isoform affects the barrier properties, decreasing basal TER, claudin 2 expression and slightly increasing FITC-dextran flux. The HDAC inhibitor SAHA which inhibits STAT6 phosphorylation increases basal TER, decreases claudin 2 and increases claudin 8 protein expression. Research shows that claudin 2 forms a cationic pore [292] and claudin 8 forms an anionic pore in kidney cells [333]. Recently HDAC inhibition has been shown to target the cytoskeletal protein α-tubulin via direct acetylation [331]; here it is speculated that this leads to reorganisation of the actin cytoskeleton and hence the TJ complex. GSK3β inhibition with 1m reduces TER and increases FITC-dextran flux, suggesting a role for GSK3β signalling in basal junctional complex maintenance. The MAPK pathway also affects barrier properties as MEK inhibition with PD0325901 increases basal TER but has no affect on FITC-flux. * IL-13 was not shown to activate MAPK in Calu-3 cells but it has been shown in other lung cell lines such as A549s [339].

7.3 Future Work

The next step in this research would be to further investigate the expression of claudin 8 in Calu-3 cells and study its interaction with claudin 2. If treatment with SAHA is eliciting its effects via the upregulation of claudin 8, as is the case for HDAC inhibition increasing claudin 1 [335], then a likely mechanism of action would be that this upregulation of claudin 8 is displacing the claudin 2 at the TJ. It would be interesting to overexpress claudin 8 and investigate the IL-13-induced decrease in TER and increase in claudin 2, which is likely to be diminished if this theory is correct. To enable accurate conclusions regarding PI3K isoform and STAT6 involvement in basal and IL-13-induced TJ regulation, overexpression or gene silencing studies should undertaken. One exciting area of research which is yet to be explored is that on the role of HDAC/HAT balance in TJ regulation, including a possible involvement of actin reorganisation. Actin reorganisation is regulated by RhoA signalling, this pathway could also be studied in connection with HDAC regulation. Finally the work in this thesis has focussed on the effect of IL-13, initial results showed that the T_H1 cytokine IFN-γ increases the TER 40% over basal levels and this finding warrants further investigation.

7.4 Final conclusions

In conclusion, this thesis has researched the effect of the cytokine IL-13 and the PI3K, STAT6, MAPK and GSK3β pathways on the modulation of epithelial barrier integrity in Calu-3 cells. It can be concluded that one way in which IL-13 disrupts the epithelial barrier is by increasing the tight junction protein claudin 2; resulting in a decrease in TER. Both ZSTK474 and SAHA treatment has proven beneficial for the epithelial barrier; measured by an increase in TER above control and a decrease in the basal level and IL-13-induced increased levels of claudin 2. Targeting the MAPK pathway using the MEK 1/2 inhibitor PD0325901 also demonstrated an increase in TER above control; however the mechanism behind this is unknown. GSK3β inhibition disrupted the epithelial barrier, reducing TER and increasing the

paracellular flux of the macromolecule FITC-dextran. Data which suggests that GSK3β signalling is vital for TJ maintenance, nonetheless the way in which this affect is produced is still unknown. These data give an important insight into the highly dynamic regulation of the TJ complex, in which further knowledge will ultimately aid in the discovery of new drug targets for asthma.

Chapter 8：Appendices

8.1 Immunnoblot buffers

Lysis Buffer	50 mM Tris-HCl pH 7.5, 150 mM NaCl, 1% Nonidet P40, 10% Glycerol (both v/v), 5 mM EDTA, 1 mM sodium vanadate, 1 mM sodium molybdate, 10 mM sodium fluoride, 40 µg/ml PMSF, 0.7 µg/ml Pepstatin A, 10 µg/ml Aprotinin, 10 µg/ml Leupeptin, 10 µg/ml and Soyabean trypsin inhibitor.
5X sample buffer	10% SDS, 50% Glycerol, 200 mM Tris-HCl pH 6.8, bromophenol blue to taste and 5% 2-mercaptoethanol (50µl/ml) to be added before use.
SDS-PAGE Running Buffer	25 mM Tris base, 192 mM glycine, 0.1% (w/v) SDS and MQ water
Semi-dry transfer buffer	39 mM glycine, 48 mM Tris base, 0.0375% SDS, 20% (v/v) methanol and MQ water
PBS	5x phosphate buffered saline tables were dissolved in 1L of MQ water
PBST	1L of PBS was supplemented with 5 ml of Tween-20
5X stripping buffer	10 g SDS, 31.25ml 1M Tris HCl at pH 7.4 and made up to 100ml with MQ water. After diluting to 1X stripping buffer 2-mercaptoethanol was added (770µl to 100ml).

8.2 Antibody table

			Western blotting		Immunofluorescence	
Target of primary antibody	**Species**	**Molecular weight kDa**	**Blocking buffer**	**Primary antibody concentration**	**Fixing method**	**Primary antibody concentration**
phospho Akt (Ser473)	rabbit	60	5% BSA in PBST	1 in 1000	N/A	N/A
phospho ERK (Thr202, Tyr204)	rabbit	42, 44	5% BSA in PBST	1 in 1000	N/A	N/A
phospho GSK (Ser21/9)	rabbit	46, 51	5% BSA in PBST	1 in 1000	N/A	N/A
phospho STAT6 (Tyr641)	rabbit	110	5% BSA in PBST	1 in 1000	N/A	N/A
Akt 1	rabbit	60	5% BSA in PBST	1 in 1000	N/A	N/A
ERK1/2	rabbit	42, 44	5% BSA in PBST	1 in 1000	N/A	N/A
GSK	rabbit	110	5% BSA in PBST	1 in 1000	N/A	N/A
STAT6	rabbit	90	5% BSA in PBST	1 in 1000	N/A	N/A
beta-actin	rabbit	45	5% milk in PBST	1 in 1000	N/A	N/A
occludin	mouse	120	5% milk in PBST	1 in 1000	1	1 in 200
claudin 2	mouse	25	5% milk in PBST	1 in 1000	1	1 in 200
claudin 1	rabbit	20	5% milk in PBST	1 in 1000	1	1 in 100
ZO-1	mouse	225	5% milk in PBST	1 in 1000	1	1 in 100
E-cadherin	mouse	135	5% milk in PBST	1 in 1000	2	1 in 100

8.3 PCR reaction mixtures

cDNA synthesis (per rxn)

10x RT Buffer	2 µl
25x dNTP Mix	0.8 µl
10x RT Random primers	2 µl
Multiscribe reverse transcriptase	1 µl
Rnasin	0.2 µl
RNA/MQ water	14 µl

Each reaction is made up 1 µg RNA diluted to 14 µl with MQ water

cDNA synthesis programme
25°C for 10 min
37°C for 120 min
85°C for 10 min
4°C hold

8.4 Primer sequences

Gene	*Forward (5'-3')*	*Reverse (5'-3')*
Occludin	GGAACACATTTATGATGAGC	GGCGTGGATTTATAGGAAGA
E-cadherin	ACCAGGACTTTGACTTGAGC	CGAGCAGAGAATCATAAGGC
Claudin 1	CCACCTGCAAACTCTCCGCC	CCAGGAGGATGCCAACCACC
Claudin 2	ATCGCTCCAACTACTACGATGC	CAGGCTGTAGGAATTGAACTCAC
Claudin 5	CTCTGCTGGTTCGCCAACAT	CACAGACGGGTCGTAAAACTC
Claudin 7	AGCTGCAAAATGTACGACTCG	GGAGACCACCATTAGGGCTC
Claudin 8	CAACCCATGCCTTAGAAATCGC	CCATTCCAACACCACCAAGAAA
Claudin 10	GCATGTAGAGGACTTATGATCGC	AGAGCGCAAATATGGAACCAAA
ZO-1	GTTGTATTGAAGATAAATGG	CAGAAGGCTCTGACCGCTGG
MUC5AC	TGACCCACCAGTGTGAGAAG	GGATGATCAGGCTCCTATCG
IL-13RA2	GGGCATTGAAGCGAAGATACA	GCCCAGGAACTTTGAACTTCTG
IL-13RA1	TCGTCGTTCAATAGAAGTACCCC	CCACTTGCAGACAAATCCTCTC
IL-4RA1	CGTGGTCAGTGCGGATAACTA	TGGTGTGAACTGTCAGGTTTC

Chapter 9 : References

1. Dal-Re, R., *Early phase drugs and biologicals clinical trials on worldwide leading causes of death: a descriptive analysis.* Eur J Clin Pharmacol, 2011. **67**(6): p. 563-71.
2. Hammad, H. and B.N. Lambrecht, *Dendritic cells and epithelial cells: linking innate and adaptive immunity in asthma.* Nat Rev Immunol, 2008. **8**(3): p. 193-204.
3. Miescher, S.M. and M. Vogel, *Molecular aspects of allergy.* Mol Aspects Med, 2002. **23**(6): p. 413-62.
4. http://www.asthma.org.uk/news_media/media_resources/for_journalists_key.html.
5. Akinbami, L.J., et al., *Trends in asthma prevalence, health care use, and mortality in the United States, 2001-2010.* NCHS Data Brief, 2012(94): p. 1-8.
6. Lazarus, S.C., *Clinical practice. Emergency treatment of asthma.* N Engl J Med, 2010. **363**(8): p. 755-64.
7. Romanet-Manent, S., et al., *Allergic vs nonallergic asthma: what makes the difference?* Allergy, 2002. **57**(7): p. 607-13.
8. Walsh, G.M., *An update on emerging drugs for asthma.* Expert Opin Emerg Drugs, 2012. **17**(1): p. 37-42.
9. Woodruff, P.G., et al., *T-helper type 2-driven inflammation defines major subphenotypes of asthma.* Am J Respir Crit Care Med, 2009. **180**(5): p. 388-95.
10. Pavord, I.D., *Asthma phenotypes.* Semin Respir Crit Care Med, 2012. **33**(6): p. 645-52.
11. Moore, W.C., et al., *Identification of asthma phenotypes using cluster analysis in the Severe Asthma Research Program.* Am J Respir Crit Care Med, 2010. **181**(4): p. 315-23.
12. Robinson, C.B., J. Leonard, and R.A. Panettieri, Jr., *Drug development for severe asthma: what are the metrics?* Pharmacol Ther, 2012. **135**(2): p. 176-81.

13. Medoff, B.D., S.Y. Thomas, and A.D. Luster, *T cell trafficking in allergic asthma: the ins and outs.* Annu Rev Immunol, 2008. **26**: p. 205-32.
14. Geraldes, L., A. Todo-Bom, and C. Loureiro, *[Airways inflammation evaluation. Upper and lower airways].* Rev Port Pneumol, 2009. **15**(3): p. 443-60.
15. Wang, X.F. and J.G. Hong, *Management of severe asthma exacerbation in children.* World J Pediatr, 2011. **7**(4): p. 293-301.
16. Kariyawasam, H.H., et al., *Remodeling and airway hyperresponsiveness but not cellular inflammation persist after allergen challenge in asthma.* Am J Respir Crit Care Med, 2007. **175**(9): p. 896-904.
17. Cohen, L., et al., *Epithelial cell proliferation contributes to airway remodeling in severe asthma.* Am J Respir Crit Care Med, 2007. **176**(2): p. 138-45.
18. Tagaya, E. and J. Tamaoki, *Mechanisms of airway remodeling in asthma.* Allergol Int, 2007. **56**(4): p. 331-40.
19. Guarino, M., et al., *Pathological relevance of epithelial and mesenchymal phenotype plasticity.* Pathol Res Pract, 1999. **195**(6): p. 379-89.
20. Acloque, H., et al., *Epithelial-mesenchymal transitions: the importance of changing cell state in development and disease.* J Clin Invest, 2009. **119**(6): p. 1438-49.
21. Kalluri, R., *EMT: when epithelial cells decide to become mesenchymal-like cells.* J Clin Invest, 2009. **119**(6): p. 1417-9.
22. Kalluri, R. and R.A. Weinberg, *The basics of epithelial-mesenchymal transition.* J Clin Invest, 2009. **119**(6): p. 1420-8.
23. Atherton, H.C., G. Jones, and H. Danahay, *IL-13-induced changes in the goblet cell density of human bronchial epithelial cell cultures: MAP kinase and phosphatidylinositol 3-kinase regulation.* Am J Physiol Lung Cell Mol Physiol, 2003. **285**(3): p. L730-9.
24. Zuhdi Alimam, M., et al., *Muc-5/5ac mucin messenger RNA and protein expression is a marker of goblet cell metaplasia in murine airways.* Am J Respir Cell Mol Biol, 2000. **22**(3): p. 253-60.

25. Widdicombe, J.G., *Airway liquid: a barrier to drug diffusion?* Eur Respir J, 1997. **10**(10): p. 2194-7.
26. Widdicombe, J.H., et al., *Regulation of depth and composition of airway surface liquid.* Eur Respir J, 1997. **10**(12): p. 2892-7.
27. Hogg, J.C., *Airway structure and function in asthma.* N Engl Reg Allergy Proc, 1986. **7**(3): p. 228-35.
28. Kuyper, L.M., et al., *Characterization of airway plugging in fatal asthma.* Am J Med, 2003. **115**(1): p. 6-11.
29. Groneberg, D.A., U. Wagner, and K.F. Chung, *Mucus and fatal asthma.* Am J Med, 2004. **116**(1): p. 66-7; author reply 67.
30. Hays, S.R. and J.V. Fahy, *The role of mucus in fatal asthma.* Am J Med, 2003. **115**(1): p. 68-9.
31. Zhu, Z., et al., *Pulmonary expression of interleukin-13 causes inflammation, mucus hypersecretion, subepithelial fibrosis, physiologic abnormalities, and eotaxin production.* J Clin Invest, 1999. **103**(6): p. 779-88.
32. Salim, S.Y. and J.D. Soderholm, *Importance of disrupted intestinal barrier in inflammatory bowel diseases.* Inflamm Bowel Dis, 2011. **17**(1): p. 362-81.
33. Nadel, J.A., *Role of epidermal growth factor receptor activation in regulating mucin synthesis.* Respir Res, 2001. **2**(2): p. 85-9.
34. Izuhara, K., et al., *The mechanism of mucus production in bronchial asthma.* Curr Med Chem, 2009. **16**(22): p. 2867-75.
35. McKenzie, A.N., et al., *Interleukin 13, a T-cell-derived cytokine that regulates human monocyte and B-cell function.* Proc Natl Acad Sci U S A, 1993. **90**(8): p. 3735-9.
36. Brown, K.D., et al., *A family of small inducible proteins secreted by leukocytes are members of a new superfamily that includes leukocyte and fibroblast-derived inflammatory agents, growth factors, and indicators of various activation processes.* J Immunol, 1989. **142**(2): p. 679-87.
37. Minty, A., et al., *Interleukin-13 is a new human lymphokine regulating inflammatory and immune responses.* Nature, 1993. **362**(6417): p. 248-50.

38. Dolganov, G., et al., *Coexpression of the interleukin-13 and interleukin-4 genes correlates with their physical linkage in the cytokine gene cluster on human chromosome 5q23-31.* Blood, 1996. **87**(8): p. 3316-26.
39. Corren, J., et al., *Lebrikizumab treatment in adults with asthma.* N Engl J Med, 2011. **365**(12): p. 1088-98.
40. Uchida, M., et al., *Periostin, a matricellular protein, plays a role in the induction of chemokines in pulmonary fibrosis.* Am J Respir Cell Mol Biol, 2012. **46**(5): p. 677-86.
41. Jia, G., et al., *Periostin is a systemic biomarker of eosinophilic airway inflammation in asthmatic patients.* J Allergy Clin Immunol, 2012. **130**(3): p. 647-654 e10.
42. Defrance, T., et al., *Interleukin 13 is a B cell stimulating factor.* J Exp Med, 1994. **179**(1): p. 135-43.
43. Horie, S., et al., *Interleukin-13 but not interleukin-4 prolongs eosinophil survival and induces eosinophil chemotaxis.* Intern Med, 1997. **36**(3): p. 179-85.
44. Provost, V., et al., *Leukotriene D4 and interleukin-13 cooperate to increase the release of eotaxin-3 by airway epithelial cells.* PLoS One, 2012. **7**(8): p. e43544.
45. Holgate, S.T. and R. Polosa, *Treatment strategies for allergy and asthma.* Nat Rev Immunol, 2008. **8**(3): p. 218-30.
46. Olson, N., et al., *Nitric oxide and airway epithelial barrier function: regulation of tight junction proteins and epithelial permeability.* Arch Biochem Biophys, 2009. **484**(2): p. 205-13.
47. Mulrennan, S.A. and A.E. Redington, *Nitric oxide synthase inhibition: therapeutic potential in asthma.* Treat Respir Med, 2004. **3**(2): p. 79-88.
48. Beckman, J.S. and W.H. Koppenol, *Nitric oxide, superoxide, and peroxynitrite: the good, the bad, and ugly.* Am J Physiol, 1996. **271**(5 Pt 1): p. C1424-37.
49. Hesse, M., et al., *Differential regulation of nitric oxide synthase-2 and arginase-1 by type 1/type 2 cytokines in vivo: granulomatous*

pathology is shaped by the pattern of L-arginine metabolism. J Immunol, 2001. **167**(11): p. 6533-44.

50. Benson, R.C., K.A. Hardy, and C.R. Morris, *Arginase and arginine dysregulation in asthma.* J Allergy (Cairo), 2011. **2011**: p. 736319.
51. Maarsingh, H., et al., *Increased arginase activity contributes to airway remodelling in chronic allergic asthma.* Eur Respir J, 2011. **38**(2): p. 318-28.
52. Yamamoto, M., et al., *Nitric oxide and related enzymes in asthma: relation to severity, enzyme function and inflammation.* Clin Exp Allergy, 2012. **42**(5): p. 760-8.
53. Yang, M., et al., *Inhibition of arginase I activity by RNA interference attenuates IL-13-induced airways hyperresponsiveness.* J Immunol, 2006. **177**(8): p. 5595-603.
54. Miloux, B., et al., *Cloning of the human IL-13R alpha1 chain and reconstitution with the IL4R alpha of a functional IL-4/IL-13 receptor complex.* FEBS Lett, 1997. **401**(2-3): p. 163-6.
55. Gauchat, J.F., et al., *A novel 4-kb interleukin-13 receptor alpha mRNA expressed in human B, T, and endothelial cells encoding an alternate type-II interleukin-4/interleukin-13 receptor.* Eur J Immunol, 1997. **27**(4): p. 971-8.
56. Andrews, A.L., et al., *Kinetic analysis of the interleukin-13 receptor complex.* J Biol Chem, 2002. **277**(48): p. 46073-8.
57. MacDonald, T.T., *Decoy receptor springs to life and eases fibrosis.* Nat Med, 2006. **12**(1): p. 13-4.
58. Caput, D., et al., *Cloning and characterization of a specific interleukin (IL)-13 binding protein structurally related to the IL-5 receptor alpha chain.* J Biol Chem, 1996. **271**(28): p. 16921-6.
59. Lacy, E.R., *Equilibrium and kinetic analysis of human interleukin-13 and IL-13 receptor alpha-2 complex formation.* J Mol Recognit, 2012. **25**(3): p. 184-91.
60. Daines, M.O., et al., *Level of expression of IL-13R alpha 2 impacts receptor distribution and IL-13 signaling.* J Immunol, 2006. **176**(12): p. 7495-501.

61. Sasaki, T., et al., *Mammalian phosphoinositide kinases and phosphatases.* Prog Lipid Res, 2009. **48**(6): p. 307-43.
62. Harris, T.K., *PDK1 and PKB/Akt: ideal targets for development of new strategies to structure-based drug design.* IUBMB Life, 2003. **55**(3): p. 117-26.
63. Vogt, P.K., et al., *Phosphatidylinositol 3-kinase: the oncoprotein.* Curr Top Microbiol Immunol, 2010. **347**: p. 79-104.
64. Vanhaesebroeck, B., L. Stephens, and P. Hawkins, *PI3K signalling: the path to discovery and understanding.* Nat Rev Mol Cell Biol, 2012. **13**(3): p. 195-203.
65. De Luca, A., et al., *The RAS/RAF/MEK/ERK and the PI3K/AKT signalling pathways: role in cancer pathogenesis and implications for therapeutic approaches.* Expert Opin Ther Targets, 2012. **16 Suppl 2**: p. S17-27.
66. Vanhaesebroeck, B., et al., *Phosphoinositide 3-kinases: a conserved family of signal transducers.* Trends Biochem Sci, 1997. **22**(7): p. 267-72.
67. Falasca, M. and T. Maffucci, *Regulation and cellular functions of class II phosphoinositide 3-kinases.* Biochem J, 2012. **443**(3): p. 587-601.
68. Stack, J.H., et al., *A membrane-associated complex containing the Vps15 protein kinase and the Vps34 PI 3-kinase is essential for protein sorting to the yeast lysosome-like vacuole.* EMBO J, 1993. **12**(5): p. 2195-204.
69. Jaber, N., et al., *Class III PI3K Vps34 plays an essential role in autophagy and in heart and liver function.* Proc Natl Acad Sci U S A, 2012. **109**(6): p. 2003-8.
70. Benistant, C., H. Chapuis, and S. Roche, *A specific function for phosphatidylinositol 3-kinase alpha (p85alpha-p110alpha) in cell survival and for phosphatidylinositol 3-kinase beta (p85alpha-p110beta) in de novo DNA synthesis of human colon carcinoma cells.* Oncogene, 2000. **19**(44): p. 5083-90.
71. Marques, M., et al., *Phosphoinositide 3-kinases p110alpha and p110beta regulate cell cycle entry, exhibiting distinct activation kinetics in G1 phase.* Mol Cell Biol, 2008. **28**(8): p. 2803-14.

72. Gaidarov, I., et al., *The class II phosphoinositide 3-kinase C2alpha is activated by clathrin and regulates clathrin-mediated membrane trafficking.* Mol Cell, 2001. **7**(2): p. 443-9.
73. Medina-Tato, D.A., S.G. Ward, and M.L. Watson, *Phosphoinositide 3-kinase signalling in lung disease: leucocytes and beyond.* Immunology, 2007. **121**(4): p. 448-61.
74. Katso, R., et al., *Cellular function of phosphoinositide 3-kinases: implications for development, homeostasis, and cancer.* Annu Rev Cell Dev Biol, 2001. **17**: p. 615-75.
75. Kou, X.X., et al., *Acetylated Sp1 inhibits PTEN expression through binding to PTEN core promoter and recruitment of HDAC1 and promotes cancer cell migration and invasion.* Carcinogenesis, 2012.
76. Karar, J. and A. Maity, *PI3K/AKT/mTOR Pathway in Angiogenesis.* Front Mol Neurosci, 2011. **4**: p. 51.
77. McCubrey, J.A., et al., *Mutations and Deregulation of Ras/Raf/MEK/ERK and PI3K/PTEN/Akt/mTOR Cascades.* Oncotarget, 2012. **3**(9): p. 954-87.
78. Luo, J.M., et al., *Possible dominant-negative mutation of the SHIP gene in acute myeloid leukemia.* Leukemia, 2003. **17**(1): p. 1-8.
79. Abbas, H.K. and C.J. Mirocha, *Isolation and purification of a hemorrhagic factor (wortmannin) from Fusarium oxysporum (N17B).* Appl Environ Microbiol, 1988. **54**(5): p. 1268-74.
80. Wymann, M.P., et al., *Wortmannin inactivates phosphoinositide 3-kinase by covalent modification of Lys-802, a residue involved in the phosphate transfer reaction.* Mol Cell Biol, 1996. **16**(4): p. 1722-33.
81. Vlahos, C.J., et al., *A specific inhibitor of phosphatidylinositol 3-kinase, 2-(4-morpholinyl)-8-phenyl-4H-1-benzopyran-4-one (LY294002).* J Biol Chem, 1994. **269**(7): p. 5241-8.
82. Crabbe, T., M.J. Welham, and S.G. Ward, *The PI3K inhibitor arsenal: choose your weapon!* Trends Biochem Sci, 2007. **32**(10): p. 450-6.
83. Ferby, I., et al., *PAF-induced MAPK activation is inhibited by wortmannin in neutrophils and macrophages.* Adv Exp Med Biol, 1996. **416**: p. 321-6.

84. Ohara-Imaizumi, M., et al., *Inhibition of Ca(2+)-dependent catecholamine release by myosin light chain kinase inhibitor, wortmannin, in adrenal chromaffin cells.* Biochem Biophys Res Commun, 1992. **185**(3): p. 1016-21.
85. Brunn, G.J., et al., *Direct inhibition of the signaling functions of the mammalian target of rapamycin by the phosphoinositide 3-kinase inhibitors, wortmannin and LY294002.* EMBO J, 1996. **15**(19): p. 5256-67.
86. Downing, G.J., et al., *Characterization of a soluble adrenal phosphatidylinositol 4-kinase reveals wortmannin sensitivity of type III phosphatidylinositol kinases.* Biochemistry, 1996. **35**(11): p. 3587-94.
87. Walker, E.H., et al., *Structural determinants of phosphoinositide 3-kinase inhibition by wortmannin, LY294002, quercetin, myricetin, and staurosporine.* Mol Cell, 2000. **6**(4): p. 909-19.
88. Puri, K.D., et al., *Mechanisms and implications of phosphoinositide 3-kinase delta in promoting neutrophil trafficking into inflamed tissue.* Blood, 2004. **103**(9): p. 3448-56.
89. Moir, L.M., et al., *Phosphatidylinositol 3-kinase isoform-specific effects in airway mesenchymal cell function.* J Pharmacol Exp Ther, 2011. **337**(2): p. 557-66.
90. Herman, S.E. and A.J. Johnson, *Molecular pathways: targeting phosphoinositide 3-kinase p110-delta in chronic lymphocytic leukemia.* Clin Cancer Res, 2012. **18**(15): p. 4013-8.
91. Chaussade, C., et al., *Evidence for functional redundancy of class IA PI3K isoforms in insulin signalling.* Biochem J, 2007. **404**(3): p. 449-58.
92. Utermark, T., et al., *The p110alpha and p110beta isoforms of PI3K play divergent roles in mammary gland development and tumorigenesis.* Genes Dev, 2012. **26**(14): p. 1573-86.
93. Ni, J., et al., *Functional characterization of an isoform-selective inhibitor of PI3K-p110beta as a potential anticancer agent.* Cancer Discov, 2012. **2**(5): p. 425-33.
94. Martin, V., et al., *Deletion of the p110beta isoform of phosphoinositide 3-kinase in platelets reveals its central role in Akt activation and*

thrombus formation in vitro and in vivo. Blood, 2010. **115**(10): p. 2008-13.

95. Mohammad, S., et al., *Gastric inhibitory peptide controls adipose insulin sensitivity via activation of cAMP-response element-binding protein and p110beta isoform of phosphatidylinositol 3-kinase.* J Biol Chem, 2011. **286**(50): p. 43062-70.
96. Bi, L., et al., *Proliferative defect and embryonic lethality in mice homozygous for a deletion in the p110alpha subunit of phosphoinositide 3-kinase.* J Biol Chem, 1999. **274**(16): p. 10963-8.
97. Lu, Z., et al., *Loss of cardiac phosphoinositide 3-kinase p110 alpha results in contractile dysfunction.* Circulation, 2009. **120**(4): p. 318-25.
98. Hayakawa, M., et al., *Synthesis and biological evaluation of sulfonylhydrazone-substituted imidazo[1,2-a]pyridines as novel PI3 kinase p110alpha inhibitors.* Bioorg Med Chem, 2007. **15**(17): p. 5837-44.
99. Kong, D. and T. Yamori, *ZSTK474 is an ATP-competitive inhibitor of class I phosphatidylinositol 3 kinase isoforms.* Cancer Sci, 2007. **98**(10): p. 1638-42.
100. Yaguchi, S., et al., *Antitumor activity of ZSTK474, a new phosphatidylinositol 3-kinase inhibitor.* J Natl Cancer Inst, 2006. **98**(8): p. 545-56.
101. Ezeamuzie, C.I., J. Sukumaran, and E. Philips, *Effect of wortmannin on human eosinophil responses in vitro and on bronchial inflammation and airway hyperresponsiveness in Guinea pigs in vivo.* Am J Respir Crit Care Med, 2001. **164**(9): p. 1633-9.
102. Duan, W., et al., *An anti-inflammatory role for a phosphoinositide 3-kinase inhibitor LY294002 in a mouse asthma model.* Int Immunopharmacol, 2005. **5**(3): p. 495-502.
103. Lee, K.S., et al., *Inhibition of phosphoinositide 3-kinase delta attenuates allergic airway inflammation and hyperresponsiveness in murine asthma model.* FASEB J, 2006. **20**(3): p. 455-65.
104. Windmiller, D.A. and J.M. Backer, *Distinct phosphoinositide 3-kinases mediate mast cell degranulation in response to G-protein-coupled*

versus FcepsilonRI receptors. J Biol Chem, 2003. **278**(14): p. 11874-8.

105. Takeda, M., et al., *Allergic airway hyperresponsiveness, inflammation, and remodeling do not develop in phosphoinositide 3-kinase gamma-deficient mice.* J Allergy Clin Immunol, 2009. **123**(4): p. 805-12.
106. Lim, D.H., et al., *PI3K gamma-deficient mice have reduced levels of allergen-induced eosinophilic inflammation and airway remodeling.* Am J Physiol Lung Cell Mol Physiol, 2009. **296**(2): p. L210-9.
107. Okkenhaug, K., et al., *Impaired B and T cell antigen receptor signaling in p110delta PI 3-kinase mutant mice.* Science, 2002. **297**(5583): p. 1031-4.
108. Bilancio, A., et al., *Key role of the p110delta isoform of PI3K in B-cell antigen and IL-4 receptor signaling: comparative analysis of genetic and pharmacologic interference with p110delta function in B cells.* Blood, 2006. **107**(2): p. 642-50.
109. Murata, T., P.D. Noguchi, and R.K. Puri, *IL-13 induces phosphorylation and activation of JAK2 Janus kinase in human colon carcinoma cell lines: similarities between IL-4 and IL-13 signaling.* J Immunol, 1996. **156**(8): p. 2972-8.
110. Lee, Y.W., et al., *Interleukin 4 induces transcription of the 15-lipoxygenase I gene in human endothelial cells.* J Lipid Res, 2001. **42**(5): p. 783-91.
111. Matsukura, S., et al., *Interleukin-13 upregulates eotaxin expression in airway epithelial cells by a STAT6-dependent mechanism.* Am J Respir Cell Mol Biol, 2001. **24**(6): p. 755-61.
112. Fritz, D.K., et al., *Oncostatin-M up-regulates VCAM-1 and synergizes with IL-4 in eotaxin expression: involvement of STAT6.* J Immunol, 2006. **176**(7): p. 4352-60.
113. Chiba, Y., M. Todoroki, and M. Misawa, *Interleukin-4 upregulates RhoA protein via an activation of STAT6 in cultured human bronchial smooth muscle cells.* Pharmacol Res, 2010. **61**(2): p. 188-92.
114. Zhang, C., et al., *Selective induction of apoptosis by histone deacetylase inhibitor SAHA in cutaneous T-cell lymphoma cells:*

relevance to mechanism of therapeutic action. J Invest Dermatol, 2005. **125**(5): p. 1045-52.

115. Richon, V.M., et al., *Second generation hybrid polar compounds are potent inducers of transformed cell differentiation.* Proc Natl Acad Sci U S A, 1996. **93**(12): p. 5705-8.
116. Marks, P.A., et al., *Histone deacetylase inhibitors.* Adv Cancer Res, 2004. **91**: p. 137-68.
117. Rosato, R.R., et al., *Simultaneous activation of the intrinsic and extrinsic pathways by histone deacetylase (HDAC) inhibitors and tumor necrosis factor-related apoptosis-inducing ligand (TRAIL) synergistically induces mitochondrial damage and apoptosis in human leukemia cells.* Mol Cancer Ther, 2003. **2**(12): p. 1273-84.
118. Rosato, R.R., J.A. Almenara, and S. Grant, *The histone deacetylase inhibitor MS-275 promotes differentiation or apoptosis in human leukemia cells through a process regulated by generation of reactive oxygen species and induction of p21CIP1/WAF1 1.* Cancer Res, 2003. **63**(13): p. 3637-45.
119. Rosato, R.R. and S. Grant, *Histone deacetylase inhibitors in cancer therapy.* Cancer Biol Ther, 2003. **2**(1): p. 30-7.
120. Drummond, D.C., et al., *Clinical development of histone deacetylase inhibitors as anticancer agents.* Annu Rev Pharmacol Toxicol, 2005. **45**: p. 495-528.
121. Gryder, B.E., Q.H. Sodji, and A.K. Oyelere, *Targeted cancer therapy: giving histone deacetylase inhibitors all they need to succeed.* Future Med Chem, 2012. **4**(4): p. 505-24.
122. Saunders, N., et al., *Histone deacetylase inhibitors as potential anti-skin cancer agents.* Cancer Res, 1999. **59**(2): p. 399-404.
123. Vigushin, D.M., et al., *Trichostatin A is a histone deacetylase inhibitor with potent antitumor activity against breast cancer in vivo.* Clin Cancer Res, 2001. **7**(4): p. 971-6.
124. Weichert, W., *HDAC expression and clinical prognosis in human malignancies.* Cancer Lett, 2009. **280**(2): p. 168-76.

125. Verdin, E., F. Dequiedt, and H.G. Kasler, *Class II histone deacetylases: versatile regulators.* Trends Genet, 2003. **19**(5): p. 286-93.
126. Duvic, M. and J. Vu, *Vorinostat: a new oral histone deacetylase inhibitor approved for cutaneous T-cell lymphoma.* Expert Opin Investig Drugs, 2007. **16**(7): p. 1111-20.
127. Marks, P.A. and W.S. Xu, *Histone deacetylase inhibitors: Potential in cancer therapy.* J Cell Biochem, 2009. **107**(4): p. 600-8.
128. Piekarz, R. and S. Bates, *A review of depsipeptide and other histone deacetylase inhibitors in clinical trials.* Curr Pharm Des, 2004. **10**(19): p. 2289-98.
129. Leoni, F., et al., *The antitumor histone deacetylase inhibitor suberoylanilide hydroxamic acid exhibits antiinflammatory properties via suppression of cytokines.* Proc Natl Acad Sci U S A, 2002. **99**(5): p. 2995-3000.
130. Buglio, D., et al., *Vorinostat inhibits STAT6-mediated TH2 cytokine and TARC production and induces cell death in Hodgkin lymphoma cell lines.* Blood, 2008. **112**(4): p. 1424-33.
131. Tran, A.D., et al., *HDAC6 deacetylation of tubulin modulates dynamics of cellular adhesions.* J Cell Sci, 2007. **120**(Pt 8): p. 1469-79.
132. Rascle, A., J.A. Johnston, and B. Amati, *Deacetylase activity is required for recruitment of the basal transcription machinery and transactivation by STAT5.* Mol Cell Biol, 2003. **23**(12): p. 4162-73.
133. Wieczorek, M., et al., *Acetylation modulates the STAT signaling code.* Cytokine Growth Factor Rev, 2012. **23**(6): p. 293-305.
134. Ray, S., et al., *Requirement of histone deacetylase1 (HDAC1) in signal transducer and activator of transcription 3 (STAT3) nucleocytoplasmic distribution.* Nucleic Acids Res, 2008. **36**(13): p. 4510-20.
135. Barnes, P.J., I.M. Adcock, and K. Ito, *Histone acetylation and deacetylation: importance in inflammatory lung diseases.* Eur Respir J, 2005. **25**(3): p. 552-63.
136. Doble, B.W. and J.R. Woodgett, *GSK-3: tricks of the trade for a multi-tasking kinase.* J Cell Sci, 2003. **116**(Pt 7): p. 1175-86.

137. Jolivalt, C.G., et al., *Defective insulin signaling pathway and increased glycogen synthase kinase-3 activity in the brain of diabetic mice: parallels with Alzheimer's disease and correction by insulin.* J Neurosci Res, 2008. **86**(15): p. 3265-74.
138. Mendes, C.T., et al., *Lithium reduces Gsk3b mRNA levels: implications for Alzheimer Disease.* Eur Arch Psychiatry Clin Neurosci, 2009. **259**(1): p. 16-22.
139. Freland, L. and J.M. Beaulieu, *Inhibition of GSK3 by lithium, from single molecules to signaling networks.* Front Mol Neurosci, 2012. **5**: p. 14.
140. Lee, Y.J. and Y.K. Kim, *The impact of glycogen synthase kinase 3beta gene on psychotic mania in bipolar disorder patients.* Prog Neuropsychopharmacol Biol Psychiatry, 2011. **35**(5): p. 1303-8.
141. Pedrosa, E., et al., *beta-catenin promoter ChIP-chip reveals potential schizophrenia and bipolar disorder gene network.* J Neurogenet, 2010. **24**(4): p. 182-93.
142. Wang, Y., et al., *The Wnt/beta-catenin pathway is required for the development of leukemia stem cells in AML.* Science, 2010. **327**(5973): p. 1650-3.
143. Bax, B., et al., *The structure of phosphorylated GSK-3beta complexed with a peptide, FRATtide, that inhibits beta-catenin phosphorylation.* Structure, 2001. **9**(12): p. 1143-52.
144. Fraser, E., et al., *Identification of the Axin and Frat binding region of glycogen synthase kinase-3.* J Biol Chem, 2002. **277**(3): p. 2176-85.
145. Fiol, C.J., et al., *Formation of protein kinase recognition sites by covalent modification of the substrate. Molecular mechanism for the synergistic action of casein kinase II and glycogen synthase kinase 3.* J Biol Chem, 1987. **262**(29): p. 14042-8.
146. Rayasam, G.V., et al., *Glycogen synthase kinase 3: more than a namesake.* Br J Pharmacol, 2009. **156**(6): p. 885-98.
147. Patel, S., et al., *Tissue-specific role of glycogen synthase kinase 3beta in glucose homeostasis and insulin action.* Mol Cell Biol, 2008. **28**(20): p. 6314-28.

148. Nikoulina, S.E., et al., *Inhibition of glycogen synthase kinase 3 improves insulin action and glucose metabolism in human skeletal muscle.* Diabetes, 2002. **51**(7): p. 2190-8.
149. Bone, H.K., et al., *Involvement of GSK-3 in regulation of murine embryonic stem cell self-renewal revealed by a series of bisindolylmaleimides.* Chem Biol, 2009. **16**(1): p. 15-27.
150. Wyrzykowska, P., et al., *Epidermal growth factor regulates PAI-1 expression via activation of the transcription factor Elk-1.* Biochim Biophys Acta, 2010. **1799**(9): p. 616-21.
151. Booy, E.P., E.S. Henson, and S.B. Gibson, *Epidermal growth factor regulates Mcl-1 expression through the MAPK-Elk-1 signalling pathway contributing to cell survival in breast cancer.* Oncogene, 2011. **30**(20): p. 2367-78.
152. Zheng, C.F. and K.L. Guan, *Activation of MEK family kinases requires phosphorylation of two conserved Ser/Thr residues.* EMBO J, 1994. **13**(5): p. 1123-31.
153. Alessi, D.R., et al., *PD 098059 is a specific inhibitor of the activation of mitogen-activated protein kinase kinase in vitro and in vivo.* J Biol Chem, 1995. **270**(46): p. 27489-94.
154. Duncia, J.V., et al., *MEK inhibitors: the chemistry and biological activity of U0126, its analogs, and cyclization products.* Bioorg Med Chem Lett, 1998. **8**(20): p. 2839-44.
155. Lorusso, P.M., et al., *Phase I and pharmacodynamic study of the oral MEK inhibitor CI-1040 in patients with advanced malignancies.* J Clin Oncol, 2005. **23**(23): p. 5281-93.
156. Rinehart, J., et al., *Multicenter phase II study of the oral MEK inhibitor, CI-1040, in patients with advanced non-small-cell lung, breast, colon, and pancreatic cancer.* J Clin Oncol, 2004. **22**(22): p. 4456-62.
157. Barrett, S.D., et al., *The discovery of the benzhydroxamate MEK inhibitors CI-1040 and PD 0325901.* Bioorg Med Chem Lett, 2008. **18**(24): p. 6501-4.
158. Brown, A.P., et al., *Pharmacodynamic and toxicokinetic evaluation of the novel MEK inhibitor, PD0325901, in the rat following oral and*

intravenous administration. Cancer Chemother Pharmacol, 2007. **59**(5): p. 671-9.

159. Doerner, A.M. and B.L. Zuraw, *TGF-beta1 induced epithelial to mesenchymal transition (EMT) in human bronchial epithelial cells is enhanced by IL-1beta but not abrogated by corticosteroids.* Respir Res, 2009. **10**: p. 100.
160. Hackett, T.L., et al., *Induction of epithelial-mesenchymal transition in primary airway epithelial cells from patients with asthma by transforming growth factor-beta1.* Am J Respir Crit Care Med, 2009. **180**(2): p. 122-33.
161. Wenzel, S.E., et al., *TGF-beta and IL-13 synergistically increase eotaxin-1 production in human airway fibroblasts.* J Immunol, 2002. **169**(8): p. 4613-9.
162. Zhou, X., et al., *MAPK regulation of IL-4/IL-13 receptors contributes to the synergistic increase in CCL11/eotaxin-1 in response to TGF-beta1 and IL-13 in human airway fibroblasts.* J Immunol, 2012. **188**(12): p. 6046-54.
163. Farquhar, M.G. and G.E. Palade, *Junctional complexes in various epithelia.* J Cell Biol, 1963. **17**: p. 375-412.
164. Wessells, N.K., et al., *Microfilaments in cellular and developmental processes.* Science, 1971. **171**(3967): p. 135-43.
165. Claude, P. and D.A. Goodenough, *Fracture faces of zonulae occludentes from "tight" and "leaky" epithelia.* J Cell Biol, 1973. **58**(2): p. 390-400.
166. Balda, M.S., et al., *Assembly of the tight junction: the role of diacylglycerol.* J Cell Biol, 1993. **123**(2): p. 293-302.
167. Kowalczyk, A.P., et al., *Desmosomes: intercellular adhesive junctions specialized for attachment of intermediate filaments.* Int Rev Cytol, 1999. **185**: p. 237-302.
168. Mese, G., G. Richard, and T.W. White, *Gap junctions: basic structure and function.* J Invest Dermatol, 2007. **127**(11): p. 2516-24.
169. Tschumperlin, D.J., et al., *Mechanotransduction through growth-factor shedding into the extracellular space.* Nature, 2004. **429**(6987): p. 83-6.

170. Furuse, M., et al., *Occludin: a novel integral membrane protein localizing at tight junctions.* J Cell Biol, 1993. **123**(6 Pt 2): p. 1777-88.
171. McCarthy, K.M., et al., *Occludin is a functional component of the tight junction.* J Cell Sci, 1996. **109 (Pt 9)**: p. 2287-98.
172. Balda, M.S., et al., *Functional dissociation of paracellular permeability and transepithelial electrical resistance and disruption of the apical-basolateral intramembrane diffusion barrier by expression of a mutant tight junction membrane protein.* J Cell Biol, 1996. **134**(4): p. 1031-49.
173. Wong, V. and B.M. Gumbiner, *A synthetic peptide corresponding to the extracellular domain of occludin perturbs the tight junction permeability barrier.* J Cell Biol, 1997. **136**(2): p. 399-409.
174. Furuse, M., et al., *Claudin-1 and -2: novel integral membrane proteins localizing at tight junctions with no sequence similarity to occludin.* J Cell Biol, 1998. **141**(7): p. 1539-50.
175. Furuse, M., et al., *A single gene product, claudin-1 or -2, reconstitutes tight junction strands and recruits occludin in fibroblasts.* J Cell Biol, 1998. **143**(2): p. 391-401.
176. Lal-Nag, M. and P.J. Morin, *The claudins.* Genome Biol, 2009. **10**(8): p. 235.
177. Trelstad, R.L., J.P. Revel, and E.D. Hay, *Tight junctions between cells in the early chick embryo as visualized with the electron microscopy.* J Cell Biol, 1966. **31**(1): p. C6-10.
178. Haskins, J., et al., *ZO-3, a novel member of the MAGUK protein family found at the tight junction, interacts with ZO-1 and occludin.* J Cell Biol, 1998. **141**(1): p. 199-208.
179. Gonzalez-Mariscal, L., A. Betanzos, and A. Avila-Flores, *MAGUK proteins: structure and role in the tight junction.* Semin Cell Dev Biol, 2000. **11**(4): p. 315-24.
180. Furuse, M., H. Sasaki, and S. Tsukita, *Manner of interaction of heterogeneous claudin species within and between tight junction strands.* J Cell Biol, 1999. **147**(4): p. 891-903.
181. Kobayashi, J., T. Inai, and Y. Shibata, *Formation of tight junction strands by expression of claudin-1 mutants in their ZO-1 binding site in MDCK cells.* Histochem Cell Biol, 2002. **117**(1): p. 29-39.

182. Itoh, M., et al., *Direct binding of three tight junction-associated MAGUKs, ZO-1, ZO-2, and ZO-3, with the COOH termini of claudins.* J Cell Biol, 1999. **147**(6): p. 1351-63.
183. Denker, B.M. and S.K. Nigam, *Molecular structure and assembly of the tight junction.* Am J Physiol, 1998. **274**(1 Pt 2): p. F1-9.
184. Howarth, A.G., M.R. Hughes, and B.R. Stevenson, *Detection of the tight junction-associated protein ZO-1 in astrocytes and other nonepithelial cell types.* Am J Physiol, 1992. **262**(2 Pt 1): p. C461-9.
185. Nishimura, M., et al., *JEAP, a novel component of tight junctions in exocrine cells.* J Biol Chem, 2002. **277**(7): p. 5583-7.
186. Kausalya, P.J., M. Reichert, and W. Hunziker, *Connexin45 directly binds to ZO-1 and localizes to the tight junction region in epithelial MDCK cells.* FEBS Lett, 2001. **505**(1): p. 92-6.
187. Bazzoni, G., et al., *Interaction of junctional adhesion molecule with the tight junction components ZO-1, cingulin, and occludin.* J Biol Chem, 2000. **275**(27): p. 20520-6.
188. Stevenson, B.R., et al., *ZO-1 and cingulin: tight junction proteins with distinct identities and localizations.* Am J Physiol, 1989. **257**(4 Pt 1): p. C621-8.
189. Beatch, M., et al., *The tight junction protein ZO-2 contains three PDZ (PSD-95/Discs-Large/ZO-1) domains and an alternatively spliced region.* J Biol Chem, 1996. **271**(42): p. 25723-6.
190. Xu, J., et al., *Early embryonic lethality of mice lacking ZO-2, but Not ZO-3, reveals critical and nonredundant roles for individual zonula occludens proteins in mammalian development.* Mol Cell Biol, 2008. **28**(5): p. 1669-78.
191. Nusrat, A., et al., *The coiled-coil domain of occludin can act to organize structural and functional elements of the epithelial tight junction.* J Biol Chem, 2000. **275**(38): p. 29816-22.
192. Walter, J.K., et al., *The oligomerization of the coiled coil-domain of occludin is redox sensitive.* Ann N Y Acad Sci, 2009. **1165**: p. 19-27.
193. Walter, J.K., et al., *Redox-sensitivity of the dimerization of occludin.* Cell Mol Life Sci, 2009. **66**(22): p. 3655-62.

194. Bamforth, S.D., et al., *A dominant mutant of occludin disrupts tight junction structure and function.* J Cell Sci, 1999. **112 (Pt 12)**: p. 1879-88.

195. Van Itallie, C.M. and J.M. Anderson, *Occludin confers adhesiveness when expressed in fibroblasts.* J Cell Sci, 1997. **110 (Pt 9)**: p. 1113-21.

196. Lacaz-Vieira, F., et al., *Small synthetic peptides homologous to segments of the first external loop of occludin impair tight junction resealing.* J Membr Biol, 1999. **168**(3): p. 289-97.

197. Tavelin, S., et al., *A new principle for tight junction modulation based on occludin peptides.* Mol Pharmacol, 2003. **64**(6): p. 1530-40.

198. Furuse, M., et al., *Direct association of occludin with ZO-1 and its possible involvement in the localization of occludin at tight junctions.* J Cell Biol, 1994. **127**(6 Pt 1): p. 1617-26.

199. Suzuki, T., et al., *PKC eta regulates occludin phosphorylation and epithelial tight junction integrity.* Proc Natl Acad Sci U S A, 2009. **106**(1): p. 61-6.

200. Itallie, C.M. and J.M. Anderson, *Caveolin binds independently to claudin-2 and occludin.* Ann N Y Acad Sci, 2012. **1257**: p. 103-7.

201. Lapierre, L.A., et al., *VAP-33 localizes to both an intracellular vesicle population and with occludin at the tight junction.* J Cell Sci, 1999. **112 (Pt 21)**: p. 3723-32.

202. Sakakibara, A., et al., *Possible involvement of phosphorylation of occludin in tight junction formation.* J Cell Biol, 1997. **137**(6): p. 1393-401.

203. Rao, R., *Occludin phosphorylation in regulation of epithelial tight junctions.* Ann N Y Acad Sci, 2009. **1165**: p. 62-8.

204. Elias, B.C., et al., *Phosphorylation of Tyr-398 and Tyr-402 in occludin prevents its interaction with ZO-1 and destabilizes its assembly at the tight junctions.* J Biol Chem, 2009. **284**(3): p. 1559-69.

205. Tsukamoto, T. and S.K. Nigam, *Role of tyrosine phosphorylation in the reassembly of occludin and other tight junction proteins.* Am J Physiol, 1999. **276**(5 Pt 2): p. F737-50.

206. Krause, G., et al., *Structure and function of extracellular claudin domains.* Ann N Y Acad Sci, 2009. **1165**: p. 34-43.
207. Angelow, S. and A.S. Yu, *Structure-function studies of claudin extracellular domains by cysteine-scanning mutagenesis.* J Biol Chem, 2009. **284**(42): p. 29205-17.
208. Robertson, S.L. and B.A. McClane, *Interactions between Clostridium perfringens enterotoxin and claudins.* Methods Mol Biol, 2011. **762**: p. 63-75.
209. Piontek, J., et al., *Formation of tight junction: determinants of homophilic interaction between classic claudins.* FASEB J, 2008. **22**(1): p. 146-58.
210. Itoh, M., et al., *Junctional adhesion molecule (JAM) binds to PAR-3: a possible mechanism for the recruitment of PAR-3 to tight junctions.* J Cell Biol, 2001. **154**(3): p. 491-7.
211. Angelow, S., R. Ahlstrom, and A.S. Yu, *Biology of claudins.* Am J Physiol Renal Physiol, 2008. **295**(4): p. F867-76.
212. Van Itallie, C.M. and J.M. Anderson, *The role of claudins in determining paracellular charge selectivity.* Proc Am Thorac Soc, 2004. **1**(1): p. 38-41.
213. Angelow, S. and A.S. Yu, *Cysteine mutagenesis to study the structure of claudin-2 paracellular pores.* Ann N Y Acad Sci, 2009. **1165**: p. 143-7.
214. Hamazaki, Y., et al., *Multi-PDZ domain protein 1 (MUPP1) is concentrated at tight junctions through its possible interaction with claudin-1 and junctional adhesion molecule.* J Biol Chem, 2002. **277**(1): p. 455-61.
215. Wen, H., et al., *Selective decrease in paracellular conductance of tight junctions: role of the first extracellular domain of claudin-5.* Mol Cell Biol, 2004. **24**(19): p. 8408-17.
216. Medina, R., et al., *Occludin localization at the tight junction requires the second extracellular loop.* J Membr Biol, 2000. **178**(3): p. 235-47.
217. Volk, T. and B. Geiger, *A 135-kd membrane protein of intercellular adherens junctions.* EMBO J, 1984. **3**(10): p. 2249-60.

218. Miyatani, S., et al., *Neural cadherin: role in selective cell-cell adhesion.* Science, 1989. **245**(4918): p. 631-5.
219. Nose, A., A. Nagafuchi, and M. Takeichi, *Isolation of placental cadherin cDNA: identification of a novel gene family of cell-cell adhesion molecules.* EMBO J, 1987. **6**(12): p. 3655-61.
220. Hatta, K., et al., *Cloning and expression of cDNA encoding a neural calcium-dependent cell adhesion molecule: its identity in the cadherin gene family.* J Cell Biol, 1988. **106**(3): p. 873-81.
221. Nagafuchi, A. and M. Takeichi, *Cell binding function of E-cadherin is regulated by the cytoplasmic domain.* EMBO J, 1988. **7**(12): p. 3679-84.
222. Schmitz, H., et al., *Epithelial barrier and transport function of the colon in ulcerative colitis.* Ann N Y Acad Sci, 2000. **915**: p. 312-26.
223. Marin, M.L., et al., *A freeze fracture study of Crohn's disease of the terminal ileum: changes in epithelial tight junction organization.* Am J Gastroenterol, 1983. **78**(9): p. 537-47.
224. Marin, M.L., et al., *Ultrastructural pathology of Crohn's disease: correlated transmission electron microscopy, scanning electron microscopy, and freeze fracture studies.* Am J Gastroenterol, 1983. **78**(6): p. 355-64.
225. Schurmann, G., et al., *Transepithelial transport processes at the intestinal mucosa in inflammatory bowel disease.* Int J Colorectal Dis, 1999. **14**(1): p. 41-6.
226. Zeissig, S., et al., *Changes in expression and distribution of claudin 2, 5 and 8 lead to discontinuous tight junctions and barrier dysfunction in active Crohn's disease.* Gut, 2007. **56**(1): p. 61-72.
227. Schulzke, J.D., et al., *Epithelial tight junctions in intestinal inflammation.* Ann N Y Acad Sci, 2009. **1165**: p. 294-300.
228. Siliciano, J.D. and D.A. Goodenough, *Localization of the tight junction protein, ZO-1, is modulated by extracellular calcium and cell-cell contact in Madin-Darby canine kidney epithelial cells.* J Cell Biol, 1988. **107**(6 Pt 1): p. 2389-99.

229. O'Keefe, E.J., R.A. Briggaman, and B. Herman, *Calcium-induced assembly of adherens junctions in keratinocytes.* J Cell Biol, 1987. **105**(2): p. 807-17.
230. Nigam, S.K., E. Rodriguez-Boulan, and R.B. Silver, *Changes in intracellular calcium during the development of epithelial polarity and junctions.* Proc Natl Acad Sci U S A, 1992. **89**(13): p. 6162-6.
231. Volberg, T., et al., *Changes in membrane-microfilament interaction in intercellular adherens junctions upon removal of extracellular Ca2+ ions.* J Cell Biol, 1986. **102**(5): p. 1832-42.
232. Zhang, L., et al., *AMP-activated protein kinase regulates the assembly of epithelial tight junctions.* Proc Natl Acad Sci U S A, 2006. **103**(46): p. 17272-7.
233. Zheng, B. and L.C. Cantley, *Regulation of epithelial tight junction assembly and disassembly by AMP-activated protein kinase.* Proc Natl Acad Sci U S A, 2007. **104**(3): p. 819-22.
234. Zhang, L., et al., *AMP-activated protein kinase (AMPK) activation and glycogen synthase kinase-3beta (GSK-3beta) inhibition induce Ca2+-independent deposition of tight junction components at the plasma membrane.* J Biol Chem, 2011. **286**(19): p. 16879-90.
235. Severson, E.A., et al., *Glycogen Synthase Kinase 3 (GSK-3) influences epithelial barrier function by regulating occludin, claudin-1 and E-cadherin expression.* Biochem Biophys Res Commun, 2010. **397**(3): p. 592-7.
236. Basuroy, S., et al., *MAPK interacts with occludin and mediates EGF-induced prevention of tight junction disruption by hydrogen peroxide.* Biochem J, 2006. **393**(Pt 1): p. 69-77.
237. Stuart, R.O. and S.K. Nigam, *Regulated assembly of tight junctions by protein kinase C.* Proc Natl Acad Sci U S A, 1995. **92**(13): p. 6072-6.
238. Banan, A., et al., *theta Isoform of protein kinase C alters barrier function in intestinal epithelium through modulation of distinct claudin isotypes: a novel mechanism for regulation of permeability.* J Pharmacol Exp Ther, 2005. **313**(3): p. 962-82.
239. Sjo, A., K.E. Magnusson, and K.H. Peterson, *Protein kinase C activation has distinct effects on the localization, phosphorylation and*

detergent solubility of the claudin protein family in tight and leaky epithelial cells. J Membr Biol, 2010. **236**(2): p. 181-9.

240. Murakami, T., E.A. Felinski, and D.A. Antonetti, *Occludin Phosphorylation and Ubiquitination Regulate Tight Junction Trafficking and Vascular Endothelial Growth Factor-induced Permeability.* J Biol Chem, 2009. **284**(31): p. 21036-46.
241. Murakami, T., et al., *Protein kinase cbeta phosphorylates occludin regulating tight junction trafficking in vascular endothelial growth factor-induced permeability in vivo.* Diabetes, 2012. **61**(6): p. 1573-83.
242. Harhaj, N.S., et al., *VEGF activation of protein kinase C stimulates occludin phosphorylation and contributes to endothelial permeability.* Invest Ophthalmol Vis Sci, 2006. **47**(11): p. 5106-15.
243. Jou, T.S., E.E. Schneeberger, and W.J. Nelson, *Structural and functional regulation of tight junctions by RhoA and Rac1 small GTPases.* J Cell Biol, 1998. **142**(1): p. 101-15.
244. Terry, S.J., et al., *Spatially restricted activation of RhoA signalling at epithelial junctions by p114RhoGEF drives junction formation and morphogenesis.* Nat Cell Biol, 2011. **13**(2): p. 159-66.
245. Heller, F., et al., *Interleukin-13 is the key effector Th2 cytokine in ulcerative colitis that affects epithelial tight junctions, apoptosis, and cell restitution.* Gastroenterology, 2005. **129**(2): p. 550-64.
246. Madden, K.B., et al., *Role of STAT6 and mast cells in IL-4- and IL-13-induced alterations in murine intestinal epithelial cell function.* J Immunol, 2002. **169**(8): p. 4417-22.
247. Rosen, M.J., et al., *STAT6 activation in ulcerative colitis: a new target for prevention of IL-13-induced colon epithelial cell dysfunction.* Inflamm Bowel Dis, 2011. **17**(11): p. 2224-34.
248. Ceponis, P.J., et al., *Interleukins 4 and 13 increase intestinal epithelial permeability by a phosphatidylinositol 3-kinase pathway. Lack of evidence for STAT 6 involvement.* J Biol Chem, 2000. **275**(37): p. 29132-7.
249. Mankertz, J., et al., *TNFalpha up-regulates claudin-2 expression in epithelial HT-29/B6 cells via phosphatidylinositol-3-kinase signaling.* Cell Tissue Res, 2009. **336**(1): p. 67-77.

250. Patrick, D.M., et al., *Proinflammatory cytokines tumor necrosis factor-alpha and interferon-gamma modulate epithelial barrier function in Madin-Darby canine kidney cells through mitogen activated protein kinase signaling.* BMC Physiol, 2006. **6**: p. 2.
251. Coyne, C.B., et al., *Regulation of airway tight junctions by proinflammatory cytokines.* Mol Biol Cell, 2002. **13**(9): p. 3218-34.
252. Ahdieh, M., T. Vandenbos, and A. Youakim, *Lung epithelial barrier function and wound healing are decreased by IL-4 and IL-13 and enhanced by IFN-gamma.* Am J Physiol Cell Physiol, 2001. **281**(6): p. C2029-38.
253. Boivin, M.A., et al., *Mechanism of interferon-gamma-induced increase in T84 intestinal epithelial tight junction.* J Interferon Cytokine Res, 2009. **29**(1): p. 45-54.
254. Betz, M. and B.S. Fox, *Prostaglandin E2 inhibits production of Th1 lymphokines but not of Th2 lymphokines.* J Immunol, 1991. **146**(1): p. 108-13.
255. Kalinski, P., et al., *IL-12-deficient dendritic cells, generated in the presence of prostaglandin E2, promote type 2 cytokine production in maturing human naive T helper cells.* J Immunol, 1997. **159**(1): p. 28-35.
256. Wang, W.C., et al., *Non-proteolytic house dust mite allergen, Der p 2, upregulated expression of tight junction molecule claudin-2 associated with Akt/GSK-3beta/beta-catenin signaling pathway.* J Cell Biochem, 2011. **112**(6): p. 1544-51.
257. Wang, X., et al., *Derp2-mutant gene vaccine inhibits airway inflammation and up-regulates Toll-like receptor 9 in an allergic asthmatic mouse model.* Asian Pac J Allergy Immunol, 2010. **28**(4): p. 287-93.
258. Qiu, J., et al., *DNA vaccine encoding Der p2 allergen down-regulates STAT6 expression in mouse model of allergen-induced allergic airway inflammation.* Chin Med J (Engl), 2006. **119**(3): p. 185-90.
259. Wan, H., et al., *Quantitative structural and biochemical analyses of tight junction dynamics following exposure of epithelial cells to house dust mite allergen Der p 1.* Clin Exp Allergy, 2000. **30**(5): p. 685-98.

260. Mehta, S., *The effects of nitric oxide in acute lung injury.* Vascul Pharmacol, 2005. **43**(6): p. 390-403.
261. Grasemann, H., et al., *Asymmetric dimethylarginine contributes to airway nitric oxide deficiency in patients with cystic fibrosis.* Am J Respir Crit Care Med, 2011. **183**(10): p. 1363-8.
262. Mhanna, M.J., et al., *Nitric oxide deficiency contributes to impairment of airway relaxation in cystic fibrosis mice.* Am J Respir Cell Mol Biol, 2001. **24**(5): p. 621-6.
263. Meng, Q.H., et al., *Lack of inducible nitric oxide synthase in bronchial epithelium: a possible mechanism of susceptibility to infection in cystic fibrosis.* J Pathol, 1998. **184**(3): p. 323-31.
264. Schmidt, A. and M.N. Hall, *Signaling to the actin cytoskeleton.* Annu Rev Cell Dev Biol, 1998. **14**: p. 305-38.
265. Olivera, D., et al., *Cytoskeletal modulation and tyrosine phosphorylation of tight junction proteins are associated with mainstream cigarette smoke-induced permeability of airway epithelium.* Exp Toxicol Pathol, 2010. **62**(2): p. 133-43.
266. Bruewer, M., et al., *RhoA, Rac1, and Cdc42 exert distinct effects on epithelial barrier via selective structural and biochemical modulation of junctional proteins and F-actin.* Am J Physiol Cell Physiol, 2004. **287**(2): p. C327-35.
267. Totsukawa, G., et al., *Distinct roles of ROCK (Rho-kinase) and MLCK in spatial regulation of MLC phosphorylation for assembly of stress fibers and focal adhesions in 3T3 fibroblasts.* J Cell Biol, 2000. **150**(4): p. 797-806.
268. Olivera, D.S., et al., *Cellular mechanisms of mainstream cigarette smoke-induced lung epithelial tight junction permeability changes in vitro.* Inhal Toxicol, 2007. **19**(1): p. 13-22.
269. Edlund, S., et al., *Transforming growth factor-beta-induced mobilization of actin cytoskeleton requires signaling by small GTPases Cdc42 and RhoA.* Mol Biol Cell, 2002. **13**(3): p. 902-14.
270. Wang, Y., et al., *Activation of ERK1/2 MAP kinase pathway induces tight junction disruption in human corneal epithelial cells.* Exp Eye Res, 2004. **78**(1): p. 125-36.

271. Samak, G., S. Aggarwal, and R.K. Rao, *ERK is involved in EGF-mediated protection of tight junctions, but not adherens junctions, in acetaldehyde-treated Caco-2 cell monolayers.* Am J Physiol Gastrointest Liver Physiol, 2011. **301**(1): p. G50-9.
272. Shen, B.Q., et al., *Calu-3: a human airway epithelial cell line that shows cAMP-dependent Cl- secretion.* Am J Physiol, 1994. **266**(5 Pt 1): p. L493-501.
273. Haghi, M., et al., *Time- and passage-dependent characteristics of a Calu-3 respiratory epithelial cell model.* Drug Dev Ind Pharm, 2010. **36**(10): p. 1207-14.
274. Stewart, C.E., et al., *Evaluation of differentiated human bronchial epithelial cell culture systems for asthma research.* J Allergy (Cairo), 2012. **2012**: p. 943982.
275. Grainger, C.I., et al., *Culture of Calu-3 cells at the air interface provides a representative model of the airway epithelial barrier.* Pharm Res, 2006. **23**(7): p. 1482-90.
276. Wisner, D.M., et al., *Opposing regulation of the tight junction protein claudin-2 by interferon-gamma and interleukin-4.* J Surg Res, 2008. **144**(1): p. 1-7.
277. Laprise, P., et al., *Phosphatidylinositol 3-kinase controls human intestinal epithelial cell differentiation by promoting adherens junction assembly and p38 MAPK activation.* J Biol Chem, 2002. **277**(10): p. 8226-34.
278. Itoh, M., et al., *The 220-kD protein colocalizing with cadherins in non-epithelial cells is identical to ZO-1, a tight junction-associated protein in epithelial cells: cDNA cloning and immunoelectron microscopy.* J Cell Biol, 1993. **121**(3): p. 491-502.
279. Foster, K.A., et al., *Characterization of the Calu-3 cell line as a tool to screen pulmonary drug delivery.* Int J Pharm, 2000. **208**(1-2): p. 1-11.
280. Hamilton, K.O., et al., *Multidrug resistance-associated protein-1 functional activity in Calu-3 cells.* J Pharmacol Exp Ther, 2001. **298**(3): p. 1199-205.
281. Peter, Y., et al., *Epidermal growth factor receptor and claudin-2 participate in A549 permeability and remodeling: implications for non-*

small cell lung cancer tumor colonization. Mol Carcinog, 2009. **48**(6): p. 488-97.

282. Ikari, A., et al., *Claudin-2 knockdown decreases matrix metalloproteinase-9 activity and cell migration via suppression of nuclear Sp1 in A549 cells.* Life Sci, 2011. **88**(13-14): p. 628-33.
283. Hirakata, Y., et al., *Monolayer culture systems with respiratory epithelial cells for evaluation of bacterial invasiveness.* Tohoku J Exp Med, 2010. **220**(1): p. 15-9.
284. Blank, F., et al., *An optimized in vitro model of the respiratory tract wall to study particle cell interactions.* J Aerosol Med, 2006. **19**(3): p. 392-405.
285. Forbes, B. and C. Ehrhardt, *Human respiratory epithelial cell culture for drug delivery applications.* Eur J Pharm Biopharm, 2005. **60**(2): p. 193-205.
286. Zhu, Y., A. Chidekel, and T.H. Shaffer, *Cultured human airway epithelial cells (calu-3): a model of human respiratory function, structure, and inflammatory responses.* Crit Care Res Pract, 2010. **2010**.
287. Stentebjerg-Andersen, A., et al., *Calu-3 cells grown under AIC and LCC conditions: implications for dipeptide uptake and transepithelial transport of substances.* Eur J Pharm Biopharm, 2011. **78**(1): p. 19-26.
288. Wynn, T.A., *Cellular and molecular mechanisms of fibrosis.* J Pathol, 2008. **214**(2): p. 199-210.
289. Cain, R.J., B. Vanhaesebroeck, and A.J. Ridley, *Different PI 3-kinase inhibitors have distinct effects on endothelial permeability and leukocyte transmigration.* Int J Biochem Cell Biol, 2012. **44**(11): p. 1929-36.
290. Morgillo, F., et al., *Antitumor activity of bortezomib in human cancer cells with acquired resistance to anti-epidermal growth factor receptor tyrosine kinase inhibitors.* Lung Cancer, 2011. **71**(3): p. 283-90.
291. Bruewer, M., et al., *Proinflammatory cytokines disrupt epithelial barrier function by apoptosis-independent mechanisms.* J Immunol, 2003. **171**(11): p. 6164-72.

292. Amasheh, S., et al., *Claudin-2 expression induces cation-selective channels in tight junctions of epithelial cells.* J Cell Sci, 2002. **115**(Pt 24): p. 4969-76.
293. Yu, A.S., et al., *Molecular basis for cation selectivity in claudin-2-based paracellular pores: identification of an electrostatic interaction site.* J Gen Physiol, 2009. **133**(1): p. 111-27.
294. Rosenthal, R., et al., *Claudin-2, a component of the tight junction, forms a paracellular water channel.* J Cell Sci, 2010. **123**(Pt 11): p. 1913-21.
295. Wada, M., et al., *Loss of Claudins 2 and 15 From Mice Causes Defects in Paracellular Na(+) Flow and Nutrient Transport in Gut and Leads to Death from Malnutrition.* Gastroenterology, 2012.
296. Tamura, A., et al., *Loss of claudin-15, but not claudin-2, causes Na+ deficiency and glucose malabsorption in mouse small intestine.* Gastroenterology, 2011. **140**(3): p. 913-23.
297. Van Itallie, C.M., et al., *Phosphorylation of claudin-2 on serine 208 promotes membrane retention and reduces trafficking to lysosomes.* J Cell Sci, 2012. **125**(Pt 20): p. 4902-12.
298. Nakano, T., et al., *Niflumic acid suppresses interleukin-13-induced asthma phenotypes.* Am J Respir Crit Care Med, 2006. **173**(11): p. 1216-21.
299. Tanabe, T., et al., *Modulation of mucus production by interleukin-13 receptor alpha2 in the human airway epithelium.* Clin Exp Allergy, 2008. **38**(1): p. 122-34.
300. Yasuo, M., et al., *Relationship between calcium-activated chloride channel 1 and MUC5AC in goblet cell hyperplasia induced by interleukin-13 in human bronchial epithelial cells.* Respiration, 2006. **73**(3): p. 347-59.
301. McManus, O.B., et al., *Ion Channel Screening.* 2004.
302. Chiba, H., et al., *The significance of interferon-gamma-triggered internalization of tight-junction proteins in inflammatory bowel disease.* Sci STKE, 2006. **2006**(316): p. pe1.

303. Wong, K.K., J.A. Engelman, and L.C. Cantley, *Targeting the PI3K signaling pathway in cancer.* Curr Opin Genet Dev, 2010. **20**(1): p. 87-90.
304. Baselga, J., *Targeting the phosphoinositide-3 (PI3) kinase pathway in breast cancer.* Oncologist, 2011. **16 Suppl 1**: p. 12-9.
305. Wojtalla, A. and A. Arcaro, *Targeting phosphoinositide 3-kinase signalling in lung cancer.* Crit Rev Oncol Hematol, 2011. **80**(2): p. 278-90.
306. Marwick, J.A., K.F. Chung, and I.M. Adcock, *Phosphatidylinositol 3-kinase isoforms as targets in respiratory disease.* Ther Adv Respir Dis, 2010. **4**(1): p. 19-34.
307. Farghaly, H.S., et al., *Interleukin 13 increases contractility of murine tracheal smooth muscle by a phosphoinositide 3-kinase p110delta-dependent mechanism.* Mol Pharmacol, 2008. **73**(5): p. 1530-7.
308. Park, S., et al., *PI-103, a dual inhibitor of Class IA phosphatidylinositide 3-kinase and mTOR, has antileukemic activity in AML.* Leukemia, 2008. **22**(9): p. 1698-706.
309. Wang, W.C., et al., *IL-6 augmented motility of airway epithelial cell BEAS-2B via Akt/GSK-3beta signaling pathway.* J Cell Biochem, 2012. **113**(11): p. 3567-75.
310. Geback, T., et al., *TScratch: a novel and simple software tool for automated analysis of monolayer wound healing assays.* Biotechniques, 2009. **46**(4): p. 265-74.
311. Rowan, W.C., et al., *Targeting phosphoinositide 3-kinase delta for allergic asthma.* Biochem Soc Trans, 2012. **40**(1): p. 240-5.
312. Buisson, A.C., et al., *Gelatinase B is involved in the in vitro wound repair of human respiratory epithelium.* J Cell Physiol, 1996. **166**(2): p. 413-26.
313. Zhao, M., *PTEN: a promising pharmacological target to enhance epithelial wound healing.* Br J Pharmacol, 2007. **152**(8): p. 1141-4.
314. Lai, J.P., J.T. Dalton, and D.L. Knoell, *Phosphatase and tensin homologue deleted on chromosome ten (PTEN) as a molecular target in lung epithelial wound repair.* Br J Pharmacol, 2007. **152**(8): p. 1172-84.

315. Lee, Y.C., et al., *Inhibitory effects of andrographolide on migration and invasion in human non-small cell lung cancer A549 cells via down-regulation of PI3K/Akt signaling pathway.* Eur J Pharmacol, 2010. **632**(1-3): p. 23-32.
316. Pankow, S., et al., *Regulation of epidermal homeostasis and repair by phosphoinositide 3-kinase.* J Cell Sci, 2006. **119**(Pt 19): p. 4033-46.
317. Bleich, M., Q. Shan, and N. Himmerkus, *Calcium regulation of tight junction permeability.* Ann N Y Acad Sci, 2012. **1258**: p. 93-9.
318. Liu, Y., et al., *Human junction adhesion molecule regulates tight junction resealing in epithelia.* J Cell Sci, 2000. **113 (Pt 13)**: p. 2363-74.
319. Zhao, J., et al., *Interleukin-13-induced MUC5AC is regulated by 15-lipoxygenase 1 pathway in human bronchial epithelial cells.* Am J Respir Crit Care Med, 2009. **179**(9): p. 782-90.
320. Kelly-Welch, A.E., et al., *Interleukin-4 and interleukin-13 signaling connections maps.* Science, 2003. **300**(5625): p. 1527-8.
321. Stambolic, V. and J.R. Woodgett, *Mitogen inactivation of glycogen synthase kinase-3 beta in intact cells via serine 9 phosphorylation.* Biochem J, 1994. **303 (Pt 3)**: p. 701-4.
322. Mandal, D., P. Fu, and A.D. Levine, *REDOX regulation of IL-13 signaling in intestinal epithelial cells: usage of alternate pathways mediates distinct gene expression patterns.* Cell Signal, 2010. **22**(10): p. 1485-94.
323. Kumagai, T., et al., *Histone deacetylase inhibitor, suberoylanilide hydroxamic acid (Vorinostat, SAHA) profoundly inhibits the growth of human pancreatic cancer cells.* Int J Cancer, 2007. **121**(3): p. 656-65.
324. Cooper, A.L., et al., *In vitro and in vivo histone deacetylase inhibitor therapy with suberoylanilide hydroxamic acid (SAHA) and paclitaxel in ovarian cancer.* Gynecol Oncol, 2007. **104**(3): p. 596-601.
325. Yi, X., et al., *Histone deacetylase inhibitor SAHA induces ERalpha degradation in breast cancer MCF-7 cells by CHIP-mediated ubiquitin pathway and inhibits survival signaling.* Biochem Pharmacol, 2008. **75**(9): p. 1697-705.

326. Sun, T., M. Rodriguez, and L. Kim, *Glycogen synthase kinase 3 in the world of cell migration.* Dev Growth Differ, 2009. **51**(9): p. 735-42.
327. Jope, R.S., C.J. Yuskaitis, and E. Beurel, *Glycogen synthase kinase-3 (GSK3): inflammation, diseases, and therapeutics.* Neurochem Res, 2007. **32**(4-5): p. 577-95.
328. Bone, H.K., et al., *A novel chemically directed route for the generation of definitive endoderm from human embryonic stem cells based on inhibition of GSK-3.* J Cell Sci, 2011. **124**(Pt 12): p. 1992-2000.
329. Williams, R., et al., *Identification of a human epidermal growth factor receptor-associated protein kinase as a new member of the mitogen-activated protein kinase/extracellular signal-regulated protein kinase family.* J Biol Chem, 1993. **268**(24): p. 18213-7.
330. Tetreault, M.P., et al., *Epidermal growth factor receptor-dependent PI3K-activation promotes restitution of wounded human gastric epithelial monolayers.* J Cell Physiol, 2008. **214**(2): p. 545-57.
331. Kaliszczak, M., et al., *A novel small molecule hydroxamate preferentially inhibits HDAC6 activity and tumour growth.* Br J Cancer, 2013. **108**(2): p. 342-50.
332. Hou, J., et al., *Claudin-4 forms paracellular chloride channel in the kidney and requires claudin-8 for tight junction localization.* Proc Natl Acad Sci U S A, 2010. **107**(42): p. 18010-5.
333. Amasheh, S., et al., *Na+ absorption defends from paracellular back-leakage by claudin-8 upregulation.* Biochem Biophys Res Commun, 2009. **378**(1): p. 45-50.
334. Angelow, S., E.E. Schneeberger, and A.S. Yu, *Claudin-8 expression in renal epithelial cells augments the paracellular barrier by replacing endogenous claudin-2.* J Membr Biol, 2007. **215**(2-3): p. 147-59.
335. Wang, H.B., et al., *Butyrate enhances intestinal epithelial barrier function via up-regulation of tight junction protein Claudin-1 transcription.* Dig Dis Sci, 2012. **57**(12): p. 3126-35.
336. Tang, X.X., et al., *Lymphocytes accelerate epithelial tight junction assembly: role of AMP-activated protein kinase (AMPK).* PLoS One, 2010. **5**(8): p. e12343.

337. Failor, K.L., et al., *Glucocorticoid-induced degradation of glycogen synthase kinase-3 protein is triggered by serum- and glucocorticoid-induced protein kinase and Akt signaling and controls beta-catenin dynamics and tight junction formation in mammary epithelial tumor cells.* Mol Endocrinol, 2007. **21**(10): p. 2403-15.
338. Petecchia, L., et al., *Cytokines induce tight junction disassembly in airway cells via an EGFR-dependent MAPK/ERK1/2-pathway.* Lab Invest, 2012. **92**(8): p. 1140-8.
339. Moynihan, B., et al., *MAP kinases mediate interleukin-13 effects on calcium signaling in human airway smooth muscle cells.* Am J Physiol Lung Cell Mol Physiol, 2008. **295**(1): p. L171-7.
340. Ciuffreda, L., et al., *Growth-inhibitory and antiangiogenic activity of the MEK inhibitor PD0325901 in malignant melanoma with or without BRAF mutations.* Neoplasia, 2009. **11**(8): p. 720-31.
341. Ishikawa-Ankerhold, H.C., R. Ankerhold, and G.P. Drummen, *Advanced fluorescence microscopy techniques--FRAP, FLIP, FLAP, FRET and FLIM.* Molecules, 2012. **17**(4): p. 4047-132.
342. Foukas, L.C., et al., *Activity of any class IA PI3K isoform can sustain cell proliferation and survival.* Proc Natl Acad Sci U S A, 2010. **107**(25): p. 11381-6.
343. Papakonstanti, E.A., et al., *Distinct roles of class IA PI3K isoforms in primary and immortalised macrophages.* J Cell Sci, 2008. **121**(Pt 24): p. 4124-33.
344. Zhang, X., et al., *Docking protein Gab2 regulates mucin expression and goblet cell hyperplasia through TYK2/STAT6 pathway.* FASEB J, 2012. **26**(11): p. 4603-13.
345. Darcan-Nicolaisen, Y., et al., *Small interfering RNA against transcription factor STAT6 inhibits allergic airway inflammation and hyperreactivity in mice.* J Immunol, 2009. **182**(12): p. 7501-8.
346. Rosen, M.J., et al., *STAT6 Deficiency Ameliorates Severity of Oxazolone Colitis by Decreasing Expression of Claudin-2 and Th2-Inducing Cytokines.* J Immunol, 2013.